The Cellular and Molecular Axis of Muscle Regeneration

Nicholas Ieronimakis

A dissertation

submitted in partial fulfillment of the

requirements for the degree of

Doctor of Philosophy

University of Washington

2014

Reading Committee:

Morayma Reyes, Chair

Hannele Ruohola-Baker

William M. Mahoney, Jr

Program Authorized to Offer Degree:

Pathology

University of Washington

Abstract

The Cellular and Molecular Axis of Muscle Regeneration

Nicholas Ieronimakis

Chair of the Supervisory Committee:

Morayma Reyes, Assistant Professor

Department of Pathology

Skeletal muscle has significant regenerative capacity, which is impaired with muscular dystrophy and aging. Muscle function and repair requires the involvement of several cellular compartments and molecular interactions. With disease cellular responses are influenced by the alteration of signaling pathways that are involved in the normal process of muscle regeneration. Disruptions in regenerative signaling coincide with the activation of pathways responsible for tissue pathology. Therefore, the cellular and molecular axis of muscle regeneration follows a strict program that when interrupted by disease, cannot sustain repair and results in muscle degeneration.

The cellular compartments of the skeletal muscle respond as a collective to repair damage. Each cellular population is influenced by distinct pathways and cellular interactions. In the absence of disease, the process of regeneration is mediated by satellite cells, endothelial cells

and collagen producing cells to respond to injury and regenerate muscle fibers, vessels, and reconstitute damaged connective tissue respectively. With disease, signaling pathways that influence cellular responses to injury are altered. As described in this dissertation, we discovered Sphingosine-1-Phosphate (S1P) and Platelet Derived Growth Factor Receptor-α (PDGFRα) are two signaling pathways with opposing effects in muscular dystrophy. With muscular dystrophy, the accumulation of fibrosis perturbs the regenerative response. Therefore, we hypothesis that alterations in the muscle's repair processes contribute to pathogenesis; pro-regenerative pathways (such as S1P) diminish as pro-fibrotic pathways (such as PDGFRα) remain active. Understanding the cellular crosstalk and both processes of degeneration and regeneration are crucial for the development of therapies that can reduce muscle pathology and promote repair. Herein, we explore the axis of molecular signaling and cellular responses that influence muscle regeneration during injury and wasting. Such a holistic approach is necessary for continuing our advance in treating muscle wasting diseases. Our main findings support our hypothesis that regeneration and degeneration are intimately linked. Two cell populations affected by muscular dystrophy (endothelial cells and satellite cells) are diverse resident cells involved in S1P signaling of the muscle. In contrast, collagen producing cells are activated by PDGFRα to promote fibrosis and perturb regeneration. In summary, our findings, support the development of combinatory therapies that target specific pathways, such as S1P and PDGFRα, to promote regenerative signaling while negating the effects of degenerative signaling on muscle repair.

Despite the potential of such cellular and molecular strategies, significant barriers exit in the culture and politics of science that I will discuss in the closing commentary. Here I will describe the current scientific crisis, which in my own opinion extends not only from a decline in funding, but abuse and misuse of resources has rampant for years. In addition the structure of

scientific training and funding has compounded this crisis, as more PhD's continue to be trained despite the recognizable and ongoing decline in scientific employment. Therefore, in the past two decades, the field of biological science has adapted a policy analogous to our government's stance on global warming; ignore the immanent catastrophe. This will not come in the form of rising oceans or temperatures, but stagnation of discoveries and treatment for diseases. This calamity can be averted if we, as a community, divert from politics and personal gain, but instead focus our efforts on conducting meaningful science with the public's best interests in mind.

Dedication

To the families and the patients who are afflicted by Duchenne muscular dystrophy, from their courage and strength I draw humility and inspiration.

Acknowledgments

I would like to acknowledge the funding agencies that have contributed to this work over the years; the Jain Foundation, the American Heart Association, the Muscular Dystrophy Association**,** UW Provost Bridge, the UW Nathan Shock Center of Excellence in the Basic Biology of Aging Genetic Approaches to Aging Training grant T32 AG000057, and the Pancretan Association of America Venizelion Scholarship.

I am also grateful to my committee members: Drs. Hannele Ruohola-Baker, Matt Kaeberlein, Bill Mahoney, and Zipora Yablonka-Reuveni.

I am grateful to my advisor Dr. Morayma Reyes, whose guidance and encouragement made this research possible.

The research outlined herein could not have proceeded without my co-authors and colleagues; whom I have had the privilege to work with.

Finally, I thank my family, friends and spouse for enduring the personal expense of my absence during all the late nights and weekends I sacrificed for this work.

Table of Contents

Introduction

Muscle Wasting and Disease

Skeletal and cardiac muscle are unique organs that sustain mechanical force for movement and the circulation. In Duchene muscular dystrophy (DMD), the absence of the dystrophin protein results in muscle wasting that leads to morbidity and heart failure (1, 2). Although great strides have been made in understanding the etiology and pathology of this disease, the molecular and cellular interactions that promote pathogenesis require further examination (3). Non-diseased skeletal muscles have a tremendous capacity for repair, yet this response is impaired with muscular dystrophy due to unknown mechanisms (4-6). The depletion and impairment of skeletal muscle stem cells (satellite cells) is a result of ongoing muscle damage and repair (7, 8). However, environmental factors, such as the accumulation of connective tissue and oxidative stress, influence satellite cell self-renewal and activation capacity (9, 10). Interestingly, satellite cells are also depleted and impaired with age-associated muscle wasting, commonly referred to as sarcopenia (11, 12). Although the etiology of sarcopenia is unknown, whereas DMD is a congenital disease, both share pathological characteristics such as fibrosis, loss of fast-twitch muscles, functional (strength) decline, and decrease in capillaries (13-18). In addition, in aged hearts the decline in dystrophin expression is associated with reduced cardiac function (19). Therefore, muscle wasting due to aging or dystrophy may follow common cellular and molecular mechanisms.

Despite similarities in pathology, DMD leads to mortality typically within 30 years of age (20). In contrast, sarcopenia is classified as a geriatric syndrome, without a known etiology, and

has only been associated with mortality (21, 22). A consequence of the anomalous etiology of sarcopenia is that appropriate animal models for studying the process of age-related muscle wasting are arguably ill-developed (23, 24). For DMD, a multitude of animal models exist that continue to shed insight on the process of muscle wasting that results from muscular dystrophy (25, 26). To date, the most utilized and characterized model of DMD is the mdx mouse (25). First developed in 1984, the mdx mouse which recapitulated much of the DMD pathogenesis, particularly in the diaphragm muscle (27-30). The availability of models is a reflection of the funding prospects and social advocacy towards DMD vs. sarcopenia. As a result, the research described herein this dissertation is focused on DMD and not sarcopenia, despite the aforementioned pathological similarities that warrant further investigation.

Cell Populations of the Skeletal Muscle

The functional unit of skeletal muscle responsible for force generation is the myofiber (31). For support, muscle contains various cellular populations that function to supply blood (endothelial cells and pericytes), produce connective tissue (collagen producing cells), and regenerate damaged myofibers (satellite cells) (32-35). Muscle function is unsustainable without vascular cells, collagen producing cells, and regenerative cells. Therefore, to gain insight on the process of muscle wasting, we sought to understand the role and response of these populations during homeostasis, injury and disease. Traditionally, such characterization has been carried out via immunohistochemical methods and cell culture of heterogeneous muscle cell preparations (4, 5, 36). Although, such studies have yielded much needed insight, the analysis has occurred at the macroscopic level; as such, methods often lack the sensitivity to distinguish specific cellular compartments or molecular interactions between different cell populations. For example, in

Figure 1A, immunostaining for blood vessels (with BS1 (37)) and collagen type I highlight the muscles architecture, but this analysis cannot distinguish which cells are transcribing collagen. In contrast, expression of cell-specific reporters can identify cellular populations based on their molecular profiles. Examples of selective reporters that highlight skeletal muscle populations (Figure 1B) include the expression of CD31-lacZ by endothelial cells (38), MLC3-nlacZ by myonuclei (39), Myf5-nlacZ by satellite cells, RGS5-nlacZ but mural cells (40), and PDGFRα-nGFP by perivascular cells (41) (Figure 1B).

Often, co-localization with specific protein targets in vivo has been deemed sufficient for classifying or identifying cellular populations. This practice has specifically been used for

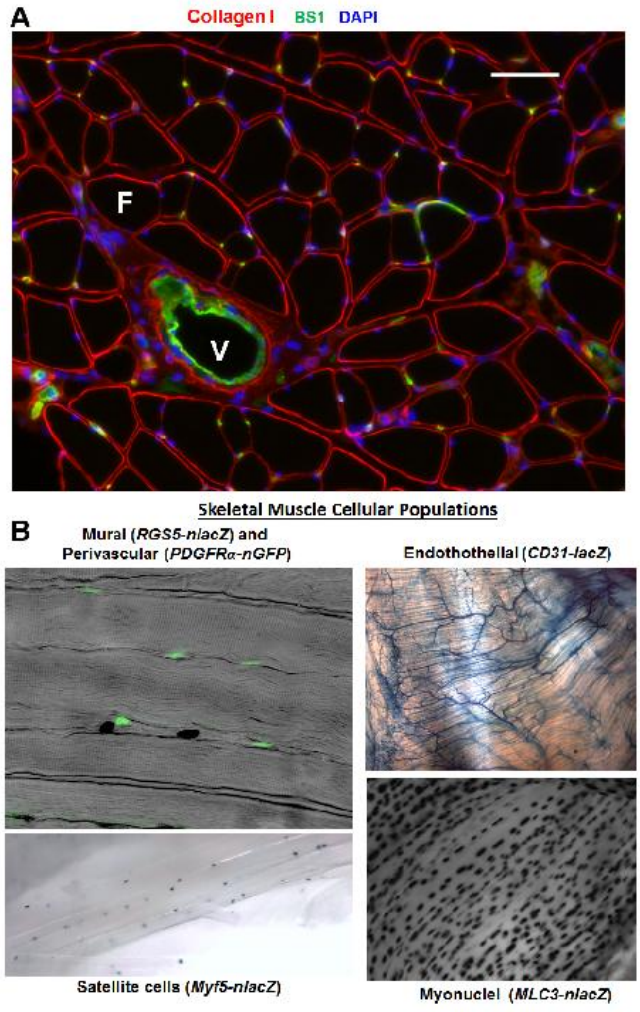

Figure 1. A. Immunofluorescence staining for type 1 collagen and BS1 (a marker of vessels) in muscle highlights skeletal muscle architecture. Myofibers (F) and green labeled capillaries and larger vessels (V) are the main components of skeletal muscle. Cross-sections were derived from a 3 month old C57BL/6, Tibialis Anterior (TA) muscle. Scale bar = 50μM. **B.** Cellular population of the skeletal muscle can be identified by their molecular signature using transgenic reporters in the mouse model. Top right: vascular endothelial cells are highlighted by CD31-lacZ. Bottom right: the nuclei of muscle fibers express MLC3-nlacZ . Bottom left: Satellite cell nuclei can be visualized by their expression of Myf5-nlacZ. Top left: supportive vascular cells such as mural and perivascular are labeled by RGS5-nlacZ and PDGFRα-GFP respectively. Photos are from whole mount of muscles stained with X-gal, which depicted as either black or blue.

identify collagen producing cells (e.g., fibroblasts) of the skeletal muscle (42, 43) . However, it is inherently biased to identify cells that produce and secret extracellular matrix proteins by co-localization alone. This paradigm has been no more apparent in the field of vascular biology exemplified by the identification of endothelial precursor cells (EPCs).

Rationale for Molecular Profiling

Bone marrow-derived peripheral blood EPCs are capable of giving rise to endothelial cells, as first reported in 1997 (44, 45). EPCs are primarily isolated from peripheral blood using markers CD34, AC133, or VEGFR2; markers that have also been utilized for isolating hematopoietic stem cells which can differentiate into vascular cells (46, 47). Therefore, the developmental origin and postnatal distinction between EPCs and hematopoietic stem cells is ambiguous (48, 49). In spite of such indifference, EPCs have been reported to integrate into the vasculature of various tissues and malignancies (44, 50). Such studies, utilized single markers, Tie2 or CD31, to evaluate contribution of putative EPCs to the vascular endothelium. However, these markers are also expressed by resident endothelial cells and inflammatory cells of hematopoietic origin (44) (51-55) .Therefore, without specific markers, EPCs are not distinguishable from other cellular components of the vasculature.

More recently, studies utilizing multiple markers to distinguish cells of hematopoietic origin have revealed that EPCs represent monocytes that can co-locate with the vasculature but do not actually integrate into the endothelium (55-58). Therefore, we have taken advantage of murine transgenic technology in combination with FACS- characterization and transcriptional profiling to identify specific cellular populations based on their molecular signature (59-61). We have characterized the role of various muscle populations via transgenic reporters (Figure1B),

fluorescent activated cells sorting (FACS), and transcriptional profiling. With this multifaceted approach, we explored the molecular mechanisms by which cell populations interact during homeostasis and disease. To date, the effects of disease and aging on individual populations and the consequences of cellular impairment are not fully understood. Therefore, utilizing the aforementioned transgenic models we took a systemic approach to define each population individually in order to understand their contributions to disease and aging. This holistic view has allowed us to identify specific signaling pathways that are altered with muscle wasting and present viable therapeutic targets for translational medicine.

Satellite Cell Potential and CD34

This dissertation begins with the investigation of the molecular hierarchy of satellite cells, based on their expression of the stem cell-associated marker CD34 (62) (Chapter 1). Although, satellite cells are unipotent stem cells, their heterogeneity and states of potential remain to be fully characterized (63). In contrast, the molecular hierarchy for hematopoetic stem cells has been defined for over 20 years (64). Analogous to hematopoietic stem cells, the majority of satellite cells express CD34 (65). Despite gaps in our understanding the role of CD34, this antigen has been pivotal for isolating hematopoietic stem cells for bone marrow transplantation (66-68). Therefore, we reasoned that CD34 may be ideal for isolating skeletal muscle satellite cells with similar clinical potential. However, more recent studies have suggested that the most primitive hematopeitic stem cells lack CD34 expression (67, 69, 70). Indeed, single $CD34^-$ hematopoietic stem cells have been reported to reconstitute the bone marrow stem cell niche and give rise to $CD34^+$ progeny (69, 70). Similarly, single satellite cells transplanted into irradiated muscle can also reconstitute the muscle niche following injury (71).

However, the potential of single satellite cells to reconstitute this population has only been evaluated with $CD34^+$ satellite cells. In addition, the potential of single $CD34^+$ satellite cells to restore the population within muscle occurs with extremely poor efficiency in comparison to hematopoetic stem cells. Specifically, only 4% of single satellite cells transplanted were reported to engraft and reconstitute the muscle niche, while single hematopoetic cell engraftment/reconstitution in the bone marrow niche is >28% (71-73). The low engraftment efficiency of satellite cells suggests that a minority of $CD34^+$ satellite cells holds significant self-renewal potency and perhaps, as with hematopoietic stem cells, the $CD34^-$ compartment holds greater potential for engraftment and self-renewal. Therefore, we explored the possibility that similar to bone marrow stem cells, the minority of $CD34^-$ satellite cells may represent the most primitive members of this population, with the greatest clinical potential.

CD34 is a cell surface glycoprotein, originally thought to be important for cell adhesion (66, 74, 75). To date, several roles for CD34 have been proposed, including cell adhesion, migration, and signaling (76). Yet, the exact purpose of CD34 remains elusive, and despite defects in hematopoiesis and regeneration, CD34 null mice are viable with no obvious phenotypes (66, 77, 78). In addition to being associated with stem cell populations, CD34 is expressed by many cells types, including vascular endothelial cells and mesenchymal cells of the skeletal muscle (34, 53, 79). Therefore, CD34 alone cannot distinguish satellite cell populations, unless in combination with markers to exclude other populations (80). More importantly, although CD34 is expressed and used to isolate stem cell populations, the expression of CD34 by committed cell populations suggests it is not a marker of stem cell plasticity. Stem cells within a given compartment may express CD34 with greater maturation along a given differentiation program (67). Therefore, we utilized a combination of markers to isolate and analyze muscle

satellite cells, with a goal of understanding their position along the myogenic program based upon the expression CD34 (Chapter1).

Regeneration of Muscle Endothelial cells

Vascular endothelial cells are an essential compartment for proper muscle function and comprise a significant proportion of the mononuclear cells in the skeletal muscle, as highlighted by Sca1-GFP expression in blood vessels (Figure2A) (81). Our own study, utilizing mononuclear muscle preps, demonstrates the proportion of endothelial cells (CD31+, Sca1+, CD45- cells) relative to other cell populations is >50% in young muscles and near 30% in aged muscles (59). A decline in endothelial cells is also observed in dystrophic muscles (Figure 2B) (18). Endothelial cell number reduction and dysfunction occur with aging and disease due to unknown mechanisms and are linked to muscle function impairment (18, 82). Interestingly, satellite cells are often in close proximity to, and in part regulated by, endothelial cells (83, 84). Since satellite and endothelial cell interactions are crucial for proper muscle repair, defining postnatal angiogenesis is essential for understanding the process of skeletal muscle regeneration. However, the response and origin of muscle endothelial cells following injury remained unresolved. The aforementioned EPCs have been reported to contribute to the endothelium following injury and in cancer (44, 45). Yet endogenous muscle endothelial cells hold angiogenic potential and can engraft into transplanted muscles (59). Therefore, we sought to investigate the mechanisms of endothelial renewal and contribution from external sources, specifically the bone marrow (Chapter 2).

During development, hemangioblasts located in the blood islands give rise to vascular endothelial cells and bone marrow hematopoietic cells (52, 85-87). Although the common

developmental origin of hematopoietic cells and endothelial cells is well established, the presence of precursors that give rise to both populations in adult tissue remains controversial (88-90). As aforementioned, the identification of EPCs presented a candidate for a putative adult "hemangioblast" (44). Yet it cannot be ignored that endothelial cells have the capacity to replicate in response to injury and disease (91-93). It is possible that the postnatal vascular endothelium can be reconstituted within a damaged tissue by a combination of bone marrow-derived precursors and endogenous endothelial cell division. Contribution by bone marrow-derived cells to the damaged vascular endothelium may represent a recapitulation of developmental programs that are reactivated in response to injury or disease (ref?). Therefore, we examined whether endothelial cell regeneration in the skeletal muscle is a mutually exclusive

Figure 2. A. A cross-section from a Tibialis Anterior muscle from a wt:Sca1-GFP mouse highlights the abundance of endothelial cells by their expression of GFP. Laminin staining highlights the muscle architecture and abundance of GFP^+ capillaries relative to myofibers. Scale bar = 50µM. **B.** Quantitative analysis of capillaries from cross-sections of 2 month old (2MO) mdx4cv vs. wt C57BL/6 quadriceps (n=3 per group), indicated a decline in endothelial cells in dystrophic muslces. * denotes P<0.05 by student's t-test.

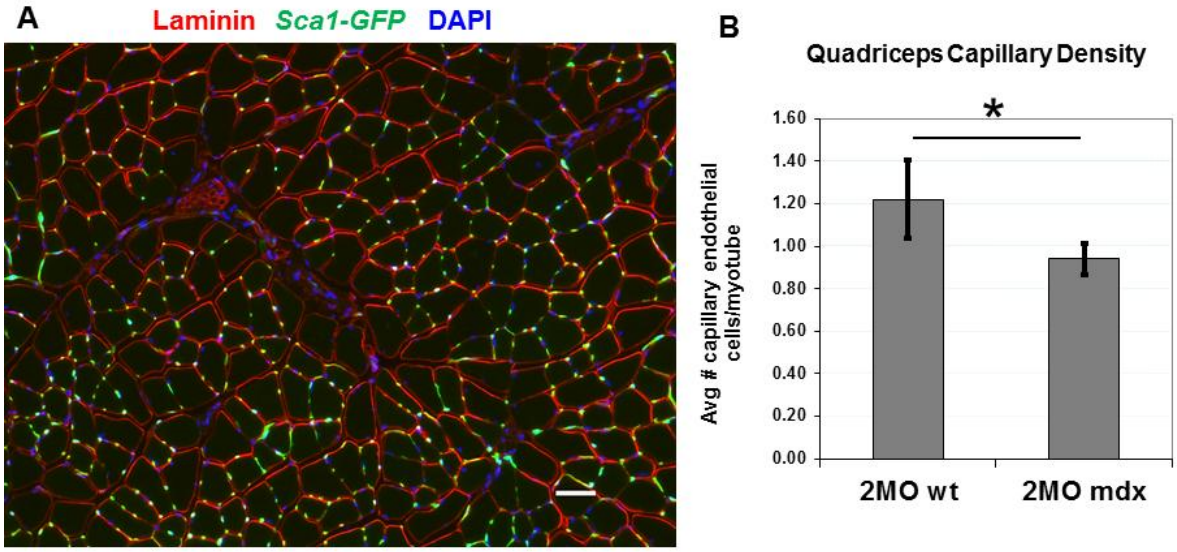

process mediated by endogenous endothelial cells or in part influenced by hematopoietic cells.

Sphingosine-1-Phospate and Muscle Regeneration

Sphingosine-1-Phosphate (S1P) is a bioactive lipid implicated in several cellular processes and tissue homeostasis (94, 95). S1P is synthesized intracellularly via the phosphorylation of sphingosine by one of two kinases (aka SPHK 1 and 2), then released to the extracellular space or stored internally (96, 97). In turn, S1P can be converted back to sphingosine via the action of two phosphatases (SGPP1 and SGPP2) or permanently degraded by the S1P lyase (96, 97). Within the last two decades, our knowledge of S1P signaling has expanded from mediation via extracellular receptors to intracellular, as a second messenger or a direct inhibitor of histone deacetylases (97-101). S1P receptors were originally identified in endothelial cells and correspondingly named Endothelial Differentiation Gene (EDG) receptors (102). To date, five such G protein-coupled receptors (GPCRs), each capable of binding S1P, have been described to mediate signaling that influences a wide variety of processes, from cell death to division (94). Since S1P receptor signaling has expanded beyond endothelial biology, these GPCRs are less commonly referred to as EDG receptors and instead now as S1PR1-5 (103). Although the biology of S1P signaling is in its infancy, S1P has been shown to be essential for immunity, angiogenesis, vascular maintenance and tumor formation (95, 104-106). However, little is known of the role S1P signaling plays in the development and homeostasis of the skeletal muscle.

S1P is important for satellite cell division and postnatal muscle regeneration (107, 108). Yet the extent and necessity for S1P signaling in satellite cells and muscle regeneration requires further investigation, particularly since SPHK1 and 2 and S1PR and 3 null mice are viable and

show no overt muscle phenotypes (104, 109-111). Of the five S1P receptors, S1PR1-3 are expressed in skeletal muscle and S1PR1 and S1PR3 are the most abundant (107). S1PR1 null mice are embryonic lethal, although this is due to impaired maturation of the vasculature (105). In contrast, S1P lyase-null mice develop to term but die within 4 months of age due an absence of lymphocytes (112). Nonetheless, alterations in S1P signaling affect muscle regeneration and therefore we sought to examine the involvement of this novel signaling phosphor-lipid, in the context of muscle wasting (107, 108, 111).

The capacity for regeneration declines with muscular dystrophy, yet little is known about the molecular mechanisms that influence satellite cell potential in dystrophic muscles. Utilizing an unbiased screen in Drosophila, genetic elevation in S1P improved the phenotype of dystrophic flies (113). In addition, S1P can influence satellite cell renewal and regeneration of acutely injured, non-diseased muscles (107, 108, 114). Endothelial cells that are closely associated with satellite cells have been reported to be the source of exogenous S1P (83, 115). Gene expression analysis indicated that the skeletal muscles vasculature is a source of S1P, as the transcripts for SPHK1 and 2 are enriched in FACS-sorted endothelial cells in comparison to whole muscle (Figure 3). Coincidently, S1P content and the expression of S1P receptors is reduced with muscular dystrophy, coordinately with a decrease in endothelial cell abundance (116) (Figure 2B) (Chapter3). Such alterations, may contribute to the depletion and impairment of myogenic cells that is observed in dystrophic muscle, as elevations in S1P promoted regeneration. Therefore, S1P alterations may directly influence the phenotype of muscle disease and can be targeted pharmacologically with S1P elevating drugs such as THI, to promote regeneration. Therefore, we extended the studies from Drosophila to the mdx mouse model for DMD to gain

insight on the potential of S1P signaling to influence muscle regeneration in mammalian dystrophic muscles (Chapter 3).

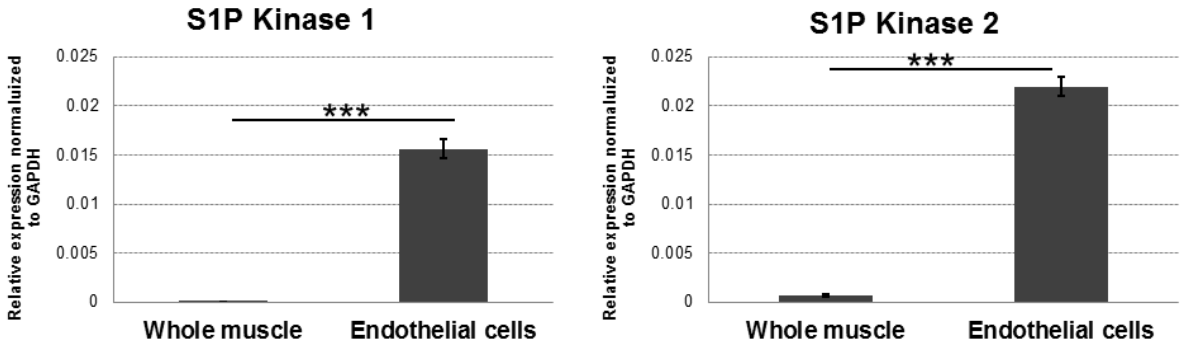

Figure 3. Quantitative-reverse PCR analysis of whole TA muscles vs. endothelial cells FACS-sorted from limb muscles (n=3 per group), indicates that S1P kinase 1 and 2 mRNA is enriched in endothelial cells. Both whole muscle and sorted cells were derived from C57BL/6 wt mice. *** indicated P<0.0005 by student's *t*-test.

PDGFRα Signaling and Muscle Fibrosis

Platelet Derived Growth Factors (PDGF) were first discovered in 1974 as a mitogen for cultured fibroblasts and smooth muscle cells (117, 118). Since this discovery, the mechanisms of PDGF signaling have been linked to two tyrosine kinase receptors that form homo- and heterodimers: PDGFRα and PDGFRβ (119). These receptors signal following the binding of dimeric ligands, consisting of either PDGF-AA, AB, BB, CC, or DD proteins (Figure 4) (120). This signaling pathway is essential for many biological processes, including cancer and embryonic development (120). The importance of PDGF signaling has been extensively studied for the development of vascular smooth muscle, and to some extent the formation of skeletal muscle (121-124). Although PDGF signaling is essential for proper muscle development, the role of this pathway in adult homeostasis and muscle diseases remains to be elucidated. Our findings indicate that PDGFRα signaling is elevated with muscular dystrophy in response to muscle fiber production of the PDGF-AA ligand (Chapter 4). During development, PDGF-AA ligand is also

produced by embryonic myogenic cells (124, 125). Therefore, PDGF signaling that occurs with muscular dystrophy may represent a recapitulation of the muscle's developmental program that is reactivated in response to degeneration and regeneration. However, as the muscles capacity to repair diminishes,, chronic activation of PDGF-mediated signaling results in disease pathology.

With muscular dystrophy, the progression of muscle wasting results in the replacement of force producing tissue with inert connective tissue. This is due to the accumulation of type I and III collagens in the muscle (126, 127). This process, fibrosis, is recognized as a barrier to the regeneration of dystrophic muscles (128). In spite of the need for anti-fibrotic intervention, the cellular interactions that dictate fibrosis in DMD are poorly understood. In comparison, cardiac fibrosis, which is also characterized by the loss of myocytes and accumulation of collagens I and III, has been extensively studied and targeted for therapeutic intervention (129, 130) (131). The lack of knowledge is evident, as skeletal muscle mesenchymal progenitors capable of giving rise to pro-collagen expressing cells have been identified only within the last 4 years (79, 132). These mesenchymal progenitors are reported to express PDGFRα, a known inducer of fibrosis, and express pro-collagens in response to stimulation with the PDGF-AA ligand in vitro (34, 133, 134). More recently, PDGFRα expressing cells have been implicated in the development of

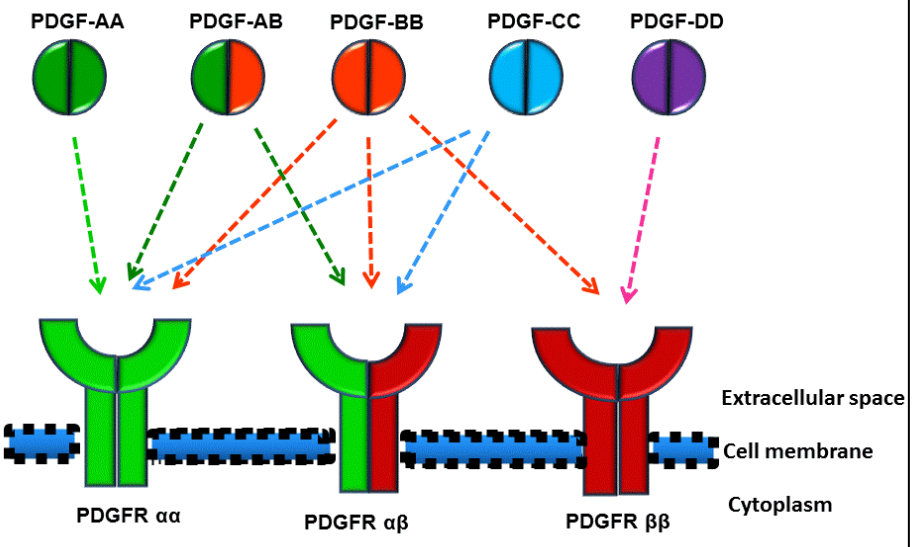

Figure 4. Overview of dimeric PDGF receptor and ligand combinations and their binding specificities. Of note, only PDGF-AA, AB and CC ligands can bind and signal through homodimer variant of the PDGFRα receptor. In contrast, the PDGF-DD ligand can only signal through the homodimer variant of the PDGFRβ receptor.

fibrosis of mdx and DMD skeletal muscle (34, 133). However, whether PDGFRα signaling potentiates fibrosis in muscular dystrophy and if mesenchymal progenitors actually produce components of fibrosis (mainly collagens) in vivo remains unknown. Therefore, to gain insight on the process of fibrosis, we examined mdx mice expressing the Collagen1α1-GFP reporter of collagen producing cells. In combination, we compared PDGFRα-nGFP and Cre alleles in mdx muscles to identify the role of this signaling pathway in the accumulation of connective tissue that occurs with muscle wasting (Chapter 4).

Hypothesis

The cellular compartments of skeletal muscle are illustrated in Figure 5 as a collective of cells supporting the muscle fibers. In the context of muscle regeneration, these populations will be systematically discussed in each respective chapter. We hypothesize that muscle regeneration and degeneration are intimately linked processes dictated by specific molecular pathways that when perturbed, contribute to muscle wasting. In contrast, our null hypothesis states that damage and repair are independent processes and consequences of muscle wasting. To test our hypothesis, we will explore how cellular responses are influenced by alterations in molecular pathways that occur with muscle wasting, specifically with S1P and PDGFRα. Our results indicate that the process of muscle regeneration is not stochastic. The extent of muscle regeneration is determined by an axis of cellular and molecular interactions that follow a defined program. This program includes the S1P (pro-regenerative) and PDGFRα (prog-fibrotic_ signaling pathways, that are both active during process of muscle repair. However, with muscular dystrophy this program falters, as pro-regenerative pathways are down-regulated and pro-pathogenic pathways remain active.

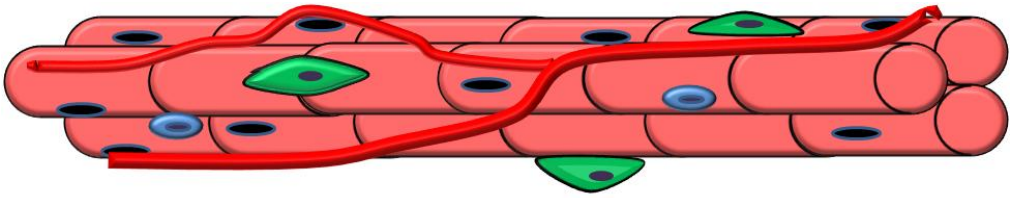

satellite cells , endothelial cells, collagen producing cells

.

Figure 5. Diagram of the cellular compartment described in this report; satellite cells, vascular endothelial cells, and collagen producing cells. Point out the muscle fibers, nuclei, satellite cells, etc.

References

1. Sultan A, Fayaz M. Prevalence of cardiomyopathy in Duchenne and Becker's muscular dystrophy. J Ayub Med Coll Abbottabad. 2008;20(2):7-13. PubMed PMID: 19385447.
2. Passamano L, Taglia A, Palladino A, Viggiano E, D'Ambrosio P, Scutifero M, et al. Improvement of survival in Duchenne Muscular Dystrophy: retrospective analysis of 835 patients. Acta myologica : myopathies and cardiomyopathies : official journal of the Mediterranean Society of Myology / edited by the Gaetano Conte Academy for the study of striated muscle diseases. 2012;31(2):121-5. PubMed PMID: 23097603; PubMed Central PMCID: PMC3476854.
3. Deconinck N, Dan B. Pathophysiology of duchenne muscular dystrophy: current hypotheses. Pediatric neurology. 2007;36(1):1-7. doi: 10.1016/j.pediatrneurol.2006.09.016. PubMed PMID: 17162189.
4. Blau HM, Webster C, Pavlath GK. Defective myoblasts identified in Duchenne muscular dystrophy. Proceedings of the National Academy of Sciences of the United States of America. 1983;80(15):4856-60. PubMed PMID: 6576361; PubMed Central PMCID: PMC384144.
5. Jasmin G, Tautu C, Vanasse M, Brochu P, Simoneau R. Impaired muscle differentiation in explant cultures of Duchenne muscular dystrophy. Laboratory investigation; a journal of technical methods and pathology. 1984;50(2):197-207. PubMed PMID: 6694359.
6. Schuierer MM, Mann CJ, Bildsoe H, Huxley C, Hughes SM. Analyses of the differentiation potential of satellite cells from myoD-/-, mdx, and PMP22 C22 mice. BMC musculoskeletal disorders. 2005;6:15. doi: 10.1186/1471-2474-6-15. PubMed PMID: 15762989; PubMed Central PMCID: PMC1079863.
7. Oexle K, Kohlschutter A. Cause of progression in Duchenne muscular dystrophy: impaired differentiation more probable than replicative aging. Neuropediatrics. 2001;32(3):123-9. doi: 10.1055/s-2001-16613. PubMed PMID: 11521207.
8. Luz MA, Marques MJ, Santo Neto H. Impaired regeneration of dystrophin-deficient muscle fibers is caused by exhaustion of myogenic cells. Brazilian journal of medical and biological research = Revista brasileira de pesquisas medicas e biologicas / Sociedade Brasileira de Biofisica [et al]. 2002;35(6):691-5. PubMed PMID: 12045834.
9. Renault V, Thornell LE, Butler-Browne G, Mouly V. Human skeletal muscle satellite cells: aging, oxidative stress and the mitotic clock. Experimental gerontology. 2002;37(10-11):1229-36. PubMed PMID: 12470836.
10. Klingler W, Jurkat-Rott K, Lehmann-Horn F, Schleip R. The role of fibrosis in Duchenne muscular dystrophy. Acta myologica : myopathies and cardiomyopathies : official journal of the Mediterranean Society of Myology / edited by the Gaetano Conte Academy for the study of striated muscle diseases. 2012;31(3):184-95. PubMed PMID: 23620650; PubMed Central PMCID: PMC3631802.
11. Gibson MC, Schultz E. Age-related differences in absolute numbers of skeletal muscle satellite cells. Muscle & nerve. 1983;6(8):574-80. doi: 10.1002/mus.880060807. PubMed PMID: 6646160.
12. Day K, Shefer G, Shearer A, Yablonka-Reuveni Z. The depletion of skeletal muscle satellite cells with age is concomitant with reduced capacity of single progenitors to

produce reserve progeny. Developmental biology. 2010;340(2):330-43. doi: 10.1016/j.ydbio.2010.01.006. PubMed PMID: 20079729; PubMed Central PMCID: PMC2854302.
13. Mann CJ, Perdiguero E, Kharraz Y, Aguilar S, Pessina P, Serrano AL, et al. Aberrant repair and fibrosis development in skeletal muscle. Skeletal muscle. 2011;1(1):21. doi: 10.1186/2044-5040-1-21. PubMed PMID: 21798099; PubMed Central PMCID: PMC3156644.
14. Webster C, Silberstein L, Hays AP, Blau HM. Fast muscle fibers are preferentially affected in Duchenne muscular dystrophy. Cell. 1988;52(4):503-13. PubMed PMID: 3342447.
15. Larsson L, Sjodin B, Karlsson J. Histochemical and biochemical changes in human skeletal muscle with age in sedentary males, age 22--65 years. Acta physiologica Scandinavica. 1978;103(1):31-9. doi: 10.1111/j.1748-1716.1978.tb06187.x. PubMed PMID: 208350.
16. Williams GN, Higgins MJ, Lewek MD. Aging skeletal muscle: physiologic changes and the effects of training. Physical therapy. 2002;82(1):62-8. PubMed PMID: 11784279.
17. Wang H, Listrat A, Meunier B, Gueugneau M, Coudy-Gandilhon C, Combaret L, et al. Apoptosis in capillary endothelial cells in ageing skeletal muscle. Aging cell. 2014;13(2):254-62. doi: 10.1111/acel.12169. PubMed PMID: 24245531.
18. Palladino M, Gatto I, Neri V, Straino S, Smith RC, Silver M, et al. Angiogenic impairment of the vascular endothelium: a novel mechanism and potential therapeutic target in muscular dystrophy. Arteriosclerosis, thrombosis, and vascular biology. 2013;33(12):2867-76. doi: 10.1161/ATVBAHA.112.301172. PubMed PMID: 24072696.
19. Townsend D, Daly M, Chamberlain JS, Metzger JM. Age-dependent dystrophin loss and genetic reconstitution establish a molecular link between dystrophin and heart performance during aging. Molecular therapy : the journal of the American Society of Gene Therapy. 2011;19(10):1821-5. doi: 10.1038/mt.2011.120. PubMed PMID: 21730971; PubMed Central PMCID: PMC3188736.
20. Schram G, Fournier A, Leduc H, Dahdah N, Therien J, Vanasse M, et al. All-cause mortality and cardiovascular outcomes with prophylactic steroid therapy in Duchenne muscular dystrophy. Journal of the American College of Cardiology. 2013;61(9):948-54. doi: 10.1016/j.jacc.2012.12.008. PubMed PMID: 23352781.
21. Cruz-Jentoft AJ, Landi F, Topinkova E, Michel JP. Understanding sarcopenia as a geriatric syndrome. Current opinion in clinical nutrition and metabolic care. 2010;13(1):1-7. doi: 10.1097/MCO.0b013e328333c1c1. PubMed PMID: 19915458.
22. Kane RL, Shamliyan T, Talley K, Pacala J. The association between geriatric syndromes and survival. Journal of the American Geriatrics Society. 2012;60(5):896-904. doi: 10.1111/j.1532-5415.2012.03942.x. PubMed PMID: 22568483.
23. Romanick M, Thompson LV, Brown-Borg HM. Murine models of atrophy, cachexia, and sarcopenia in skeletal muscle. Biochimica et biophysica acta. 2013;1832(9):1410-20. doi: 10.1016/j.bbadis.2013.03.011. PubMed PMID: 23523469; PubMed Central PMCID: PMC3687011.
24. Augustin H, Partridge L. Invertebrate models of age-related muscle degeneration. Biochimica et biophysica acta. 2009;1790(10):1084-94. doi: 10.1016/j.bbagen.2009.06.011. PubMed PMID: 19563864.

25. Willmann R, Possekel S, Dubach-Powell J, Meier T, Ruegg MA. Mammalian animal models for Duchenne muscular dystrophy. Neuromuscul Disord. 2009;19(4):241-9. doi: 10.1016/j.nmd.2008.11.015. PubMed PMID: 19217290.
26. Partridge T. Animal models of muscular dystrophy--what can they teach us? Neuropathology and applied neurobiology. 1991;17(5):353-63. PubMed PMID: 1758568.
27. Bulfield G, Siller WG, Wight PA, Moore KJ. X chromosome-linked muscular dystrophy (mdx) in the mouse. Proceedings of the National Academy of Sciences of the United States of America. 1984;81(4):1189-92. PubMed PMID: 6583703; PubMed Central PMCID: PMC344791.
28. Tanabe Y, Esaki K, Nomura T. Skeletal muscle pathology in X chromosome-linked muscular dystrophy (mdx) mouse. Acta neuropathologica. 1986;69(1-2):91-5. PubMed PMID: 3962599.
29. Chapman VM, Miller DR, Armstrong D, Caskey CT. Recovery of induced mutations for X chromosome-linked muscular dystrophy in mice. Proceedings of the National Academy of Sciences of the United States of America. 1989;86(4):1292-6. PubMed PMID: 2919177.
30. Stedman HH, Sweeney HL, Shrager JB, Maguire HC, Panettieri RA, Petrof B, et al. The mdx mouse diaphragm reproduces the degenerative changes of Duchenne muscular dystrophy. Nature. 1991;352(6335):536-9. doi: 10.1038/352536a0. PubMed PMID: 1865908.
31. Huijing PA. Muscle as a collagen fiber reinforced composite: a review of force transmission in muscle and whole limb. Journal of biomechanics. 1999;32(4):329-45. PubMed PMID: 10213024.
32. Mauro A. Satellite cell of skeletal muscle fibers. The Journal of biophysical and biochemical cytology. 1961;9:493-5. PubMed PMID: 13768451; PubMed Central PMCID: PMC2225012.
33. Lepper C, Partridge TA, Fan CM. An absolute requirement for Pax7-positive satellite cells in acute injury-induced skeletal muscle regeneration. Development. 2011;138(17):3639-46. doi: 10.1242/dev.067595. PubMed PMID: 21828092; PubMed Central PMCID: PMC3152922.
34. Uezumi A, Ito T, Morikawa D, Shimizu N, Yoneda T, Segawa M, et al. Fibrosis and adipogenesis originate from a common mesenchymal progenitor in skeletal muscle. Journal of cell science. 2011;124(Pt 21):3654-64. PubMed PMID: 22045730.
35. Lee J, Schmid-Schonbein GW. Biomechanics of skeletal muscle capillaries: hemodynamic resistance, endothelial distensibility, and pseudopod formation. Annals of biomedical engineering. 1995;23(3):226-46. PubMed PMID: 7631979.
36. Tamaki T, Akatsuka A, Okada Y, Matsuzaki Y, Okano H, Kimura M. Growth and differentiation potential of main- and side-population cells derived from murine skeletal muscle. Experimental cell research. 2003;291(1):83-90. PubMed PMID: 14597410.
37. Kirchmair R, Gander R, Egger M, Hanley A, Silver M, Ritsch A, et al. The neuropeptide secretoneurin acts as a direct angiogenic cytokine in vitro and in vivo. Circulation. 2004;109(6):777-83. doi: 10.1161/01.CIR.0000112574.07422.C1. PubMed PMID: 14970115.
38. Zambrowicz BP, Friedrich GA, Buxton EC, Lilleberg SL, Person C, Sands AT. Disruption and sequence identification of 2,000 genes in mouse embryonic stem cells. Nature. 1998;392(6676):608-11. doi: 10.1038/33423. PubMed PMID: 9560157.

39. Kelly R, Alonso S, Tajbakhsh S, Cossu G, Buckingham M. Myosin light chain 3F regulatory sequences confer regionalized cardiac and skeletal muscle expression in transgenic mice. The Journal of cell biology. 1995;129(2):383-96. PubMed PMID: 7721942; PubMed Central PMCID: PMC2199907.
40. Nisancioglu MH, Mahoney WM, Jr., Kimmel DD, Schwartz SM, Betsholtz C, Genove G. Generation and characterization of rgs5 mutant mice. Molecular and cellular biology. 2008;28(7):2324-31. PubMed PMID: 18212066.
41. Hamilton TG, Klinghoffer RA, Corrin PD, Soriano P. Evolutionary divergence of platelet-derived growth factor alpha receptor signaling mechanisms. Molecular and cellular biology. 2003;23(11):4013-25. PubMed PMID: 12748302; PubMed Central PMCID: PMC155222.
42. Dulauroy S, Di Carlo SE, Langa F, Eberl G, Peduto L. Lineage tracing and genetic ablation of ADAM12(+) perivascular cells identify a major source of profibrotic cells during acute tissue injury. Nature medicine. 2012;18(8):1262-70. doi: 10.1038/nm.2848. PubMed PMID: 22842476.
43. Murphy MM, Lawson JA, Mathew SJ, Hutcheson DA, Kardon G. Satellite cells, connective tissue fibroblasts and their interactions are crucial for muscle regeneration. Development. 2011;138(17):3625-37. doi: 10.1242/dev.064162. PubMed PMID: 21828091; PubMed Central PMCID: PMC3152921.
44. Asahara T, Masuda H, Takahashi T, Kalka C, Pastore C, Silver M, et al. Bone marrow origin of endothelial progenitor cells responsible for postnatal vasculogenesis in physiological and pathological neovascularization. Circulation research. 1999;85(3):221-8. PubMed PMID: 10436164.
45. Asahara T, Murohara T, Sullivan A, Silver M, van der Zee R, Li T, et al. Isolation of putative progenitor endothelial cells for angiogenesis. Science. 1997;275(5302):964-7. PubMed PMID: 9020076.
46. Ribatti D. The discovery of endothelial progenitor cells. An historical review. Leukemia research. 2007;31(4):439-44. doi: 10.1016/j.leukres.2006.10.014. PubMed PMID: 17113640.
47. Sata M, Saiura A, Kunisato A, Tojo A, Okada S, Tokuhisa T, et al. Hematopoietic stem cells differentiate into vascular cells that participate in the pathogenesis of atherosclerosis. Nature medicine. 2002;8(4):403-9. doi: 10.1038/nm0402-403. PubMed PMID: 11927948.
48. Chao H, Hirschi KK. Hemato-vascular origins of endothelial progenitor cells? Microvascular research. 2010;79(3):169-73. doi: 10.1016/j.mvr.2010.02.003. PubMed PMID: 20149806; PubMed Central PMCID: PMC2857563.
49. Yoder MC. Endothelial progenitor cell: a blood cell by many other names may serve similar functions. Journal of molecular medicine. 2013;91(3):285-95. doi: 10.1007/s00109-013-1002-8. PubMed PMID: 23371317; PubMed Central PMCID: PMC3704045.
50. Nolan DJ, Ciarrocchi A, Mellick AS, Jaggi JS, Bambino K, Gupta S, et al. Bone marrow-derived endothelial progenitor cells are a major determinant of nascent tumor neovascularization. Genes & development. 2007;21(12):1546-58. doi: 10.1101/gad.436307. PubMed PMID: 17575055; PubMed Central PMCID: PMC1891431.

51. Venneri MA, De Palma M, Ponzoni M, Pucci F, Scielzo C, Zonari E, et al. Identification of proangiogenic TIE2-expressing monocytes (TEMs) in human peripheral blood and cancer. Blood. 2007;109(12):5276-85. doi: 10.1182/blood-2006-10-053504. PubMed PMID: 17327411.
52. Motoike T, Loughna S, Perens E, Roman BL, Liao W, Chau TC, et al. Universal GFP reporter for the study of vascular development. Genesis. 2000;28(2):75-81. PubMed PMID: 11064424.
53. Pusztaszeri MP, Seelentag W, Bosman FT. Immunohistochemical expression of endothelial markers CD31, CD34, von Willebrand factor, and Fli-1 in normal human tissues. J Histochem Cytochem. 2006;54(4):385-95. doi: 10.1369/jhc.4A6514.2005. PubMed PMID: 16234507.
54. Kim SJ, Kim JS, Papadopoulos J, Wook Kim S, Maya M, Zhang F, et al. Circulating monocytes expressing CD31: implications for acute and chronic angiogenesis. The American journal of pathology. 2009;174(5):1972-80. doi: 10.2353/ajpath.2009.080819. PubMed PMID: 19349357; PubMed Central PMCID: PMC2671284.
55. Rehman J, Li J, Orschell CM, March KL. Peripheral blood "endothelial progenitor cells" are derived from monocyte/macrophages and secrete angiogenic growth factors. Circulation. 2003;107(8):1164-9. PubMed PMID: 12615796.
56. Rohde E, Malischnik C, Thaler D, Maierhofer T, Linkesch W, Lanzer G, et al. Blood monocytes mimic endothelial progenitor cells. Stem cells (Dayton, Ohio). 2006;24(2):357-67. doi: 10.1634/stemcells.2005-0072. PubMed PMID: 16141361.
57. Rohde E, Bartmann C, Schallmoser K, Reinisch A, Lanzer G, Linkesch W, et al. Immune cells mimic the morphology of endothelial progenitor colonies in vitro. Stem cells (Dayton, Ohio). 2007;25(7):1746-52. doi: 10.1634/stemcells.2006-0833. PubMed PMID: 17395771.
58. Purhonen S, Palm J, Rossi D, Kaskenpaa N, Rajantie I, Yla-Herttuala S, et al. Bone marrow-derived circulating endothelial precursors do not contribute to vascular endothelium and are not needed for tumor growth. Proceedings of the National Academy of Sciences of the United States of America. 2008;105(18):6620-5. doi: 10.1073/pnas.0710516105. PubMed PMID: 18443294; PubMed Central PMCID: PMC2365563.
59. Ieronimakis N, Balasundaram G, Reyes M. Direct isolation, culture and transplant of mouse skeletal muscle derived endothelial cells with angiogenic potential. PloS one. 2008;3(3):e0001753. PubMed PMID: 18335025.
60. Ieronimakis N, Balasundaram G, Rainey S, Srirangam K, Yablonka-Reuveni Z, Reyes M. Absence of CD34 on murine skeletal muscle satellite cells marks a reversible state of activation during acute injury. PloS one. 2010;5(6):e10920. doi: 10.1371/journal.pone.0010920. PubMed PMID: 20532193; PubMed Central PMCID: PMC2880004.
61. Ieronimakis N, Hays AL, Janebodin K, Mahoney WM, Jr., Duffield JS, Majesky MW, et al. Coronary adventitial cells are linked to perivascular cardiac fibrosis via TGFbeta1 signaling in the mdx mouse model of Duchenne muscular dystrophy. Journal of molecular and cellular cardiology. 2013;63:122-34. doi: 10.1016/j.yjmcc.2013.07.014. PubMed PMID: 23911435; PubMed Central PMCID: PMC3834000.

62. Stella CC, Cazzola M, De Fabritiis P, De Vincentiis A, Gianni AM, Lanza F, et al. CD34-positive cells: biology and clinical relevance. Haematologica. 1995;80(4):367-87. PubMed PMID: 7590508.
63. Biressi S, Rando TA. Heterogeneity in the muscle satellite cell population. Seminars in cell & developmental biology. 2010;21(8):845-54. doi: 10.1016/j.semcdb.2010.09.003. PubMed PMID: 20849971; PubMed Central PMCID: PMC2967620.
64. Bryder D, Rossi DJ, Weissman IL. Hematopoietic stem cells: the paradigmatic tissue-specific stem cell. The American journal of pathology. 2006;169(2):338-46. doi: 10.2353/ajpath.2006.060312. PubMed PMID: 16877336; PubMed Central PMCID: PMC1698791.
65. Beauchamp JR, Heslop L, Yu DS, Tajbakhsh S, Kelly RG, Wernig A, et al. Expression of CD34 and Myf5 defines the majority of quiescent adult skeletal muscle satellite cells. The Journal of cell biology. 2000;151(6):1221-34. PubMed PMID: 11121437; PubMed Central PMCID: PMC2190588.
66. Gangenahalli GU, Singh VK, Verma YK, Gupta P, Sharma RK, Chandra R, et al. Hematopoietic stem cell antigen CD34: role in adhesion or homing. Stem cells and development. 2006;15(3):305-13. doi: 10.1089/scd.2006.15.305. PubMed PMID: 16846369.
67. Goodell MA, Rosenzweig M, Kim H, Marks DF, DeMaria M, Paradis G, et al. Dye efflux studies suggest that hematopoietic stem cells expressing low or undetectable levels of CD34 antigen exist in multiple species. Nature medicine. 1997;3(12):1337-45. PubMed PMID: 9396603.
68. Silvestri F, Banavali S, Baccarani M, Preisler HD. The CD34 hemopoietic progenitor cell associated antigen: biology and clinical applications. Haematologica. 1992;77(3):265-73. PubMed PMID: 1385274.
69. Osawa M, Hanada K, Hamada H, Nakauchi H. Long-term lymphohematopoietic reconstitution by a single CD34-low/negative hematopoietic stem cell. Science. 1996;273(5272):242-5. PubMed PMID: 8662508.
70. Zanjani ED, Almeida-Porada G, Livingston AG, Flake AW, Ogawa M. Human bone marrow CD34- cells engraft in vivo and undergo multilineage expression that includes giving rise to CD34+ cells. Experimental hematology. 1998;26(4):353-60. PubMed PMID: 9546319.
71. Sacco A, Doyonnas R, Kraft P, Vitorovic S, Blau HM. Self-renewal and expansion of single transplanted muscle stem cells. Nature. 2008;456(7221):502-6. doi: 10.1038/nature07384. PubMed PMID: 18806774; PubMed Central PMCID: PMC2919355.
72. Notta F, Doulatov S, Laurenti E, Poeppl A, Jurisica I, Dick JE. Isolation of single human hematopoietic stem cells capable of long-term multilineage engraftment. Science. 2011;333(6039):218-21. doi: 10.1126/science.1201219. PubMed PMID: 21737740.
73. Camargo FD, Chambers SM, Drew E, McNagny KM, Goodell MA. Hematopoietic stem cells do not engraft with absolute efficiencies. Blood. 2006;107(2):501-7. doi: 10.1182/blood-2005-02-0655. PubMed PMID: 16204316; PubMed Central PMCID: PMC1895609.
74. Hu MC, Chien SL. The cytoplasmic domain of stem cell antigen CD34 is essential for cytoadhesion signaling but not sufficient for proliferation signaling. Blood. 1998;91(4):1152-62. PubMed PMID: 9454744.

75. Healy L, May G, Gale K, Grosveld F, Greaves M, Enver T. The stem cell antigen CD34 functions as a regulator of hemopoietic cell adhesion. Proceedings of the National Academy of Sciences of the United States of America. 1995;92(26):12240-4. PubMed PMID: 8618877; PubMed Central PMCID: PMC40332.
76. Nielsen JS, McNagny KM. Novel functions of the CD34 family. Journal of cell science. 2008;121(Pt 22):3683-92. doi: 10.1242/jcs.037507. PubMed PMID: 18987355.
77. Suzuki A, Andrew DP, Gonzalo JA, Fukumoto M, Spellberg J, Hashiyama M, et al. CD34-deficient mice have reduced eosinophil accumulation after allergen exposure and show a novel crossreactive 90-kD protein. Blood. 1996;87(9):3550-62. PubMed PMID: 8611677.
78. Alfaro LA, Dick SA, Siegel AL, Anonuevo AS, McNagny KM, Megeney LA, et al. CD34 promotes satellite cell motility and entry into proliferation to facilitate efficient skeletal muscle regeneration. Stem cells (Dayton, Ohio). 2011;29(12):2030-41. doi: 10.1002/stem.759. PubMed PMID: 21997891; PubMed Central PMCID: PMC3638793.
79. Joe AW, Yi L, Natarajan A, Le Grand F, So L, Wang J, et al. Muscle injury activates resident fibro/adipogenic progenitors that facilitate myogenesis. Nature cell biology. 2010;12(2):153-63. doi: 10.1038/ncb2015. PubMed PMID: 20081841.
80. Kuang S, Kuroda K, Le Grand F, Rudnicki MA. Asymmetric self-renewal and commitment of satellite stem cells in muscle. Cell. 2007;129(5):999-1010. PubMed PMID: 17540178.
81. Day K, Shefer G, Richardson JB, Enikolopov G, Yablonka-Reuveni Z. Nestin-GFP reporter expression defines the quiescent state of skeletal muscle satellite cells. Developmental biology. 2007;304(1):246-59. doi: 10.1016/j.ydbio.2006.12.026. PubMed PMID: 17239845; PubMed Central PMCID: PMC1888564.
82. Muller-Delp JM, Spier SA, Ramsey MW, Delp MD. Aging impairs endothelium-dependent vasodilation in rat skeletal muscle arterioles. American journal of physiology Heart and circulatory physiology. 2002;283(4):H1662-72. doi: 10.1152/ajpheart.00004.2002. PubMed PMID: 12234821.
83. Christov C, Chretien F, Abou-Khalil R, Bassez G, Vallet G, Authier FJ, et al. Muscle satellite cells and endothelial cells: close neighbors and privileged partners. Molecular biology of the cell. 2007;18(4):1397-409. doi: 10.1091/mbc.E06-08-0693. PubMed PMID: 17287398; PubMed Central PMCID: PMC1838982.
84. Abou-Khalil R, Le Grand F, Pallafacchina G, Valable S, Authier FJ, Rudnicki MA, et al. Autocrine and paracrine angiopoietin 1/Tie-2 signaling promotes muscle satellite cell self-renewal. Cell stem cell. 2009;5(3):298-309. doi: 10.1016/j.stem.2009.06.001. PubMed PMID: 19733541.
85. Kubo H, Alitalo K. The bloody fate of endothelial stem cells. Genes & development. 2003;17(3):322-9. doi: 10.1101/gad.1071203. PubMed PMID: 12569121.
86. Motoike T, Markham DW, Rossant J, Sato TN. Evidence for novel fate of Flk1+ progenitor: contribution to muscle lineage. Genesis. 2003;35(3):153-9. doi: 10.1002/gene.10175. PubMed PMID: 12640619.
87. Ema M, Takahashi S, Rossant J. Deletion of the selection cassette, but not cis-acting elements, in targeted Flk1-lacZ allele reveals Flk1 expression in multipotent mesodermal progenitors. Blood. 2006;107(1):111-7. doi: 10.1182/blood-2005-05-1970. PubMed PMID: 16166582.

88. Bailey AS, Fleming WH. Converging roads: evidence for an adult hemangioblast. Experimental hematology. 2003;31(11):987-93. PubMed PMID: 14585360.
89. Basile DP, Yoder MC. Circulating and tissue resident endothelial progenitor cells. Journal of cellular physiology. 2014;229(1):10-6. doi: 10.1002/jcp.24423. PubMed PMID: 23794280; PubMed Central PMCID: PMC3908443.
90. Yoder MC. Is endothelium the origin of endothelial progenitor cells? Arteriosclerosis, thrombosis, and vascular biology. 2010;30(6):1094-103. doi: 10.1161/ATVBAHA.109.191635. PubMed PMID: 20453169.
91. Schwartz SM, Benditt EP. Aortic endothelial cell replication. I. Effects of age and hypertension in the rat. Circulation research. 1977;41(2):248-55. PubMed PMID: 872300.
92. Hansson GK, Chao S, Schwartz SM, Reidy MA. Aortic endothelial cell death and replication in normal and lipopolysaccharide-treated rats. The American journal of pathology. 1985;121(1):123-7. PubMed PMID: 2996359; PubMed Central PMCID: PMC1888033.
93. Reidy MA, Schwartz SM. Endothelial injury and regeneration. IV. Endotoxin: a nondenuding injury to aortic endothelium. Laboratory investigation; a journal of technical methods and pathology. 1983;48(1):25-34. PubMed PMID: 6337296.
94. Rosen H, Gonzalez-Cabrera PJ, Sanna MG, Brown S. Sphingosine 1-phosphate receptor signaling. Annual review of biochemistry. 2009;78:743-68. doi: 10.1146/annurev.biochem.78.072407.103733. PubMed PMID: 19231986.
95. Maceyka M, Harikumar KB, Milstien S, Spiegel S. Sphingosine-1-phosphate signaling and its role in disease. Trends in cell biology. 2012;22(1):50-60. doi: 10.1016/j.tcb.2011.09.003. PubMed PMID: 22001186; PubMed Central PMCID: PMC3253987.
96. Yatomi Y, Ozaki Y, Ohmori T, Igarashi Y. Sphingosine 1-phosphate: synthesis and release. Prostaglandins & other lipid mediators. 2001;64(1-4):107-22. PubMed PMID: 11324700.
97. Kunkel GT, Maceyka M, Milstien S, Spiegel S. Targeting the sphingosine-1-phosphate axis in cancer, inflammation and beyond. Nature reviews Drug discovery. 2013;12(9):688-702. doi: 10.1038/nrd4099. PubMed PMID: 23954895; PubMed Central PMCID: PMC3908769.
98. Olivera A, Spiegel S. Sphingosine-1-phosphate as second messenger in cell proliferation induced by PDGF and FCS mitogens. Nature. 1993;365(6446):557-60. doi: 10.1038/365557a0. PubMed PMID: 8413613.
99. Spiegel S. Sphingosine 1-phosphate: a prototype of a new class of second messengers. Journal of leukocyte biology. 1999;65(3):341-4. PubMed PMID: 10080537.
100. Spiegel S, Milstien S. Sphingosine 1-phosphate, a key cell signaling molecule. The Journal of biological chemistry. 2002;277(29):25851-4. doi: 10.1074/jbc.R200007200. PubMed PMID: 12011102.
101. Hait NC, Allegood J, Maceyka M, Strub GM, Harikumar KB, Singh SK, et al. Regulation of histone acetylation in the nucleus by sphingosine-1-phosphate. Science. 2009;325(5945):1254-7. doi: 10.1126/science.1176709. PubMed PMID: 19729656; PubMed Central PMCID: PMC2850596.

102. Hla T, Maciag T. An abundant transcript induced in differentiating human endothelial cells encodes a polypeptide with structural similarities to G-protein-coupled receptors. The Journal of biological chemistry. 1990;265(16):9308-13. PubMed PMID: 2160972.
103. Strub GM, Maceyka M, Hait NC, Milstien S, Spiegel S. Extracellular and intracellular actions of sphingosine-1-phosphate. Advances in experimental medicine and biology. 2010;688:141-55. PubMed PMID: 20919652; PubMed Central PMCID: PMC2951632.
104. Mizugishi K, Yamashita T, Olivera A, Miller GF, Spiegel S, Proia RL. Essential role for sphingosine kinases in neural and vascular development. Molecular and cellular biology. 2005;25(24):11113-21. doi: 10.1128/MCB.25.24.11113-11121.2005. PubMed PMID: 16314531; PubMed Central PMCID: PMC1316977.
105. Liu Y, Wada R, Yamashita T, Mi Y, Deng CX, Hobson JP, et al. Edg-1, the G protein-coupled receptor for sphingosine-1-phosphate, is essential for vascular maturation. The Journal of clinical investigation. 2000;106(8):951-61. doi: 10.1172/JCI10905. PubMed PMID: 11032855; PubMed Central PMCID: PMC314347.
106. Rivera J, Proia RL, Olivera A. The alliance of sphingosine-1-phosphate and its receptors in immunity. Nature reviews Immunology. 2008;8(10):753-63. doi: 10.1038/nri2400. PubMed PMID: 18787560; PubMed Central PMCID: PMC2600775.
107. Danieli-Betto D, Peron S, Germinario E, Zanin M, Sorci G, Franzoso S, et al. Sphingosine 1-phosphate signaling is involved in skeletal muscle regeneration. American journal of physiology Cell physiology. 2010;298(3):C550-8. doi: 10.1152/ajpcell.00072.2009. PubMed PMID: 20042733.
108. Nagata Y, Partridge TA, Matsuda R, Zammit PS. Entry of muscle satellite cells into the cell cycle requires sphingolipid signaling. The Journal of cell biology. 2006;174(2):245-53. doi: 10.1083/jcb.200605028. PubMed PMID: 16847102; PubMed Central PMCID: PMC2064184.
109. Kono M, Mi Y, Liu Y, Sasaki T, Allende ML, Wu YP, et al. The sphingosine-1-phosphate receptors S1P1, S1P2, and S1P3 function coordinately during embryonic angiogenesis. The Journal of biological chemistry. 2004;279(28):29367-73. doi: 10.1074/jbc.M403937200. PubMed PMID: 15138255.
110. Allende ML, Sasaki T, Kawai H, Olivera A, Mi Y, van Echten-Deckert G, et al. Mice deficient in sphingosine kinase 1 are rendered lymphopenic by FTY720. The Journal of biological chemistry. 2004;279(50):52487-92. doi: 10.1074/jbc.M406512200. PubMed PMID: 15459201.
111. Germinario E, Peron S, Toniolo L, Betto R, Cencetti F, Donati C, et al. S1P2 receptor promotes mouse skeletal muscle regeneration. Journal of applied physiology. 2012;113(5):707-13. doi: 10.1152/japplphysiol.00300.2012. PubMed PMID: 22744969.
112. Vogel P, Donoviel MS, Read R, Hansen GM, Hazlewood J, Anderson SJ, et al. Incomplete inhibition of sphingosine 1-phosphate lyase modulates immune system function yet prevents early lethality and non-lymphoid lesions. PloS one. 2009;4(1):e4112. doi: 10.1371/journal.pone.0004112. PubMed PMID: 19119317; PubMed Central PMCID: PMC2606024.
113. Pantoja M, Fischer KA, Ieronimakis N, Reyes M, Ruohola-Baker H. Genetic elevation of sphingosine 1-phosphate suppresses dystrophic muscle phenotypes in Drosophila. Development. 2013;140(1):136-46. doi: 10.1242/dev.087791. PubMed PMID: 23154413; PubMed Central PMCID: PMC3513996.

114. Sanchez T, Hla T. Structural and functional characteristics of S1P receptors. Journal of cellular biochemistry. 2004;92(5):913-22. doi: 10.1002/jcb.20127. PubMed PMID: 15258915.
115. Venkataraman K, Lee YM, Michaud J, Thangada S, Ai Y, Bonkovsky HL, et al. Vascular endothelium as a contributor of plasma sphingosine 1-phosphate. Circulation research. 2008;102(6):669-76. doi: 10.1161/CIRCRESAHA.107.165845. PubMed PMID: 18258856; PubMed Central PMCID: PMC2659392.
116. Loh KC, Leong WI, Carlson ME, Oskouian B, Kumar A, Fyrst H, et al. Sphingosine-1-phosphate enhances satellite cell activation in dystrophic muscles through a S1PR2/STAT3 signaling pathway. PloS one. 2012;7(5):e37218. doi: 10.1371/journal.pone.0037218. PubMed PMID: 22606352; PubMed Central PMCID: PMC3351440.
117. Kohler N, Lipton A. Platelets as a source of fibroblast growth-promoting activity. Experimental cell research. 1974;87(2):297-301. PubMed PMID: 4370268.
118. Ross R, Glomset J, Kariya B, Harker L. A platelet-dependent serum factor that stimulates the proliferation of arterial smooth muscle cells in vitro. Proceedings of the National Academy of Sciences of the United States of America. 1974;71(4):1207-10. PubMed PMID: 4208546; PubMed Central PMCID: PMC388193.
119. Heldin CH, Westermark B. Mechanism of action and in vivo role of platelet-derived growth factor. Physiological reviews. 1999;79(4):1283-316. PubMed PMID: 10508235.
120. Andrae J, Gallini R, Betsholtz C. Role of platelet-derived growth factors in physiology and medicine. Genes & development. 2008;22(10):1276-312. doi: 10.1101/gad.1653708. PubMed PMID: 18483217; PubMed Central PMCID: PMC2732412.
121. Crosby JR, Seifert RA, Soriano P, Bowen-Pope DF. Chimaeric analysis reveals role of Pdgf receptors in all muscle lineages. Nature genetics. 1998;18(4):385-8. doi: 10.1038/ng0498-385. PubMed PMID: 9537425.
122. Hoch RV, Soriano P. Roles of PDGF in animal development. Development. 2003;130(20):4769-84. doi: 10.1242/dev.00721. PubMed PMID: 12952899.
123. Soriano P. The PDGF alpha receptor is required for neural crest cell development and for normal patterning of the somites. Development. 1997;124(14):2691-700. PubMed PMID: 9226440.
124. Tallquist MD, Weismann KE, Hellstrom M, Soriano P. Early myotome specification regulates PDGFA expression and axial skeleton development. Development. 2000;127(23):5059-70. PubMed PMID: 11060232.
125. Tallquist M, Kazlauskas A. PDGF signaling in cells and mice. Cytokine & growth factor reviews. 2004;15(4):205-13. doi: 10.1016/j.cytogfr.2004.03.003. PubMed PMID: 15207812.
126. Hantai D, Labat-Robert J, Grimaud JA, Fardeau M. Fibronectin, laminin, type I, III and IV collagens in Duchenne's muscular dystrophy, congenital muscular dystrophies and congenital myopathies: an immunocytochemical study. Connective tissue research. 1985;13(4):273-81. PubMed PMID: 3161692.
127. Goldspink G, Fernandes K, Williams PE, Wells DJ. Age-related changes in collagen gene expression in the muscles of mdx dystrophic and normal mice. Neuromuscul Disord. 1994;4(3):183-91. PubMed PMID: 7919967.
128. Kharraz Y, Guerra J, Pessina P, Serrano AL, Munoz-Canoves P. Understanding the process of fibrosis in Duchenne muscular dystrophy. BioMed research international.

2014;2014:965631. doi: 10.1155/2014/965631. PubMed PMID: 24877152; PubMed Central PMCID: PMC4024417.
129. Brown RD, Ambler SK, Mitchell MD, Long CS. The cardiac fibroblast: therapeutic target in myocardial remodeling and failure. Annual review of pharmacology and toxicology. 2005;45:657-87. doi: 10.1146/annurev.pharmtox.45.120403.095802. PubMed PMID: 15822192.
130. Fan D, Takawale A, Lee J, Kassiri Z. Cardiac fibroblasts, fibrosis and extracellular matrix remodeling in heart disease. Fibrogenesis & tissue repair. 2012;5(1):15. doi: 10.1186/1755-1536-5-15. PubMed PMID: 22943504; PubMed Central PMCID: PMC3464725.
131. Biernacka A, Frangogiannis NG. Aging and Cardiac Fibrosis. Aging and disease. 2011;2(2):158-73. PubMed PMID: 21837283; PubMed Central PMCID: PMC3153299.
132. Uezumi A, Fukada S, Yamamoto N, Takeda S, Tsuchida K. Mesenchymal progenitors distinct from satellite cells contribute to ectopic fat cell formation in skeletal muscle. Nature cell biology. 2010;12(2):143-52. doi: 10.1038/ncb2014. PubMed PMID: 20081842.
133. Uezumi A, Fukada S, Yamamoto N, Ikemoto-Uezumi M, Nakatani M, Morita M, et al. Identification and characterization of PDGFRalpha+ mesenchymal progenitors in human skeletal muscle. Cell death & disease. 2014;5:e1186. doi: 10.1038/cddis.2014.161. PubMed PMID: 24743741; PubMed Central PMCID: PMC4001314.
134. Olson LE, Soriano P. Increased PDGFRalpha activation disrupts connective tissue development and drives systemic fibrosis. Developmental cell. 2009;16(2):303-13. doi: 10.1016/j.devcel.2008.12.003. PubMed PMID: 19217431; PubMed Central PMCID: PMC2664622.

Chapter 1

Satellite cell heterogeneity

Primer

Since their discovery in 1961 (1), satellite cells are recognized as the bona fide stem cells responsible for postnatal muscle regeneration (2). Satellite cells are essential for muscle repair, as their ablation results in complete muscle wasting and scar formation (3). The potency of satellite cells for muscle repair has also been demonstrated as single satellite cells transplanted into irradiated muscle can reconstitute the entire population (4). Despite our understanding of the central role of satellite cells in regenerating muscle, the "essence" of this population is underscored by its heterogeneity. Irrespective of the almost homogenous expression of myogenic regulatory factors Myf5 and Pax7 (5, 6), clonal analysis has indicated that a great variation of myogenic potential exists between satellite cells (4, 7). Yet, the molecular mechanisms that dictate states of potential remain poorly defined. Therefore, we sought to understand satellite cell heterogeneity based on CD34 expression, a marker used to distinguish the most primitive hematopoietic stem cells (8).Characterization is not only essential for understanding satellite cell biology, but also for enriching the most potent members of this population for their potential use in stem cell based therapies.

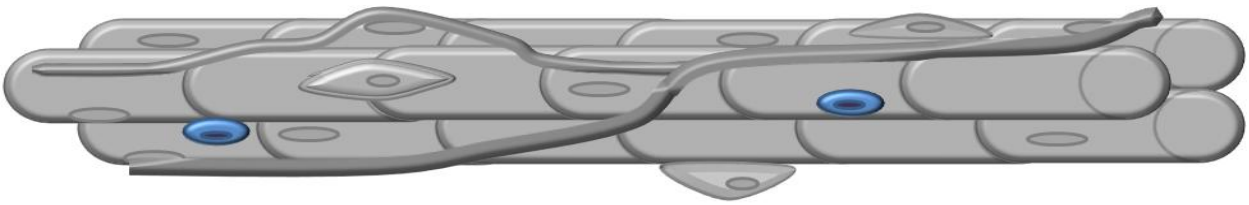

satellite cells

1. Mauro A. Satellite cell of skeletal muscle fibers. The Journal of biophysical and biochemical cytology. 1961;9:493-5. PubMed PMID: 13768451; PubMed Central PMCID: PMC2225012.

2. Biressi S, Rando TA. Heterogeneity in the muscle satellite cell population. Seminars in cell & developmental biology. 2010;21(8):845-54. doi: 10.1016/j.semcdb.2010.09.003. PubMed PMID: 20849971; PubMed Central PMCID: PMC2967620.
3. Lepper C, Partridge TA, Fan CM. An absolute requirement for Pax7-positive satellite cells in acute injury-induced skeletal muscle regeneration. Development. 2011;138(17):3639-46. doi: 10.1242/dev.067595. PubMed PMID: 21828092; PubMed Central PMCID: PMC3152922.
4. Sacco A, Doyonnas R, Kraft P, Vitorovic S, Blau HM. Self-renewal and expansion of single transplanted muscle stem cells. Nature. 2008;456(7221):502-6. PubMed PMID: 18806774.
5. Seale P, Ishibashi J, Scime A, Rudnicki MA. Pax7 is necessary and sufficient for the myogenic specification of CD45+:Sca1+ stem cells from injured muscle. PLoS biology. 2004;2(5):E130. doi: 10.1371/journal.pbio.0020130. PubMed PMID: 15138500; PubMed Central PMCID: PMC406392.
6. Beauchamp JR, Heslop L, Yu DS, Tajbakhsh S, Kelly RG, Wernig A, et al. Expression of CD34 and Myf5 defines the majority of quiescent adult skeletal muscle satellite cells. The Journal of cell biology. 2000;151(6):1221-34. PubMed PMID: 11121437; PubMed Central PMCID: PMC2190588.
7. Day K, Shefer G, Richardson JB, Enikolopov G, Yablonka-Reuveni Z. Nestin-GFP reporter expression defines the quiescent state of skeletal muscle satellite cells. Developmental biology. 2007;304(1):246-59. doi: 10.1016/j.ydbio.2006.12.026. PubMed PMID: 17239845; PubMed Central PMCID: PMC1888564.
8. Stella CC, Cazzola M, De Fabritiis P, De Vincentiis A, Gianni AM, Lanza F, et al. CD34-positive cells: biology and clinical relevance. Haematologica. 1995;80(4):367-87. PubMed PMID: 7590508.

Absence of CD34 on Murine Skeletal Muscle Satellite Cells Marks a Reversible State of Activation during Acute Injury.

Nicholas Ieronimakis[1], Gayathri Balasundaram[1], Sabrina Rainey[1], Kiran Srirangam[1], Zipora Yablonka-Reuveni[2], Morayma Reyes[1]*

1 Department of Pathology, School of Medicine, University of Washington, Seattle, Washington, United States of America, 2 Department of Biological Structure, School of Medicine, University of Washington, Seattle, Washington, United States of America

Reproduced from PLoS One, published June 02, 2010. Pone.0010920.

Abstract

Background: Skeletal muscle satellite cells are myogenic progenitors that reside on myofiber surface beneath the basal lamina. In recent years satellite cells have been identified and isolated based on their expression of CD34, a sialomucin surface receptor traditionally used as a marker of hematopoietic stem cells. Interestingly, a minority of satellite cells lacking CD34 has been described.

Methodology/Principal Findings: In order to elucidate the relationship between CD34+ and CD34-satellite cells we utilized fluorescence-activated cell sorting (FACS) to isolate each population for molecular analysis, culture and transplantation studies. Here we show that unless used in combination with a7 integrin, CD34 alone is inadequate for purifying satellite cells. Furthermore, the absence of CD34 marks a reversible state of activation dependent on muscle injury.

Conclusions/Significance: Following acute injury CD34-cells become the major myogenic population

whereas the percentage of CD34+ cells remains constant. In turn activated CD34-cells can reverse their activation to maintain the pool of CD34+ reserve cells. Such activation switching and maintenance of reserve pool suggests the satellite cell compartment is tightly regulated during muscle regeneration.

Introduction

Since their discovery, satellite cells have been characterized as the resident stem cells of the skeletal muscle, responsible for postnatal myofiber growth and regeneration [1,2]. Classically, satellite cells have been defined by their position underneath the basal lamina of muscle fibers. More recently, satellite cells have been distinguished by nuclear Pax7 immunostaining and/or nlacZ/+ Myf5 reporter expression, and the presence of various surface receptors including a7 integrin (herein referred as a7), b1 integrin, CD34, NCAM, c-met, and CXCR4 [3,4,5,6,7,8,9,10,11,12]. Although satellite cells are unanimously recognized by anatomical location, there is no single surface marker specific or exclusive to the entire population. This issue is compounded by the heterogeneity of satellite cells between muscles, as reported with Pax3 expression, and within muscles, based on non-uniform expression levels of Myf5-driven reporters [13,14,15]. Such heterogeneity between and within various muscles exemplifies the complexity of the satellite cell pool that has yet an established canonical differentiation lineage.

Beauchamp et al. (2000) reported that the majority of satellite cells could be identified by Myf5-knock-in reporter activity and CD34 expression. In this study approximately 20% of satellite cells monitored in freshly isolated myofibers from extensor digitorum longus (EDL) muscle, could not be detected by CD34 immunostaining. Although the CD34-satellite cell population was not characterized, it was suggested these cells may represent a more primitive population of muscle stem cells [5]. In separate studies using Pax3 and Pax7 reporter mice, it was observed that the majority of myogenic cells of skeletal muscle reside within the CD34+ fraction [16,17]. It has been further described that myogenic cells can be isolated by fluorescence-activated cell sorting (FACS) as CD45-/Sca1-/CD34+, and more recently as CD45-/CD31-

/Sca1-/CD11b-/a7+/CD34+ [18,19].

Although CD34 has been used to identify and isolate satellite cells, many cell types, including muscle endothelial cells, express CD34 [20]. Thus, in order to study satellite cell heterogeneity, we initially set out to develop a method to isolate pure populations of satellite cells using the CD34 antigen while excluding other cells that may also express CD34. Utilizing FACS based on previously published reports from this and other laboratories, we initially isolated satellite cells by removing CD45+ hematopoietic cells, CD31+ endothelial cells, other non-satellite Sca1+ cells, and then selecting the remaining CD34+ fraction [18,20,21]. Although the bulk of CD45-/CD31-/Sca1-/CD34+ sorted cells were myogenic, we repeatedly observed non-myogenic cells in culture. Next, in accordance with the literature, we incorporated a7 for satellite cell FACS isolation [10,14,19,22]. Indeed, this approach eliminated non-myogenic cells in culture. Subsequently, we observed by FACS-analysis that the CD45-/CD31-/Sca1-/ a7+ population was comprised of a CD34+ majority and CD34- minority. In the murine hematopoietic system it has been observed that single CD34-/low stem cells can reconstitute the entire hematopoietic system and give rise to both CD34+/- cells [23]. Therefore, in analogy with the hematopoietic system, we initially hypothesized that within the satellite cell compartment the minority of CD34- cells may represent more primitive cells upstream of the more abundant CD34+ population. However, our results described herein indicate the absence of CD34 on skeletal muscle satellite cells in vivo marks a state of activation dependent on muscle injury and not necessarily a hierarchy as initially predicted.

Results

Despite CD45/CD31/Sca1 Negative Selection, CD34 is Insufficient for Purifying Satellite Cell by Flow Cytometry. Using our previously developed method to isolate endothelial cells from a collection of skeletal muscles (pooled hind limb, pectorals and triceps muscles), we initially FACS-sorted satellite cells as CD45-/CD31-/Sca1-/CD34+ [20]. Reverse-transcription PCR (RT-PCR) of these freshly sorted cells

revealed expression of Pax7 and myogenic factors Myf5 and MyoD (data not shown). In culture, the majority of CD45-/CD31-/Sca1-/CD34+ sorted cells produced colonies comprised of small round cells that ultimately formed twitching myotubes. However, cultured CD45-/CD31-/Sca1-/CD34+ + cells also gave rise to larger non-myogenic cells that never formed myotubes (data not shown).

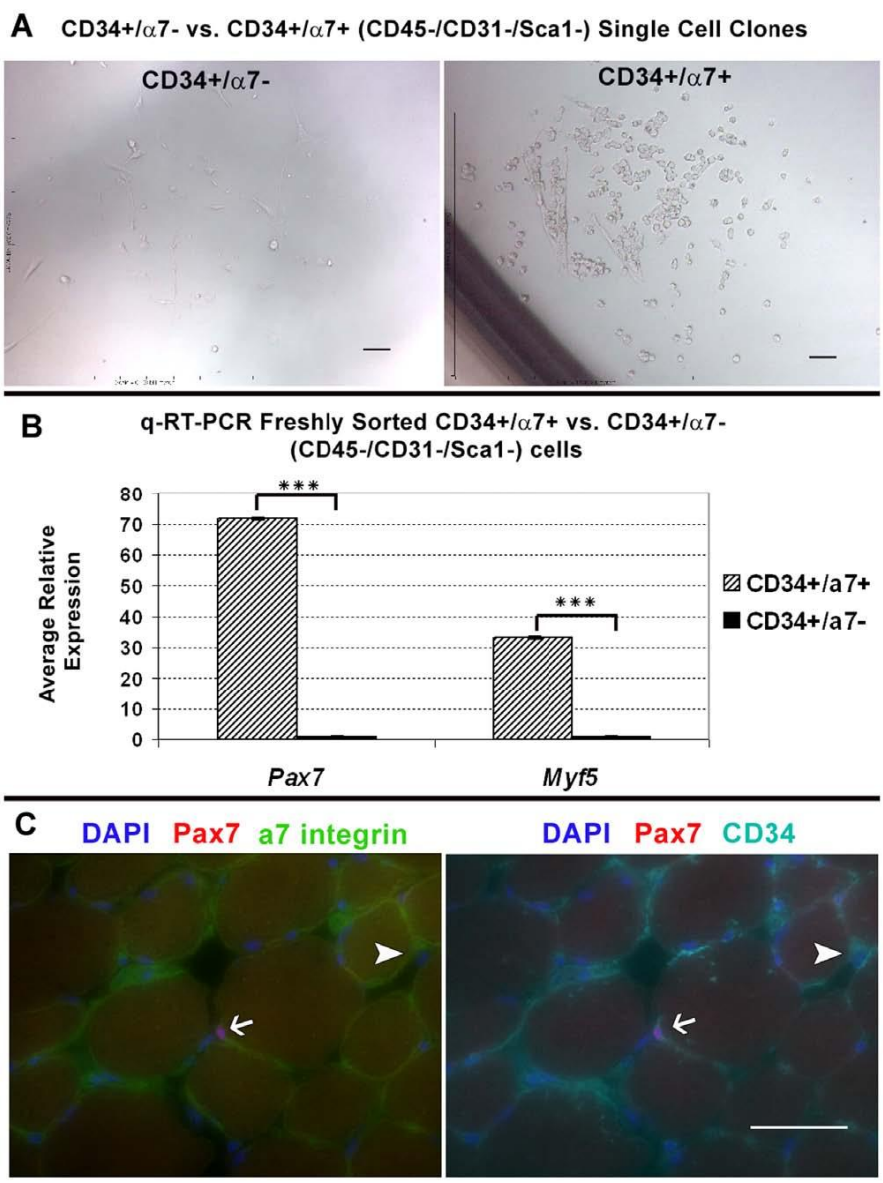

Figure 1. CD34+/a7 integrin-cells are not myogenic nor anatomically defined satellite cells. (A) Colonies derived from FACS-mediated single cell deposition of CD34+/a72 and CD34+/a7+ (CD452/CD312/Sca12) cells (n = 3). Only a7+ sorted cells gave rise to colonies of small round myogenic cells. (B) q-RT-PCR of freshly sorted cells (n = 2) indicates only a7+ cells express Pax7 and Myf5. *** denotes P#0.00005 calculated by Student's t-test. Error bars represent ±SEM. (C) Immunostained TA cryosections reveal Pax7+ satellite cells are CD34+/a7+ (arrow) while CD34+/a72 cells sighted within interstitium were Pax7-(arrow head). Negative controls for all stainings are depicted in Figure S4. Scale bars = 50 mm.

To improve satellite cell purification we incorporated a7 and investigated the myogenic potential within the CD45/CD31/Sca1 population based on the presence or absence of a7 and CD34 antigens. By FACS-mediated single cell deposition only CD34+/a7+ (CD45-/CD31-/Sca1-) sorted cells, which were small and round, gave rise to myogenic colonies (n = 3). In contrast, CD34+/a7+ (CD45-/CD31-/Sca1-) cells appeared larger and more spread-out and did not form myotubes (n = 3)(Figure 1A). Quantitative reverse-transcription PCR (q-RT-PCR) of freshly sorted cells (n = 2) revealed that between these two populations, only CD34+/a7+ cells express the definitive satellite cells genes Pax7 and Myf5 (Figure 1B). Cryosections from uninjured tibialis anterior (TA) muscle, immunostainied for Pax7, a7 and CD34, revealed the presence of both populations. However, only CD34+/a7+

Figure 2. CD34+ and CD34-cells are Pax7+ satellite cells of the skeletal muscle. Cryosections of tibialis anterior (TA) muscle immunostained for Pax7, laminin, and CD34 show the existence of CD342 satellite cells. Both CD342/Pax7+ (arrow head) and CD34+/Pax7+ (arrow) cells were sighted in the satellite position under the basal lamina. Scale bar =50uM.

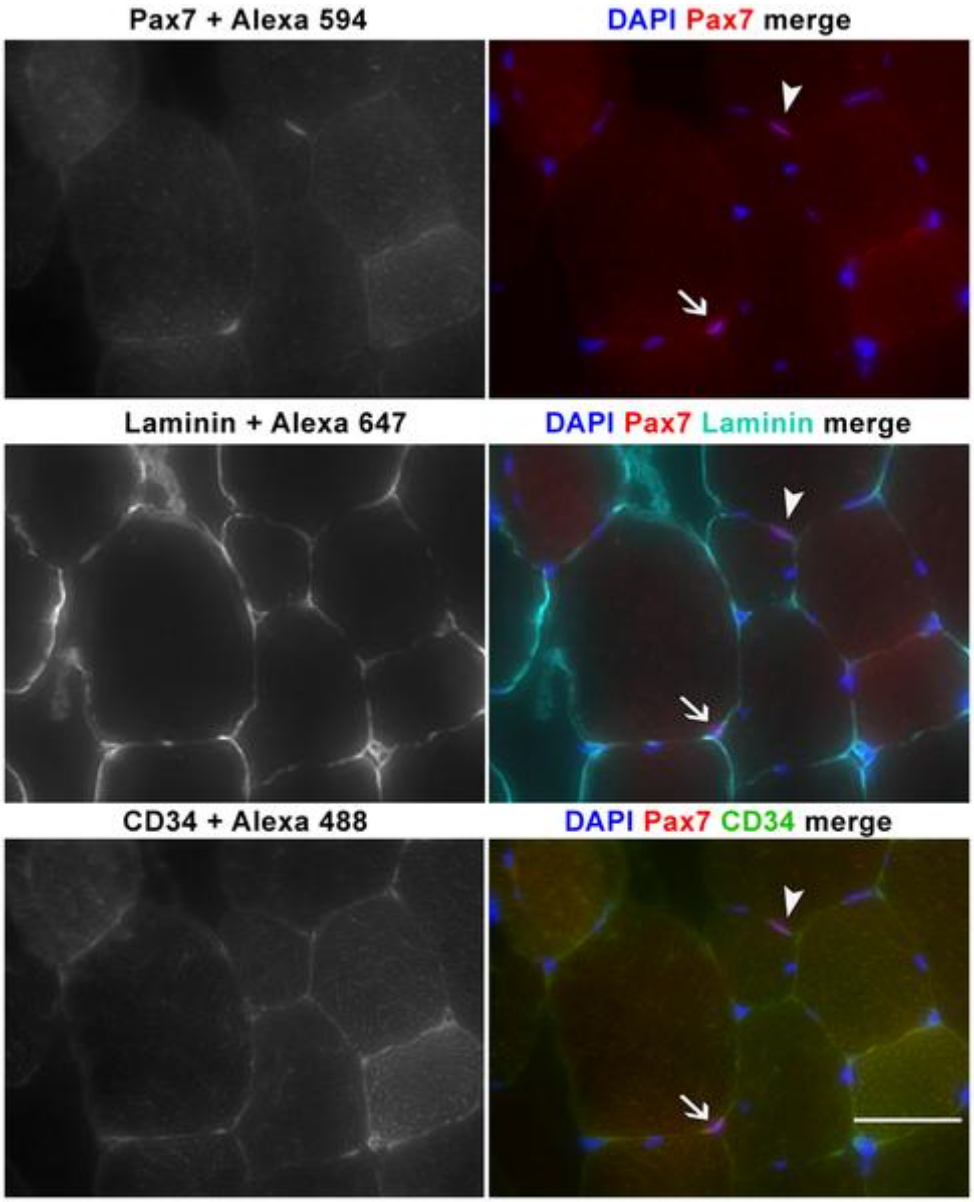

cells were Pax7+ and within the satellite cell position. CD34+/a72 cells were Pax72 and located in the interstitium (Figure 1C). Altogether, our results indicate CD34+/a7+ cells are present in the satellite cell compartment while CD34+/a72 cells are not myogenic in culture nor satellite cells by anatomical definition. By FACS-analysis we determined that a7- cells constitute 11.8% (61.2% SEM) of the CD45-/CD31-/Sca1-/CD34+ population (n = 5); note with the exception of transplant studies and reporter mice, all experiments characterizing CD34+/- cells were completed with 2 month old C57BL/6 male mice. We believe sorted CD34+/a72 cells, which correspond with CD34+/ a7+/Pax7+ cells observed by immunostaining, were the source of non-myogenic CD45-/CD31-/Sca1-/CD34+ cells. Collectively, our results are consistent with previous reports that CD34 is present on the majority of skeletal muscle satellite cells. However, because CD34 cell surface expression is not exclusive to satellite cells, it is insufficient to FACS purify satellite cells unless used in conjunction with a second positive antigen such as a7.

CD34-/a7+ (CD45-/CD31-/Sca1-) Cells Represent a Minority of Limb Muscle Pax7+ Satellite Cells

When purifying a7+ (CD45-/CD31-/Sca1-) cells, we observed CD34+ majority and CD34- minority populations, both of which produced myogenic colonies in culture. These CD34+/- populations sorted as CD45-/CD31-/Sca1-/a7+ shall be abbreviated CD34+ and CD34- for the remainder of this manuscript. FACS-analysis indicates CD34- cells make up ,17.6% (62.2% SEM) of the a7+ (CD45-/CD31-/Sca1-) population in pooled muscle preparations from individual mice (n = 5). Further antibody staining revealed the presence of CD34-/Pax7+ cells in the satellite cell position underneath the basal lamina; confirming CD34- cells are an integral part of the satellite cell niche in vivo and not a mere product of cell isolation procedures (Figure 2). Satellite cells constitute only 2–5% of the nuclei in adult muscles and their abundance varies between muscle type and age [24,25]. Therefore, direct quantification from cross sections would have required that many samples and cross sections be analyzed for accurate numbers of CD34+ and CD34-, Pax7+ satellite cells. Thus in order to quantify the abundance of these two satellite cell populations, we performed flow cytometry analysis of pooled muscles as well as individual muscles.

Analysis of myogenic colonies generated by FACS-mediated single cell deposition of CD34+/- satellite cells (1 cell per well, 96 wells per cell type from each mouse, n = 3) revealed that both populations contributed myogenic clones with similar growth pattern based on the number of nuclei counted from each colony (Figure 3A, cell doubling). However, clonability was higher in the CD34+ versus the CD34- population (Figure 3A, #colonies/per 96 wells). The difference observed between the number of wells with colonies, suggests the CD34+ population exhibits greater cloning efficiency. Alternatively, our culture conditions may not be optimal for seeding CD34- sorted cells.

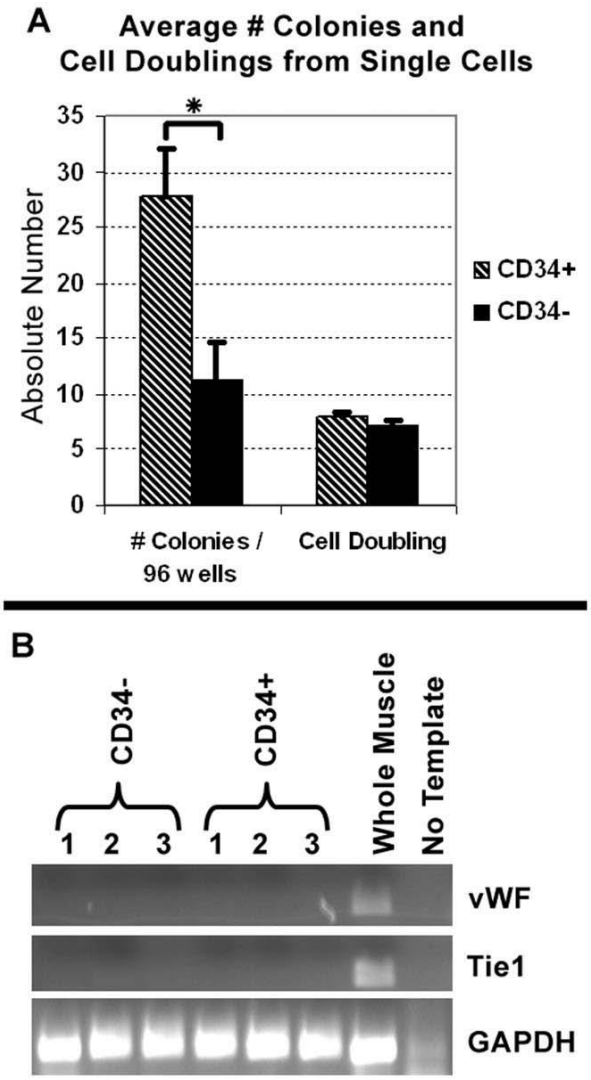

Figure 3. CD34+/- sorted cells represent clonal non-endothelial myogenic populations. (A) FACS-mediated single cell deposition indicates both populations had similar proliferation rates, although CD34+ cells gave rise to more colonies. Y-axis denotes the average number of colonies per 96 well plate or cell doublings. Although CD34+ single cells gave rise to more colonies, both populations were equally myogenic in culture (B) RT-PCR of freshly sorted cells for endothelial cell expressed genes von Willenbrand Factor (vWF)and Tie1 confirms no contamination from CD34+/a7+ capillaries. Both A and B are from 2 month old, n = 3 C57BL/6 mice. Student's t-test, * P = 0.05. Error bars represent ±SEM.

As noted above, all Pax7+ cells were a7+ (Figure 1C). However, not all a7+ cells were Pax7+. The microvascular bed, especially vascular smooth muscle cells stained positive for a7 (data not shown)[26,27]. However, in the event that any endothelial cells may be a7+, such putative endothelial cells are CD31+ and are excluded from the CD45-/CD31-/Sca1-/a7+ population. Indeed, RT-PCR of freshly sorted cells (n = 3) for von Willebrand Factor and Tie1, genes expressed by skeletal muscle endothelium, confirms the absence of endothelial cells within both sorted cell populations (Figure 3B) [20]. Additionally vascular smooth

muscle cells within skeletal muscles immunostained negative for CD34 and thus were presumed to be excluded from the sorted CD34+ population (not shown)[28]. Although such vascular smooth muscle cells could potentially be present in the CD34- satellite cell population, our sort approach should eliminate the presence of such cells from the final population. As previously published, satellite cells have also been defined as small non-granulated cells based on FACS-analysis [13]. Likewise, in our FACS isolation of satellite cells, we gate on smaller events by forward scatter (FSC)Area vs. FSC-Height to remove larger a7+ cells that may originate from vascular smooth muscle (Figure S1).

To assess satellite cell purity within each population, we cytocentrifuged freshly sorted CD34+/- cells (n = 3 mice) and immunostained with anti-Pax7. From both sorted populations we obtained a high purity of myogenic cells as indicated by the tions. In this transgenic mouse, muscle fibers and cultured presence of nuclear Pax7 staining (Figure 4A, left panels). On differentiated myoblasts and myotubes express nuclear localized average, 89% (61.7% SEM) of CD34+ and 70% (62.6% SEM) of LacZ [5,15,29]. Nuclei positive for b-galactosidase (b-gal) were CD34- cells stained positive for Pax7. Although the majority of identified by X-gal staining (data not shown). We observed that cytocentrifuged cells from both populations stained positive, the CD34- cells were completely negative, while approximately 0.01% of CD34+ cells stained positive for β-gal activity with X-gal. With the exception of the few CD34+/β−gal+

Figure 4. CD34+/- sorted populations contain a similar number of satellite cells that vary in gene expression. (A) The majority of freshly sorted cytocentrifuged CD34+/- cells stained positive for Pax7 DAB; 89% (61.7% SEM) of CD34+ and 70% (62.6% SEM) of CD34- cells were positive (n = 3, 2 month old C57BL/6). Although this difference was statistically significant (Students t-test, P#0.05), the majority of CD34+ and CD34- cells were Pax7+ indicating a high purity of satellite cells within both populations. Arrowheads indicate Pax7+ cells while line arrows point to Pax7-cells. Cultured CD34+/- cells from Myf5$^{nlacZ/+}$ and 3F-nlacZ-2F mice gave rise to b-galactosidase+ myogenic colonies as indicated by X-gal staining. The presence of Myf5$^{nlacZ/+}$ and 3F-nlacZ-2F reporters in culture suggests both populations have similar myogenic potential. 606 scale bar for cytocentrifuged photos was unavailable. Scale bars for cultured cells = 50 mm. (B) q-RT-PCR of freshly sorted cells confirms a7 expression in both populations and low CD34 expression in CD34- cells (n = 3, 2 month old C57BL/6). Although higher in CD34+ cells, both populations expressed satellite cell markers Pax3/7, and myogenic regulatory factors Myf5, MyoD, and myogenin. Expression of satellite cell associated genes CXCR4, c-met, and NCAM was also higher in CD34+ cells. Student's t-test calculated * P#0.05 and ** P#0.005. Error bars represent ±SEM.

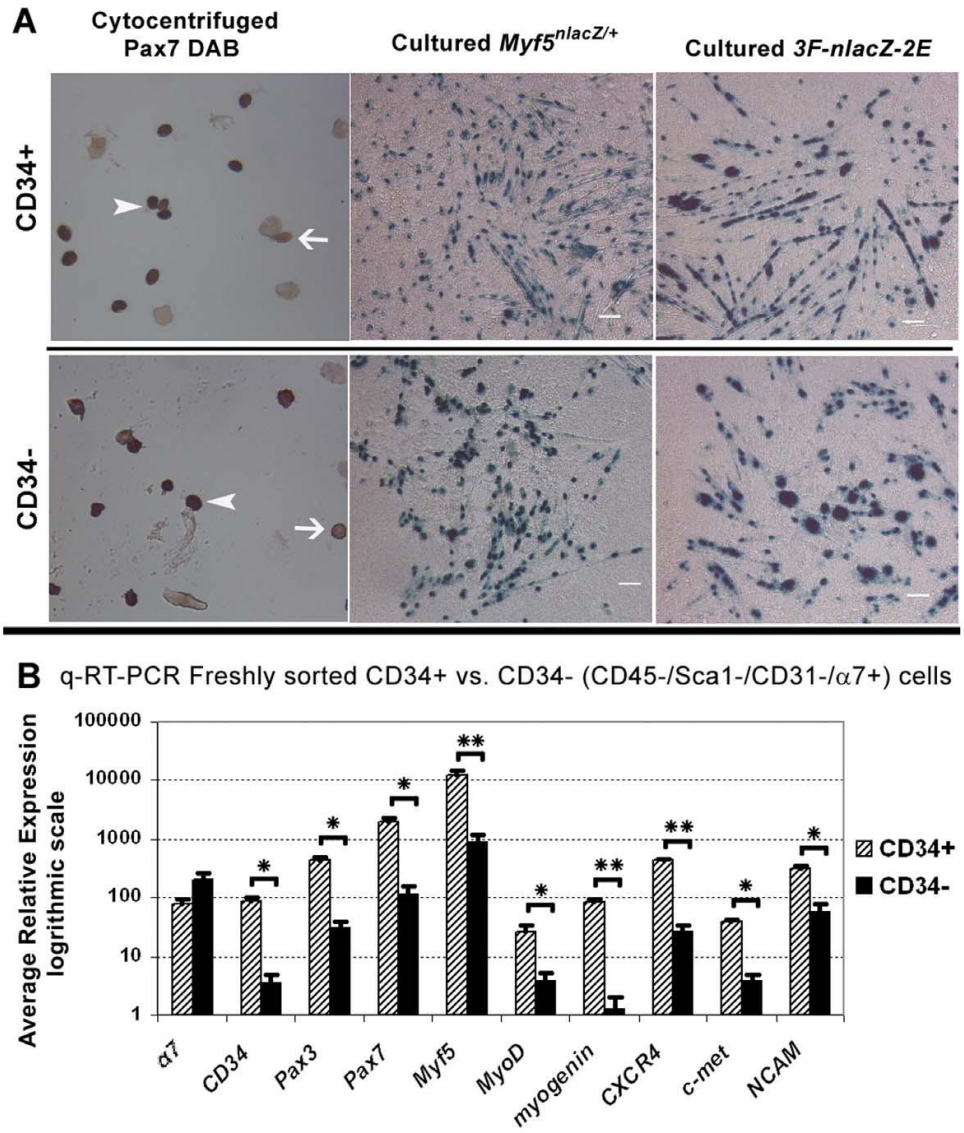

cells observed, lack of 3F-nlacZ-2F reporter activity indicated the vast majority of cells in the CD34+/− sorted populations were not differentiated myoblasts (the phase at which this transgene is activated) [5], [29]. In contrast, we did identify β-gal+ cells from cytocentrifuged 3F-nlacZ-2F unsorted cells stained with X-gal as a positive control (not shown).

To assess the in vitro myogenic potential of these two populations, we cultured CD34+/- sorted cells from 3F-nlacZ2F (n = 2, pooled) and Myf5$^{nlacZ/+}$ mice (n = 3). Cultured CD34+/- cells sorted from Myf5$^{nlacZ/+}$ and 3F-nlacZ-2F mice produced progeny that looked identical in culture (Figure 4A, middle and right panels). From Myf5$^{nlacZ/+}$ mice, both populations formed myogenic colonies with numerous b-gal+ myonuclei and myoblasts. Myonuclei from Myf5$^{nlacZ/+}$ mice stained positive with X-gal due to the presence of residual b-gal expressed also in differentiating cells [15]. In contrast, 3F-nlacZ-2F reporter activity was predominantly localized in myonuclei. To further compare the CD34+/- populations, we surveyed the expression of genes known to be transcribed by satellite cells (Figure 4B). Due to possible gene regulation changes in culture that may not necessarily

represent in vivo expression, we chose to analyze only freshly sorted cells by q-RT-PCR. Initially we checked CD34 and a7 expression to validate our FACS-analysis (Figure 4B). In accordance with antigen levels, CD34- cells express very low levels of CD34 mRNA, whereas CD34+ cells transcribe much higher levels (25 times greater than CD34- cells). The expression of a7 was similar in both CD34+/- populations and not statistically significant (Student's t-test, P.0.05). Next, we compared the two populations for the expression of a panel of genes that are associated with different phases of myogenesis (Figure 4B). Pax3, Pax7, and Myf5 are expressed by quiescent and proliferating satellite cells [4,12,30,31]. MyoD expression is initiated upon satellite cell activation and sustained in proliferating and differentiating progeny, while myogenin expression is associated specifically with myogenic differentiation [11,32]. Interestingly, expression levels of Pax3/7 genes and muscle regulatory factors

(MRF's) Myf5, MyoD, and myogenin were significantly higher in CD34+ vs. CD34- cells (Student's t-test, P#0.05). The detection of myogenin suggests the presence of some differentiating myogenic cells, which may account for the presence of a minute number of cytocentrifuged CD34+ cells that stained positive with X-gal for the differentiation-linked 3F-nlacZ-2F reporter as detailed above. Our detection of myogenin and MyoD transcripts, in addition to Myf5, in preparation of freshly isolated satellite cells is in agreement with previous studies describing gene expression in freshly isolated satellite cells [33,34]. Expression of satellite cell associated genes CXCR4, c-met and NCAM was also significantly higher in CD34+ cells (Student's t-test, P#0.05). Collectively, this expression comparison suggests that CD34+ cells transcribe higher levels of satellite cell characteristic genes than CD34- cells. Alternatively, the CD34- population may contain a residual population of non-myogenic cells that contributes to the apparent reduced expression of these genes.

The CD34+ and CD34- Populations are Consistently Maintained Across Different Muscles In the aforementioned experiments, we isolated CD34+/- cells from pooled hindlimb, pectoralis and triceps muscles. In contrast, the study by Beauchamp et al. (2000) quantified the percentage of CD34+ satellite

cells only on EDL single fiber isolations. Thus, to address the possibility that CD34- satellite cells reside only in specific skeletal muscles, we FACS-analyzed individual muscles (n = 5) using same selection strategy used for pooled muscle isolations (Figure 5A). Because the number of hematopoietic cells can vary between mice depending on circulatory responses, such as mild inflammation, we restricted our analysis to the CD45- fraction. For each muscle, Figure 5B represents the average percentage of CD34+/- cells compared to the total number of non-hematopoietic mononuclear cells. Figure 5C represents the average percentage within the a7+ (CD45-/CD31-/Sca1-) population in order to determine if CD34+ cells consistently represent the majority.

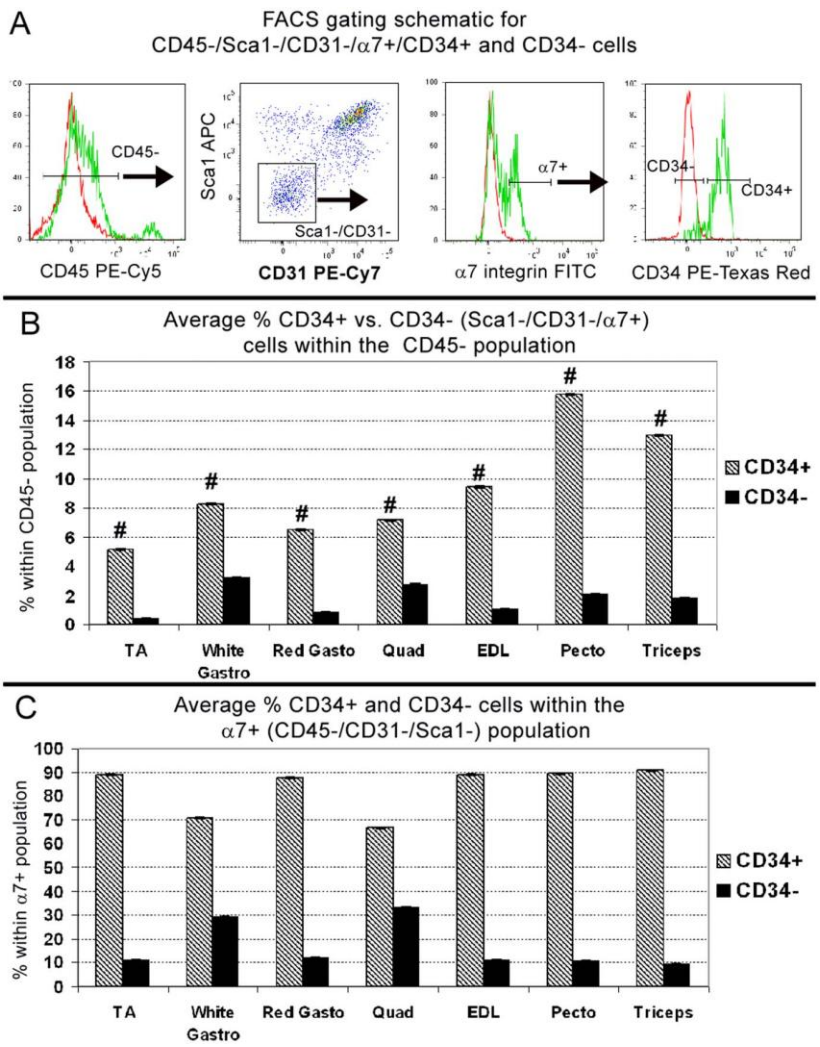

Figure 5. The distribution of CD34+/- cells is maintained among individual muscles. (A) Gating schematic for sorting and analyzing CD34+/- populations. Following size selection, hematopoietic cells are removed by selecting only CD45- cells. Endothelial and other non-satellite cells are then removed by gating on CD31-/Sca1- cells. Finally within the a7+ (CD45-/CD31-/Sca1-) population, CD34+/- cells are selected. Red peaks represent unstained controls, green peaks are experimental stained sample. (B) The average percentage of each population per muscle group relative to all CD45-, non-hematopoietic cells. By single factor ANOVA, differences between muscles was statistically significant for CD34+ (# P#0.05) but not CD34- (P = 0.076). (C) The average percentage of CD34+ and CD34- cells within the a7+ (CD45-/CD31-/Sca1-) population. The ratio of CD34+ over CD34- cells was not statistically significant by single factor ANOVA. A–C are from n = 5, 2 month old C57BL/6 mice. Error bars represent ±SEM.

Results from individual muscle analyses indicate that the

average percentage of CD34+ cells compared to the CD45- fraction is consistent between hindlimb muscles, whereas pectoralis and triceps contain nearly twice the amount of CD34+ cells. Such variation in the number of CD34+ cells may be attributed to individual muscle demands for myogenic cells and/or myofiber types. Consequently, the percentage of CD34+ cells was statistically different (single factor ANOVA, p#0.05) between muscle groups, whereas the percentage of CD34- cells was not (P = 0.075), indicating this population is consistently present in all muscle groups analyzed. Despite this variation, CD34+ cells were consistently the majority within the a7+ (CD45-/CD31-/ Sca1-) population. The ratio of CD34+ over CD34- cells was not statistically significant (single factor ANOVA, p.0.05), suggesting the distribution of these two populations is maintained between muscle groups.

Following Acute Injury, CD34- Cells Represent the Majority of Activated a7+ (CD45-/CD31-/Sca1-) Myogenic Cells

To elucidate the role of CD34- skeletal muscle cells of the skeletal muscle we examined their response to acute injury using the cardiotoxin (CTX) model. Such injury is characterized by a massive myogenic response leading to almost full muscle regeneration by week two following initial tissue destruction [35,36]. We injected CTX in left TA's and FACS-analyzed each damaged muscle individually at 3, 7, and 14 days post injury (n = 5 per time point)(Figure 6A&B). Just as the previous analysis of individual muscles, we compared here the percentage of CD34+/- cells within the CD45- fraction (Figure 6A) and the relative percentage within all a7+ (CD45-/CD31-/Sca1-) cells (Figure 6B). For this experiment we predicted that the more differentiated population will increase early after injury and continuously decrease from day 7 to14 as the muscle reaches full regeneration. In addition, if there is a canonical relationship between CD34+/- cells, we have anticipated an inverse trend where one population decreases while the other increases during the course of regeneration.

As expected, 3 days post injury there was a massive increase in declined to near uninjured levels by day

14. In contrast, the the number of a7+ (CD45-/CD31-/Sca1-) cells which by average percentage of CD34+ cells remained between 3–5% histology were not vascular smooth muscle cells as indicated by a-within the CD45- fraction (Figure 6A) despite becoming the smooth muscle actin (aSMA) staining (Figure S2). Surprisingly minority within a7+ (CD45-/CD31-/Sca1-) population after CTX injury, the CD34-cells became the majority and (Figure 6B). The fluctuation of CD34- cells between time points within CD45- fraction and a7+ population was statistically significant (single factor ANOVA, p#0.05). However, the percentage of CD34+ cells within the CD45- fraction remained relatively constant ($p = 0.076$).

Since CD34+ cells became the minority within the a7+ (CD45-/CD31-/Sca1-) population early in injury but the overall percentage of these cells did not increase, we postulated this population remained quiescent while CD34- cells were activated. Thus, we compared Myf5, MyoD, and myogenin expression by q-RT-PCR in freshly sorted cells from damaged limb muscles at 3 days post CTX injury (Figure 6C). Cells were sorted from pooled CTX injected muscles (single TA, quadriceps and gastrocnemius) from individual mice ($n = 3$). Without injury both CD34+/- cells expressed relative high levels of Myf5 but low levels of MyoD and myogenin mRNA, indicating both populations are committed to the myogenic pathway, but remain quiescent in uninjured muscle (Figure 4B). In contrast, following injury the average relative expression of all three MRF's increased in both populations (Figure 6C). Myf5 and MyoD expression was similar between both populations whereas myogenin was 3.9 times greater and statistically significant (Student's t-test, p#0.05) in CD34- cells. In accordance with MRF expression during myogenesis, upregulation of Myf5 and MyoD following injury indicates both CD34+/- cells are activated while higher myogenin expression suggests that more differentiated cells reside within the CD34- population [11]. The significance of myogenin expression was confirmed by immunostaining as the majority of myogenin+ cells observed within damaged areas 3 days post CTX injury, were a7+/CD34- (Figure 7A). Taking into account myogenin histological and FACS data we concluded CD34- cells were directly responding to

injury. In contrast, significant upregulation of MyoD but not myogenin by CD34+ cells suggested this population was activated but not differentiating. However, the role of CD34+ cells following injury was unclear as their overall numbers did not increase while the majority of a7+ cells observed within damaged areas were CD34-.

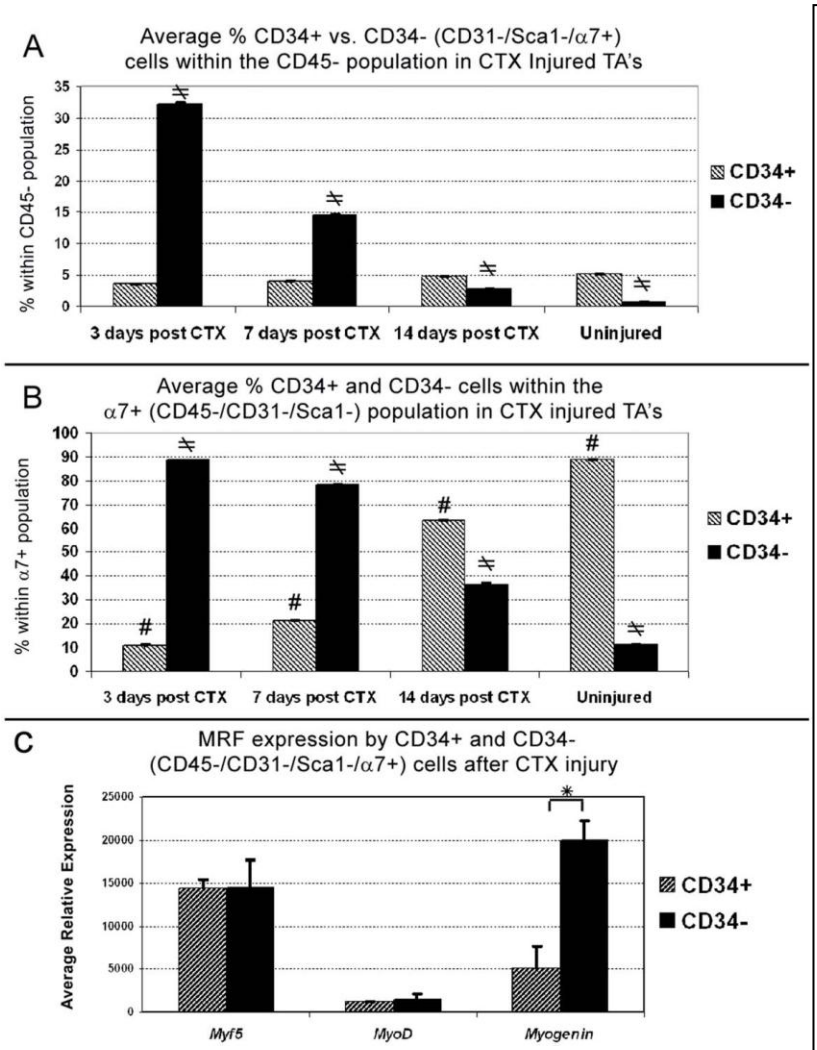

Figure 6. Following acute injury, CD34- cells are the more responsive myogenic majority. (A) Relative to all CD45- cells, the average percentage of CD34- cells in Cardiotoxin (CTX) injected TA's (n = 5 per time point) significantly increased 3 days post injury and declines to near uninjured levels by day 14 (single factor ANOVA, ?P= #0.05). In contrast, the percentage of CD34+ cells remained relatively constant during course of regeneration and was not statistically significant. (B) 3 days post injury the average percentage of CD34- within the a7+ (CD45/CD31-/Sca1-) population drastically increases. This proportion reverts back to near uninjured levels by day 14 and by single factor ANOVA was statistically significant for both CD34+ (# P=0.05) and CD34- (≠P=0.05) populations. (C) q-RT-PCR analysis of cells sorted 3 days post injury from CTX treated limb muscles (n = 3), indicates the average relative expression of all three MRF's increased in both populations as compared to uninjured muscles depicted in Figure 4B. Comparison of MRF's levels in injury reveals both populations express equal levels of key myogenic genes Myf5 and MyoD, while CD34- cells express significantly elevated levels of the differentiation factor myogenin.Student's t-test, * P#0.05. Error bars represent ±SEM. A–C are from 2 month old C57BL/6 mice.

Although Both CD34+/- Populations Proliferate in Response to Injury, CD34+ Cells Retain More BrdU

Because the percentage of CD34+ cells did not increase with CTX damage, it was possible that there was a general increase in all cell types or that CD34+ cells did not proliferate in response to injury. To explore this alternative, we compared BrdU incorporation in

order to quantify proliferation between CD34+/- cells and asses if the absence of CD34 simply marks mitotically active myogenic cells. In order to test this hypothesis we analyzed BrdU incorporation without injury, 2.5–3 days post injury within the peak of proliferation, and after regeneration 14 days post injury (n = 3 for each timepoint analyzed)(Figure 7B)[35]. Bone marrow cells isolated from the same animals as a positive control had a high degree of BrdU incorporation following 3 days pulse. In contrast, BrdU was not detected in CD34+ or CD34- cells from uninjured limb. However, upon injury, BrdU was incorporated into the CD34+/- populations. When isolated from mice pulsed for 12 hours between day 2.5–3 post CTX injury, both CD34+/- populations had incorporated equally high levels of BrdU.

Interestingly, in cells isolated from mice pulsed for the first 3 days following injury and then chased to day 14, BrdU incorporation declined in CD34- cells but remained the same for CD34+ cells. Consequently, the amount BrdU retention by day 14 was roughly 10 fold greater for CD34+ vs. CD34- cells as represented by the log distance from the mean of each fluorescence peak. Given that the level of BrdU uptake at day 2.5–3 was similar for both populations, we estimate that the CD34- population divided .3 cell doublings during the day 4–14 chase.

Figure 7. Although CD34- cells were more differentiated, both CD34+/- populations proliferated in response to injury. (A) Immunostaining of damaged TA, 3 days post injury, reveals that myogenin+ cells within the sight of injury are a7+/CD34-. Insets show colocalization of DAPI with nuclear myogenin and membranous a7 but not CD34 staining. Insets were produced from the original sized merged photographs. Scale bar = 50 mm. (B) FACS-analysis of BrdU incorporation in sorted CD34+/- cells after 3 days pulse, indicates relative to bone marrow (BM) cells (top right histogram), without injury both populations are quiescent (top histogram). In mice pulsed for 12 hours between 2.5–3 days post CTX injection, both CD34+/- cells show nearly equal levels of BrdU incorporation (middle histogram). Mice pulsed for the first 3 days following injury and then chased to day 14 reveal that CD34- cells retain less BrdU whereas CD34+ cells maintained a similar levels to the day 2.5–3 pulse (bottom histogram). Green peaks represent IgG Isotype controls, Violet BM mononuclear cells, Blue CD34+ cells, and Red CD34- cells. Schematics next to histograms portray timelines for each BrdU experiment. Each experimental pulse was conducted with n = 3, 2 month old C57BL/6 mice.

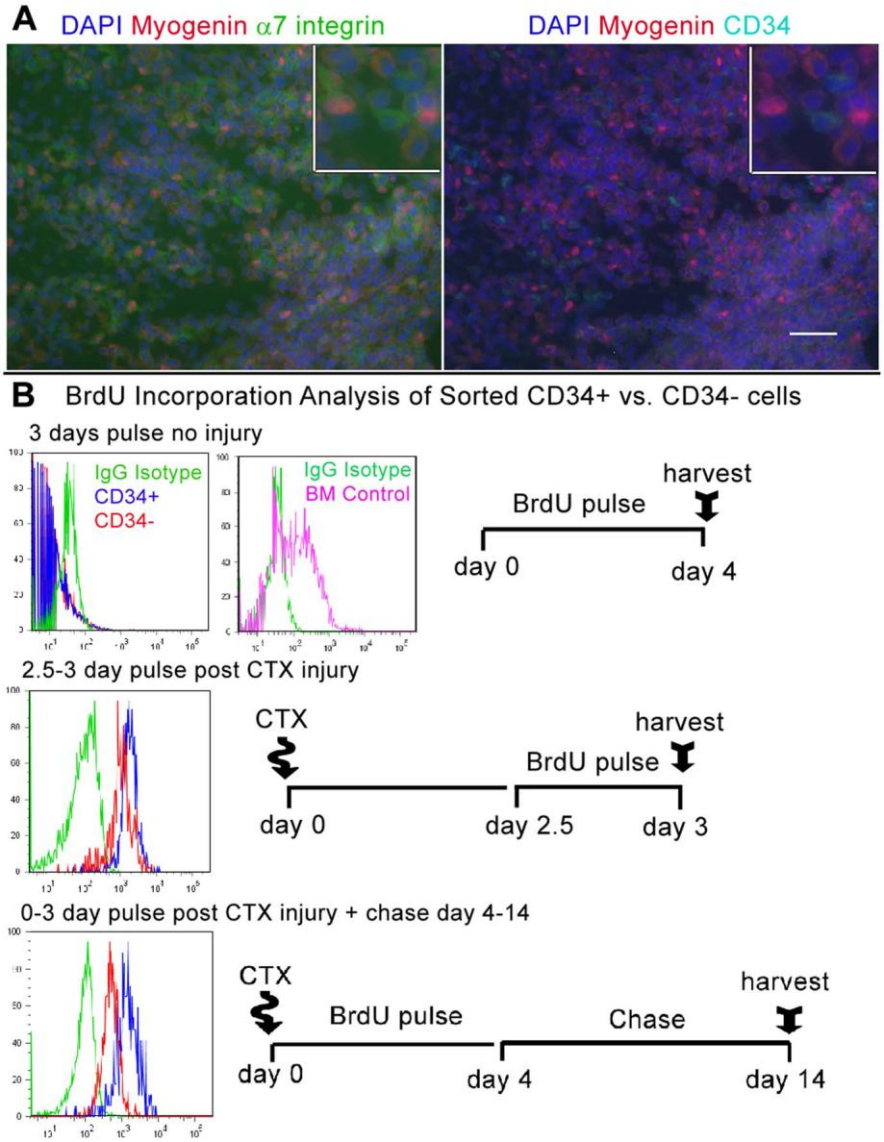

Without injury, the lack of detectable BrdU incorporation correlates with q-RT-PCR data to indicate both populations are quiescent. Following injury both populations have equal levels of BrdU incorporation indicating a similar degree of cell division occurred within the peak of proliferation. Beyond 3 days after injury, CD34+ cells retained a similar level of BrdU indicating they ceased dividing, while CD34- continued to proliferate as their incorporation decreased during the chase. Interestingly, although CD34+ cells did incorporate BrdU following injury, their percentage did not increase but remained relatively constant. Therefore we postulated CD34+ cells give rise to more committed cells while tightly maintaining the parent population during the course of regeneration. All together, FACS, histological, and BrdU results indicate CD34+ cells divided early in response to injury and perhaps gave rise to CD34- cells, which further proliferated during the course of regeneration.

CD34+/- Switching is Dependent on Muscle Injury

To test the possibility that activated CD34+ cells are becoming or giving rise to CD34- cells, we sorted

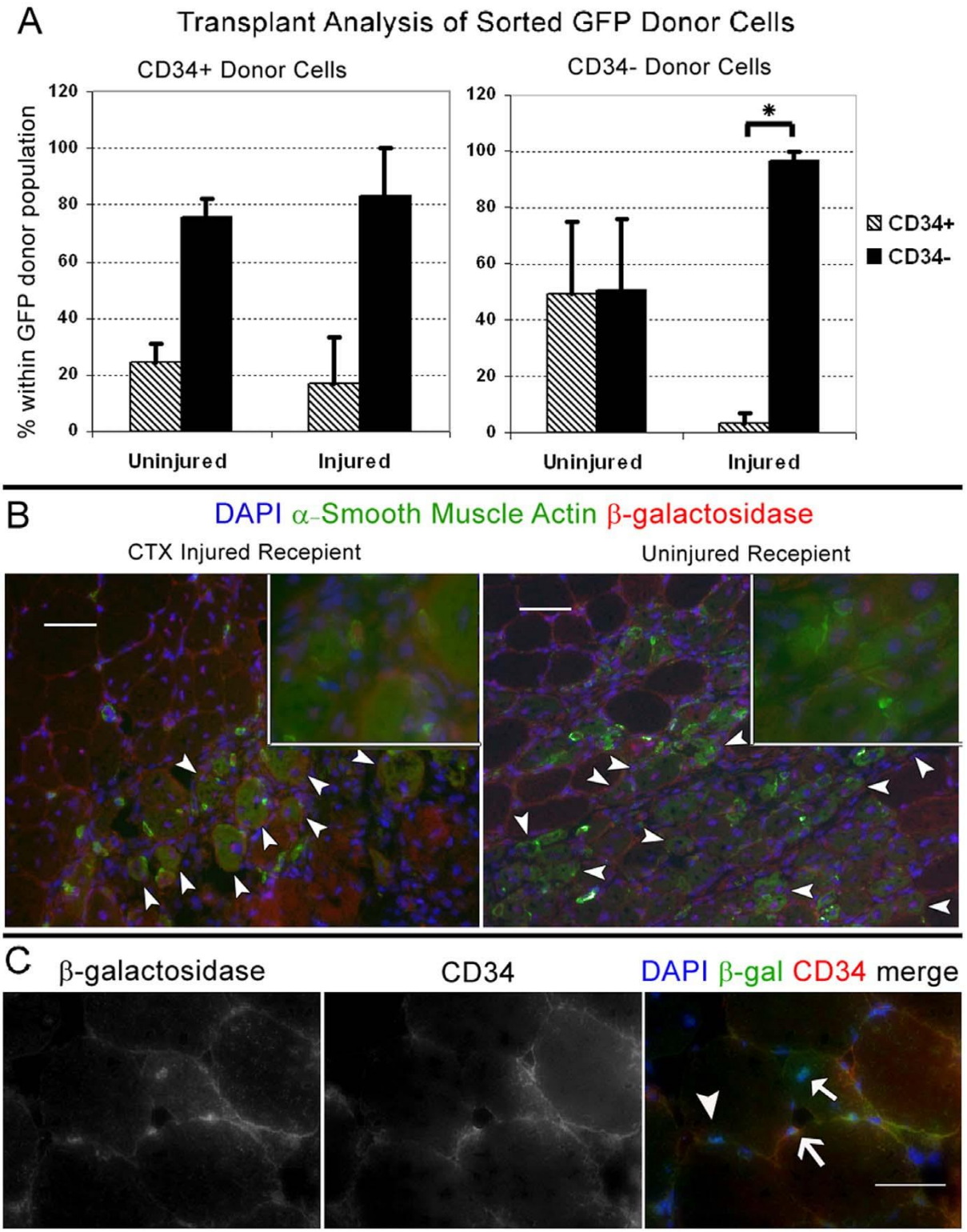

Figure 8. Following injury repair CD34- cells can revert to CD34+. (A) CD34+/- cells sorted from injured (3 days prior) limb muscles of chicken actin promoter driven EGFP reporter mice, were transplanted into uninjured and injured (1 day prior) quadriceps of C57BL/6 recepients. Quadriceps were FACS-analyzed 3 days post transplant. Values in the Y-axis correspond to the percentage of GFP CD34+/- cells detected from each respective donor cell type. The X-axis indicates the state of each recipient muscle prior to transplant (n = 3 per condition). Irrespective of the recipient state, the majority of CD34+ donor cell became or gave rise to CD34- after transplant. Although not statistically significant, this switch slightly increased in CTX injured recipients. In contrast a large proportion of CD34- cells became or gave rise to CD34+ when transplanted into uninjured muscle but significantly remained CD34- in injured muscle. Student's t-test calculated * P#0.05. Error bars represent ±SEM. (B) Sorted CD34- from CTX injured Myf5$^{nlacZ/+}$ mice were transplanted into uninjured (n = 3) and injured (n = 3) quadriceps muscles. In addition to a mock injection, a7(CD45/CD31-/Sca1-) sorted cell were transplanted into uninjured quadriceps as negative controls (Figures S3 and S4). Recipient muscles were harvested 7 days after transplant and stained for a-smooth muscle actin (aSMA), b-galactosidase (b-gal) and CD34. Cells engrafted under both conditions as indicated by b-gal+ central nuclei in aSMA+ fibers (arrowheads). Insets show co-localization of nuclear b-gal with DAPI and cytoplasmic a-SMA staining. Insets were produced from 40xmagnification photographs taken within the same field. (C) Engraftment of CD34-cells into uninjured muscle reveals conversion of CD34- cells to CD34+ cells. Interestingly CD34+ (line arrow) and CD34- (arrowhead), b-gal+ cells were observed near b-gal+ myonuclei (solid arrow) indicating donor CD34- cells can form new myofibers, remain CD34- or gain CD34 expression. Scale bars = 50 mm

both populations from injured chicken actin promoter driven EGFP transgenic mice and transplanted into injured and uninjured quadriceps of C57BL/6 mice. Recipient muscles were then analyzed by FACS to examine if GFP donor cells gained or lost CD34 when transplanted into each respective environment. Injured recipient quadriceps were injected with CTX one day prior to cell transplants. All recipient muscles were analyzed 3 days post transplant in order to detect donor cells prior to fusion (n = 3 for each condition). CD34 analysis of transplanted GFP cells indicated a distinct pattern of switching dependent on the state of muscle injury. As predicted, the majority of injury activated CD34+ donor cells gave rise to, or directly became CD34 negative. The percentage of CD34- cells generated from CD34+ donors was slightly more in injured recipient muscles, although this difference was not significant (Student's t-test, p.0.05)(Figure 8A, left graph). Conversely, the majority of CD34- cells transplanted into injured muscle remained CD34- (Figure 8A, right graph). To our surprise a large portion of CD34- cells transplanted into

uninjured muscle became and/or gave rise to CD34+ cells. In contrast to the CD34 expressing phenotype acquired from negative donors following transplant into uninjured muscles, the percentage of CD34- cells detected in transplanted injured muscles was very consistent and statistically significant (Student's t-test, P#0.05)(Figure 8A, right graph). These results indicated that the presence or absence of CD34 on satellite cells is conditionally dependent on muscle environmental demands and not necessarily hierarchal as initially hypothesized. Because we only studied a short timeframe after injury, it was conversion following the peak of proliferation, we sorted and unclear if later during the course of regeneration, CD34- cells transplanted CD34- cells isolated from muscles of Myf5$^{nlacZ/+}$ ever transitioned back to CD34+. To examine the possibility of mice 3 days post CTX injury directly into uninjured(n=3)and injured (n = 3) quadriceps injected the previous day with CTX (C57BL/6 recipients). In order to detect the Myf5$^{nlacZ/+}$ transgene in donor cells that may have recently fused or formed immature myofibers, we harvested recipient muscles 7 days post transplant. Cyrosections were initially stained with X-gal to identify and validate the presence of Myf5$^{nlacZ/+}$ donor cells. Once b-gal+ cells were identified (Figure S3), adjacent cryosections were stained with antibodies against b-gal, CD34, and aSMA as a marker of newly regenerated myofibers [37,38,39]. Results indicate that activated CD34- donor cells were myogenic as in both injured and uninjured recipient muscles they formed new muscle fibers identified as a-SMA+ with b-gal+ centrally located nuclei (Figure 8B). In addition, we observed mononuclear b-gal+/ CD34+ cells indicating some CD34- cells revert back to a reserve state following injury repair (Figure 8C). Altogether, the analysis of the FACS population dynamics during regeneration and BrdU pulse-chase studies, suggest that the CD34- population is the major myogenic population responsive of regeneration after injury. In addition, the transplant studies indicate that some CD34- negative cells can localize to the satellite cell position and express CD34. We propose a mechanism for this reversible switching of CD34 in response to injury to generate enough differentiating progeny while maintaining the pool of reserve satellite cells during regeneration (Figure 9).

Discussion

In recent years several surface receptors, including CD34, have been described to recognize satellite cells of the skeletal muscle [5]. However, no single surface receptor has proven exclusive to satellite cells, and CD34 is no exception. By utilizing FACS we set out to isolate pure populations of satellite cells using a host of antigens in order to select out contaminating cells that also express CD34. Our results reveal the population of skeletal muscle cells characterized as CD45-/CD31-/Sca1-/CD34+/a72, lack expression of myogenic transcription factors Pax7 and Myf5,do not form myotubes in vitro, nor conform to the satellite cell anatomically defined position under the basal lamina. Therefore, we conclude CD34 alone is inadequate for selecting pure populations of satellite cells from the skeletal muscle.

Since the initial observation by Beauchamp et al. (2000), CD34 has been widely used to identify and isolate satellite cells [9,13,19,40,41,42]. Contrary to the multitude of studies that have examined CD34+ satellite cells, the CD34- minority remained uncharacterized. Initially, we predicted that similar to the hematopoietic system, a linear relationship existed within the satellite cell compartment of skeletal muscle, where more primitive CD34- cells give rise to more committed CD34+ cells. Contrary to our initial hypothesis, our results indicate that following acute injury CD34- cells represent the more myogenically active population. Furthermore, the absence or presence of CD34 is reversible depending on the state of injury.

Currently, an inducible CD34 Cre-Lox reporter model is not available to directly distinguish between downregulation of CD34 or asymmetric division as possible means for CD34 conversion. However, BrdU analysis, myogenin expression/staining and transplant data indicate CD34- cells directly respond and contribute to muscle regeneration following acute injury. Remarkably, despite similar BrdU incorporation at the peak of proliferation between day 2.5–3

post injury, the percentage of CD34+ cells did not change over the course regeneration. Because the absence of CD34 marks a state of activation which seems reversible, the steady percentage of CD34+ cells throughout injury suggests a proportion of myogenic cells are programmed and/or stimulated to maintain a reserve pool of satellite cells during the course of regeneration. This reversible switch from activation to dormancy has also been observed with hematopoietic stem cells as they maintain the stem cell pool following bone marrow injury [43].

Despite their response following acute injury, CD34- cells were quiescent in uninjured muscle. This leaves into question the role of this population during normal muscle homeostasis. Although both CD34+/- populations were equally myogenic in culture, freshly sorted CD34- cells had lower expression of myogenic-related genes such as Pax7, Pax3, Myf5, MyoD, myogenin, CXCR4, and c-met. Furthermore, we and other groups have observed that within 24 hours of being seeded satellite cells lose CD34 in culture, suggesting CD34 is downregulated upon activation [5]. Therefore, CD34- cells appear to represent more ‘‘primed’’ satellite cells poised for injury response that can advance further in the myogenic pathway or upregulate CD34 and revert back to a reserve state depending on the muscle microenvironment. Although CD34’s function has yet to be elucidated, reversibility has been reported with hematopoietic stem cells, suggesting a similar role or pathway of CD34 regulation may exists between tissue specific stem cells [44,45]. Interestingly, despite the major myogenic potential and contribution of CD34+/- cells to muscle regeneration, a minority of Sca1+ (CD45-/CD31-/CD34+) cells sorted from injured muscle was myogenic in culture, suggesting another possible state of transition or stem cell reservoir exists within limb muscles (data not shown)[46].

Although the true function(s) of CD34 remains uncertain, it has been described that this highly glycosylated sialomucin receptor not only plays a role in signaling but is important in promoting both cellular adhesion and repulsion [44], [47]. Interestingly in one study it has been reported that CD34 functions in mast cells to prevent adhesion [48]. Conversely a separate study has reported that CD34 functions to promote lymphocyte adhesion via L-selectin in high endothelial venule cells [49]. Thus, it is possible that the adhesion role of CD34 is dependent on the presence

Figure 9. Summary of significant results and proposed model of CD34 switching by satellite cells following injury. (A) Following acute injury the proportion of CD34- cells drastically increases while the CD34+ populations remains to near uninjured levels. Despite the increase of only CD34- cells, BrdU analysis indicates both populations proliferate shortly after injury (day 3) while CD34+ cells retain BrdU following regeneration (day 14). Such trends indicate that CD34+ population represents the pool of less advanced satellite cells that can generate more differentiated CD34- cells while maintaining their numbers during injury repair. In turn, CD34- cells continue proliferating beyond day 3, indicating this population supplies the differentiated progeny required for complete muscle regeneration. (B) Although more differentiated cells reside within the CD34- population following injury, the absence of CD34 does not terminally mark differentiation as CD34- cells can revert back to the CD34+ pool of less advanced satellite cells. Thus activated myogenic cells can switch CD34 expression in response to injury, suggesting that CD34 may play a role in maintaining a reserve pool of satellite cell in order to prevent depletion during muscle regeneration.

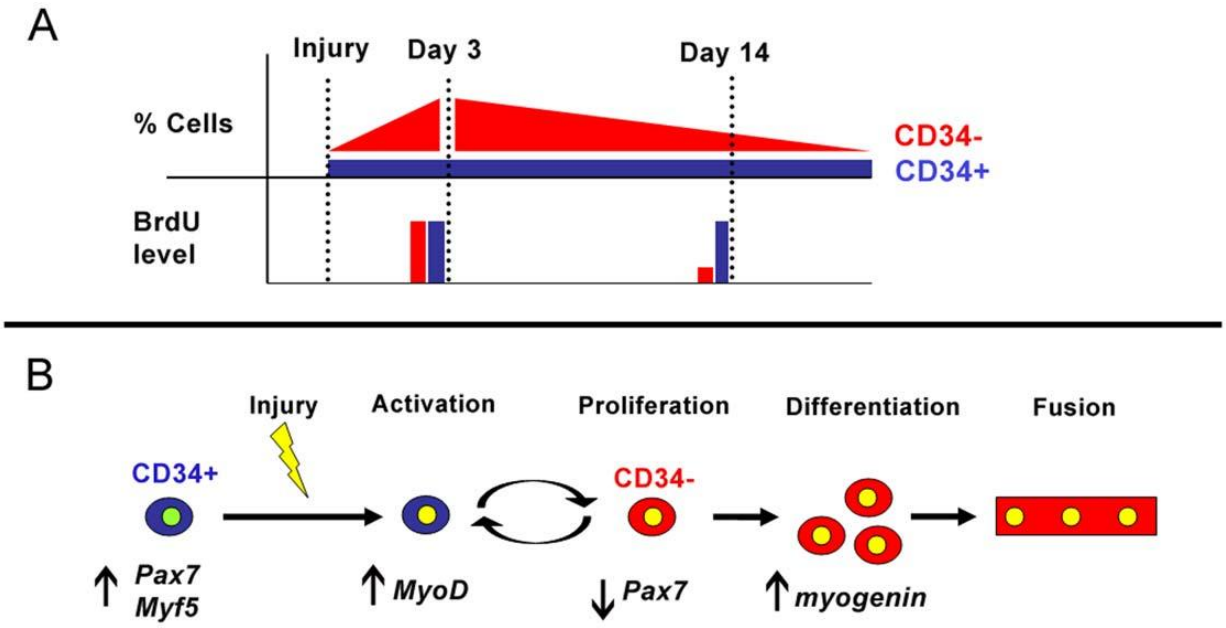

or absence of additional surface receptors as a means to modulate binding or repulsion by various cell types. As aforementioned satellite cells downregulate CD34 in culture, suggesting this receptor functions in maintaining an undifferentiated state. Perhaps such maintenance is linked to adhesion and therefore downregulation of CD34 is required for migration and subsequent engraftment within regions of damaged muscle.

By characterizing skeletal muscle satellite cells based on the presence or absence of CD34 we have identified a key myogenic population responsible for muscle regenerating following acute injury as CD34− (α7+/CD45−/CD31−/Sca1−). In addition we show that the fraction of CD34+ cells remains steady during homeostasis and injury regeneration. Such evidence suggests, despite much heterogeneity, the satellite cell pool is highly regulated in vivo to maintain a reserve pool of CD34+ (α7+/CD45−/CD31−/Sca1−) cells while producing sufficient numbers of differentiated progeny for muscle regeneration.

Materials and Methods

Ethics Statement

This study has been reviewed and approved by the University of Washington's Institution Animal Care and Use Committee.

Mice and Animal Care

All mice used for satellite cell characterization (histology, FACS-analysis of individual muscles and injury, single cell culture, cytocentrifugation, BrdU and expression analysis) were C57BL/6, predominantly 2 month old males. Reporter mice used for cytocentrifugation and/or culture were 1.5 month old $Myf5^{nLacZ/+}$ and 4 month old 3F-nlacZ-2F [5], [50], [51], previously

described in our studies [12], [29]. Transplant donor cells were derived from chicken β-actin promoter driven EGFP or Myf5$^{nLacZ/+}$ reporter mice ages ranging from 6–9 month old [52]. Recipients were C57BL/6, ages ranging from 2–12 months old. Unless specified otherwise, each experimental replicate (n =) represents samples derived from individual animals that were independently processed and analyzed. Mice were housed and maintained in a modified barrier facility located at the University of Washington. All animal experiments were performed in accordance with guidelines approved by the University of Washington's Institution Animal Care and Use Committee

FACS

Methods for muscle processing and FACS were followed as previously described [20]. Typically from pooled preparations including both hind limb muscles, pectorals and triceps ofindividual 2 month old C57BL/6 males, we recover 1.5610^{6} cytocentrifugation, BrdU and expression analysis) were C57BL/6, mononuclear cells per gram of muscle processed. Samples were predominantly 2 month old males. Reporter mice used for initially stained with biotinylated anti-CD34 in 100 ml PBS with cytocentrifugation and/or culture were 1.5 month old Myf5$^{nLacZ/+}$ 0.3% BSA per 10^{6} cells for 45 minutes (min) on ice, then washed and 4 month old 3F-nlacZ-2F [5,50,51], previously described in and resuspended in an antibody cocktail including conjugated our studies [12,29]. Transplant donor cells were derived from streptavidin and directly conjugated anti-CD45/CD31/Sca-1/a7 chicken b-actin promoter driven EGFP or Myf5$^{nLacZ/+}$ reporter for a second 45 min incubation. For single cell deposition DAPI mice ages ranging from 6–9 month old [52]. Recipients were (Sigma) was added for viability and left in solution prior to sorting in order to remove DAPI+ non-viable cells. FACS antibody data, dilutions, combinations

and machine specifications are listed in Methods S1. Data was acquired at 10,000 events per sample and cells sorted with a BD Aria I and later Aria II, both using Diva software. Subsequent analysis and flow cytometry plots were generated using FlowJo v7.2.5 (TreeStar, Inc.). Average population values and standard deviations used for error bars were calculated from the analysis of individual mice. Graphs, Student's t-test and ANOVA statistical analyses were generated using Microsoft Excel 2003. For transplants, culture and cytocentrifugation sorted cells were collected in culture media. For reverse and quantitative PCR, sorted cells were collected in 350 ml RLT lysis buffer (Qaigen) supplemented with b-mercaptoethanol per manufacturers instructions and immediately placed on dry ice and stored at 280uC.

Cell Culture

Clonal cultures were prepared by FACS-Aria mediated single cell deposition into 96 well trays. Non-clonal cultures cells were directly sorted into 1.7 ml tubes containing 750 ml media and seeded manually onto 24 well dishes. All tissue culture dishes were coated with 0.67% (w/v) Type-A Gelatin (Sigma) in H2O and allowed to dry prior to use. Culture media consisted of Ham's F10 supplemented with 15% Horse Serum and final concentration of 2 mM CaCl2, 100 units/ml Penicillin with 100 mg/ml Streptomycin (all from HyClone), and 20 ng/ml bFGF (R&D). Cells were maintained at 37uC, 5%O2, and 5%CO2 and media was changed after 4 days. At day 8 in culture, cells were fixed with 2% formaldehyde (diluted formalin in PBS) and stained with DAPI for counting clones or X-gal for presence of Myf5$^{nlacZ/+}$ or 3F-nlacZ-2F reporter activity. After DAPI staining, photographs of each single cell derived colony was taken and used to quantify proliferation. To avoid counting errors we utilized the ImageJ v1.40 g (Wayne Rasband, NIH) cell counter plugin (Kurt De Vos, University of Sheffield) which automatically tallies events labeled by users. Subsequently every DAPI labeled nuclei including

myonuclei were accounted for in the final cell count. The average cell doubling for each CD34+/- population was calculated based on the number of DAPI+ nuclei counted per colony using the following formula in Microsoft Excel; colony cell doubling = log (# nuclei counted/2).

Stainings

All muscle cryosections were cut 8 mm, fixed with 2% formaldehyde for 5 min, washed 36 with PBS, then stained with respective antibodies. For cytocentrifugation staining, freshly sorted cells were spun onto microscope slides at 800 g RCF, fixed with 4% formaldehyde for 5 min, washed, and then stained. Stainings utilizing biotinylated antibodies were first blocked with Vector labs Streptavidin-Avidin blocking kit. Stainings using mouse primary antibodies were completed using the M.O.M staining kit (Vector labs) with some modification to manufacturer's instruction. Cryosections were incubated overnight at 4uC with the

M.O.M. mouse IgG blocking reagent and streptavidin conjugated fluorophores were used in place of avidin conjugates. All antibodies were diluted in PBS containing 1% BSA (fraction IV, from Fisher) except when prescribed by M.O.M. kit instructions. DAB staining for Pax7 (performed on freshly isolated, cytocentrifuged cells) was completed using the R.T.U. Vectastain Elite and ImmPact DAB substrate kits (both from Vector labs) following manufacturer's instructions. For X-gal staining, cells and tissue sections were fixed for 10 min at room temperature with 2% formaldehyde/0.2% glutaraldehyde and incubated overnight at 37uC with staining solution containing a final concentration of 1 mg/ml X-gal, 5 mM potassium ferricyonide, 5 mM potassium ferrocyonide, and 2 mM CaCl2 (all from Fisher). All stainings included negative controls in which primary antibodies or X-gal was omitted (depicted in Figure S4). Brightfield photographs were taken with Fisher Micromaster digital inverted microscope with Infinity optics using Micron v1.05 software. Immunofluorescent stainings were acquired

with a Zeiss Axiovert 200 microscope equipped with monochrome camera. Controls for immunofluorescent stainings were taken at the same or greater exposure time as primary stained samples. Monochromatic photographs were colored then merged with Adobe Photoshop v9.0.2. When necessary to reduce background, certain photos' brightness and contrast levels were adjusted within individual channels prior to coloring. A list of primary and secondary antibodies, dilutions and microscope specifications are described in the Methods S1.

Reverse-Transcription and Quantitative-RT-PCR

Methods and reagents for PCR reactions have been previously described by us [20]. Briefly RNA was purified from sorted cells using Qaigens RNeasy kit. All reactions were two-step beginning with cDNA synthesis followed by conventional or quantitative PCR for specific target genes. The following thermal cycling conditions were used: 95uC-79 initial activation followed by 94uC300;57uC-300;72uC-450, for 35 cycles. Quantitative PCR reactions were run on an ABI 7900HT PCR system using sybr green PCR master mix. Results were analyzed using SDS 2.2 software and relative expressions calculated by comparative Ct method. cDNA from unsorted muscle mononuclear cells (Figure 1B) or whole muscle (Figures 4B and 6C) were used for calibration. The endogenous control was GAPDH. Ct values are listed in the Table S1. Each sample was derived from specific cell populations sorted from individual mice. Reactions for each respective sample and gene were run in triplicate. The relative expression between samples was used to calculate the average expression values and SEM for error bars represented in each figure. Primer sequences for each target gene are listed in Methods S1.

Injury and Transplants

Muscle injury was induced by directly injecting 50 ml and 100 ml per TA and quadriceps, respectively, of 10 mM Naja nigrcollis cardiotoxin (Calbiochem) in PBS. Donor cells were

sorted as CD45-/CD31-/Sca1-/a7+/CD34+ and CD34- from injured chicken actin promoter driven EGFP or Myf5$^{nlacZ/+}$ limb muscles injected with CTX 3 days prior to isolation. Cells were directly injected in 15–20 ml collection media, into uninjured or injured quadriceps treated with CTX the day prior to cell transplantation. For GFP cell analysis each recipients qaudricep (n = 12, 6 injured 1 day prior and 6 uninjured) was transplanted with 50,000 sorted CD34+/- cells. Recipients of GFP cells were euthanized 3 days post transplant and GFP donor cells were analyzed by FACS vs. uninjected injured and uninjured controls. Donor GFP cells represented ,1% of all a7+ (CD45-/CD31-/ Sca1-) cells. Quadriceps (n = 6, 3 injured/3 uninjured) injected with 10,000 Myf5$^{nlacZ/+}$ CD34- sorted cells were harvested 7 days post transplant and frozen in OCT for subsequent staining. For negative control, 50,000–150,000 sorted Myf5$^{nlacZ/+}$ (CD45-/ CD31-/Sca1-) a7-cells (n = 2) were transplanted along with a single SHAM (media only) injection into uninjured quadriceps.

BrdU Incorporation and Analysis

For each pulse 250 ml of 4 mg/ml BrdU (Sigma) in PBS was administered daily via intraperitoneal injection. CD34+/- cells were sorted from limb muscles, fixed with 4% formaldehyde for 5 minutes, washed with PBS and left overnight at 4uC. Tibialis and femur bone marrows were collected as a positive control for BrdU incorporation by flushing the tibia and femur with a 28 gauge needle. Fixed cells were processed and stained with PE conjugated anti-BrdU antibody (BD) according to manufacturer's protocol. Briefly cells were further fixed with 70% EtOH, denatured with 2 M HCL, and stained in PBS containing 0.5% Tween20 and 0.5% BSA. Sorted cells were identified as DAPI positive and BrdU incorporation was defined by comparing positive bone marrow cells with IgG isotype stained controls.

Chapter 1Supplementary Material: Available online at PLoS One.org. pone.0010920.

Chapter 1 References

1. Collins CA, Olsen I, Zammit PS, Heslop L, Petrie A, et al. (2005) Stem cell function, self-renewal, and behavioral heterogeneity of cells from the adult muscle satellite cell niche. Cell 122: 289–301.

2. Mauro A (1961) Satellite cell of skeletal muscle fibers. J Biophys Biochem Cytol 9: 493–495.

3. Seale P, Sabourin LA, Girgis-Gabardo A, Mansouri A, Gruss P, et al. (2000) Pax7 is required for the specification of myogenic satellite cells. Cell 102:777–786.

4. Relaix F, Montarras D, Zaffran S, Gayraud-Morel B, Rocancourt D, et al. (2006) Pax3 and Pax7 have distinct and overlapping functions in adult muscle progenitor cells. J Cell Biol 172: 91–102.

5. Beauchamp JR, Heslop L, Yu DSW, Tajbakhsh S, Kelly RG, et al. (2000) Expression of CD34 and Myf5 defines the majority of quiescent adult skeletal muscle satellite cells. Journal of Cell Biology 151: 1221–1233.

6. Cornelison DD, Wold BJ (1997) Single-cell analysis of regulatory gene expression in quiescent and activated mouse skeletal muscle satellite cells. DevBiol 191: 270–283.

7. Covault J, Sanes JR (1986) Distribution of N-CAM in synaptic and extrasynaptic portions of developing and adult skeletal muscle. J Cell Biol 102: 716–730.

8. Cerletti M, Jurga S, Witczak CA, Hirshman MF, Shadrach JL, et al. (2008) Highly efficient, functional engraftment of skeletal muscle stem cells in dystrophic muscles. Cell 134: 37–47.

9. Ratajczak MZ, Majka M, Kucia M, Drukala J, Pietrzkowski Z, et al. (2003) Expression of functional CXCR4 by muscle satellite cells and secretion of SDF-1 by muscle-derived fibroblasts

is associated with the presence of both muscle progenitors in bone marrow and hematopoietic stem/progenitor cells in muscles.Stem Cells 21: 363–371.

10. Rooney JE, Gurpur PB, Yablonka-Reuveni Z, Burkin DJ (2009) Laminin-111 restores regenerative capacity in a mouse model for alpha7 integrin congenital myopathy. Am J Pathol 174: 256–264.

11. Yablonka-Reuveni Z, Day K, Vine A, Shefer G (2008) Defining the transcriptional signature of skeletal muscle stem cells. J Anim Sci 86: E207–216. 12. Day K, Shefer G, Richardson JB, Enikolopov G, Yablonka-Reuveni Z (2007) Nestin-GFP reporter expression defines the quiescent state of skeletal muscle satellite cells. Dev Biol 304: 246–259.

13. Montarras D, Morgan J, Collins C, Relaix F, Zaffran S, et al. (2005) Direct Isolation of Satellite Cells for Skeletal Muscle Regeneration. Science 309:2064–2067.

14. Kuang S, Kuroda K, Le Grand F, Rudnicki MA (2007) Asymmetric self-renewal and commitment of satellite stem cells in muscle. Cell 129: 999–1010. 15. Day K, Shefer G, Shearer A, Yablonka-Reuveni Z (2010) The depletion of
skeletal muscle satellite cells with age is concomitant with reduced capacity of single progenitors to produce reserve progeny. Developmental Biology 340: 330–343.

16. Montarras D, Morgan J, Collins C, Relaix F, Zaffran S, et al. (2005) Direct isolation of satellite cells for skeletal muscle regeneration. Science 309: 2064–2067.

17. Bosnakovski D, Xu Z, Li W, Thet S, Cleaver O, et al. (2008) Prospective isolation of skeletal muscle stem cells with a Pax7 reporter. Stem Cells 26: 3194–3204

18. Sherwood RI, Christensen JL, Conboy IM, Conboy MJ, Rando TA, et al. (2004) Isolation of adult mouse myogenic progenitors: functional heterogeneity of cells within and engrafting skeletal muscle. Cell 119: 543–554.

19. Sacco A, Doyonnas R, Kraft P, Vitorovic S, Blau HM (2008) Self-renewal and expansion of single transplanted muscle stem cells. Nature 456: 502–506. 20. Ieronimakis N, Balasundaram G, Reyes M (2008) Direct isolation, culture and transplant of mouse skeletal muscle derived endothelial cells with angiogenic potential. PLoS One 3: e0001753.

21. Asakura A, Seale P, Girgis-Gabardo A, Rudnicki MA (2002) Myogenic specification of side population cells in skeletal muscle. J Cell Biol 159: 123–134. 22. Blanco-Bose WE, Yao CC, Kramer RH, Blau HM (2001) Purification of mouse primary myoblasts based on alpha 7 integrin expression. Exp Cell Res 265: 212–220.

23. Osawa M, Hanada K, Hamada H, Nakauchi H (1996) Long-term lymphohe- matopoietic reconstitution by a single CD34-low/negative hematopoietic stem cell. Science 273: 242–245.

24. Hawke TJ, Garry DJ (2001) Myogenic satellite cells: physiology to molecular biology. J Appl Physiol 91: 534–551.

25. Halevy O, Piestun Y, Allouh MZ, Rosser BW, Rinkevich Y, et al. (2004) Pattern of Pax7 expression during myogenesis in the posthatch chicken establishes a model for satellite cell differentiation and renewal. Dev Dyn 231: 489–502.

26. Yao CC, Breuss J, Pytela R, Kramer RH (1997) Functional expression of the alpha 7 integrin receptor in differentiated smooth muscle cells. J Cell Sci 110(Pt13): 1477–1487.

27. Silva R, D'Amico G, Hodivala-Dilke KM, Reynolds LE (2008) Integrins: the keys to unlocking angiogenesis. Arterioscler Thromb Vasc Biol 28: 1703–1713.

28. Zammit P, Beauchamp J (2001) The skeletal muscle satellite cell: stem cell or son of stem cell? Differentiation 68: 193–204.

29. Kirillova I, Gussoni E, Goldhamer DJ, Yablonka-Reuveni Z (2007) Myogenic reprogramming of retina-derived cells following their spontaneous fusion with myotubes. Dev Biol 311: 449–463.

30. Zammit PS, Relaix F, Nagata Y, Ruiz AP, Collins CA, et al. (2006) Pax7 and myogenic progression in skeletal muscle satellite cells. Journal of Cell Science 119: 1824–1132.

31. Day K, Paterson B, Yablonka-Reuveni Z (2009) A distinct profile of myogenic regulatory factor detection within Pax7+ cells at S phase supports a unique role of Myf5 during posthatch chicken myogenesis. Dev Dyn 238: 1001–1009.

32. Yablonka-Reuveni Z, Rivera AJ (1994) Temporal expression of regulatory and structural muscle proteins during myogenesis of satellite cells on isolated adult rat fibers. Dev Biol 164: 588–603.

33. Kastner S, Elias MC, Rivera AJ, Yablonka-Reuveni Z (2000) Gene expression patterns of the fibroblast growth factors and their receptors during myogenesis of rat satellite cells. J Histochem Cytochem 48: 1079–1096.

34. Gnocchi VF, White RB, Ono Y, Ellis JA, Zammit PS (2009) Further characterisation of the molecular signature of quiescent and activated mouse muscle satellite cells. PLoS ONE 4: e5205.

35. Yan Z, Choi S, Liu X, Zhang M, Schageman JJ, et al. (2003) Highly coordinated gene regulation in mouse skeletal muscle regeneration. J Biol Chem 278:8826–8836.

36. d'Albis A, Couteaux R, Janmot C, Roulet A, Mira JC (1988) Regeneration after cardiotoxin injury of innervated and denervated slow and fast muscles of mammals. Myosin isoform analysis. Eur J Biochem 174: 103–110.

37. Springer ML, Ozawa CR, Blau HM (2002) Transient production of alpha- smooth muscle actin by skeletal myoblasts during differentiation in culture and following intramuscular implantation. Cell Motil Cytoskeleton 51: 177–186.

38. Shefer G, Wleklinski-Lee M, Yablonka-Reuveni Z (2004) Skeletal muscle satellite cells can spontaneously enter an alternative mesenchymal pathway.J Cell Sci 117: 5393–5404.

39. Graves DC, Yablonka-Reuveni Z (2000) Vascular smooth muscle cells spontaneously adopt a skeletal muscle phenotype: a unique Myf5(-)/MyoD(+) myogenic program. J Histochem Cytochem 48: 1173–1193.

40. Volonte D, Liu Y, Galbiati F (2005) The modulation of caveolin-1 expression controls satellite cell activation during muscle repair. Faseb J 19: 237–239. 41. Oustanina S, Hause G, Braun T (2004) Pax7 directs postnatal renewal and propagation of myogenic satellite cells but not their specification. Embo J 23: 3430–3439.

42. Le Grand F, Jones AE, Seale V, Scime A, Rudnicki MA (2009) Wnt7a activates the planar cell polarity pathway to drive the symmetric expansion of satellite stem cells. Cell Stem Cell 4: 535–547.

43. Wilson A, Laurenti E, Oser G, van der Wath RC, Blanco-Bose W, et al. (2008) Hematopoietic stem cells reversibly switch from dormancy to self-renewal during homeostasis and repair. Cell 135: 1118–1129.

44. Nielsen JS, McNagny KM (2008) Novel functions of the CD34 family. J Cell Sci 121: 3683–3692.

45. Sato T, Laver JH, Ogawa M (1999) Reversible expression of CD34 by murine hematopoietic stem cells. Blood 94: 2548–2554.

46. Kafadar KA, Yi L, Ahmad Y, So L, Rossi F, et al. (2009) Sca-1 expression is required for efficient remodeling of the extracellular matrix during skeletal muscle regeneration. Dev Biol 326: 47–59.

47. Lanza F, Healy L, Sutherland DR (2001) Structural and functional features of the CD34 antigen: an update. J Biol Regul Homeost Agents 15: 1–13.

48. Nielsen JS, McNagny KM (2009) CD34 is a key regulator of hematopoietic stem cell trafficking to bone marrow and mast cell progenitor trafficking in the periphery. Microcirculation 16: 487–496.

49. Baumheter S, Singer MS, Henzel W, Hemmerich S, Renz M, et al. (1993) Binding of L-selectin to the vascular sialomucin CD34. Science 262: 436–438.

50. Tajbakhsh S, Bober E, Babinet C, Pournin S, Arnold H, et al. (1996) Gene targeting the myf-5 locus with nlacZ reveals expression of this myogenic factor in mature skeletal muscle fibres as well as early embryonic muscle. Dev Dyn 206: 291–300.

51. Kelly R, Alonso S, Tajbakhsh S, Cossu G, Buckingham M (1995) Myosin light chain 3F regulatory sequences confer regionalized cardiac and skeletal muscle expression in transgenic mice. J Cell Biol 129: 383–396.

52. Okabe M, Ikawa M, Kominami K, Nakanishi T, Nishimune Y (1997) 'Green mice' as a source of ubiquitous green cells. FEBS Lett 407: 313–319.

Chapter 2

Endothelial cell response to injury

Primer

Blood flow is essential for proper muscle function, maintenance and repair. Endothelial cells of the vasculature play a prominent role in regulating blood pressure and flow (1). In skeletal muscle, satellite cells reside in close proximity to vascular endothelial cells and conduct paracrine signaling (2). Although studies have suggested that satellite cells can adopt non-myogenic fates (3), lineage tracing has confirmed the commitment of satellite cells exclusively towards myogenesis (4). While satellite cells function to reconstitute damaged muscle fibers (ref), the source of vascular endothelial cells during the course of regeneration remaines unknown. Circulating endothelial progenitor cells (EPCs) have the potential to reconstitute damaged macrovasculature (5). Yet, the contribution of EPCs to the skeletal muscle microvasculature remains in question. Therefore, we sought to understand the origin of the regenerating muscle vasculature, a vital component of the skeletal muscle that is crucial for muscle function.

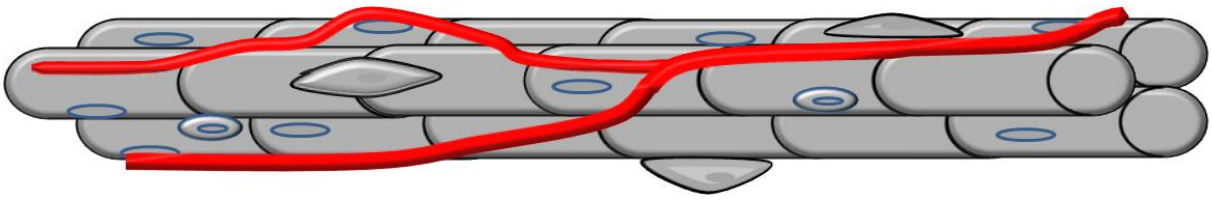

1. Duplain H, Burcelin R, Sartori C, Cook S, Egli M, Lepori M, et al. Insulin resistance, hyperlipidemia, and hypertension in mice lacking endothelial nitric oxide synthase. Circulation. 2001;104(3):342-5. PubMed PMID: 11457755.
2. Christov C, Chretien F, Abou-Khalil R, Bassez G, Vallet G, Authier FJ, et al. Muscle satellite cells and endothelial cells: close neighbors and privileged partners. Molecular biology of the cell. 2007;18(4):1397-409. doi: 10.1091/mbc.E06-08-0693. PubMed PMID: 17287398; PubMed Central PMCID: PMC1838982.
3. Shefer G, Wleklinski-Lee M, Yablonka-Reuveni Z. Skeletal muscle satellite cells can spontaneously enter an alternative mesenchymal pathway. Journal of cell science. 2004;117(Pt 22):5393-404. doi: 10.1242/jcs.01419. PubMed PMID: 15466890.
4. Kanisicak O, Mendez JJ, Yamamoto S, Yamamoto M, Goldhamer DJ. Progenitors of skeletal muscle satellite cells express the muscle determination gene, MyoD. Developmental biology. 2009;332(1):131-41. doi: 10.1016/j.ydbio.2009.05.554. PubMed PMID: 19464281; PubMed Central PMCID: PMC2728477.
5. Asahara T, Masuda H, Takahashi T, Kalka C, Pastore C, Silver M, et al. Bone marrow origin of endothelial progenitor cells responsible for postnatal vasculogenesis in physiological and pathological neovascularization. Circulation research. 1999;85(3):221-8. PubMed PMID: 10436164.

Bone marrow-derived cells do not engraft into skeletal muscle microvasculature but promote angiogenesis after acute injury.

Nicholas Ieronimakis, Aislinn Hays, and Morayma Reyes

Departments of Pathology and Lab Medicine, University of Washington School of Medicine, Seattle, Wash., USA

Reproduced from Experimental Hematology, published Dec 03, 2011. 40:238-249.

Abstract

The skeletal muscle is supported by a vast network of microvessels with the capacity to regenerate in response to injury. However, the dynamics of microvascular repair and the origin of reconstituted endothelial cells in the skeletal muscle are poorly understood. A growing body of literature exists to indicate bone marrow (BM)Lderived cells engraft into regenerating vascular endothelium and muscle macrovasculature. Therefore, we investigated the extent of BM contribution to skeletal muscle microvasculature after acute injury. Because reporters and markers commonly used to trace donor BM cells are not endothelial specific but are also expressed by leukocytes, we generated novel BM chimeras utilizing Tie2-green fluorescent protein BM cells transplanted into CD31 and Caveolin-1 knockout recipients. In turn, we surveyed BM vascular contribution, not just by the presence of green fluorescent protein, but also CD31 and Caveolin-1, respectively. After stable BM reconstitution, chimera limb muscles were cardiotoxin (CTX) injured and examined 21 days post-injury for the presence of green fluorescent protein, CD31, and Caveolin-1. Acute muscle injury by CTX is characterized by

initial microvasculature death followed by rapid endothelial regeneration within 14 days post-damage. Histological analysis of injured and uninjured contralateral limb muscles revealed a complete absence of BM engraftment in the muscle vasculature of wild-type and CD31/Caveolin-1 knockout chimeras. In contrast, F4/80+ cells isolated from CTX-injured muscle, expressed endothelial-related markers and promoted angiogenesis in vitro. Therefore, despite the absence of BM engraftment to regenerated skeletal muscle microvasculature, macrophages recruited after injury promote angiogenesis and, in turn, vascular regeneration

Introduction

For proper function and maintenance, the skeletal muscle relies on an extensive vascular network. Damage to muscle vasculature by injury or disease can lead to ischemia, which promotes debilitating and sometimes fatal conditions such as gangrene, nonhealing wounds, and peripheral artery disease. In contrast to muscle fiber regeneration, which has been extensively studied in acute injury models, regeneration of the skeletal muscle microvasculature has not been critically examined [1]. To date, various cell populations, including peripheral blood and bone marrow (BM)derived cells, have been reported to promote angiogenesis and contribute to muscle vasculature [2–6]. However, many of the markers used to evaluate vascular contribution, including Tie2 and CD31, are not exclusive to endothelial cells and can be expressed by circulating leukocytes, including monocytes [7–11]. Due to such overlap, putative vascular regeneration by BMderived populations is not easily distinguished from inflammatory cells responding to injury. Therefore, it remains unclear whether cells of BM origin actually contribute to regenerated endothelium or assist in the muscle repair process.

In this study, we examined muscle vascular regeneration using the cardiotoxin (CTX) model of acute injury. CTX injury is characterized by initial massive tissue destruction followed by full

regeneration within 3 weeks [12,13].To assess the effects of CTX on muscle vasculature in vivo, we surveyed different time points after injury and observed an initial decline in skeletal muscle endothelial cells, followed by regeneration to almost uninjured levels by day 14 post-injury. 5-Bromo-2-deoxyuridine (BrdU) and 5-ethynyl-2 deoxyuridine (EdU) incorporation indicates that endothelial cells, irrespective of their origin, proliferated in response to injury. To elucidate if vascular regeneration could be attributed to BM-derived cells, we generated Tie2-green fluorescent protein (GFP) BM chimeras utilizing CD31 and Caveolin-1 knockout (KO) mice [14,15]. Such models allowed us to effectively distinguish BM contribution into regenerating vasculature, not just by the presence of the Tie2-promoterdriven GFP, but also CD31 and Caveolin-1, respectively [16]. Because impaired angiogenesis has been reported in both KO models, we hypothesized that these environments will favor Tie2-GFP BM contribution to vasculature after injury [14,15,17,18]. Mobilization defects of BM endothelial progenitors have been reported in Caveolin1deficient mice, adding to the selective advantage of normal BM in Caveolin-1 KO mice [19]. To exclude inflammatory monocytes responding to injury that may also express these markers, we examined chimeric animals 21 days after injury. Our results show the muscle endothelium was void of GFP in all chimeras and CD31/Caveolin-1 in each respective KO model, indicating that after acute injury, BM cells do not engraft in regenerated vasculature. In turn, as suggested by previous studies, we demonstrate that macrophages recruited in response to muscle injury promote angiogenesis [20–22].

Methods

All mouse models used in this study were procured from Jackson Labs and are detailed in the Supplementary Methods (online only, available at www.exphem.org). Animals were housed and

maintained at the University of Washington in a modified barrier facility. Procedures used in this study were performed under the approval and guidance of the University of Washington's Institution Animal Care and Use Committee. Detailed experimental procedures and antibody specifics are included in the Supplementary Methods and Tables E1 and E2 (online only, available at www.exphem.org).

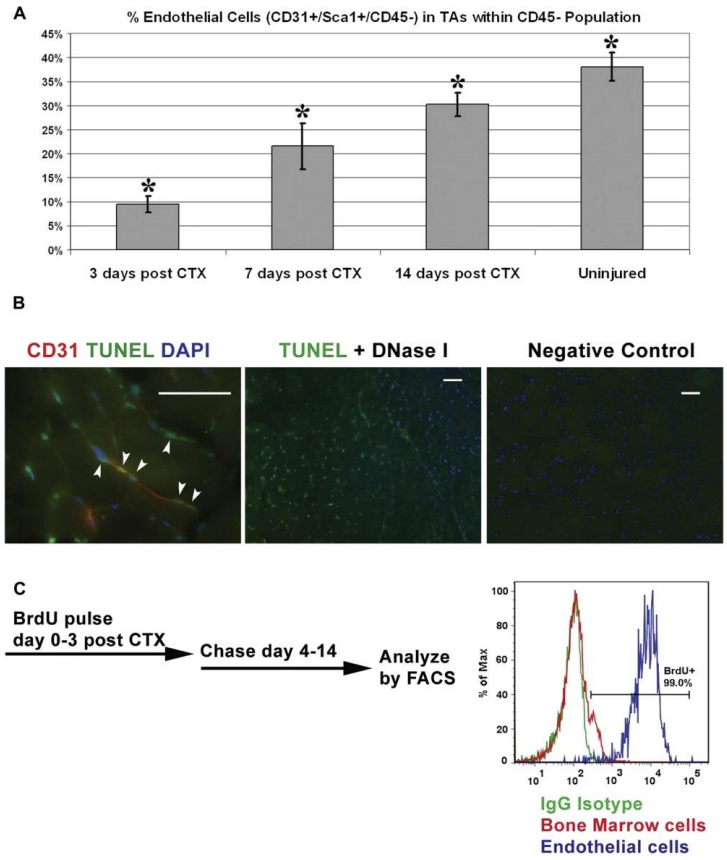

Figure 1. Endothelial cell decline after acute injury is attributed to cell death. (**A**) Time course FACS analysis of left TA muscles (n = 5 C57BL/6 per time point) after CTX injury reveals the proportion of endothelial cells (EC) identified as $CD45^{-}$, $Sca1^{+}$, $CD31^{+}$, initially declines but returns to near uninjured levels by day 14 post-injury. TAs of uninjured animals were used for comparison. *Statistically significant between each group by single factor analysis of variance; $p < 0.0005$. Error bars = standard error of mean. (**B**) Staining of injured C57BL/6 muscle, 3 days post-CTX injury for cell death, reveals $CD31^{+}$, terminal deoxynucleotidyl transferase dUTP nick end labeling (TUNEL)–positive vessels (arrowheads). DNase1-treated muscle served as a positive control. TUNEL staining in green corresponds to fluorescein isothiocyanate and CD31 in red with Alexa Fluor 594. Scale bar = 50 μm. (**C**) FACS analysis of BrdU pulse-chase in CTX injured limb muscles (TA, quadriceps, gastrocnemius) indicates EC ($CD45^{-}$, $Sca1^{+}$, $CD31^{+}$ sorted cells) retain a high levels of BrdU incorporated within the first 3 days post-injury vs BM mononuclear cells (n = 3 C57BL/6). As indicated by the gate, approximately 99% of all EC retained BrdU by day 14 post-injury.

Results

After acute muscle injury, endothelial cells decline but quickly regenerate

To investigate vascular regeneration in skeletal muscle, we induced acute injury with CTX and examined endothelial decline by fluorescent-activated cell sorting (FACS) analysis in wild-type

(WT) C57BL/6 mice [23]. In order to establish the kinetics of injury response, we analyzed three time points at days 3, 7, and 14 post-injury as compared to undamaged tibialis anterior (TA) muscles (n 5 5 animals per time point). Only left TAs were injured and analyzed, while uninjured TAs from a separate group of mice were used as control for comparison. It has been demonstrated that endothelial cells are susceptible to CTX in vitro and the muscle capillary density declines with CTX injury [24–26]. In accordance with these reports, we observed, by FACS analysis, a rapid decline in the proportion of CD45- , Sca1+, CD31+ endothelial cells, 3 days post-injury (Fig. 1A) [23]. Terminal deoxynucleotidyl transferase dUTP nick end labeling assay confirmed the initial endothelial cell decline observed 3 days post-injury was due to cell death (Fig. 1B). Roughly 56% of CD31+ cells observed in fields of CTX injury were positive for nuclear localized terminal deoxynucleotidyl transferase dUTP nick end labeling staining. In contrast to the initial decline, during the course of regeneration, the proportion of endothelial cells increased at 7 days post-injury and reached almost uninjured levels by day 14.

To assess if myogenic proliferation precedes endothelial cell regeneration, we conducted a BrdU pulse-chase experiment. CTX injury activates myogenic cells, with proliferation climaxing at day 3 post-injury [13,27]. Thus, we chose to pulse animals (n=3 C57BL/6) for the first 3 days of injury and chase from days 4 to 14. We predicted that if endothelial cells and/or progenitors followed the same course of myogenic proliferation, there would be a significant amount of BrdU incorporation and retention. Alternatively, if endothelial cells proliferate after the peak of myogenic cell division beyond 3 days post-injury, there would be low BrdU incorporation by day 14. Thus, low BrdU incorporation would indicate the vascular response is stimulated after the peak of myogenic cell proliferation. In contrast, results indicate proliferation occurred early after injury, as endothelial cells retained a high degree of BrdU relative to BM cells, which

continuously turn over and thus retained low amounts after the 10-day chase (Fig. 1C). Early proliferation indicated that resident surviving endothelial cells or circulating progenitors are activated and orchestrated with the myogenic response immediately after injury.

To further evaluate the course of vascular proliferation after injury, we examined by histology, EdU incorporation in injured muscles from Tie2-GFP transgenic mice. Analogous to BrdU, EdU is incorporated into DNA during replication [16]. In contrast, EdU can be surveyed without acid or heat-mediated DNA denaturization, which often leads to loss of GFP and antigen recognition. To identify vascular cells, we stained with Caveolin-1 and examined EdU incorporation in muscles 3 and 7 days post-CTX injury. Contralateral uninjured muscles were also surveyed for EdU incorporation. Staining revealed EdU+, Caveolin1+ cells in regenerating vasculature of injured muscles, confirming that vascular cells had proliferated directly after injury (Fig. 2). To our surprise, GFP fluorescence at days 3 and 7 post-CTX injury was absent in Caveolin-1^{þ} cells, suggesting the Tie2-GFP transgene is not active or expression is not sufficient for GFP to be

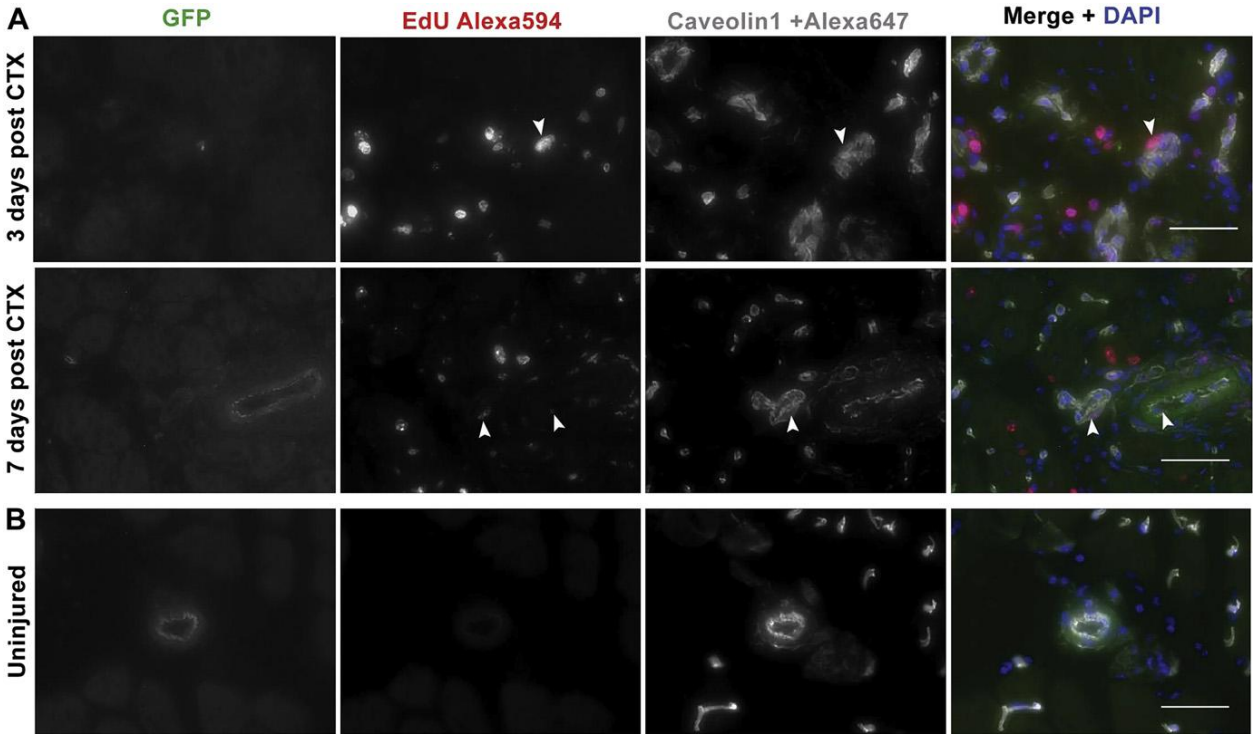

Figure 2. Vascular regeneration begins directly following muscle injury. (**A**) Staining for EdU incorporation and vascular cells with anti−Caveolin-1 at 3 days and 7 days post-CTX injury in muscles from Tie2-GFP reporter animals, reveals vascular cells proliferated directly after injury to replace the damaged endothelium. Arrows point to EdU^+, $Caveolin^+$ cells within injured areas of muscle. Surprisingly, GFP was not readily visible, suggesting the transgene is not expressed during the early stages of vascular regeneration and remodeling. (**B**) Staining for EdU in uninjured contralateral muscles indicates an absence of incorporation. However, Tie2-promoter−driven GFP was visible in the undamaged endothelium. Scale bars = 50 μm

visible above background fluorescence during the early stages of vascular regeneration. In contrast, Tie2-promoterdriven GFP was visible in vessels of uninjured contralateral muscles. However, we did not observe EdU incorporation in uninjured contralateral muscles. Therefore, vascular regeneration is not mediated by proliferating endothelial cells residing in distal muscles, but occurs from resident cells that survive injury or cells adjacent to the injured areas within the same muscle or adjacent muscles. Moreover, these data indicate damaged or dead skeletal muscle endothelium can repair itself after acute injury.

Chimera KO models are effective systems for identifying BM-derived vascular contribution

High BrdU/EdU incorporation and retention during the first 3 days after injury suggested angiogenesis from regenerating damaged endothelium or neighboring undamaged vessels may be accompanied by alternate sources, such as BM-derived progenitors. Because the majority of endothelial regeneration after CTX injury occurs within 14 days, we hypothesized that such rapid vascular reconstitution could not occur without contribution from cells of BM origin. To test our hypothesis, we generated BM chimeras using Tie2-GFP donor BM. Muscle vasculature in this reporter model expresses Tie2-promoterdriven GFP and stains positive for CD31 and Caveolin-1 (Fig. 3A). Because no single marker is exclusive to endothelial cells, and Tie2 is no exception, we generated BM chimeras in CD31 and Caveolin-1 KO models (n 5 6 chimeras, 2= C57BL/6,

2= CD31 KO, 2= Caveolin-1 KO) (Fig. 3B). Such models allowed us to identify vascular contribution not only by the presence of GFP, but also CD31 and Caveolin-1 protein, respectively. In addition, due to delayed angiogenesis in these KO models, normal donor BM cells would incur a selective advantage over resident endothelial cells or progenitors [17,18]. o assess BM vascular contribution in response to injury, we injected CTX in left limb muscles; TA, quadriceps, and gastrocnemius. Contralateral limb muscles were left uninjured to survey potential contribution in the absence of injury. Our characterization in the aforementioned results

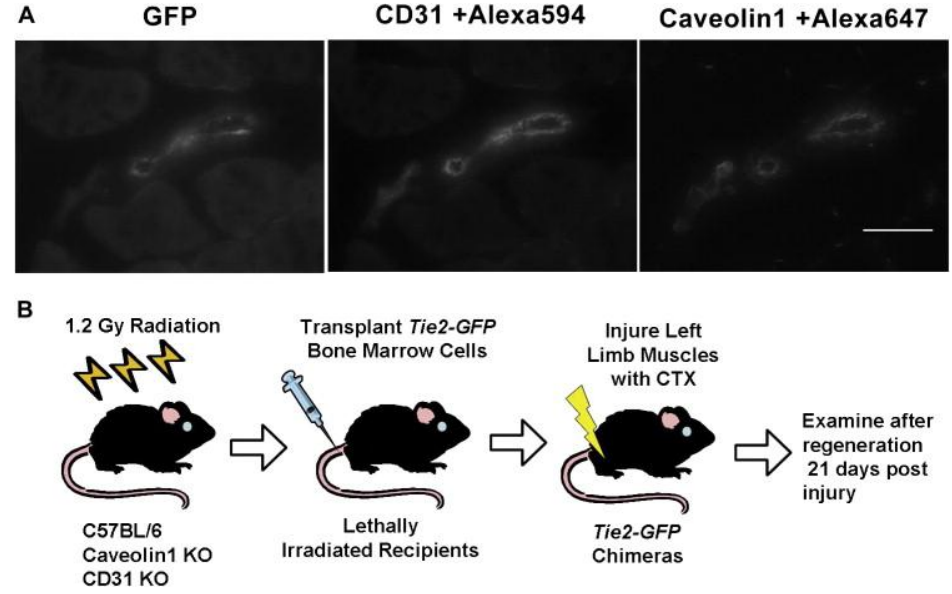

indicates CTX injury is ideal for studying endothelial regeneration, as the majority of microvessels are massively damaged immediately after injury and rapidly repaired within 2 weeks. To distinguish definitive vascular contribution from vessel-associated

Figure 3. Tie2-GFP reporter animals express GFP in skeletal muscle vasculature and harbor the CD45.1 alloantigen, making them ideal for chimera generation. (**A**) Analysis of muscle cross sections reveals Tie2-promoter−driven GFP is expressed by muscle endothelial cells and colocalizes with CD31 and Caveolin-1 staining. Scale bar = 50 μm. (**B**) Experimental schematic of allogeneic chimera generation using Tie2-GFP BM into donors and C57BL/6, CD31, and Caveolin-1 KO mice, and subsequent injury. (**C**) FACS analysis of chimera limb-derived BM mononuclear cells reveals the average reconstitution of donor BM based on the percentage of $CD45^+$ cells was ~90% between all chimeras analyzed (n = 6). C57BL/6 BM cells express the CD45.2 alloantigen (left graph). Conveniently, we discovered that Tie2-GFP animals on the FVB/N background express the CD45.1 (middle graph). Thus donor cells in BM chimeras are easily distinguishable from recipients that express CD45.2 (right graph). (**D**) FACS analysis of endothelial cells from Tie2-GFP limb muscles indicates detecting of GFP by flow cytometry after enzymatic muscle digestion is compromised. As compared to the unstained control, 95% to 97% of endothelial cells identified as $CD45^-$, $CD31^+$ in Tie2-GFP and C57BL/6 muscles, stained positive for Tie2. In contrast, GFP was detected in only 57% of $Tie2^+$ endothelial cells. Therefore, FACS is not an accurate method for detecting Tie2-GFP^+ endothelial cells in skeletal muscles of BM chimeras.

inflammation that occurs in response to damage, we chose to survey muscles after complete repair, 21 days post-CTX injury (Fig. 3B). At this time point, WT muscles are fully regenerated with little or no inflammatory cells remaining. To quantify BM reconstitution, we mismatched alloantigen donors and recipients. Conveniently, we discovered that the FVB/N background Tie2-GFP reporter model harbors the strain-specific CD45.1 alloantigen. Thus, donor BM cells are easily distinguished from the CD45.2 expressed by C57BL/6 and related models, including CD31 and Caveolin-1 KO mice. FACS analysis of BM mononuclear cells collected from each recipient at the end of the experiment indicated 90% of all CD45+ cells were donor (CD45.1+)-derived (Fig. 3C).

To date, a number of studies have identified BM engraftment to vasculature via histological analysis [2,3,5,6]. For our study, we initially sought to utilize a combination of histological and FACS analysis for identifying and quantifying BM-derived endothelial cells. By histological analysis, capillary, venous, and arteriole endothelial cells in uninjured Tie2-GFP skeletal muscles

are all visibly positive for GFP. In order to assess the sensitivity and immunophenotype of GFP+ endothelial cells by flow cytometry, we conducted a validation experiment comparing Tie2-GFP and C57BL/6 limb muscles by FACS (Fig. 3D). Following our previously published FACS methods and characterization, we identified muscle endothelial cells as CD45- and CD31+ [23]. In turn, the majority (95% to 97%) of endothelial cells analyzed from both Tie2-GFP and C57BL/6 limb muscles stained positive for Tie2. However, from Tie2-GFP muscles, GFP was not detectable in 38% of Tie2+ (CD45-, CD31+) endothelial cells. The discrepancy between Tie2 immunostaining and GFP may be attributed to the loss of GFP in cells whose membranes have been compromised by mechanical processing and enzymatic digestion. Such processing is commonly utilized and necessary for disassociating mononuclear cells from myofibers for FACS analysis and/or cell sorting [28–30]. In turn, mononuclear cell isolation preserved antigen detection, but severely compromised detection of cells that express GFP under the Tie2 promoter, making this approach impractical for detecting Tie2-GFP BM engraftment in skeletal muscle vasculature. Therefore, we chose to detect vascular engraftment by histological analysis for GFP and anti-GFP staining in order to ensure accurate detection of Tie2-GFP+ cells in BM chimeras.

BM cells did not engraft into regenerated muscle vasculature

After muscle regeneration 21 days post-CTX injury, we harvested and froze injured and uninjured limb muscles (e.g., TAs, gastrocnemius, and quadriceps) for histological analysis. Initially, we sectioned and surveyed transverse cross sections for the presence of GFP. Relative to limb muscles processed the same day from Tie2-GFP mice, we did not detect any GFP signal in the vessels of BM chimeric animals (Fig. 4A). Few GFP+ cells were present only in regions with persistent inflammation in injured muscles of Caveolin-1 and CD31 KO mice. In contrast,

C57BL/6 chimera muscles did not harbor significant inflammation 21 days post-injury and were

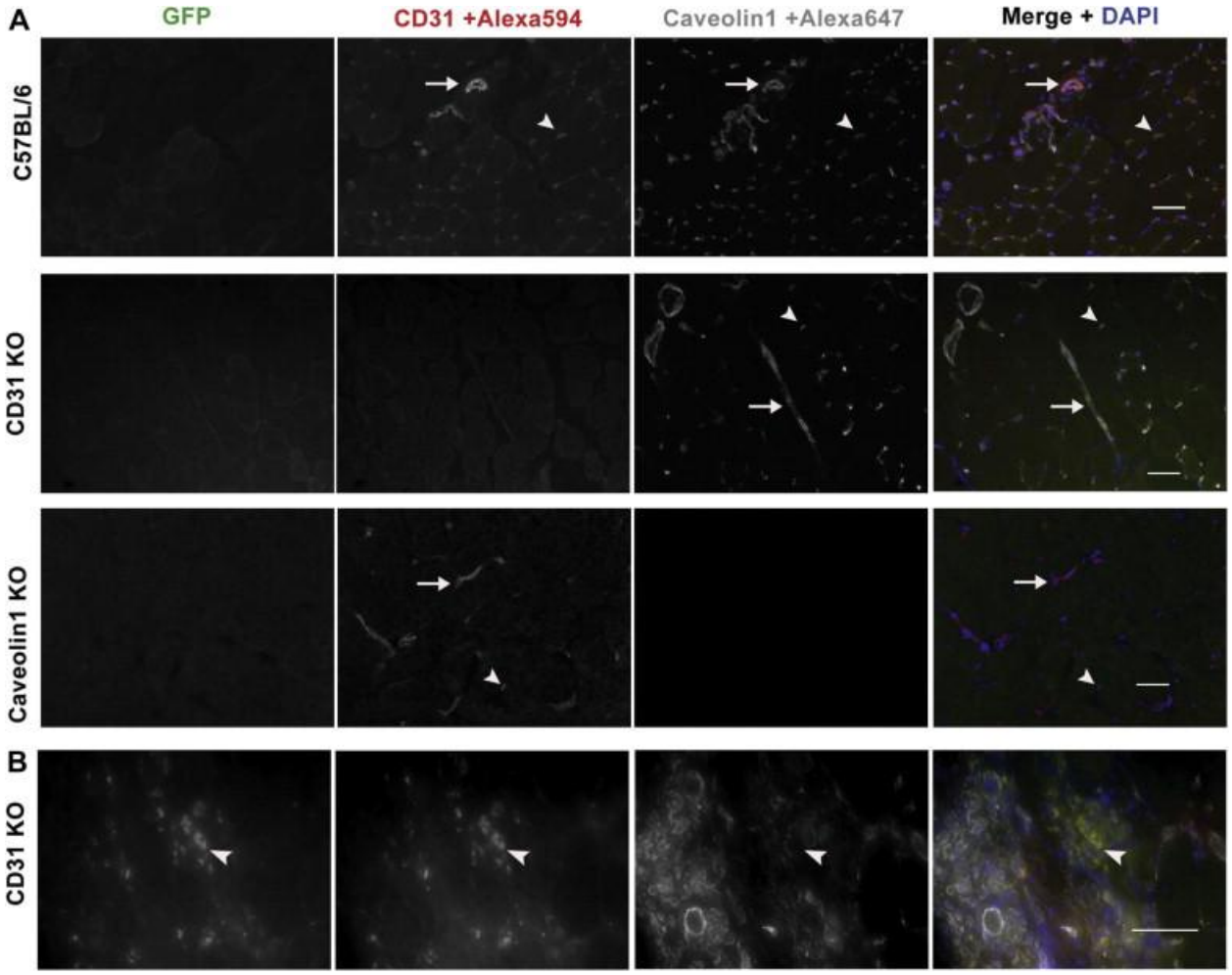

Figure 4. Absence of BM vascular contribution after acute injury. (**A**) Histological analysis revealed an absence of GFP in the regenerated muscle vasculature of all chimeric animals. Staining for CD31 and Caveolin-1 confirm the absence of BM-derived cells in the endothelium of larger vessels (arrow) and capillaries (arrowhead pointing to one of many) of injured muscles (quadriceps shown) of KO animals. Vessels in uninjured contralateral muscles were also negative for GFP and CD31/Caveolin-1 in each respective KO (not shown). (**B**) GFP^+ cells were only observed in regions of persistent inflammation only in CD31 and Caveolin-1 KO mice (CD31 KO shown). *Tie2-GFP*$^+$ BM-derived inflammatory cells were positive for CD31 but negative for Caveolin-1 (arrowhead). Scale bars = 50 μm.

completely void of GFP-positive cells. To confirm our findings, we surveyed multiple cross sections (six per muscle, spaced out 200 mm longitudinal distance) stained for CD31 and Caveolin-1 from each BM recipient. Staining confirmed the absence of BM cell contribution to

vasculature, as indicated by the lack of CD31 and Caveolin-1 immunoreactivity in the vessels of each respective KO chimera (Fig. 4A). Once more, we only observed GFP^{þ} inflammatory cells that stained positive for CD31, but negative for Caveolin-1, in CD31 and Caveolin-1 KO mice (Fig. 4B). Negative vascular staining in each respective KO demonstrated antibody specificity. In contrast, the presence of antigen was validated by staining C57BL/6 control chimeras, which showed robust signals for CD31 and Caveolin-1 in vessels. Interestingly, analogous to our results in CTX-injured muscles, uninjured contralateral muscles surveyed in parallel were completely void of GFP and immunostaining for each respective KO protein. As a final test to confirm our finding, we conducted anti-GFP staining. In line with the aforementioned results, we did not observe GFP staining in the vessels of injured or uninjured chimeric muscles relative to control Tie2-GFP muscle (Fig. 5A). Once more, only in Caveolin-1 and CD31 KO chimeras, where inflammatory cells persisted in injured muscles, did we observe cells that stained positive for anti-GFP. These GFP+ cells also stained positive for vascular endothelial growth factor receptor 2 (VEGFR2 or Flk-1), but were not incorporated into vessels (Fig. 5B). Although BM-derived endothelial progenitors have been reported to express VEGFR2, recent reports have shown macrophages and blood-derived hematopoietic progenitors that do not give rise to endothelial cells also express VEGFR2 [6,31,32].

Figure 5. BM-derived cells were present only in areas with persistent inflammation in the injured muscles of KO chimeras. (**A**) Staining for anti-GFP confirmed a complete absence of BM cells in regenerated muscles of C57BL/6 chimeras. GFP was detected only in areas with persistent inflammation in the injured muscles of CD31 and Caveolin-1 KO animals (not shown here). Tie2-GFP muscle processed in parallel with chimeras indicates GFP was preserved and colocalized with antibody staining. (**B**) BM-derived Tie2-GFP^{+} cells (arrowheads) detected with anti-GFP in KO chimeras (CD31 KO shown), stained positive for VEGFR2 and were adjacent to VEGFR2^{+} vessels (arrows). Inset (top left of merge) highlights the proximity of VEGFR2^{+} vessels and anti-GFP^{+}, VEGFR2^{+} cells. Scale bar = 50 μm.

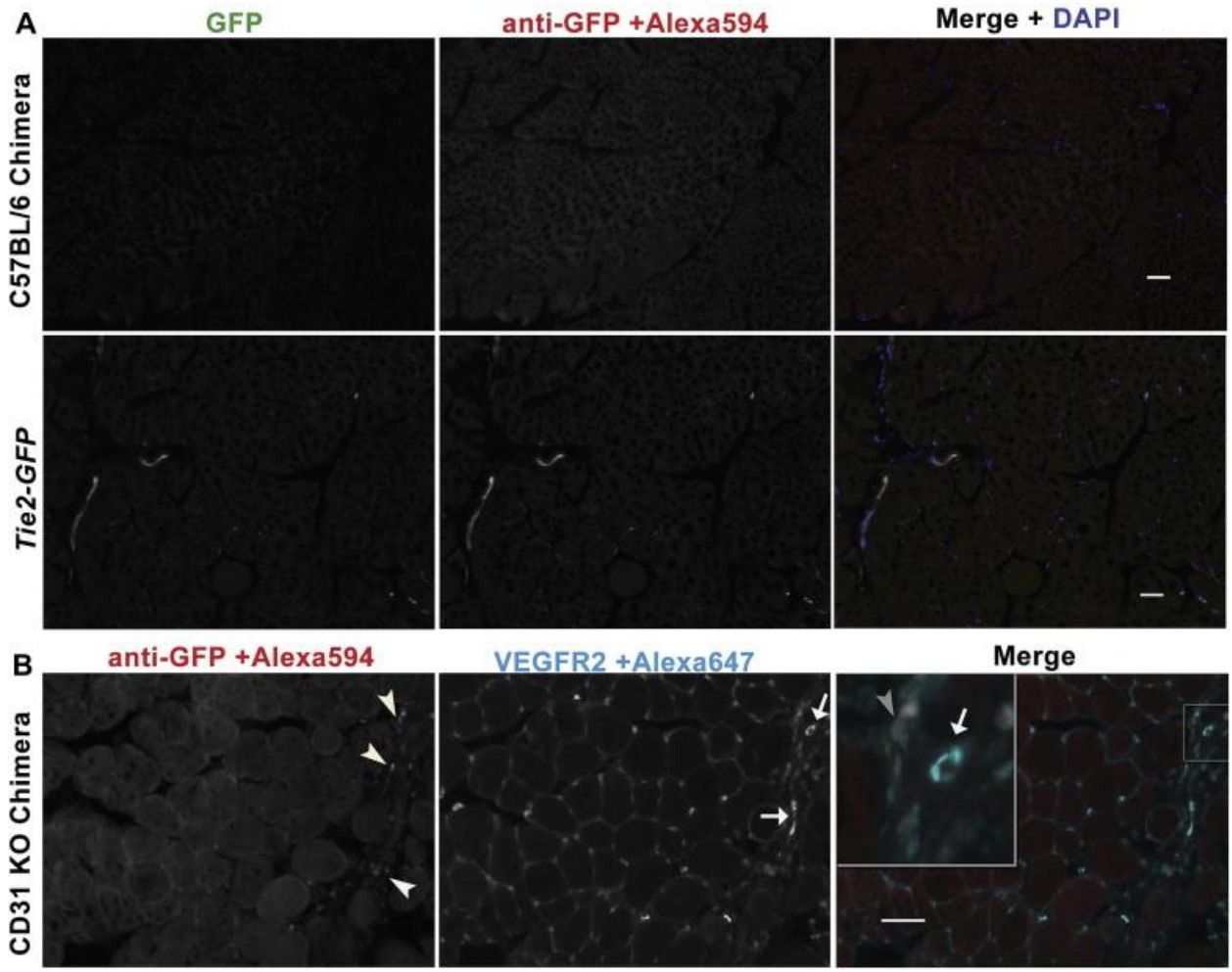

Although we did not observe GFP+ cells in vessels, we stained for CD45 to confirm the hematopoietic phenotype of Tie2-GFP+, VEGFR2+ cells observed in the injured muscles of

CD31 and Caveolin-1 KO BM chimeras. Staining results demonstrate BM-derived Tie2-GFP+

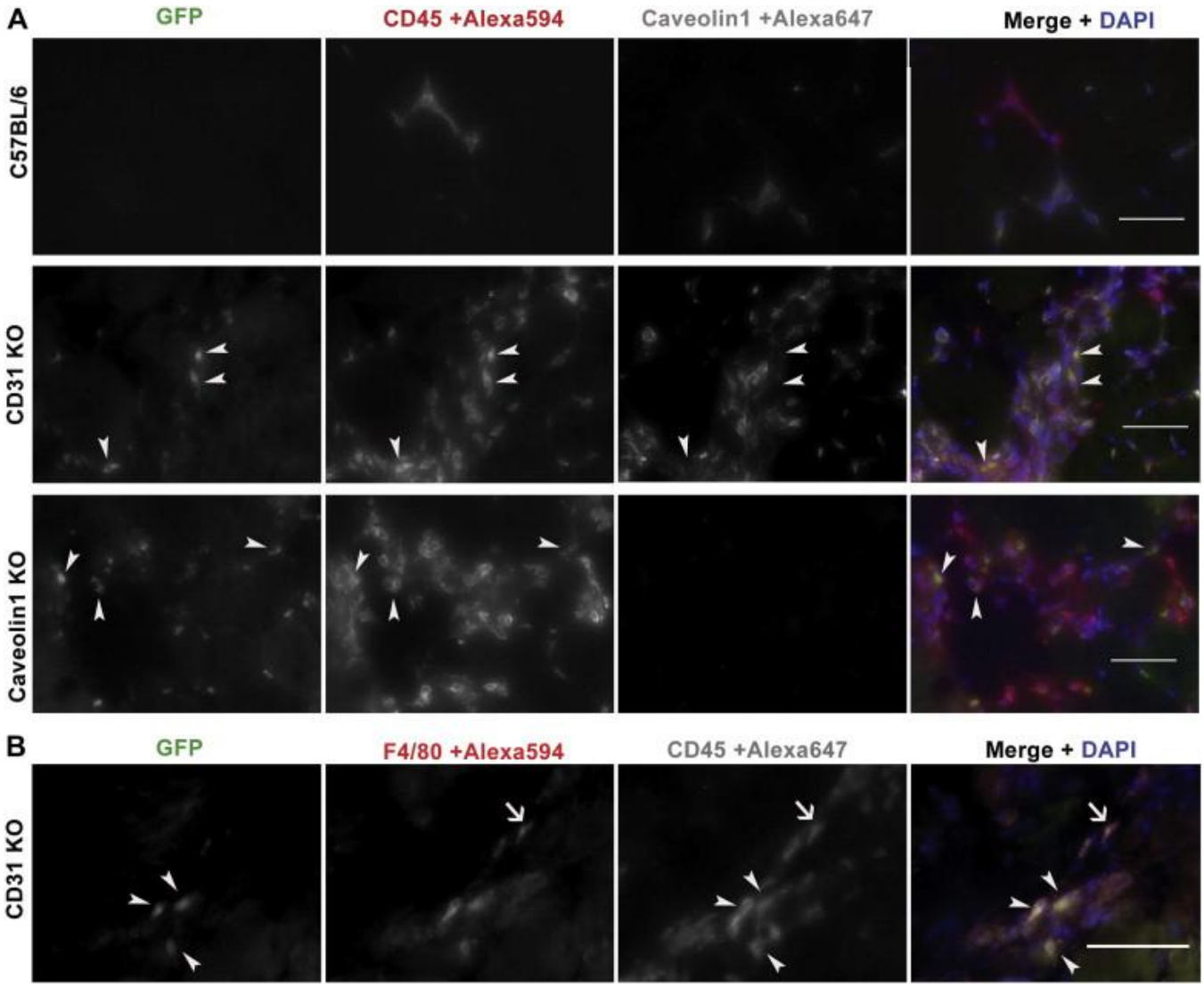

Figure 6. Tie2-GFP$^+$ BM cells represent inflammatory cells that do not engraft to regenerated muscle microvasculature. (**A**) Tie2-GFP$^+$ cells (arrowheads) observed only in CD31 and Caveolin-1 KO chimeras are remnant or persistent inflammatory cells that stain positive for CD45, but negative for Caveolin-1. The absence of Caveolin-1 staining in Caveolin-1 KO chimeras confirms that only vascular cells, but not Tie2-GFP$^+$ and/or CD45$^+$ inflammatory cells, are positive for Caveolin-1. The observed close proximity of Tie2-GFP$^+$ BM-derived cells to Caveolin-1$^+$ vascular cells may obscure the identification of engraftment from vessel-associated inflammation, when only one marker or reporter common to both cell types is used. Scale bar = 50 μm. (**B**) Staining for the macrophage marker F4/80 reveals a proportion of F4/80$^+$ cells express Tie2-GFP (arrowheads). Although all F4/80$^+$ cells were CD45$^+$, not all were positive for GFP (arrow). Scale bar = 50 μm.

cells present only in CD31 and Caveolin-1 KO chimeras are CD45+, Caveolin-1+ , and localized near and sometimes adjacent to Tie2-GFP+ Caveolin-1+ vascular cells (Fig. 6). BM-derived endothelial progenitor cells have been reported to express Caveolin-1, but not CD45 [19,31]. Therefore, we inferred Tie2-GFP+ cells were remnant inflammatory cells and not BM-derived endothelial cells or progenitors, as they were positive for CD45 but negative for Caveolin-1. In some cases, due to very close proximity, some Caveolin-1+ vascular cells appear to overlap with CD45+ inflammatory cells. However, the absence of Caveolin-1 staining in Caveolin-1 KO chimeras confirms Tie2-GFP+ and/or CD45+ inflammatory cells are indeed negative for Caveolin-1. Therefore, we did not detect BM-derived vascular incorporation in regenerated muscle microvasculature, but rather persistent inflammatory cells that express Tie2, CD31, and VEGFR2, all markers associated with leukocytes and endothelial cells. Further characterization revealed that some Tie2-GFP+,CD45+ cells observed in KO chimeras were also positive for F4/80, a marker of murine macrophages [33]. All F4/80+ cells were consistently positive for CD45, but not for GFP (Fig. 6B). Tie2+ macrophages have been reported proangiogenic and, therefore, the presence of F4/80+, Tie2-GFP+ cells indicates that persistent inflammatory cells remain to promote angiogenesis, which is perturbed in CD31 and Caveolin-1 KO chimeras [8,10,21,22,34,35].

Macrophages responding to muscle injury promote angiogenesis

Recently, it has been reported that a reduction of F4/80+ cells in muscle 3 days post-CTX injury from CCR2 null mice was associated with lower levels of VEGF and decreased capillary density during the course of regeneration [21]. Therefore, we hypothesized that F4/80+ macrophages, which infiltrate muscle immediately after injury, directly promote angiogenesis. To investigate the angiogenic role of macrophages, we isolated CD45+, F4/80+ cells 3 days post-CTX injury

for coculture with skeletal muscle endothelial cells on Matrigel and monitored vascular tube formation (Fig. 7A, B). In order to account for potential vascular engraftment in vitro, CD45+, F4/80+ cells were isolated from animals that ubiquitously express GFP in all cells [36]. For comparison, CD45+, F4/80- cells were also cocultured and analyzed for endothelial-related markers vs CD45+, F4/80+ cells by FACS (Fig. 7A). Interestingly, although a large proportion of CD45+ cells present in limb muscles 3 days post-CTX injury were Tie2+ and Sca1+, few CD45+, F4/80- cells were positive for VEGFR2 and vascular endothelial cadherin. In contrast, 30% of F4/80+ cells were positive for VEGFR2 and vascular endothelial cadherin. Coculture experiments revealed both FACS-sorted CD45+,F4/80- populations did not form vascular tubes,

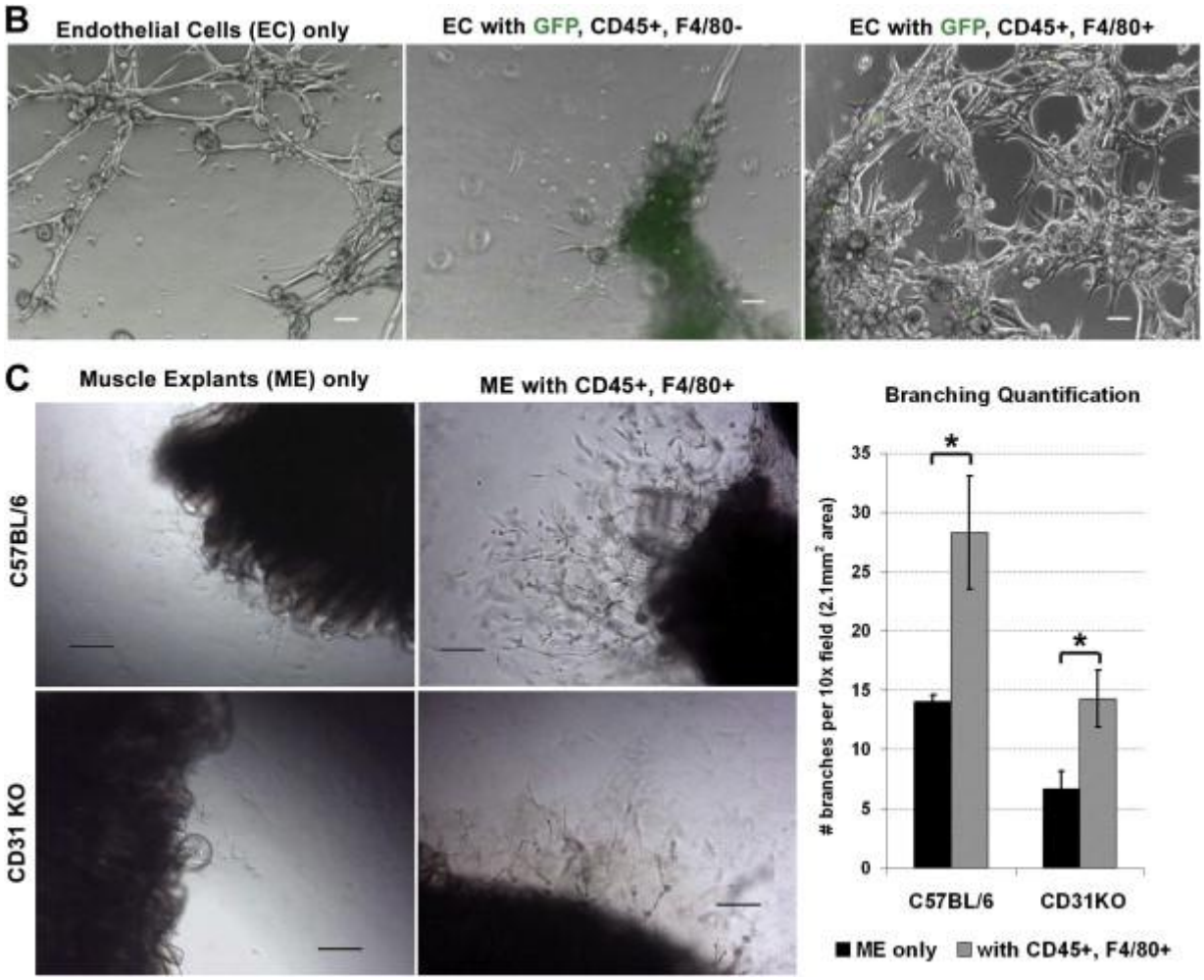

Figure 7. F4/80^{+} macrophages recruited following muscle injury promote skeletal muscle microvascular angiogenesis in vitro. (**A**) FACS analysis and sorting schematic from a pool of limb muscles 3 days post-CTX injury, the time point preceding vascular regeneration. CD45^{+} cells from injured muscles were selected and sorted as F4/80^{+} and F4/80^{-} for coculture experiments. An IgG isotype control conjugated to phycoerythrin (PE) was used to confirm the absence of nonspecific staining. Aliquots taken from the same preparation labeled with CD45 and F4/80 were stained with PE-conjugated antibodies against Tie2, VEGFR2, vascular endothelial cadherin, and Sca1 to analyze the presence of each respective antigen on CD45^{+}, F4/80^{+} (middle row of histograms) and CD45^{+}, F4/80^{-} cells (bottom row of histograms). Histogram red peaks represent the unstained control, blue peaks represent stained experimental samples. Percentages represent the proportion of event within gates (horizontal black bars) for each respective population. (**B**) Coculture of skeletal muscle microvascular endothelial cells with GFP expressing CD45^{+}, F4/80^{-}, or F4/80^{+} cells, reveals only F4/80^{+} cells (macrophages) promote vascular tube formation on Matrigel. Although neither population engrafted with vascular tubes, GFP^{+} cells were observed in close proximity to endothelial cells. Scale bar = 50 μm. (**C**) CD45^{+}, F4/80^{+} cells FACS-sorted 3 days post-CTX injury, promote vascular sprouting from both uninjured C57BL/6 and CD31 KO TA muscle explants (n = 3 explants per condition) seeded on Matrigel. Scale bar = 100 μm *$p \leq 0.05$ by two-tailed Student's t-test.

as indicated by the absence of GFP in vascular tubes, but were closely associated with GFP endothelial cells. However, only F4/80- cells promoted angiogenesis, while F4/80- cells appeared to impede vascular tube formation (Fig. 7B).

To further investigate the role of macrophages in promoting angiogenesis, we examined vascular branching from uninjured muscle explants plated on Matrigel, in the presence or absence of F4/80+ cells, once more isolated 3 days post-CTX injury. In contrast to aorta ring explants, skeletal muscle explants produce little vascular sprouting without robust proangiogenic intervention [37–39]. Therefore, muscle explants are ideal for evaluating the proangiogenic role or F4/80+ macrophages. [18]. 10 days of culture, vascular sprouting was signifi-ined [5]. BM-derived endothelial progenitors not only share scantly greater with F4/80+ cells in both WT and CD31 marker profiles with leukocytes, but have also been re-KO explants (Fig. 7C). Altogether, such results indicate ported to be indistinguishable from monocytes in vitro that macrophages responding to muscle injury directly [11,40,41]. Therefore, legitimate endothelial contribution

promote angiogenesis. Furthermore, neither CD45+, F4/80+ macrophages nor CD45+, F/4/80- cells formed individual vascular tubes or engrafted with cocultured endothelial cell vascular tubes, supporting the absence of BM suggesting previous studies may have misinterpreted results engraftment in muscle vasculature observed in vivo.

Discussion

Although vasculature contribution by BM-derived cells has been reported for hindlimb ischemia injury, only single markers that are also expressed by leukocytes were examined [5]. BM-derived endothelial progenitors not only share marker profiles with leukocytes, but have also been reported to be indistinguishable from monocytes in vitro [11,40,41]. Therefore, legitimate endothelial contribution

by BM-derived cells is difficult to distinguish from inflammatory cells present after injury. Furthermore, the engraftment of BM cells to tumor vasculature has been challenged, suggesting previous studies may have misinterpreted results by relying on single reporters, such as Tie2, that alone are not exclusive to endothelial cells [42]. Alternatively, differences in hindlimb ischemia may be permissive to BM cell vascular contribution, which varies from localized toxin injury that does not target the macrovasculature. With CTX injury, microvascular endothelial cell death and decline precedes massive vascular regeneration within 3 weeks of injury. In contrast, hindlimb ischemia injury models target the macrovasculature but have also been reported to result in muscle microvascular decline [43,44]. Therefore, although hindlimb ischemia injury models present more obvious clinical relevance, CTX injury is a simple and technically straightforward model to study localized microvascular regeneration.

In this report, utilizing novel system chimeras, we conclude that BM-derived cells do not engraft with regenerating muscle microvasculature. In concordance with many reports, we

observed that BM-derived cells express common endothelial markers, such as Tie2, CD31, and VEGFR, but were not present in the regenerated vascular endothelium. Rather, BM-derived cells, which stained negative for Caveolin-1, were in close proximity to Caveolin-1+ vascular cells and not clearly distinguished by single-marker characterization. Although leukocytes play a significant role in injury repair, our data indicate an absence of BM-derived endothelial contribution to skeletal muscle vascular regeneration in vivo [22,45]. Alternatively, BM contribution is transient and regresses once bona fide endothelial cells reconstitute damaged vasculature. Furthermore, we did not detect any BM-derived cells in the vessels of uninjured muscles or with in vitro vascular tube formation, supporting the notion that BM contribution occurs in a transient manner under muscle duress or is injury model specific. Thus, we conclude that if BM engraftment occurs, the event is temporary and not a permanent facet of vascular regeneration in skeletal muscle after toxin-induced acute injury. In contrast, the presence of macrophages in KO chimeras highlights the role of BM cells in vascular regeneration. Subsequent experiments demonstrated that, in contrast to CD45+, F4/80- cells present after injury, a greater proportion of macrophages (CD45+, F4/80+) were positive for endothelial-related markers VEGFR2 and vascular endothelial cadherin, and promoted vessel formation in vitro. Future research is warranted to elucidate the role(s) of macrophage/monocyte subpopulations in skeletal muscle vascular regeneration and in angiogenic impaired models, such as CD31 and Caveolin-1 KO animals.

Chapter 2 Supplementary Material: Available online at ScienceDirect., Experimental Hematology Volume42, Issue 3.

Chapter 2 References

1. Ciciliot S, Schiaffino S. Regeneration of mammalian skeletal muscle. Basic mechanisms and clinical implications. Curr Pharm Des. 2010; 16:906–914.

2. Al-Khaldi A, Al-Sabti H, Galipeau J, Lachapelle K. Therapeutic angiogenesis using autologous bone marrow stromal cells: improved blood flow in a chronic limb ischemia model. Ann Thorac Surg. 2003;75:204–209.

3. Fan CL, Gao PJ, Che ZQ, Liu JJ, Wei J, Zhu DL. Therapeutic neovascularization by autologous transplantation with expanded endothelial progenitor cells from peripheral blood into ischemic hind limbs. Acta Pharm Sin. 2005;26:1069–1075.

4. Zhang HK, Zhang N, Wu LH, et al. Therapeutic neovascularization with autologous bone marrow CD34 þ cells transplantation in hin- dlimb ischemia. Chin J Surg. 2005;43:1275–1278.

5. Asahara T, Masuda H, Takahashi T, et al. Bone marrow origin of endothelial progenitor cells responsible for postnatal vasculogenesis in physiological and pathological neovascularization. Circ Res. 1999;85:221–228.

6. Asahara T, Murohara T, Sullivan A, et al. Isolation of putative progenitor endothelial cells for angiogenesis. Science. 1997;275:964–967.

7. Kim SJ, Kim JS, Papadopoulos J, et al. Circulating monocytes expressing CD31: implications for acute and chronic angiogenesis. AmJ Pathol. 2009;174:1972–1980.

8. De Palma M, Venneri MA, Galli R, et al. Tie2 identifies a hematopoietic lineage of proangiogenic monocytes required for tumor vessel formation and a mesenchymal population of pericyte progenitors.Cancer Cell. 2005;8:211–226.

9. Fujiyama S, Amano K, Uehira K, et al. Bone marrow monocyte lineage cells adhere on injured endothelium in a monocyte chemoattractant protein-1-dependent manner and accelerate reendothelialization as endothelial progenitor cells. Circ Res. 2003;93:980–989.

10. Venneri MA, De Palma M, Ponzoni M, et al. Identification of proangiogenic TIE2-expressing monocytes (TEMs) in human peripheral blood and cancer. Blood. 2007;109:5276–5285.

11. Rehman J, Li J, Orschell CM, March KL. Peripheral blood ‘‘endothelial progenitor cells’’ are derived from monocyte/macrophages and secrete angiogenic growth factors. Circulation. 2003;107:1164–1169.

12. d’Albis A, Couteaux R, Janmot C, Roulet A, Mira JC. Regenerationafter cardiotoxin injury of innervated and denervated slow and fast muscles of mammals. Myosin isoform analysis. Eur J Biochem. 1988;174:103–110.

13. Yan Z, Choi S, Liu X, et al. Highly coordinated gene regulation in mouse skeletal muscle regeneration. J Biol Chem. 2003;278:8826– 8836.

14. Duncan GS, Andrew DP, Takimoto H, et al. Genetic evidence for functional redundancy of platelet/endothelial cell adhesion molecule-1 (PECAM-1): CD31-deficient mice reveal PECAM-1-dependent and PECAM-1-independent functions. J Immunol. 1999;162:3022–3030.

15. Razani B, Engelman JA, Wang XB, et al. Caveolin-1 null mice are viable but show evidence of hyperproliferative and vascular abnormalities. J Biol Chem. 2001;276:38121–38138.

16. Motoike T, Loughna S, Perens E, et al. Universal GFP reporter for the study of vascular development. Genesis. 2000;28:75–81.

17. Woodman SE, Ashton AW, Schubert W, et al. Caveolin-1 knockout mice show an impaired angiogenic response to exogenous stimuli. Am J Pathol. 2003;162:2059–2068.

18. Solowiej A, Biswas P, Graesser D, Madri JA. Lack of platelet endothelial cell adhesion molecule-1 attenuates foreign body inflammation because of decreased angiogenesis. Am J Pathol. 2003;162:953–962.

19. Sbaa E, Dewever J, Martinive P, et al. Caveolin plays a central role in endothelial progenitor cell mobilization and homing in SDF-1-driven postischemic vasculogenesis. Circ Res. 2006;98:1219–1227.

20. Arnold L, Henry A, Poron F, et al. Inflammatory monocytes recruited after skeletal muscle injury switch into antiinflammatory macrophages to support myogenesis. J Exp Med. 2007;204:1057–1069.

21. Ochoa O, Sun D, Reyes-Reyna SM, et al. Delayed angiogenesis and VEGF production in CCR2-/- mice during impaired skeletal muscle regeneration. Am J Physiol. 2007;293:R651–R661.

22. Martinez CO, McHale MJ, Wells JT, et al. Regulation of skeletal muscle regeneration by CCR2-activating chemokines is directly related to macrophage recruitment. Am J Physiol. 2011;299:R832–R842.

23. Ieronimakis N, Balasundaram G, Reyes M. Direct isolation, culture and transplant of mouse skeletal muscle derived endothelial cells with angiogenic potential. PloS One. 2008;3:e0001753.

24. Wu PL, Lee SC, Chuang CC, et al. Non-cytotoxic cobra cardiotoxin A5 binds to alpha(v)beta3 integrin and inhibits bone resorption. Identification of cardiotoxins as non-RGD integrin-binding proteins of the Ly-6 family. J Biol Chem. 2006;281:7937–7945.

25. Ou YJ, Leung YM, Huang SJ, Kwan CY. Dual effects of extracellular Ca2+ on cardiotoxin-induced cytotoxicity and cytosolic Ca2+ changes in cultured single cells of rabbit aortic endothelium. Biochim Biophys Acta. 1997;1330:29–38.

26. Vignaud A, Hourde C, Medja F, Agbulut O, Butler-Browne G, FerryA. Impaired skeletal muscle repair after ischemia-reperfusion injury in mice. J Biomed Biotechnol. 2010;724914.

27. Ieronimakis N, Balasundaram G, Rainey S, Srirangam K, Yablonka-Reuveni Z, Reyes M. Absence of CD34 on murine skeletal muscle satellite cells marks a reversible state of activation during acute injury. PloS One. 2010;5:e10920.

28. Sacco A, Doyonnas R, Kraft P, Vitorovic S, Blau HM. Self-renewal and expansion of single transplanted muscle stem cells. Nature.2008;456:502–506.

29. Kuang S, Kuroda K, Le Grand F, Rudnicki MA. Asymmetric self- renewal and commitment of satellite stem cells in muscle. Cell. 2007;129:999–1010.

30. Joe AW, Yi L, Natarajan A, et al. Muscle injury activates resident fibro/adipogenic progenitors that facilitate myogenesis. Nat Cell Biol. 2010;12:153–163.

31. Case J, Mead LE, Bessler WK, et al. Human CD34+ AC133+ VEGFR-2+ cells are not endothelial progenitor cells but distinct, primitive hematopoietic progenitors. Exp Hematol. 2007;35:1109–1118.

32. Dineen SP, Lynn KD, Holloway SE, et al. Vascular endothelial growth factor receptor 2 mediates macrophage infiltration into orthotopic pancreatic tumors in mice. Cancer Res. 2008;68:4340–4346. 33. Austyn JM, Gordon S. F4/80, a monoclonal antibody directed specif-ically against the mouse macrophage. Eur J Immunol. 1981;11:805–815.

34. Prokopi M, Mayr M. Proteomics: a reality-check for putative stem cells. Circ Res. 2011;108:499–511.

35. Coffelt SB, Tal AO, Scholz A, et al. Angiopoietin-2 regulates gene expression in Tie2-expressing monocytes and augments their inherent proangiogenic functions. Cancer Res.

2010;70:5270–5280. 36. Okabe M, Ikawa M, Kominami K, Nakanishi T, Nishimune Y. ‘Green mice’ as a source of ubiquitous green cells. FEBS Lett. 1997;407:313–319.

37. Zhu WH, Iurlaro M, MacIntyre A, Fogel E, Nicosia RF. The mouse aorta model: influence of genetic background and aging on bFGF- and VEGF-induced angiogenic sprouting. Angiogenesis. 2003;6: 193–199.

38. Masson VV, Devy L, Grignet-Debrus C, et al. Mouse aortic ring assay: a new approach of the molecular genetics of angiogenesis. Biol Proc Online. 2002;4:24–31.

39. Jang HS, Kim HJ, Kim JM, et al. A novel ex vivo angiogenesis assay based on electroporation-mediated delivery of naked plasmid DNA to skeletal muscle. Mol Ther. 2004;9:464–474.

40. Rohde E, Bartmann C, Schallmoser K, et al. Immune cells mimic the morphology of endothelial progenitor colonies in vitro. Stem Cells. 2007;25:1746–1752.

41. Rohde E, Malischnik C, Thaler D, et al. Blood monocytes mimic endothelial progenitor cells. Stem Cells. 2006;24:357–367.

42. Purhonen S, Palm J, Rossi D, et al. Bone marrow-derived circulating endothelial precursors do not contribute to vascular endothelium and are not needed for tumor growth. PNAS. 2008;105:6620–6625.

43. Vignaud A, Hourde C, Medja F, Agbulut O, Butler-Browne G, Ferry A. Impaired skeletal muscle repair after ischemia-reperfusion injury in mice. J Biomed Biotechnol. 2010;2010:724914.

44. Bailey AM, O’Neill TJ, Morris CE, Peirce SM. Arteriolar remodeling following ischemic injury extends from capillary to large arteriole in the microcirculation. Microcirculation. 2008;15:389–404.

Chapter 3.

Sphingosine-1-Phosphate in muscle regeneration

Primer

Skeletal muscle regeneration is dependent on the proper reconstitution of the vasculature and myofibers. With muscular dystrophy, this process is disrupted as dysfunction of both satellite cells and endothelial cells occurs (1, 2). The molecular mechanisms that dictate such dysfunction are poorly understood. Recently, genetic elevation of sphingosine-1-phosphate (S1P) in dystrophic flies promoted function and reduced pathology (3). S1P is a bioactive lipid that was first described as a ligand for the endothelial differentiation gene-1 receptor (EDG1 or S1PR1) (4), which is expressed during endothelial cell formation of vascular tubes in vitro (5). To date, five receptors for S1P have been implicated in many cellular processes and expressed by several cellular populations (6). Coincidently, S1P is produced by endothelial cells and is important for satellite cell renewal and muscle repair (7, 8). Therefore, we examined the role of S1P pathway in muscular dystrophy and its potential to promote satellite cell-mediated regeneration.

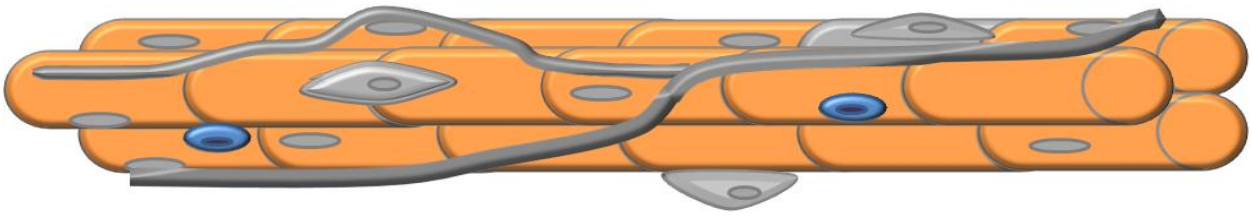

Satellite cell regeneration with muscular dystrophy

1. Palladino M, Gatto I, Neri V, Straino S, Smith RC, Silver M, et al. Angiogenic impairment of the vascular endothelium: a novel mechanism and potential therapeutic target in muscular dystrophy. Arteriosclerosis, thrombosis, and vascular biology. 2013;33(12):2867-76. doi: 10.1161/ATVBAHA.112.301172. PubMed PMID: 24072696.
2. Blau HM, Webster C, Pavlath GK. Defective myoblasts identified in Duchenne muscular dystrophy. Proceedings of the National Academy of Sciences of the United States of America. 1983;80(15):4856-60. PubMed PMID: 6576361; PubMed Central PMCID: PMC384144.
3. Pantoja M, Fischer KA, Ieronimakis N, Reyes M, Ruohola-Baker H. Genetic elevation of sphingosine 1-phosphate suppresses dystrophic muscle phenotypes in Drosophila. Development. 2013;140(1):136-46. doi: 10.1242/dev.087791. PubMed PMID: 23154413; PubMed Central PMCID: PMC3513996.
4. Lee MJ, Van Brocklyn JR, Thangada S, Liu CH, Hand AR, Menzeleev R, et al. Sphingosine-1-phosphate as a ligand for the G protein-coupled receptor EDG-1. Science. 1998;279(5356):1552-5. PubMed PMID: 9488656.
5. Hla T, Maciag T. An abundant transcript induced in differentiating human endothelial cells encodes a polypeptide with structural similarities to G-protein-coupled receptors. The Journal of biological chemistry. 1990;265(16):9308-13. PubMed PMID: 2160972.
6. Spiegel S, Milstien S. Sphingosine 1-phosphate, a key cell signaling molecule. The Journal of biological chemistry. 2002;277(29):25851-4. doi: 10.1074/jbc.R200007200. PubMed PMID: 12011102.
7. Venkataraman K, Lee YM, Michaud J, Thangada S, Ai Y, Bonkovsky HL, et al. Vascular endothelium as a contributor of plasma sphingosine 1-phosphate. Circulation research. 2008;102(6):669-76. doi: 10.1161/CIRCRESAHA.107.165845. PubMed PMID: 18258856; PubMed Central PMCID: PMC2659392.
8. Nagata Y, Partridge TA, Matsuda R, Zammit PS. Entry of muscle satellite cells into the cell cycle requires sphingolipid signaling. The Journal of cell biology. 2006;174(2):245-53. doi: 10.1083/jcb.200605028. PubMed PMID: 16847102; PubMed Central PMCID: PMC2064184.

Increased sphingosine-1-phosphate improves muscle regeneration in acutely injured mdx mice.

Nicholas Ieronimakis,[1] Mario Pantoja,[2] Aislinn L Hays,[1] Timothy L Dosey,[2] Junlin Qi,[2] Karin A Fischer,[2] Andrew N Hoofnagle,[3] Martin Sadilek,[4] Jeffrey S Chamberlain,[5] Hannele Ruohola-Baker,[2] and Morayma Reyes[1,3]

[1]Department of Pathology, School of Medicine, University of Washington, Seattle, WA 98195, USA

[2]Department of Biochemistry, Institute for Stem Cell and Regenerative Medicine, University of Washington, Seattle, WA 98195, USA

[3]Department of Laboratory Medicine, School of Medicine, University of Washington, Seattle, WA 98195, USA

[4]Department of Chemistry, University of Washington, Seattle, WA 98195, USA

[5]Department of Neurology, Senator Paul D Wellstone Muscular Dystrophy Cooperative Research Center, University of Washington, Seattle, WA 98195, USA

Reproduced from Skeletal Muscle, published Aug 01, 2013. 2044-5040-3-20.

Abstract

Background

Presently, there is no effective treatment for the lethal muscle wasting disease Duchenne muscular dystrophy (DMD). Here we show that increased sphingosine-1-phoshate (S1P) through direct injection or via the administration of the small molecule 2-acetyl-4(5)-tetrahydroxybutyl imidazole (THI), an S1P lyase inhibitor, has beneficial effects in acutely injured dystrophic muscles of mdx mice.

Methods

We treated mdx mice with and without acute injury and characterized the histopathological and functional effects of increasing S1P levels. We also tested exogenous and direct administration of S1P on mdx muscles to examine the molecular pathways under which S1P promotes regeneration in dystrophic muscles.

Results

Short-term treatment with THI significantly increased muscle fiber size and extensor digitorum longus (EDL) muscle specific force in acutely injured mdx limb muscles. In addition, the accumulation of fibrosis and fat deposition, hallmarks of DMD pathology and impaired muscle regeneration, were lower in the injured muscles of THI-treated mdx mice. Furthermore, increased muscle force was observed in uninjured EDL muscles with a longer-term treatment of THI. Such regenerative effects were linked to the response of myogenic cells, since intramuscular injection of S1P increased the number of $Myf5^{nlacz/+}$ positive myogenic cells and newly regenerated myofibers in injured mdx muscles. Intramuscular injection of biotinylated-S1P localized to muscle fibers, including newly regenerated fibers, which also stained positive for S1P receptor 1 (S1PR1). Importantly, plasma membrane and perinuclear localization of phosphorylated S1PR1 was observed in regenerating muscle fibers of mdx muscles. Intramuscular increases of S1P levels, S1PR1 and phosphorylated ribosomal protein S6 (P-rpS6), and elevated EDL muscle specific force, suggest S1P promoted the upregulation of anabolic pathways that mediate skeletal muscle mass and function.

Conclusions

These data show that S1P is beneficial for muscle regeneration and functional gain in dystrophic mice, and that THI, or other pharmacological agents that raise S1P levels systemically, may be developed into an effective treatment for improving muscle function and reducing the pathology of DMD.

Background

Duchenne muscular dystrophy (DMD) is a muscle wasting disease for which there is no cure. This severe X-linked recessive disease affects 1 in 3,500 male births [1]. In dystrophic muscles, rounds of contractions result in degeneration/regeneration cycles. In turn, dystrophic muscle cannot regenerate sufficiently to overcome degeneration, leading to muscle wasting over time. Since no effective treatment presently exists and the immune response to dystrophin has hampered gene therapy approaches, new advances for the treatment of DMD are imperative [2,3].

Previously, sphingosine-1-phosphate (S1P) has been implicated in muscle repair, satellite cell proliferation, myoblast differentiation in vitro and in non-diseased mouse models in vivo[2,4-6]. These essential roles for S1P in skeletal muscle regeneration suggested that elevation of S1P may have therapeutically beneficial effects in models of disease [7]. More recently, S1P has been shown beneficial for activating satellite cells in dystrophic muscles [8]. Furthermore, an unbiased genetic modifier screen in Drosophila revealed that by increasing S1P levels via reduction of the lipid phosphate phosphatase 3 (LPP3) homolog, wunen, or the S1P lyase, sply, prevents to a large degree dystrophic muscle wasting in flies [9]. In mice, elevation of S1P by the genetic reduction of S1P lyase can be phenocopied pharmacologically via treatment with the small molecule 2-acetyl-4(5)-tetrahydroxybutyl imidazole (THI) [10,11]. Furthermore, in Drosophila, THI treatment also significantly suppresses the dystrophic muscle phenotype [9].

Utilizing the mdx mouse model, we initiated studies on the effect of increasing S1P levels in dystrophic mice, and found that short-term treatment with THI improves muscle integrity and function following acute injury with cardiotoxin (CTX). THI treatment also leads to significant

improvements of the pathology of dystrophic muscles, as indicated by the reduced accumulation of fibrosis and fat deposition in acutely injured muscles. In turn, intramuscular injection of S1P resulted in an increased number of myogenic cells and newly regenerating fibers in vivo. S1P receptor 1 (S1PR1) is expressed by many muscle cell types, particularly muscle fibers, and phosphorylated S1PR1 is localized in the plasma membrane and intracellularly (perinuclear localization) of muscle fibers. Intramuscular S1P administration results in increased levels of total and phosphorylated S1PR1 and ribosomal protein S6 (rpS6). This suggests that increases in fiber size are mediated by anabolic pathways that promote greater skeletal muscle mass and function, potentially through S1PR1 signaling. Furthermore, ex vivo administration of S1P improved specific force in uninjured dystrophic muscle. Similarly, longer-term THI treatment of uninjured young mdx mice resulted in increased extensor digitorum longus (EDL) muscle force in the absence of CTX injury. Altogether, S1P acts at multiple levels in muscles, particularly in myogenic cells and muscle fibers, and collectively the actions of S1P in muscle are beneficial for regeneration in the setting of muscular dystrophy.

Methods

Animal procedure

Experiments involving animals were undertaken in accordance with approved guidelines and ethical approval from the Institutional Animal Care and Use Committee, University of Washington, Seattle, WA, USA.

THI injections in injured mice

Peripheral blood cells from 1.5-month-old (MO) wild type (wt) C57BL/k6 and mdx mice on a C57BL/k6 background (B6Ros.Cg-Dmd$^{mdx\text{-}4Cv}$/J, herein referred to as mdx^{4cv}) were analyzed (Figure 1A). Blood was collected before and 12 hours following the last of two 250 µl intraperitoneal (IP) injections of 0.15 mg/ml THI in PBS. Injections were 6 hours apart. This injection regimen and dose was repeated for all subsequent experiments involving THI, but for longer-treatment durations as outlined. Six 5-MO mdx^{4cv} males were used for the experiments in Figure 1B, and Additional file 1: Figure S1 and S2. For Figures 2 and and3,3, and Additional file 1: Figures S3 to S7, six 11-MO females and seven 16-MO males mdx^{4cv} were used for these experiments. In these mice, the left tibialis anterior (TA) and quadriceps femoris (quads) were injured with 10 nM CTX (Calbiochem, Darmstadt, Germany) from Naja nigricollis. Once more, THI-treated mice were injected IP with 250 µl 0.15 mg/ml THI in PBS, twice daily (injections 6 hours apart) immediately after injury and for the first 3 days following injury. The vehicle controls were injected IP with PBS. On day 4 post injury, 5-MO mdx^{4cv} animals were euthanized for S1P and creatine kinase (CK) analysis. On day 17 post CTX, 11-MO and 16-MO mdx^{4cv} mice were also injected IP with 1% Evans Blue dye (EBD) to label persistently damaged (dye permeable) muscle fibers [12], and euthanized on day 18 post injury for histopathology analysis. Muscles for S1P and expression analysis (from 5-MO mdx^{4cv}) were frozen directly in liquid nitrogen, while muscles taken for histopathology were frozen under liquid nitrogen cooled isopentane in optimal cutting temperature (OCT) compound. All myofibers were measured for the minimum diameters on the cross-sections of mouse quadriceps muscle using ImageJ software (Bethesda, MD, USA). Between 750 and 850 myofibers were counted for three mice treated with PBS or THI, with or without CTX injury. For functional analysis outlined in Figure 4B, 4.75- to

5-MO male mdx on a C57BL/10 background (C57BL/10ScSn-Dmd$^{mdx/J}$) were used for the 14-day treatment of THI or vehicle. Following the same dose and treatment regimen, mdx were treated with THI (n = 10) or vehicle (n = 9) for 14 days following CTX injury to left TAs and quadriceps. The same mdx strain was compared to wt C57BL/10 animals in Figure 4C and for exogenous S1P treatment depicted in Figure 4D. Animals used to evaluate the degree of CTX injury in EDL (Additional file 1: Figure S8) were 4-MO female mdx (n = 4, C57BL/10ScSn-Dmd$^{mdx/J}$ background), injected in left TAs with CTX and with approximately 3 μl India ink, added to the tip of the needle to mark injection penetration. Following CTX injections, mice were immediately injected IP with 1% EBD. Both left (injured) and contralateral uninjured TA and EDL muscles were harvested and frozen in OCT compound 12 hours post injury.

THI treatment in drinking water of young, uninjured mdx mice

Beginning at 4 weeks of age, male mdx^{4cv} were treated with THI (n = 4) or vehicle (n = 3) for 4 weeks, and analyzed by EDL myography at 8 weeks of age. For this treatment we followed the dose and conditions described by Schwab et al. [11]. Briefly, 50 mg/l THI was administered ad libitum. The vehicle consisted of water at pH 2.8 containing 10 g/l glucose.

Peripheral blood cell analysis

Blood was collected via retro-orbital blood collection using heparinized capillaries and transferred to blood collection tubes containing a final concentration of 1.6 mg/ml EDTA (SARSTEDT, Nümbrecht, Germany) for analysis. Analysis of whole blood was undertaken with 20 μl per sample using the Hemavet 950 FS system (Drew Scientific, Dallas, TX, USA).

Analysis of gene expression by quantitative reverse transcription-PCR (RT-PCR)

Total RNA (RNeasy Kit, Qiagen, Venlo, Netherlands) was prepared from mdx^{4cv} TA muscles homogenized under liquid nitrogen by mortar and pestle. Methods for RNA isolation and cDNA generation were in accordance with manufacturer's protocols using reverse transcriptase (Applied Biosystems, Carlsbad, CA, USA) as previously described [13]. RNA (0.5 μg) was reverse transcribed using the Omniscript RT Kit (Qiagen). For reverse transcription-PCR (RT-PCR), 10 ng cDNA was combined with SYBR Green (Thermo Scientific, Waltham, MA, USA) following published conditions and primer sequences for S1P-related genes by Grabski et al. [14] and by Au et al. [15] for 18S.

Functional analysis: myography

Animals treated with THI or PBS (vehicle) via IP injection as aforementioned for 14 days were analyzed between 1 and 4 days following the final day of injection. Prior to euthanasia animals were anesthetized with 0.5 mg/g weight avertin diluted in PBS. EDLs were then excised and equilibrated in Ringer's solution (120 mM NaCl, 4.7 mM KCl, 3.15 mM $MgCl_2$, 1.3 mM NaH_2PO_4, 25 mM $NaHCO_3$, 11 mM glucose, 1.25 mM $CaCl_2$, pH 7.2) with 95% O_2/5% CO_2 for a minimum of 15 minutes prior to stimulation [16]. For assessment of direct S1P administration, EDL muscles from uninjured and untreated 3.5-MO male mdx (C57BL/10ScSn-Dmd$^{mdx/J}$) were incubated with oxygenated Ringer's solution containing 10 μM S1P or vehicle (PBS with 4 mg/ml fatty acid free BSA) for 15 minutes prior to stimulation [16]. All functional experiments were carried out with buffer solutions at 25°C under constant oxygenation. Myography was conducted using a 820S myograph (DMT, Ann Arbor, MI, USA) and data was recorded using a PowerLab 4/30 acquisition system with LabChart Pro software v7.3.1 (both from

ADInstruments, Dunedin, New Zealand). Stimulations were conducted with S88X dual systems (Grass Technologies, Middleton, WI, USA). Muscles were stimulated to establish optimal fiber length (Lf) and voltage at which maximum tetanic force was measured at 120 Hz using 4.15 ms pulses within 450 ms train duration [17]. Force frequency was carried out using the same pulse duration at 10, 20, 40, 60, 80, 100 and 120 Hz, as outlined in the x-axis of Figure 3B. Specific force was calculated as previously described [18] by normalizing to the muscle cross-sectional area (CSA). CSA is the quotient of dry muscle mass (mg) over Lo (mm), which is defined as the product of Lf with the fiber length ratio (0.44 for EDL) and mammalian muscle density (1.06 mg/mm^3).

Measurement of S1P in mouse tissue

S1P was quantified in tissue after homogenization and extraction using liquid chromatography-tandem mass spectrometry (LC-MS/MS). Tissue was pulverized in liquid nitrogen using a mortar and pestle. Collected tissue was weighed and an internal standard (C17 base D-erythro-sphingosine-1-phosphate in methanol (Avanti Polar Lipids, Alabaster, AL, USA)) was added at 1 pmol/mg tissue. Tissue was then vortexed/extracted in 16 volumes (mg/μl) of acetonitrile:water (80:20, v/v) for 10 minutes at room temperature. Supernatants were collected after centrifugation (10 minutes at 14,000 rpm) and concentrated to dryness using a SpeedVac Concentrator (Thermo Scientific). Pellets were resuspended in methanol to a calculated concentration of 0.05 μM C17 base D-erythro-sphingosine-1-phosphate. Then 10 μl was analyzed by LC-MS/MS using C17 base D-erythro-sphingosine-1-phosphate plus C18 base D-erythro-sphingosine-1-phosphate (both at 0.05 μM) as a standard. Separation of analytes was undertaken by liquid chromatography using a Chromolith RP-C18e 100 × 2 mm column (EMD, Gibbstown, NJ, USA)

and analysis by tandem mass spectrometry with a Quattro Micro mass spectrometer (Waters, Milford, MA, USA) in positive ion mode. The HPLC gradient using two pumps was linear from 50% MeOH to 99% MeOH using solvent A (water, 0.1% formic acid) and solvent B (MeOH, 0.1% formic acid) over 1 minute at a flow rate of 0.35 ml/min. To wash the column, the gradient was repeated twice before equilibrating for 3 minutes before running the next sample. The transitions analyzed were 380.25 >264.50 and 380.25 >82.00 for endogenous S1P, and 366.25 >250.50 and 366.25 >82.00 for internal standard with a dwell time of 0.07 seconds. Data collection was by MassLynx software (Waters) and processed with QuanLynx software (Waters).

Measurement of S1P in mouse plasma

S1P was quantified in plasma using butanol extraction and liquid LC-MS/MS [19]. Internal standard (5 µl 3 µM C17 base D-erythro-sphingosine-1-phosphate in ethanol (Avanti Polar Lipids)) was added to 10 µl EDTA-anticoagulated plasma and mixed thoroughly on an orbital shaker (Thermomixer, Eppendorf, Hauppauge, NY, USA) for 10 minutes at 1,400 rpm at 20°C. The sample was then acidified using 50 µl 30 mM citric acid/40 mM Na_2HPO_4, pH 4.0, and extracted for 10 minutes at 1,400 rpm at 20°C with 125 µl water-saturated butanol (Fisher Scientific, Waltham, MA, USA). The butanol layer was removed and lyophilized in a centrifugal evaporator at 20°C. The residue was stored at −20°C until analyzed. The residue was resuspended in 125 µl HPLC buffer A (50% methanol, 1% formic acid, 5 mM ammonium formate in water (JT Baker) and sonicated in a bath sonicator for 1 minute at 20°C. Analytes in a portion of the sample (10 µl) were then separated using liquid chromatography (Shimadzu, Nakagyo-ku, Kyoto, Japan) with a Luna 3 µm C18(2) 100Å 50 × 2 mm column (Phenomenex,

Torrance, CA, USA) and analyzed by tandem mass spectrometry on a 4000 QTRAP mass spectrometer (AB SCIEX, Framingham, MA, USA) in positive ion mode. The HPLC gradient was linear from buffer A to buffer B (10% isopropyl alcohol, 1% formic acid, 5 mM ammonium formate in methanol) over 1 minute at a flow rate of 0.4 ml/min. To wash the column, the gradient was repeated twice before equilibrating for the next sample. The transitions analyzed were 380.3/264.3 and 380.3/81.9 for endogenous S1P, and 366.2/93.0, 366.2/82.0 and 366.2/250.3 for internal standard with a dwell time of 15 milliseconds. Calibrators were in mouse plasma (C18 base D-erythro-sphingosine-1-phosphate, Avanti Polar Lipids). Between-day coefficient of variation was 7.7%. Pertinent instrument specific parameters were empirically derived and included curtain gas: 15, ion source voltage: 5000 V, emitter temperature: 550°C, desolvation gas 1: 20, desolvation gas 2: 70, collision gas: 6, entrance potential: 10, and collision cell exit potential: 10. Chromatographic data were analyzed using Analyst 1.4.2 (AB SCIEX) by summing transitions for each analyte.

Creatine kinase (CK) assay

mdx^{4cv} mouse plasma samples were diluted 1:50 and total CK activity was measured by an enzymatic rate method at the clinical laboratory of the Department of Laboratory Medicine, University of Washington, using the Beckman Coulter instrument (Brea, CA, USA) as previously described [20]. Relative levels were then normalized to body weight.

S1P injections

Right and left TAs of three 3-MO male mdx^{4cv}:Myf5$^{nlacZ/+}$ were injured once more with 10 nM CTX (Figure 5). S1P (Enzo Life Sciences, Farmingdale, NY, USA; Calbiochem) preparation was

undertaken according to manufacturer's instructions. Briefly, S1P was dissolved in methanol (0.5 mg/ml) and aliquoted, then the solvent was evaporated with a stream of nitrogen to deposit a thin film on the inside of the tube. Prior to use, aliquots were resuspended in PBS with 4 mg/ml BSA (fatty acid free) to a concentration of 500 μM. Directly following CTX injection, 20 μl 500 μM S1P was injected in left TAs, daily until day 3 post injury, at which time animals were euthanized and muscles were harvested for freezing. Right TAs were injected with an equal volume of PBS with 4 mg/ml BSA as vehicle controls. In a separate experiment (Figure 6), TAs of four 2.5-MO female mdx^{4cv} were injected with S1P or vehicle under the same conditions stated above, in the absence of injury. AJ/SCID mice (n = 4, 9-MO, B6. Cg-$Dysf^{prmd}Prkdc^{scid}$/J) were also injected for 3 days with S1P or vehicle in TAs post CTX injury, following the same concentration and injection regimen used in mdx^{4cv}. For measurement of S1P muscle content (Figure 7A) following intramuscular injections, 11-MO mdx^{4cv} (n = 3) were injected 20 μl 500 μM S1P in left TAs and 20 μl vehicle in right TAs. Muscles were harvested and frozen in liquid nitrogen 15 minutes post injection, and then processed using the aforementioned methods for analyzing S1P in muscle by LC-MS/MS. For injection of biotinylated-S1P, TAs from 11-MO mdx^{4cv} (n = 2) were injected intramuscularly with 20 μl 500 μM S1P-biotin or vehicle (Echelon Biosciences, Salt Lake City, UT, USA). TAs were harvested and frozen in OCT compound 15 minutes following injection.

Mouse histology and immunohistochemistry

All mouse muscles were frozen directly in OCT compound with liquid nitrogen cooled in isopentane and sectioned 8 μm thick. Tissue for X-gal staining was fixed for 10 minutes with 2% formaldehyde/0.2% glutaraldehyde and incubated overnight at 37°C with staining buffer (PBS

with 1 mg/ml X-gal, 5 mM potassium ferricyanide, 5 mM potassium ferrocyanide, 2 mM $CaCl_2$ (all from Fisher Scientific)). Picrosirius red with fast green, hematoxylin and eosin, and Oil Red O staining were conducted following established protocols [21]. Fibrosis was quantified as percentage of area stained red within each 20 × field analyzed using ImageJ v1.40 or Adobe Photoshop CS2 (San Jose, CA, USA). For evaluating fibrosis, the mean value from three separate sections (200 μm apart in longitudinal distance) were analyzed from each muscle and used to calculate the overall mean for each muscle group outlined in the x-axis of Figure 1D. Lipid accumulation was quantified with the ImageJ cell counter plugin by counting fatty infiltrates in montages (stitched from 10 × photos) covering the entire CSA of each muscle. Muscles injected with S1P-biotin or vehicle were cut 8 μm thick, fixed for 5 minutes with 4% formaldehyde, and then stained with streptavidin conjugated to Alexa Fluor 594 (Life Technologies, Carlsbad, CA, USA) at 1:1000 in PBS and 1% BSA for 1 hour.

Immunohistological staining

Staining was undertaken using freshly frozen mdx^{4cv} muscles. Pax7 staining was performed as outlined by Clever et al. [22] with slight modification. Sections were fixed overnight in 4% formaldehyde (from paraformaldehyde powder) at 4°C. Following fixation, antigen retrieval was performed with 10 mM citrate buffer (with 0.05% Tween 20 at pH 6.0) warmed in a water bath at 90°C for 20 minutes. Slides were then permeated with ice cold methanol for 5 minutes at room temperature. Streptavidin/biotin blocking (Vector Laboratories, Burlingame, CA, USA) was performed according to manufacturer's instructions. Staining was undertaken using the Mouse on Mouse (MOM) Kit (Vector Laboratories) with immunoglobulin G (IgG) blocking for 5 hours at 4°C prior to addition of mouse monoclonal anti-Pax7 (clone PAX7, R&D Systems,

Minneapolis, MN, USA) diluted at 1:20 and incubated overnight at 4°C. Biotinylated anti-mouse secondary was supplied with and used as prescribed by MOM Kit instructions. Streptavidin conjugated to Alexa Fluor 488 (Life Technologies) was added at 1:1000. As a negative control for Pax7 staining, a mouse IgG isotype was applied to separate ribbons and treated in parallel. For BS1 staining, muscles were initially fixed with 4% formaldehyde for 5 minutes at room temperature then stained with BS1 directly conjugated to fluorescein isothiocyanate (FITC), diluted at 1:400 in PBS with 1% BSA and applied for 1 hour at room temperature. Following BS1 staining, wheat germ agglutinin (WGA) directly conjugated to rhodamine was administered at 1:400 dilution as a counterstain for identifying myofibers. CD3e staining was undertaken in the same manner as BS1, using rat monoclonal anti-CD3e (clone 145-2C11, eBioscience, San Diego, CA, USA) at 1:100 dilution, followed by anti-rat IgG conjugated to Alexa Fluor 594 at 1:1000 dilution.

For laminin staining, tissue was also fixed with 2% formaldehyde for 5 minutes then treated with polyclonal rabbit anti-laminin (Sigma-Aldrich, St Louis, MO, USA) for 1 hour at 1:400 dilution in PBS and 1% BSA. Following washes, Alexa Fluor 488 conjugated goat anti-rabbit IgG (Life Technologies) was administered at 1:800 dilution for 1 hour. Controls omitting the primary antibody were included with all staining. For embryonic myosin heavy chain (eMyHC), tissue was first fixed with 2% formaldehyde for 5 minutes, treated with streptavidin/avidin blocking and blocked with IgG block from MOM Kit for 5 hours at 4°C. Following blockade, concentrated mouse anti-eMyHC (clone F1.652, received concentrated at 357 μg/ml IgG, Developmental Studies Hybridoma Bank (DSHB), University of Iowa, IA, USA) was administered at 1:400 dilution overnight at 4°C. The remainder of the staining was undertaken following MOM Kit staining instruction. 3,3'-diaminobenzidine (DAB) was used for visualizing

and quantifying eMyHC fibers. For fluorescence, eMyHC was visualized using streptavidin conjugated to Alexa Fluor 594 used at 1:1000 dilution for 1 hour. For S1P receptor staining, slides were fixed with 4% formaldehyde for 5 minutes and stained with rabbit polyclonal IgG antibodies against S1PR1, S1PR3 (Cayman Chemical, Ann Arbor, MI, USA) and phosphorylated S1PR1 (raised against Thr236, Assay Biotechnology, Sunnyvale, CA, USA), all applied at a dilution of 1:200 for 2 hours. Following receptor staining, goat anti-rabbit IgG conjugated to Alexa Fluor 488 was added at 1:1000 for 1 hour. In parallel, we stained additional slides with rabbit polyclonal IgG isotype at the same final concentrations to exclude non-specific staining of these antibodies in mdx^{4cv} muscles.

Staining quantifications were all undertaken using ImageJ cell counter plugin. Calculations, statistics and graphs were generated with Microsoft Excel (Redmond, WA, USA). Bright field photographs were captured using either a Fisher Scientific Micromaster digital inverted or upright microscopes with Micron software. Fluorescent photographs were captured with a monochromatic camera using an Axiovert 200 microscope (Zeiss, Oberkochen, Germany). Individual fluorescent channels were colored and merged using Adobe Photoshop. Brightness contrast levels were adjusted to increase visibility and reduce background in most photographs.

Western blot analysis

Tissue for western blot analysis was snap frozen in liquid nitrogen and subsequently homogenized. Freshly isolated TA muscles were harvested and snap frozen in liquid nitrogen prior to homogenization with disposable tissue grinders. Tissue was homogenized under liquid nitrogen then resuspended in lysis buffer containing 50 mM Tris–HCl (pH 7.4), 1 mM EDTA, 150 mM NaCl, 5 mM NaF, 0.25% (w/v) sodium deoxycholate, 2 mM $NaVO_3$, 1% Triton X-100

(v/v), supplemented with complete protease inhibitor cocktail (Roche, Basel, Switzerland), and complete phosphatase inhibitor cocktails 1 and 2 (Sigma-Aldrich). Protein extracts were separated using Ready Gel Tris–HCl (BioRad, Hercules, CA, USA), 4 to 20% linear gradient and transferred to polyvinylidene fluoride (PVDF) membranes with a wet transfer system (BioRad). Membranes were blocked for 1 hour with Tris-buffered saline with 0.1% (v/v) Tween 20 containing 5% (w/v) BSA. For S1PR1 analysis, rabbit polyclonal anti-S1PR1 was used at a 1:500 dilution (Santa Cruz Biotechnology, Santa Cruz, CA, USA). Rabbit polyclonal antibodies were used to blot against phosphorylated (Thr308) Akt, total Akt, phosphorylated (Ser2448) mammalian target of rapamycin (mTOR), total mTOR, phosphorylated (Ser240/Ser244) rpS6, total rpS6 (1:1000, Cell Signaling Technology, Danvers, MA, USA) and β-actin (1:10000, Sigma-Aldrich). The signals were detected using an enhanced chemiluminescence kit (Millipore, Billerica, MA, USA) and CL-XPosure films (Thermo Scientific) were analyzed using ImageJ.

Statistics

Student's t-test was used to determine statistical significance for the majority of experiments. P values generated by analysis of variance (ANOVA) are specified in the text.

Results

Alterations of S1P regulation and content following IP injection of THI in mdx mice

To determine the effect of elevating S1P levels in dystrophic animals, we studied the effects of THI in the mdx mouse model for DMD [23,24]. Recently, Loh et al. (2012) showed that compared to wt, mdx muscles are in a state of S1P deprivation as they exhibit increased levels of the enzymes that degrade S1P (S1P lyase and S1P phosphatase 1) [8]. THI is a hydrophilic small

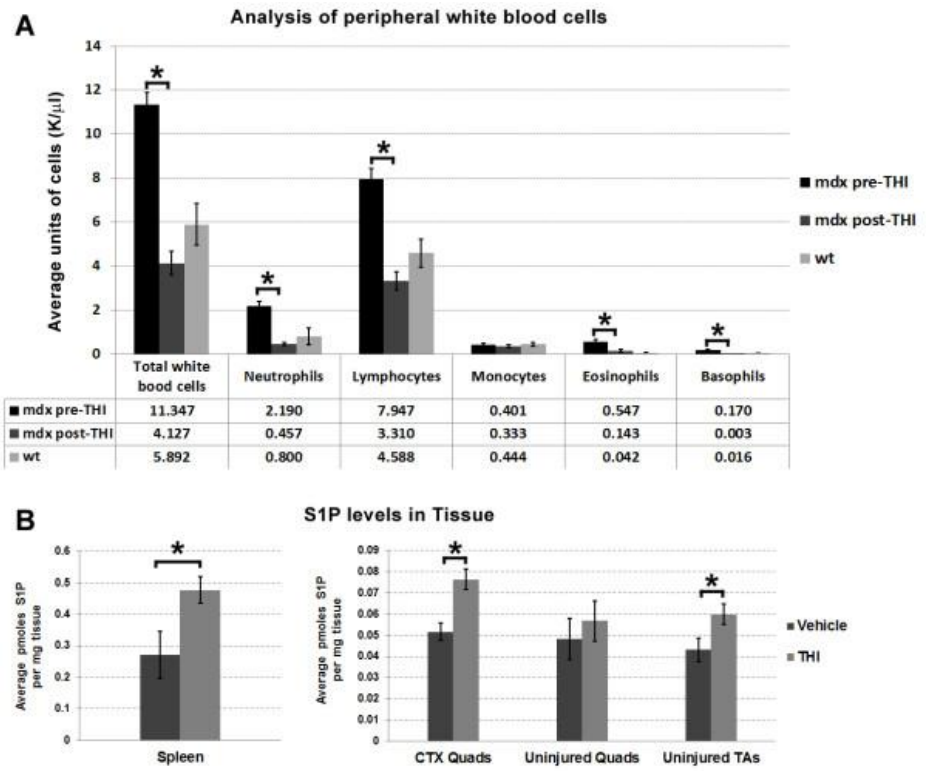

Figure1. IP injection of THI reduces peripheral blood leukocytes and increases S1P levels in most tissues. (A) Leukocytes were analyzed from the peripheral blood of 1.5-MO mdx^{4cv} mice (n = 3) before and 12 hours following treatment with THI (2 × 250 µl 0.15 mg/ml IP injections, 6 hours apart). IP administration of THI significantly reduced circulating leukocytes to values below or near age-matched wt (n = 4). The average value of each population is listed in the table below the bar graph. Values between pre and post THI, and wt were also significant by ANOVA (P <0.05) for all leukocytes except monocytes. **(B)** mdx^{4cv} mice (n = 6, 5-MO) were treated with THI or vehicle for 3 days (2 × 250 µl 0.15 mg/ml IP injections per day) following CTX injury to assess changes in S1P muscle content. Muscles and spleens were harvested on day 4 post injury for S1P analysis by LC-MS/MS. Results indicate S1P levels in spleen and injured quadriceps (quads) were significantly elevated with THI treatment. Interestingly, uninjured quadriceps did not show a significant increase of S1P, whereas uninjured TA muscles did. *P <0.05 by student's *t*-test. Error bars represent SEM. CTX, cardiotoxin; IP, intraperitoneal; LC-MS/MS, liquid chromatography-tandem mass spectrometry; MO, month-old; S1P, sphingosine-1-phoshate; SEM, standard error of the mean; TA, tibialis anterior; THI, 2-acetyl-4(5)-tetrahydroxybutyl imidazole; wt, wild type.

molecule that increases S1P levels by inhibiting the lyase that irreversibly degrades S1P [11,25,26]. In turn, low doses of THI may be sufficient to cause mild lymphocytopenia but the presumable increase of S1P levels in muscle have not been reported [8,11]. To corroborate the effects of THI in mdx^{4cv} mice, we analyzed changes in lymphocytes before and after treatment, and measured S1P content in muscle (Figure 1). THI has low oral bioavailability; Bagdanoff et al. showed 10 to 12%

bioavailability of THI when administered orally [10]. Thus we evaluated IP injections of THI as a parenteral delivery route for elevating systemic levels of THI. Peripheral blood was collected and analyzed before and 12 hours after two IP injections of THI (each injection was 250 μl 0.15 mg/ml THI, administered 6 hours apart). Following THI treatment, we observed a significant drop of all leukocytes except monocytes in mdx^{4cv} (n = 3, 1.5-MO) (Figure 1A). Of note, prior to treatment with THI, the total number of white blood cells and amount of individual leukocyte populations except monocytes, was significantly elevated in 1.5-MO mdx^{4cv} mice (n = 3) versus age-matched wt mice (n = 4). Interestingly, the number of platelets was also elevated twofold in mdx^{4cv} versus wt, but declined to near wt following THI administration (Additional file 1: Figure S1). This systemic effect in lymphocyte count indicates that THI functions efficiently when delivered systemically via IP injection. In addition, for short-term treatments, IP administration is desirable to ensure that all mice received the same dose. Thus for the majority of experiments described herein, we opted to administer THI via IP administration.

Loh et al. also demonstrated that following acute injury, the expression of S1P lyase increases in wt muscle [8]. Thus we analyzed the expression of enzymes that regulate S1P production and degradation following CTX injury in the mdx background with and without THI treatment. Right TA and quadriceps muscles were uninjured, while left counterparts were injured using CTX, a well characterized model of acute injury where initial muscle destruction is followed by a rapid myogenic response [27-30]. mdx^{4cv} mice (n = 6, 3.5-MO males) were injected IP immediately following CTX and thereafter five additional times during a 3-day period (for example 2 × IP injections per day) with either the previously used dose of THI or vehicle. For this analysis, muscles were harvested at day 4 post injury; the peak of myogenic gene expression following CTX-induced damage [28]. In the absence of THI, expression of the S1P lyase was significantly

elevated following injury (Additional file 1: Figure S2A). Surprisingly, expression of S1P

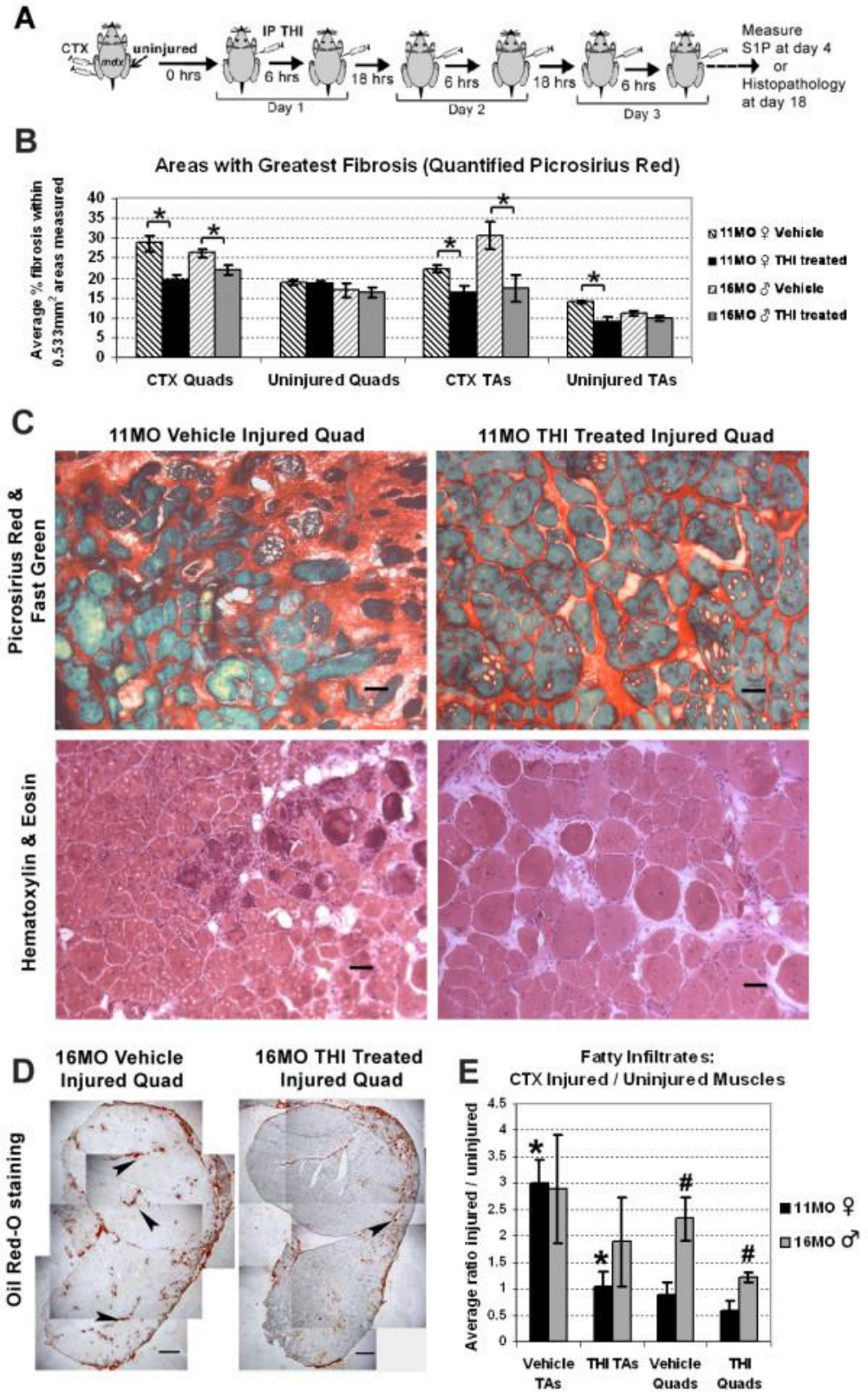

Figure 2. Dystrophic pathology following muscle injury is improved with THI treatment. (A) Experimental schematic of THI (0.075 μg/day) and PBS (vehicle)-treated mdx mice injected IP twice daily for the first 72 hours following CTX injury. Muscles from aged mdx^{4cv} mice (n = 7, THI-treated: 3 × 11-MO females, 4 × 16-MO males; n = 6 vehicle-treated: 3 × 11-MO females, 3 × 16-MO males) were harvested for histopathology analysis 18 days post CTX injury. **(B)** Histological quantification of picrosirius red staining indicates lower fibrotic accumulation following injury in both TA and quadriceps (quads) muscles from mice treated with THI. For CTX-injected muscles, damaged regions of muscle (for example fields with the greatest accumulation of sirius red staining) were quantified for both THI and vehicle-treated mice. The level of fibrosis was not significantly different between treated and control (vehicle) uninjured quadriceps; however, uninjured TA muscles from 11-MO THI-treated mice had lower fibrosis compared to control TA muscles. For each muscle, three separate sections (200 μm apart in longitudinal distance) were analyzed. **(C)** Representative photographs of injured quadriceps stained with picrosirius red and fast green depict collagen deposition (red staining), while muscle morphology and organization is depicted with hematoxylin and eosin staining. Scale bars = 50 μm. **(D)** Oil Red O staining depicts fat deposits (arrows) over the entire CSA of THI-treated and vehicle-injured quadriceps from 16-MO males. Scale bars = 500 μm. **(E)** The ratio of fat deposition in injured TAs over uninjured contralateral TAs quantified from Oil Red O staining was significantly reduced in THI-treated versus control animals in 11-MO (*) but not 16-MO mdx^{4cv} mice. In contrast, the ratio of injured over uninjured fat deposits in quadriceps was significantly reduced in 16-MO (#) but not in 11-MO mdx mice. *P <0.05, **P <0.01 by student's *t*-test. Error bars represent SEM. CSA, cross-sectional area; CTX, cardiotoxin; IP, intraperitoneal; MO, month-old; SEM, standard error of the mean; TA, tibialis anterior; THI, 2-acetyl-4(5)-tetrahydroxybutyl imidazole.

phosphatase 1 and lyase were greater in the injured muscles with THI treatment, suggesting a possible compensation in the S1P degradation pathways in response to the inhibition of the S1P lyase. Analogous to these results, expression levels of S1P kinase 1 were also increased with injury and at higher levels with THI (Additional file 1: Figure S2B). In contrast, the expression of S1P kinase 2 was only significantly elevated in the injured muscles from THI-treated animals. These results suggest that acute injury in mdx^{4cv} muscles induces upregulation of enzymes that regulate S1P metabolism. In turn, elevated expression of both S1P kinases with THI treatment may be beneficial for muscle regeneration in mdx mice. However, with THI treatment S1P phosphatase 1 and lyase expression were also greatly increased. Therefore we examined S1P

content, to determine if THI treatment results in increased intramuscular S1P levels and in turn promotes muscle regeneration following CTX injury.

In order to determine if THI treatment results in increased intramuscular S1P levels, a second group of mdx^{4cv} animals was treated with THI or PBS (n = 6, 5-MO males), following the same dosing schedule (2 × IP injections per day for the first 3 days post CTX injury) and sacrificed at day 4 to analyze the efficacy of THI in increasing S1P levels (Figure 1B). In concordance with published work, treatment with THI increased S1P levels in spleen but not plasma (Figure 1B, Additional file 1: Figure S3A) [10,11]. S1P levels were also significantly increased in CTX-injured quadriceps from THI-treated animals (Figure 1B). This indicates that despite increased expression of S1P phosphatase 1 and lyase following injury, the counteracting increased expression of both S1P kinases results in elevated levels of intramuscular S1P. In addition, we also observed increased S1P levels in the uninjured TA muscles from mice treated with THI compared to vehicles. To examine if such extravascular increases of S1P correlated with a beneficial effect in dystrophic mice, we analyzed the level of plasma CK, which are elevated in humans and mice with muscular dystrophy activity in the same group of THI-treated mdx^{4cv} mice [31]. Results indicate a trending, but not statistically significant decline in CK activity levels in plasma collected on day 4 post injury from THI versus vehicle-treated mice (Additional file 1: Figure S3B).

Reduction of dystrophic muscle pathology in acutely injured mdx muscles via administration of THI IP

Although young mdx mice exhibit robust muscle repair, regeneration becomes impaired with aging, resulting in muscle atrophy and dystrophy [3]. Therefore, in a third experiment, the effects

of THI on histopathology were assessed in injured and uninjured muscles from two groups of aged mdx^{4cv} mice (n = 6, 11-MO females; n = 7, 16-MO males), to determine the effects of increasing levels of S1P in dystrophic animals at a stage of severe muscle wasting. Importantly, it has been reported that mdx females older than 6 months of age exhibit greater fibrosis than males [32]. Once more, right TA and quadriceps muscles were uninjured, while left counterparts were injured with CTX (Figure 2A). Regeneration following CTX injury is well orchestrated in normal muscle but impaired in older mdx mice [29]. Therefore in these studies we analyzed the muscles from 11- and 16-MO mdx mice 18 days following CTX injury, a time point expected for non-diseased muscles to fully regenerate [28]. In the 16-MO mice, muscles were weighed immediately after collection and normalized to body weight (grams muscle weight over grams mouse weight). As expected, injured muscles were lighter than uninjured muscles in vehicle mice, an approximate weight loss greater than 20% (Additional file 1: Figure S4A). However, in the THI-treated mice the weight of injured quadriceps was similar to uninjured quadriceps (muscle weight ratio injured/uninjured approximates one), suggesting that THI treatment promotes muscle repair and protects from muscle loss following acute injury.

Fibrosis and fat deposition are both hallmarks of muscle wasting and dystrophic muscle pathology [32,33]. In addition, when regeneration is impaired, fibrosis and fat accumulate in place of muscle following acute injury [34,35]. Histological quantification revealed that THI treatment reduced accumulation of both fibrosis and fat deposition following acute injury in quadriceps and TA muscles (Figure 2B,C). Results for lower fibrosis were confirmed by third party hydroxyproline analysis of injured TAs from 16-MO animals (Additional file 1: Figure S4B). Interestingly, fibrosis was also significantly lower in uninjured TAs of 11-MO females, which correlates with the capacity of THI to elevate S1P levels in uninjured TAs (Figure 1B,

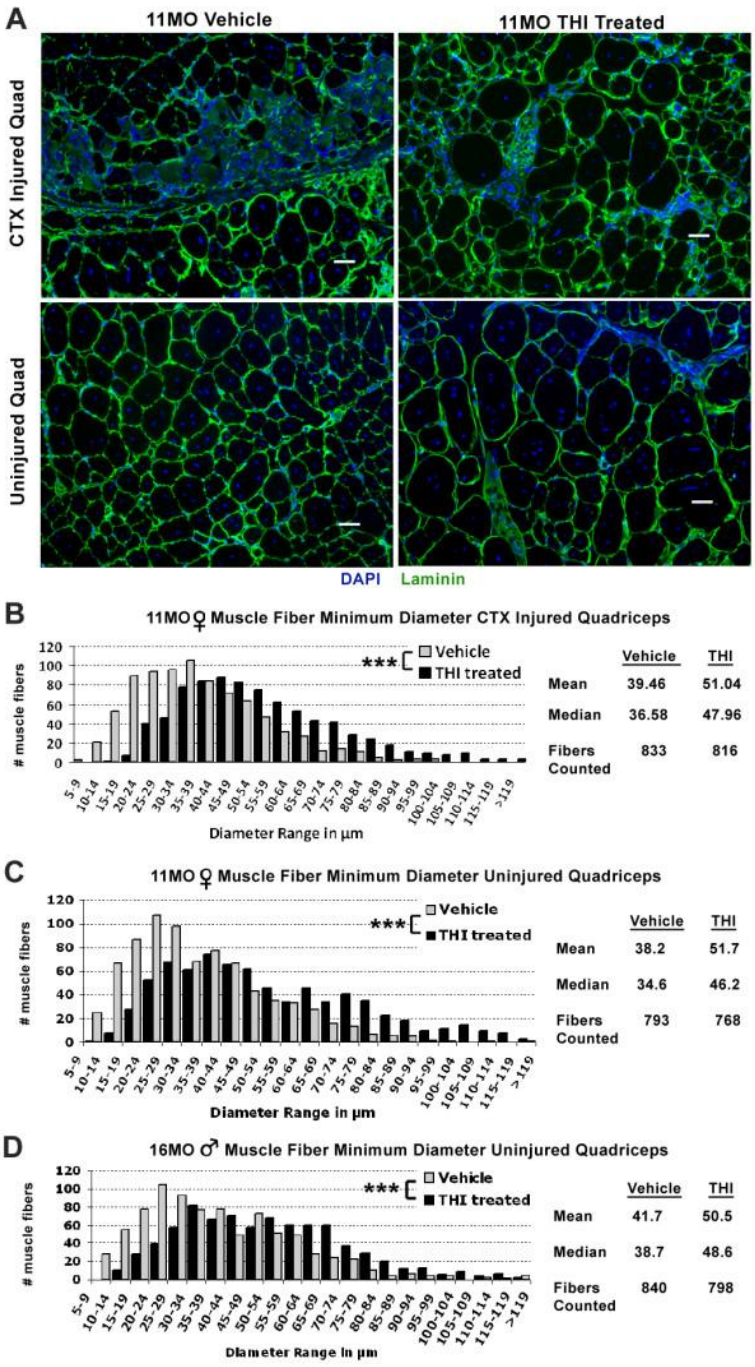

Figure3. Elevating S1P levels with THI increases muscle fiber size. **(A)** Staining for laminin (green) and DAPI (blue) depict a dramatic increase in muscle fiber size in both injured and uninjured quadriceps (quads) with THI treatment. Depicted are quadriceps muscles from 11-MO mdx^{4cv} mice. Scale bars = 50 µm. **(B,C,D)** Quantification of minimum muscle fiber diameter reveals a significant increase in myofiber size in THI-treated animals. Increased myofiber diameter was observed in both **(B)** injured and **(C)** uninjured quadriceps from THI-treated 11-MO mdx^{4cv} mice, whereas only **(D)** uninjured quadriceps in THI-treated 16-MO mdx^{4cv} mice showed increased myofiber size compared to vehicle controls. As indicated by the distributions, mean and median values of muscle fiber minimum diameters, there is an overall increase in muscle fiber size with THI treatment. Quantifications were undertaken in random fields in both injured and uninjured muscles in order to obtain an overall representation of fiber size increase for each muscle.*P <0.05, ***P <0.0005 by student's

Additional file 1: Figure S5). Although only left TAs and quadriceps were injected with CTX, fibrosis accumulation in uninjured muscles was likely elevated as mice disuse injured limbs and bear most of the use/weight on the uninjured contralateral limb. Therefore, the differences observed in

uninjured TAs are likely due to reductions in the amount of fibrotic deposition that would otherwise accumulate without THI treatment, since it is unlikely THI can reverse already accrued fibrosis. Along with lower fibrosis observed in injured muscles, the overall morphology appeared more organized with THI treatment compared to vehicle-treated animals (Figure 2C). In addition, the number of EBD-positive fibers, an indicator of muscle fiber damage, was lower in injured 11-MO muscles and significantly reduced in uninjured 11-MO quadriceps (Additional file 1: Table S1) [12,36]. In these muscles the number of centrally nucleated fibers was comparable between THI and vehicle-treated animals (Additional file 1: Figure S6).

To test whether THI-treated mice show decreased fat deposition in injured muscles, we quantified the fat deposits within entire cross-sections of THI and vehicle-treated muscles (Figure 2D). The ratio of fat deposits between injured and uninjured contralateral muscles was then compared to THI and vehicle-treated mice (Figure 2E). This analysis indicates that THI significantly reduced fat deposition resulting from injury in 11-MO female TAs and 16-MO male quadriceps. These results demonstrate that THI treatment reduces injury-induced fat deposition and fibrosis in mdx muscles.

Further analysis of THI-treated mdx^{4cv} mice revealed an increase in muscle fiber size in quadriceps (Figure 3A). Although mdx mice undergo muscle hypertrophy as compared to wild type, we observed a significant increase in the minimum fiber diameter with THI treatment in diaphragms, and in both uninjured and injured quadriceps of 11-MO mice (Figure 3B,C and Additional file 1: Figure S7) [37]. Uninjured quadriceps of THI-treated 16-MO males also showed a significant increase in fiber size (Figure 3D). In summary, 3 days of THI treatment is sufficient to increase muscle fiber size in older mdx mice.

To assess if increases in muscle fiber size observed with THI treatment are accompanied by an increase in the number of satellite cells, we quantified the number of Pax7+ cells. Within skeletal muscle, Pax7 is specifically expressed by satellite cells, which have been reported to decline in older mdx^{4cv} muscles [38-40]. As expected, few satellite cells (Pax7+ nuclei) were visible in cross-sections of 11-MO mdx muscles. However, there was a significant increase in the mean number of Pax7+ nuclei, collectively in limb muscles (TAs and quadriceps) from THI-treated 11-MO animals (Additional file 1: Figure S8).

S1P is a potent angiogenic factor [41-43]. Thus we studied the effects of THI treatment on the skeletal muscle microvasculature. We quantified the number of vessels using BS1, a lectin that highlights endothelial cells [44]. In contrast to the increase in Pax7+ cells, we did not observe an increase in BS1+ vessels in injured 11-MO TA muscles. Quantitative RT-PCR analysis of endothelial related genes eNOS and CD31 in 5-MO mdx^{4cv} TA muscles at day 4 post injury, show no significant difference in the levels of expression of these endothelial associated genes in THI treatment compared to vehicle (Additional file 1: Figure S9). This suggests that THI benefits on muscle repair do not depend on increasing microvasculature density.

THI treatment elevates isometric force in acutely injured mdx EDL muscles

To assess if increasing S1P levels promotes dystrophic muscle function, in a fourth experiment we conducted myography analysis following longer treatment with THI. For this experiment, another group of mdx mice (male 4.75- to 5-MO C57BL/10ScSn-Dmd$^{mdx/J}$) was injured and treated with daily IP injections using the same THI dose and injection interval, for 14 consecutive days; the maximum duration for IP administration allowed by our approved animal protocol. Animals were treated with THI (n = 10) or vehicle (n = 9) for 14 days following injury,

Figure 4. S1P promotes functional improvement of mdx **(**C57BL/10ScSn-Dmd$^{mdx/J}$**)** muscle. (A) Experimental schematic of longer-term, 14-day treatment of THI or PBS (vehicle) following CTX injury. THI was administered following the aforementioned dose and injection regimen. Following treatment, EDL muscles were harvested and specific isometric force was analyzed by in vitro myography from both injured and uninjured limbs. **(B)** Force frequency analysis reveals that EDL muscles isolated from injured limbs of THI-treated animals (n = 10) have significantly greater specific force compared to injured vehicle controls (n = 9). **(C)** Analysis of untreated and uninjured wt (C57BL/10ScSn) and mdx (C57BL/10ScSn-Dmd$^{mdx/J}$) indicate specific force improved in injured but not uninjured THI-treated EDL muscles. **(D)** Incubation of uninjured and untreated mdx *(*C57BL/10ScSn-Dmd$^{mdx/J}$) EDL muscles with a high concentration of S1P (10 μM) leads to a significant increase in maximal specific force. *P <0.05, **P <0.005 by student's *t*-test. Error bars represent SEM. CTX, cardiotoxin; EDL, extensor digitorum longus; S1P, sphingosine-1-phoshate; SEM, standard error of the mean; THI, 2-acetyl-4(5)-tetrahydroxybutyl imidazole; wt, wild type.

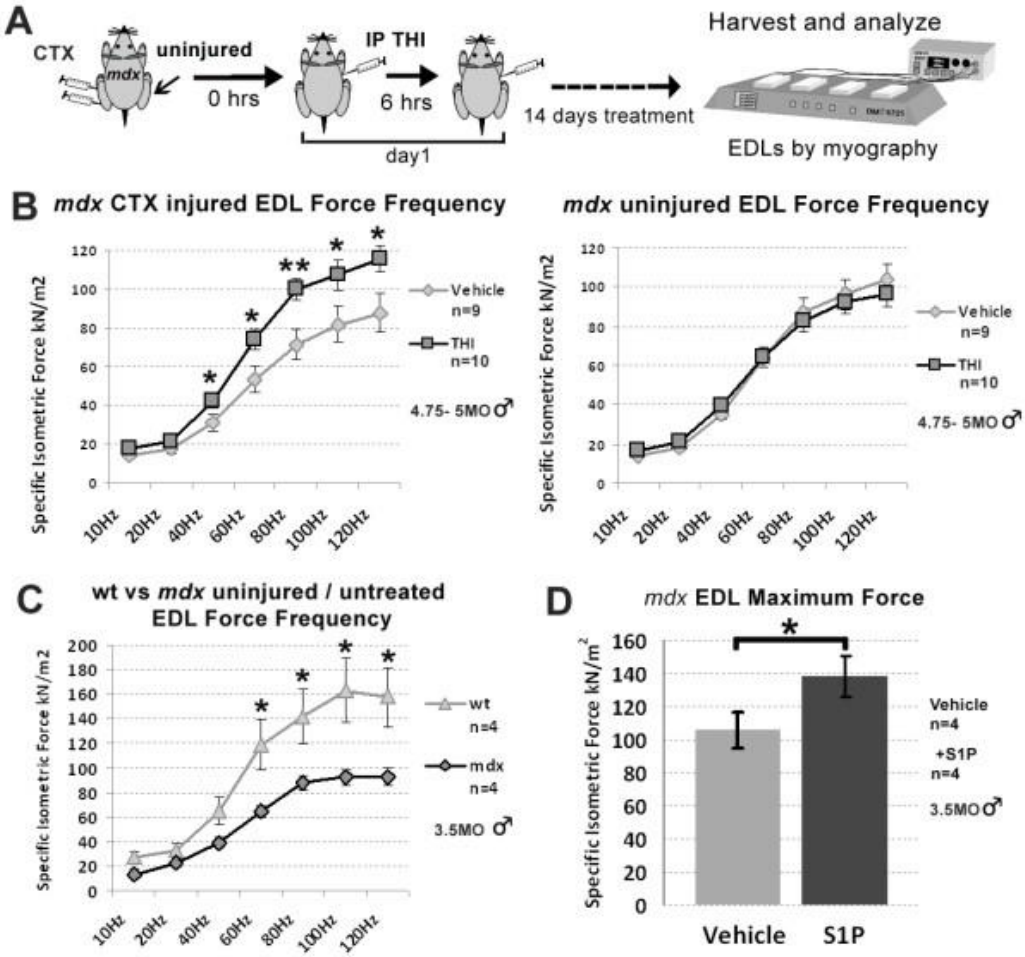

and analyzed between day 15 and 19 (Figure 4A). EDL muscles from injured and uninjured contralateral limbs were analyzed for isometric specific force; a physiological

measurement of muscle force that is reduced with muscular dystrophy in mice and humans [18,45,46].

To assess if the EDL is damaged as a consequence of CTX injection in the TA, we injured and analyzed a separate group of mdx mice (n = 4) 12 hours post injury. For this fifth experiment, CTX injections included India ink to label needle penetration [47]. To assess muscle fiber damage, a consequence of CTX injury, animals were injected IP with EBD immediately following CTX injection. The presence of EBD indicates EDL muscles are damaged. However, EDL damage is not due to direct penetration by the needle since India ink was only present in the CTX-injected TA muscles (Additional file 1: Figure S10).

Force frequency analysis revealed a significantly higher specific force by EDL muscles isolated from injured limbs of THI-treated mice (Figure 4B). These values were similar to EDL muscles isolated from contralateral uninjured limbs, indicating that THI prevented wasting and preserved muscle function following acute injury (Figure 4B). However, the specific force observed after THI treatment was still lower than wt control animals (Figure 4C). Two weeks of THI treatment was not sufficient to improve specific force in uninjured EDL muscles. However, as shown in Figure 1B, the THI dose of 0.75 μg/day used for all our experiments does not significantly raise S1P levels in all uninjured mdx muscles. In addition, although peripheral lymphocytes declined with THI (Figure 1A), we did not observe a decline of CD3e+ T-cells present in the diaphragm following 2 weeks of THI (Additional file 1: Figure S11) [48]. Therefore, it is plausible that a higher dose of THI is required to sufficiently elevate S1P levels needed to improve specific force in uninjured mdx muscles. However, since THI is insoluble in PBS at higher concentrations and has low oral bioavailability, we chose to directly study the effects of high levels of S1P on

uninjured mdx muscles ex vivo. For this experiment, EDLs from uninjured and untreated mdx mice were analyzed following incubation with 10 μM S1P [16]. Analysis of the maximal specific force indicates that direct administration of S1P significantly increases force output in uninjured mdx muscle (Figure 4D). Such results indicate that treatment with high concentrations of S1P can promote functional improvement of dystrophic muscles.

Overall, reduction in fibrosis and fat deposition, and increase in myofiber size and satellite cell numbers, indicate that elevating S1P levels, pharmacologically or by direct administration, has a profound benefit in dystrophic muscle repair and function.

Direct administration of S1P promotes muscle regeneration in mdx mice following CTX injury

S1P is essential for satellite cell turnover, myoblast differentiation and muscle regeneration in non-diseased mice, and more recently shown to promote satellite cell activation in mdx muscle [4,5,8,47]. To determine if the increase in satellite cell number observed in the THI-treated muscles was a result of increased S1P muscle content, we examined the effects of direct S1P administration following CTX-induced acute injury in dystrophic muscles. In order to identify satellite cells and their progeny, we utilized mdx^{4cv}:Myf5$^{nlacz/+}$ mice carrying the nuclear lacZ reporter driven by the endogenous Myf5 gene, a marker of myogenic cells [49-51]. CTX was applied to both TA muscles (n = 3, 3-MO mdx^{4cv}:Myf5$^{nlacz/+}$ males), then S1P was immediately injected intramuscularly into left TAs and a vehicle control into right TAs. Injections were repeated daily for the first 72 hours following injury and TAs were harvested on day 4 post injury, directly following the peak of injury-induced myogenic cell proliferation for analysis of Myf5+ nuclei (Figure 5A) [28]. S1P-treated muscles showed a dramatic, fourfold increase in the

number of Myf5+ nuclei in areas with severe CTX damage compared to vehicle controls (Figure 5B top row and 5C left graph). Furthermore, a significant increase in the number of Myf5+ nuclei was observed over the entire CSA of S1P-treated TAs (Figure 5C middle graph, Additional file 1: Figure S12). These data demonstrate that S1P treatment increases the number of myogenic cells in mdx muscles following injury and suggests that S1P promotes satellite cell proliferation in vivo.

We then determined whether the increase in myogenic cells promotes dystrophic muscle repair by staining for eMyHC, a marker of regenerating muscle fibers [27]. In concurrence with the rise of

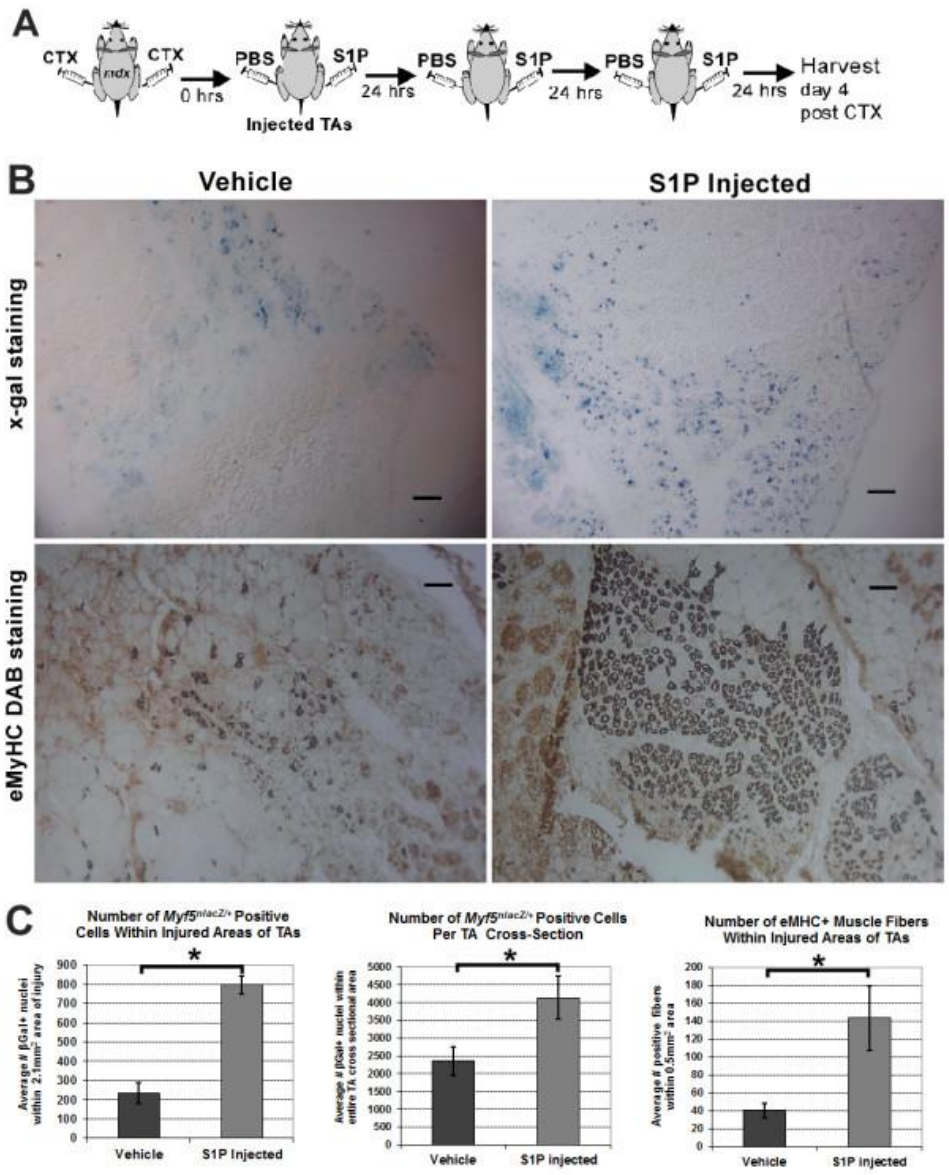

Figure 5. Direct administration of S1P promotes muscle regeneration following acute injury. (A) Experimental schematic of S1P and PBS (vehicle) injected daily for the first 72 hours into TAs of 3-MO mdx^{4cv}:Myf5$^{nlacZ/+}$ *mice* (n = 3, left TAs injected S1P, right TAs injected PBS) following CTX injury. **(B)** Top row: X-gal staining reveals an increased number of β-galactosidase+ nuclei at the sites of injury in S1P-treated TA muscles compared to vehicle controls. Bottom row: staining for eMyHC with DAB reveals a significant increase in the number of newly regenerated muscle fibers in S1P-treated TA muscles. Scale bars = 50 μm. **(C)** Left graph: quantification of β-galactosidase+ nuclei indicates the number of Myf5+ cells is significantly increased at the site of injury in S1P-treated compared to untreated muscles. Middle graph: a significant increase in β-galactosidase+ nuclei was also observed over the entire CSA of each S1P-treated TA muscle. Right graph: quantification of the number of eMyHC fibers within areas of regeneration was significantly greater with S1P treatment. *P <0.05 by student's *t*-test. Error bars represent SEM. CSA, cross-sectional area; CTX, cardiotoxin; DAB, 3,3'-diaminobenzidine; eMyHC, embryonic myosin heavy chain; MO, month-old; S1P, sphingosine-1-phoshate; SEM, standard error of the mean; TA, tibialis anterior.

Myf5+ myogenic cells, a 3.6 fold increase in the number of eMyHC+ fibers was observed in S1P-treated TAs (Figure 5B bottom row, 5C right graph). This increase in eMyHC+ fibers, corresponded with elevated numbers of centrally nucleated muscle fibers in the injured regions of S1P-treated muscles (Additional file 1: Figure S13A). Furthermore, the size of regenerating myofibers in S1P-treated TAs was significantly greater, as indicated by the minimum diameter quantified for the largest eMyHC+ fibers (Additional file 1: Figure S13B). Collectively, these data show that local administration of S1P promotes dystrophic muscle repair by improving satellite cell response and contribution to muscle fiber regeneration.

S1P directly acts on mdx muscle fibers, and elevates levels of total and phosphorylated S1PR1

In mammals there are five S1P receptors that share homology to G-protein coupled receptors [52]. It has been recently reported that S1P receptor 2 (S1PR2) is specifically activated in myogenic cells and that downstream effectors of S1P action in satellite cells include components of the JAK-STAT signaling pathway [8]. In contrast, our results and others, of exogenous S1P treatment resulting in increased EDL force, suggests that S1P also acts directly on muscle fibers [16]. The amount of exogenous S1P added in the bath was super-physiological and thus we measured S1P muscle levels following intramuscular injection of S1P. In this experiment, left TAs from mdx^{4cv} mice (n = 3, 11-MO) were injected with the same dose of S1P as the mdx^{4cv}:$Myf5^{nlacz/+}$ mice depicted in Figure 5A, while contralateral TAs received the same vehicle. In contrast to the previous experiment depicted in Figure 5A, TA muscles were injected in the absence of injury and were harvested for S1P analysis 15 minutes post injection (Figure 6A); the same time used for S1P incubation prior to EDL force measurement shown in Figure 4D. Results indicate that within this timeframe, intramuscular injection of S1P does significantly increase S1P levels in mdx muscle (Figure 6A).

To directly observe where S1P binds in the muscle, a separate group of mdx^{4cv} (n = 2, 11-MO) were injected with the same amount of biotinylated-S1P in left and vehicle in right TAs. Once more, TAs were harvested 15 minutes post injection for histological visualization of S1P. Staining with streptavidin conjugated to Alexa Fluor 594 reveals that biotinylated-S1P is present in many cells, but particularly localized to the perimeter of muscle fibers (Figure 5B). Among the three S1P receptors (S1PR1, S1PR2, S1PR3) expressed in muscle, S1PR3 and S1PR1 are the

most abundant in wt muscle [5]. Importantly, expression of these three S1P receptors is reduced in mdx muscle cells, especially S1PR1, which shows more than five fold reduction in relative mRNA levels (Additional file 1: Figure S14). Staining of mdx^{4cv} muscles (3.5-MO) for S1PR1 and S1PR3, reveals that S1PR1 is present at the perimeter of muscle fibers and myonuclei, whereas S1PR3 appears localized to the vasculature (Figure 6C). S1PR1 is a G protein-coupled receptor (GPCR) that can be activated via phosphorylation, resulting in translocation to the endosomal compartment and/or the perinuclear compartment [53-55]. Therefore, perinuclear localization of S1PR1 suggested that in response to S1P treatment, receptor 1 signaling is activated in mdx^{4cv} muscle fibers. To evaluate the presence of active S1PR1 signaling during muscle fiber regeneration, we surveyed the same CTX-injured muscles depicted in Figure 5A for the presence of phosphorylated S1PR1. Results indicate S1PR1 is localized around the perimeter of muscle fibers and intracellularly near or within the myonuclei (perinuclear) of newly regenerated eMyHC+ fibers (Figure 6D). In parallel, we observed more concentrated staining for phosphorylated S1PR1 localized perinuclearly and less so around the perimeter of eMyHC+ fibers (Figure 6E). These results indicate that S1PR1 signaling is active in regenerating muscle fibers and suggests that the beneficial actions that S1P exerts on mdx muscle fibers may be mediated through S1PR1.

S1P administration correlates with increased levels of S1PR1 and P-rpS6, an indicator of protein synthesis

S1PR1 has been implicated in myoblast proliferation and shown to steadily increase during the course of regeneration in non-diseased muscle [4,5]. Therefore to gain more insight on the potential action that S1P exerts via S1PR1 in dystrophic muscle, we injected S1P in uninjured

TAs of mdx^{4cv} (n = 3, 2.5-MO), and quantified the level of S1PR1 and some downstream effectors (Figure 7A) [56]. In turn, S1P treatment resulted in significantly elevated levels of S1PR1 in mdx^{4cv} TAs (Figure 7B). In a separate experiment, we injected S1P in left TAs and vehicle in right TAs of mdx^{4cv} (n = 3, 10-MO), following the same dose and experimental design (three injections, one per day, harvest on day 4), and analyzed TA muscles for phosphorylated S1PR1. Results from this experiment show that phosphorylated S1PR1 is also significantly elevated with S1P treatment (Additional file 1: Figure S15).

A result of S1P injection was larger eMyHC+ fibers that were positive for phosphorylated S1PR1 (Figure 6E, Additional file 1: Figure S13B). Therefore, we examined if elevated S1PR1

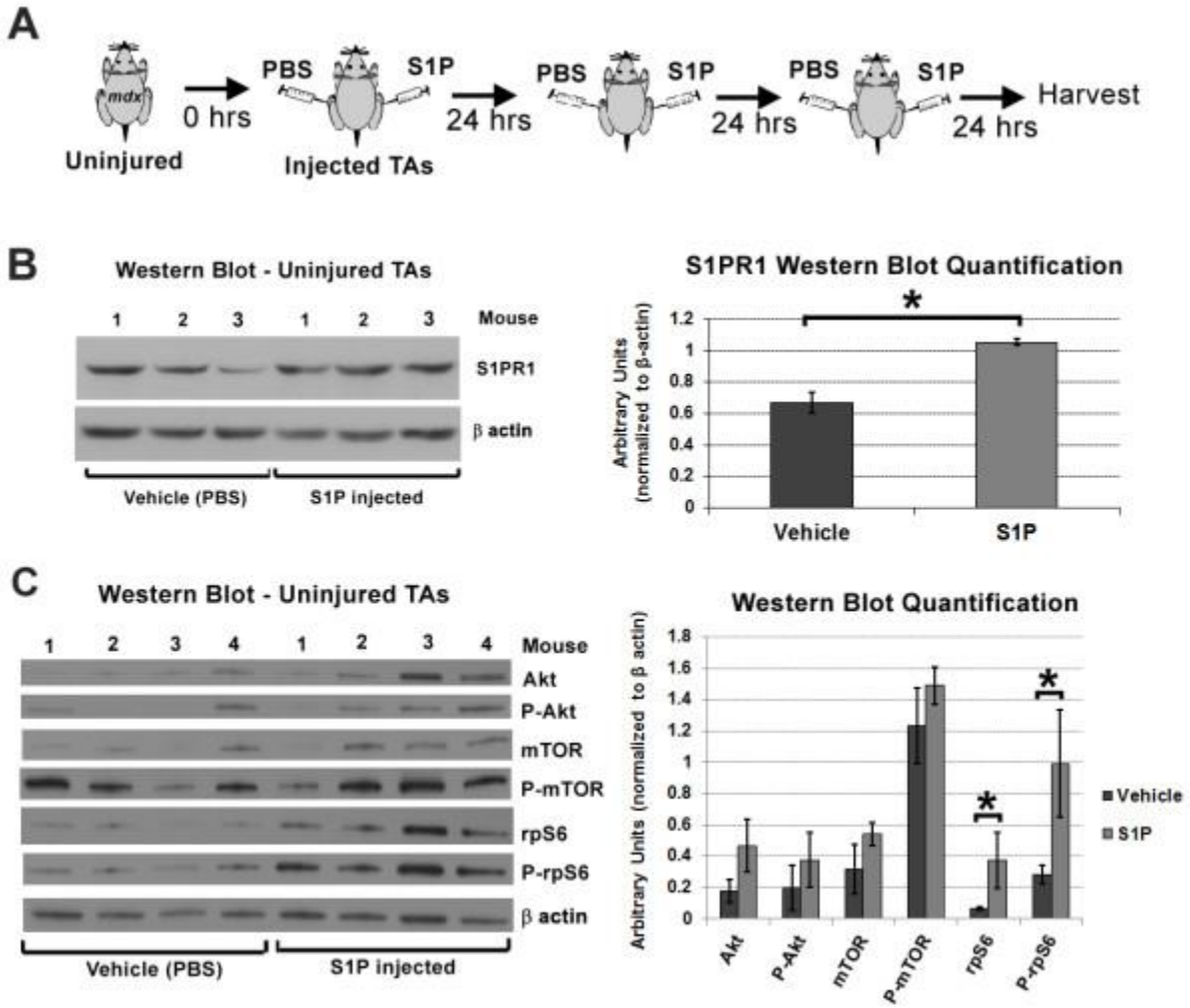

Figure 6. Administration of S1P leads to increased levels of S1PR1 and P-rpS6 in vivo**.** (A) Experimental schematic of S1P and PBS (vehicle) injected daily for the first 72 hours into TAs of uninjured mdx^{4cv} mice (n = 4, 2.5-MO, left TAs injected S1P, right TAs injected PBS**).** (B) Western blot analysis of injected TAs (n = 3, 2.5-MO mdx^{4cv}) indicates that administration of S1P significantly increases S1PR1 levels. **(C)** Western blot analysis of injected TAs (n = 4, 2.5-MO mdx^{4cv}) for total, and P-Akt, P-mTOR and P-rpS6, reveals that total and P-rpS6 were significantly higher with S1P treatment. Increased levels of total and P-rpS6 suggest that S1P administration promotes protein synthesis in mdx muscles. **P* <0.05 by student's *t*-test. Error bars represent SEM. MO, month-old; P-Akt, phosphorylated Akt; P-mTOR, phosphorylated mammalian target of rapamycin; P-rpS6, phosphorylated ribosomal protein S6; rpS6, ribosomal protein S6; S1P, sphingosine-1-phoshate; S1PR1, S1P receptor 1; SEM, standard error of the mean; TA, tibialis anterior.

levels corresponded with known regulators of cell size and protein synthesis; Akt, mTOR, S6 kinase and rpS6. S1P-induced hypertrophy has been described in cultured cardiomyocytes, which was accompanied by activation of Akt and S6 kinase [57]. In addition, S1PR1 activation of S6 kinase via a Gi-dependent pathway has been reported in vascular smooth muscle cells [56]. Akt and mTOR signaling via S6 kinase, an activator of rpS6 implicated in protein synthesis, has been described as sufficient to induce skeletal muscle hypertrophy [58-60]. Therefore, we evaluated if direct injection of S1P induces activation of these pathways in uninjured TA muscles of mdx^{4cv} mice (n = 4, 2.5-MO). Western blot analysis of TA muscles injected for 3 days with S1P (Figure 7A) revealed that the levels of phosphorylated Akt (P-Akt) and mTOR (P-mTOR), though increased, were not significantly higher in S1P-treated muscles (Figure 7C). However, the levels of rpS6 and phosphorylated rpS6 (P-rpS6) were significantly increased with S1P treatment compared to control muscles, suggesting an increase in protein synthesis. Although a more detailed study is required to elucidate the role of S1P in skeletal muscle protein synthesis, our data suggest that S1P can activate muscle anabolic pathways in the mdx mouse.

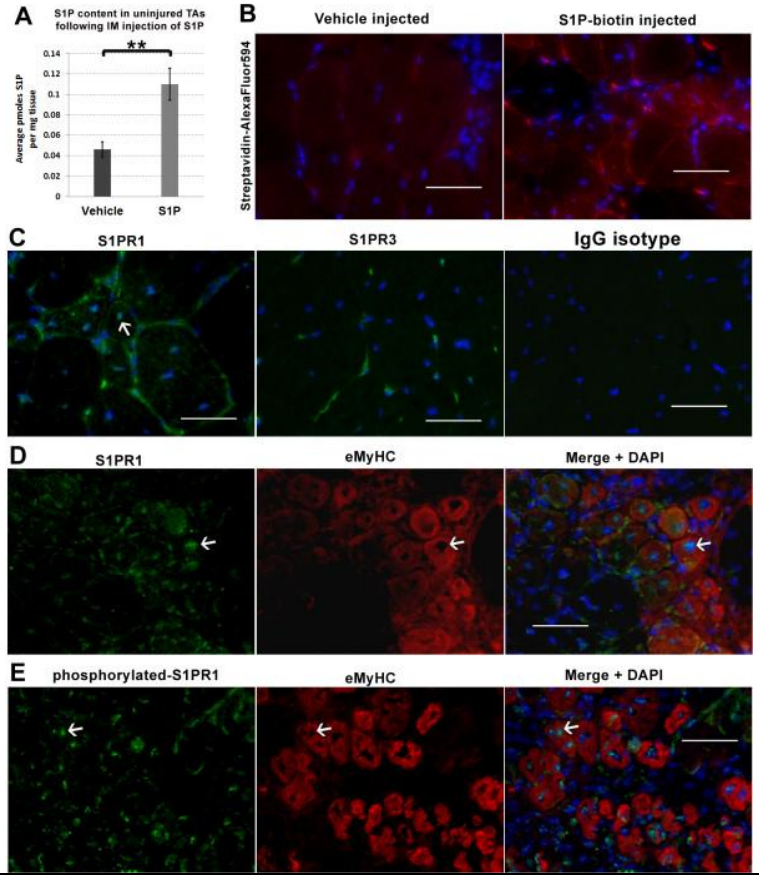

Direct administration of S1P promotes muscle regeneration in dysferlinopathy mice following acute injury

The role of dysferlin is currently unknown, but its absence in humans and mice results in chronic muscle wasting that primarily affects limb and girdle muscles [61-63]. Although dysferlinopathy is less severe than DMD [64], dysferlinopathy patients

Figure 7. Direct injection results in elevated S1P levels which correlate with the activation of receptor 1 in muscle fibers. (A) To quantify the elevation of S1P following direct administration, we injected a single dose (same dose as Figure5) of S1P in left TAs and vehicle in right TAs of uninjured mdx^{4cv} (n = 3, 11-MO) mice. TA muscles were harvested 15 minutes post injection for analysis by LC-MS/MS. Results indicate a significant elevation of S1P following direct injection. **(B)** To visualize the location of S1P following injection, biotinylated-S1P was injected in left TAs versus vehicle in right TAs of uninjured mdx^{4cv} mice (n = 2, 11-MO). Once more, TAs were harvested 15 minutes following injection. Staining with streptavidin conjugated to Alexa Fluor 594 reveals the presence of S1P-biotin around the perimeter of muscle fibers. **(C)** Staining of mdx^{4cv} TAs for S1PR1 and S1PR3 reveals S1PR1 is localized to the perimeter and perinuclear area (arrow) of muscle fibers (left photo). In contrast, staining for S1PR3 was mainly localized to the muscle vasculature (middle photo). Staining in parallel with an IgG isotype control for both antibodies shows the absence of non-specific staining (right graph). **(D)** Staining for S1PR1 in CTX-injured TAs (same tissue from Figure 5) reveals S1PR1 is present at the perimeter and perinuclear area of regenerating eMyHC+ fibers. **(E)** Staining for phosphorylated S1PR1 in the same mdx^{4cv} TAs was more prominent in the perinuclear area of eMyHC+ fibers, indicating the presence of active S1PR1 signaling in regenerating fibers. Scale bars = 50 μm. **P <0.005 by student's t-test. Error bars represent SEM. CTX, cardiotoxin; eMyHC, embryonic myosin heavy chain; IgG, immunoglobulin G; LC-MS/MS, liquid chromatography-tandem mass spectrometry; MO, month-old; S1P, sphingosine-1-phoshate; S1PR1, S1P receptor 1; S1PR3, S1P receptor 3; SEM, standard error of the mean; TA, tibialis anterior.

are often wheelchair bound between 30 and 40 years of age [65]. Much like DMD, muscles in humans and mice lacking functional dysferlin exhibit chronic atrophy, resulting in the accumulation of fibrosis and fat [66]. Therefore we tested the effects of S1P administration after CTX injury in a model of dysferlinopathy (AJ/SCID) to evaluate if the benefits of S1P are exclusive to the mdx background or can be applied to other muscle wasting diseases [67]. We followed the same experimental design outlined in Figure 5A, injecting left TAs of AJ/SCID mice (n = 4, 9-MO) with the same dose of S1P and vehicle in right TAs for 3 days following CTX injury. In contrast to the experiments in mdx^{4cv}, we harvested TAs on day 6 post injury in order to also evaluate the onset of fibrosis. In accordance to the results observed in mdx, we observed improved muscle regeneration with the administration of S1P in AJ muscles. Specifically, we observed lower fibrosis and increased centrally nucleated fibers, as well as improved muscle architecture in the damaged regions of muscle with S1P administration (Additional file 1: Figure S16). These results indicate that approaches aimed at elevating muscle S1P may be beneficial to promote muscle regeneration in additional muscle wasting diseases.

Longer-term treatment with THI shows a functional benefit in uninjured mdx muscle

To this point we have largely examined the role of S1P in promoting muscle regeneration in acutely injured dystrophic muscles. Since long-term intramuscular injections of S1P are neither feasible nor practical (the injections also cause damage), we decided to revisit the use of THI for elevating S1P muscle content. Although our initial experiments with THI showed little benefit in uninjured mdx muscles, they were short-term and in older animals with severe pathology (Figures 2, ,3),3), or adult animals (Figure 4) at a point when hypertrophy and robust regeneration compensate for degeneration in limb muscles [24,68,69]. Therefore, we examined

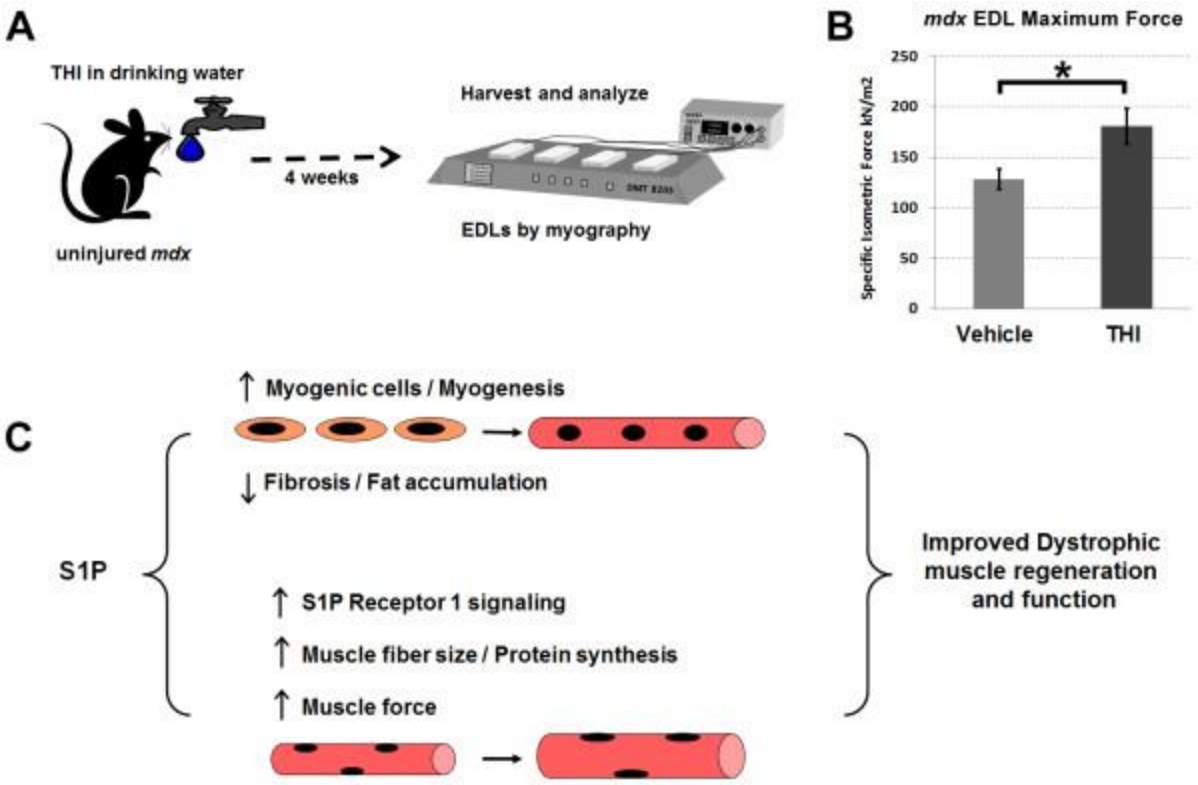

Figure 8. Longer-term treatment with THI elevated muscle force in uninjured ***mdx*** EDL muscles. (A) Experimental schematic outlining the treatment regimen. Beginning at 4 weeks of age, mdx^{4cv} mice (1-MO males) were treated for 4 weeks ad libitum with 50 mg/l THI (n = 4) or vehicle (n = 3) in drinking water. **(B)** Myography analysis of EDL muscles reveals a significant increase in maximal specific force with THI treatment. **P* <0.05 by student's *t*-test. Error bars represent SEM. **(C)** Summary of findings: S1P can act to not only promote myogenic cell activation and muscle repair, but also enhance muscle fiber size and force, possibly through S1PR1 mediated signaling. EDL, extensor digitorum longus; MO, month-old; S1P, sphingosine-1-phoshate; S1PR1, S1P receptor 1; SEM, standard error of the mean; THI, 2-acetyl-4(5)-tetrahydroxybutyl imidazole.

longer-term treatment of THI in younger mdx mice at 4 weeks of age, a time point characterized by significant muscle degeneration prior to the compensatory period [70]. For this experiment, uninjured mdx^{4cv} animals were treated for 1 month, beginning at 4 weeks of age, with THI or vehicle in the drinking water (Figure 8A) [11]. At 8 weeks of age, we assessed the functional benefit of THI treatment by analyzing EDL specific force via myography. In turn, EDLs from THI-treated animals showed significantly greater specific force compared to vehicle-treated

controls (Figure 8B). This data demonstrates that elevating S1P levels is beneficial for the chronic muscle injury that occurs early in muscular dystrophy.

Discussion

We have shown that systemic administration of the pharmacological agent THI by IP injection to dystrophic mdx mice led to elevated levels of S1P in recovering injured muscle tissue, as well as a reduction of fibrosis and fat infiltration, both pathological indicators of muscle wasting (Figure 2). Additionally, systemic THI led to a significant increase in muscle fiber size and specific force of CTX-injured muscles (Figures 3 and and4).4). In turn, ex vivo administration of high levels of S1P resulted in specific force levels in uninjured mdx EDL muscles (Figure 4D). To pursue a better understanding of how elevated S1P reduces DMD pathology, we found that direct administration of S1P via intramuscular injection doubles muscle S1P content compared to the S1P levels reached with IP injections of THI. In addition, intramuscular S1P injections led to an increase in myogenic cells (Myf5+) and induced phosphorylation of S1PR1, which was particularly abundant in newly regenerating fibers (Figure 7, Additional file 1: Figure S15), as well as a significant increase in rpS6 and P-rpS6 levels (Figure 6). These results suggest that S1P not only works to activate myogenic precursors but also elevates protein synthesis in muscle fibers, potentially through S1PR1 mediated signaling (summarized in Figure 8C). In summary, THI/S1P administration led to improved regeneration and pathology, higher muscle specific force, an increase in the number of myogenic cells, and larger muscle fibers.

Our results indicate that S1P mediates satellite cell-dependent and muscle fiber-dependent effects on skeletal muscle. If amelioration of muscle wasting occurs through receptor-mediated signaling then S1P, elevated intracellularly via THI, must be exported to activate the S1P

receptors. THI has been reported to inhibit the S1P lyase, an enzyme whose active site is on the cytoplasmic side of the endoplasmic reticulum. Therefore elevations of S1P levels mediated via THI inhibition of the S1P lyase presumably occur within the cytoplasm [71]. S1P may also act intracellularly before possible export to promote muscle wasting suppression. This alternative is supported by our work with Drosophila, which have no known S1P receptors [9], as well as by a recent report that showed S1P interacts directly, intracellularly, with histone deacetylases (HDACs) [72]. As HDAC inhibitors have been previously shown to suppress dystrophic phenotypes in mdx mice, the actions of S1P on the suppression of muscle wasting may occur in part through such mechanisms [73]. It has also been reported that reductions in HDAC activity result in an increase of follistatin, an inhibitor of myostatin, which may explain the amelioration of DMD pathology [74]. Our data support this possibility and suggest that the molecular mechanism for the suppression of muscle degeneration involves the anabolic pathways for muscle formation rpS6. These components have been shown to lie downstream of myostatin and insulin-like growth factor [75].

Conclusion

Based on the work reported here, elevation of S1P may be a fruitful strategy for ameliorating the pathology manifested in patients afflicted with DMD and possibly other muscle wasting diseases (for example dysferlinopathy). Therapies based on promoting S1P levels in dystrophic muscle have the potential to improve pathology by promoting satellite cell and anabolic-mediated regeneration. An obvious candidate for a small molecule therapeutic is THI. Our work has shown that short-term treatment of THI has significant efficacy in increasing regenerative capacity in the mdx mouse following acute muscle injury, while longer treatment can improve muscle

function in younger uninjured mdx muscle. Moreover, significant increases in muscle fiber size have been suggested as a viable approach in overcoming dystrophic muscle damage by promoting strength and function [76]. Additionally, there are other THI derivatives with increased oral bioavailability that may be more effective at increasing and maintaining high intramuscular S1P levels in long-term treatments, which was necessary for functional improvement of uninjured EDL muscles [10]. Alternatively there are inhibitors of lipid phosphate phosphatases and/or S1P phosphatases that may also increase intramuscular S1P levels [10,77]. In addition, there are specific S1P receptor agonists (for example FTY720) that are currently FDA approved or in clinical trials [78,79]. Based on our present results and those of others, future studies focused on S1P-based therapeutics for the treatment of DMD and related myopathies are warranted.

Chapter 3 Supplementary Material: Available online at SkeletalMuscleJournal.com. 2044-5040-3-20

Chapter 3 References

1. Deconinck N, Dan B: Pathophysiology of duchenne muscular dystrophy: current hypotheses.Pediatr Neurol 2007, 36:1–7.

2. Mendell JR, Rodino-Klapac LR, Malik V: Molecular therapeutic strategies targeting Duchenne muscular dystrophy.J Child Neurol 2010, 25:1145–1148.

3. Palmieri B, Tremblay JP, Daniele L: Past, present and future of myoblast transplantation in the treatment of Duchenne muscular dystrophy.Pediatr Transplant 2010, 14:813–819.

4. Rapizzi E, Donati C, Cencetti F, Nincheri P, Bruni P: Sphingosine 1-phosphate differentially regulates proliferation of C2C12 reserve cells and myoblasts.Mol Cell Biochem 2008, 314:193–199.

5. Danieli-Betto D, Peron S, Germinario E, Zanin M, Sorci G, Franzoso S, Sandona D, Betto R: Sphingosine 1-phosphate signaling is involved in skeletal muscle regeneration.Am J Physiol 2010, 298:C550–C558.

6. Bernacchioni C, Cencetti F, Blescia S, Donati C, Bruni P: Sphingosine kinase/sphingosine 1-phosphate axis: a new player for insulin-like growth factor-1-induced myoblast differentiation.Skelet Muscle 2012, 2:15.

7. Bruni P, Donati C: Pleiotropic effects of sphingolipids in skeletal muscle.Cell Mol Life Sci 2008, 65:3725–3736.

8. Loh KC, Leong WI, Carlson ME, Oskouian B, Kumar A, Fyrst H, Zhang M, Proia RL, Hoffman EP, Saba JD: Sphingosine-1-phosphate enhances satellite cell activation in dystrophic muscles through a S1PR2/STAT3 signaling pathway.PLoS One 2012, 7:e37218.

9. Pantoja M, Fischer KA, Ieronimakis N, Reyes M, Ruohola-Baker H: Genetic elevation of Sphingosine 1-phosphate suppresses dystrophic muscle phenotypes in Drosophila.Development 2013, 140:136–146.

10. Bagdanoff JT, Donoviel MS, Nouraldeen A, Tarver J, Fu Q, Carlsen M, Jessop TC, Zhang H, Hazelwood J, Nguyen H, Baugh SD, Gardyan M, Terranova KM, Barbosa J, Yan J, Bednarz M, Layek S, Courtney LF, Taylor J, Digeorge-Foushee AM, Gopinathan S, Bruce D, Smith T,

Moran L, O'Neill E, Kramer J, Lai Z, Kimball SD, Liu Q, Sun W, et al: Inhibition of sphingosine-1-phosphate lyase for the treatment of autoimmune disorders.J Med Chem 2009, 52:3941–3953.

11. Schwab SR, Pereira JP, Matloubian M, Xu Y, Huang Y, Cyster JG: Lymphocyte sequestration through S1P lyase inhibition and disruption of S1P gradients.Science (New York, NY 2005, 309:1735–1739.

12. Matsuda R, Nishikawa A, Tanaka H: Visualization of dystrophic muscle fibers in mdx mouse by vital staining with Evans blue: evidence of apoptosis in dystrophin-deficient muscle.J Biochem 1995, 118:959–964.

13. Ieronimakis N, Balasundaram G, Rainey S, Srirangam K, Yablonka-Reuveni Z, Reyes M: Absence of CD34 on murine skeletal muscle satellite cells marks a reversible state of activation during acute injury.PLoS One 2008, 5:e10920.

14. Grabski AD, Shimizu T, Deou J, Mahoney WM Jr, Reidy MA, Daum G: Sphingosine-1-phosphate receptor-2 regulates expression of smooth muscle alpha-actin after arterial injury.Arterioscler Thromb Vasc Biol 2009, 29:1644–1650.

15. Au CG, Butler TL, Sherwood MC, Egan JR, North KN, Winlaw DS: Increased connective tissue growth factor associated with cardiac fibrosis in the mdx mouse model of dystrophic cardiomyopathy.Int J Exp Pathol 2011, 92:57–65.

16. Danieli-Betto D, Germinario E, Esposito A, Megighian A, Midrio M, Ravara B, Damiani E, Libera LD, Sabbadini RA, Betto R: Sphingosine 1-phosphate protects mouse extensor digitorum longus skeletal muscle during fatigue.Am J Physiol 2005, 288:C1367–C1373.

17. Gregorevic P, Plant DR, Leeding KS, Bach LA, Lynch GS: Improved contractile function of the mdx dystrophic mouse diaphragm muscle after insulin-like growth factor-I administration.Am J Pathol 2002, 161:2263–2272.

18. Gregorevic P, Plant DR, Lynch GS: Administration of insulin-like growth factor-I improves fatigue resistance of skeletal muscles from dystrophic mdx mice.Muscle Nerve 2004, 30:295–304.

19. Baker DL, Desiderio DM, Miller DD, Tolley B, Tigyi GJ: Direct quantitative analysis of lysophosphatidic acid molecular species by stable isotope dilution electrospray ionization liquid chromatography-mass spectrometry.Anal Biochem 2001, 292:287–295.

20. Oliver IT: A spectrophotometric method for the determination of creatine phosphokinase and myokinase.Biochem J 1955, 61:116–122.

21. Kiernan J: Histological and Histochemical Methods: Theory and Practice, 4th edition. New York: Cold Spring Harbor Laboratory Press; 2008.

22. Clever JL, Sakai Y, Wang RA, Schneider DB: Inefficient skeletal muscle repair in inhibitor of differentiation knockout mice suggests a crucial role for BMP signaling during adult muscle regeneration.Am J Physiol 2010, 298:C1087–C1099.

23. Chapman VM, Miller DR, Armstrong D, Caskey CT: Recovery of induced mutations for X chromosome-linked muscular dystrophy in mice.Proc Natl Acad Sci USA 1989, 86:1292–1296.

24. Pastoret C, Sebille A: mdx mice show progressive weakness and muscle deterioration with age.J Neurol Sci 1995, 129:97–105.

25. Zhou J, Saba JD: Identification of the first mammalian sphingosine phosphate lyase gene and its functional expression in yeast.Biochem Biophys Res Commun 1998, 242:502–507.

26. Mendel J, Heinecke K, Fyrst H, Saba JD: Sphingosine phosphate lyase expression is essential for normal development in Caenorhabditis elegans.J Biol Chem 2003, 278:22341–22349.

27. d'Albis A, Couteaux R, Janmot C, Roulet A, Mira JC: Regeneration after cardiotoxin injury of innervated and denervated slow and fast muscles of mammals. Myosin isoform analysis.E J Biochem 1988, 174:103–110.

28. Yan Z, Choi S, Liu X, Zhang M, Schageman JJ, Lee SY, Hart R, Lin L, Thurmond FA, Williams RS: Highly coordinated gene regulation in mouse skeletal muscle regeneration.J Biol Chem 2003, 278:8826–8836.

29. Mouisel E, Vignaud A, Hourde C, Butler-Browne G, Ferry A: Muscle weakness and atrophy are associated with decreased regenerative capacity and changes in mTOR signaling in skeletal muscles of venerable (18-24-month-old) dystrophic mdx mice.Muscle Nerve 2010, 41:809–818.

30. Ieronimakis N, Balasundaram G, Rainey S, Srirangam K, Yablonka-Reuveni Z, Reyes M: Absence of CD34 on murine skeletal muscle satellite cells marks a reversible state of activation during acute injury.PLoS One 2010, 5:e10920.

31. Glesby MJ, Rosenmann E, Nylen EG, Wrogemann K: Serum CK, calcium, magnesium, and oxidative phosphorylation in mdx mouse muscular dystrophy.Muscle Nerve 1988, 11:852–856.

32. Salimena MC, Lagrota-Candido J, Quirico-Santos T: Gender dimorphism influences extracellular matrix expression and regeneration of muscular tissue in mdx dystrophic mice.Histochem Cell Biol 2004, 122:435–444.

33. Cros D, Harnden P, Pellissier JF, Serratrice G: Muscle hypertrophy in Duchenne muscular dystrophy. A pathological and morphometric study. J Neurol 1989, 236:43–47.

34. Murphy MM, Lawson JA, Mathew SJ, Hutcheson DA, Kardon G: Satellite cells, connective tissue fibroblasts and their interactions are crucial for muscle regeneration.Development 2011, 138:3625–3637.

35. Mann CJ, Perdiguero E, Kharraz Y, Aguilar S, Pessina P, Serrano AL, Munoz-Canoves P: Aberrant repair and fibrosis development in skeletal muscle.Skelet Muscle 2011, 1:21.

36. Hamer PW, McGeachie JM, Davies MJ, Grounds MD: Evans Blue Dye as an in vivo marker of myofibre damage: optimising parameters for detecting initial myofibre membrane permeability.J Anat 2002, 200:69–79.

37. Peter AK, Crosbie RH: Hypertrophic response of Duchenne and limb-girdle muscular dystrophies is associated with activation of Akt pathway.Exp Cell Res 2006, 312:2580–2591.

38. Halevy O, Piestun Y, Allouh MZ, Rosser BW, Rinkevich Y, Reshef R, Rozenboim I, Wleklinski-Lee M, Yablonka-Reuveni Z: Pattern of Pax7 expression during myogenesis in the

posthatch chicken establishes a model for satellite cell differentiation and renewal.Dev Dyn 2004, 231:489–502.

39. Reimann J, Irintchev A, Wernig A: Regenerative capacity and the number of satellite cells in soleus muscles of normal and mdx mice.Neuromuscul Disord 2000, 10:276–282.

40. Seale P, Sabourin LA, Girgis-Gabardo A, Mansouri A, Gruss P, Rudnicki MA: Pax7 is required for the specification of myogenic satellite cells.Cell 2000, 102:777–786.

41. Heo K, Park KA, Kim YH, Kim SH, Oh YS, Kim IH, Ryu SH, Suh PG: Sphingosine 1-phosphate induces vascular endothelial growth factor expression in endothelial cells.BMB Rep 2009, 42:685–690.

42. Kimura T, Watanabe T, Sato K, Kon J, Tomura H, Tamama K, Kuwabara A, Kanda T, Kobayashi I, Ohta H, Ui M, Okajima F: Sphingosine 1-phosphate stimulates proliferation and migration of human endothelial cells possibly through the lipid receptors, Edg-1 and Edg-3.Biochem J 2000, 348(Pt 1):71–76.

43. Rikitake Y, Hirata K, Kawashima S, Ozaki M, Takahashi T, Ogawa W, Inoue N, Yokoyama M: Involvement of endothelial nitric oxide in sphingosine-1-phosphate-induced angiogenesis.Arterioscler Thromb Vasc Biol 2002, 22:108–114.

44. Yeh HI, Dupont E, Coppen S, Rothery S, Severs NJ: Gap junction localization and connexin expression in cytochemically identified endothelial cells of arterial tissue.J Histochem Cytochem 1997, 45:539–550.

45. Beenakker EA, Maurits NM, Fock JM, Brouwer OF, van der Hoeven JH: Functional ability and muscle force in healthy children and ambulant Duchenne muscular dystrophy patients.Eur J Paediatr Neurol 2005, 9:387–393.

46. Lynch GS, Hinkle RT, Chamberlain JS, Brooks SV, Faulkner JA: Force and power output of fast and slow skeletal muscles from mdx mice 6–28 months old.J Physiol 2001, 535:591–600.

47. Nagata Y, Partridge TA, Matsuda R, Zammit PS: Entry of muscle satellite cells into the cell cycle requires sphingolipid signaling.J Cell Biol 2006, 174:245–253.

48. Frank SJ, Engel I, Rutledge TM, Letourneur F: Structure/function analysis of the invariant subunits of the T cell antigen receptor.Semin Immunol 1991, 3:299–311.

49. Tajbakhsh S, Bober E, Babinet C, Pournin S, Arnold H, Buckingham M: Gene targeting the myf-5 locus with nlacZ reveals expression of this myogenic factor in mature skeletal muscle fibres as well as early embryonic muscle.Dev Dyn 1996, 206:291–300.

50. Beauchamp JR, Heslop L, Yu DS, Tajbakhsh S, Kelly RG, Wernig A, Buckingham ME, Partridge TA, Zammit PS: Expression of CD34 and Myf5 defines the majority of quiescent adult skeletal muscle satellite cells.J Cell Biol 2000, 151:1221–1234.

51. Day K, Shefer G, Richardson JB, Enikolopov G, Yablonka-Reuveni Z: Nestin-GFP reporter expression defines the quiescent state of skeletal muscle satellite cells.Dev Biol 2007, 304:246–259.

52. Rosen H, Gonzalez-Cabrera PJ, Sanna MG, Brown S: Sphingosine 1-phosphate receptor signaling.Annu Rev Biochem 2009, 78:743–768.

53. Liu CH, Thangada S, Lee MJ, Van Brocklyn JR, Spiegel S, Hla T: Ligand-induced trafficking of the sphingosine-1-phosphate receptor EDG-1.Mol Biol Cell 1999, 10:1179–1190.

54. Oo ML, Chang SH, Thangada S, Wu MT, Rezaul K, Blaho V, Hwang SI, Han DK, Hla T: Engagement of S1P(1)-degradative mechanisms leads to vascular leak in mice.J Clin Invest 2011, 121:2290–2300.

55. Estrada R, Wang L, Jala VR, Lee JF, Lin CY, Gray RD, Haribabu B, Lee MJ: Ligand-induced nuclear translocation of S1P(1) receptors mediates Cyr61 and CTGF transcription in endothelial cells.Histochem Cell Biol 2009, 131:239–249.

56. Kluk MJ, Hla T: Role of the sphingosine 1-phosphate receptor EDG-1 in vascular smooth muscle cell proliferation and migration.Circ Res 2001, 89:496–502.

57. Robert P, Tsui P, Laville MP, Livi GP, Sarau HM, Bril A, Berrebi-Bertrand I: EDG1 receptor stimulation leads to cardiac hypertrophy in rat neonatal myocytes.J Mol Cell Cardiol 2001, 33:1589–1606.

58. Bodine SC, Stitt TN, Gonzalez M, Kline WO, Stover GL, Bauerlein R, Zlotchenko E, Scrimgeour A, Lawrence JC, Glass DJ, Yancopoulos GD: Akt/mTOR pathway is a crucial regulator of skeletal muscle hypertrophy and can prevent muscle atrophy in vivo.Nat Cell Biol 2001, 3:1014–1019.

59. Lai KM, Gonzalez M, Poueymirou WT, Kline WO, Na E, Zlotchenko E, Stitt TN, Economides AN, Yancopoulos GD, Glass DJ: Conditional activation of akt in adult skeletal muscle induces rapid hypertrophy.Mol Cell Biol 2004, 24:9295–9304.

60. Thomas G: The S6 kinase signaling pathway in the control of development and growth.Biol Res 2002, 35:305–313.

61. Anderson LV, Davison K, Moss JA, Young C, Cullen MJ, Walsh J, Johnson MA, Bashir R, Britton S, Keers S, Argov Z, Mahjneh I, Fougerousse F, Beckmann JS, Bushby KM: Dysferlin is a plasma membrane protein and is expressed early in human development.Hum Mol Genet 1999, 8:855–861.

62. Ho M, Post CM, Donahue LR, Lidov HG, Bronson RT, Goolsby H, Watkins SC, Cox GA, Brown RH Jr: Disruption of muscle membrane and phenotype divergence in two novel mouse models of dysferlin deficiency.Hum Mol Genet 2004, 13:1999–2010.

63. Millay DP, Maillet M, Roche JA, Sargent MA, McNally EM, Bloch RJ, Molkentin JD: Genetic manipulation of dysferlin expression in skeletal muscle: novel insights into muscular dystrophy.Am J Pathol 2009, 175:1817–1823.

64. Han R, Rader EP, Levy JR, Bansal D, Campbell KP: Dystrophin deficiency exacerbates skeletal muscle pathology in dysferlin-null mice.Skelet Muscle 2011, 1:35.

65. Aoki M, Takahashi T: [Mutational and clinical features of Japanese patients with dysferlinopathy (Miyoshi myopathy and limb girdle muscular dystrophy type 2B)].Rinsho shinkeigaku 2005, 45:938–942. [Article in Japanese]

66. Fanin M, Angelini C: Muscle pathology in dysferlin deficiency.Neuropathol Appl Neurobiol 2002, 28:461–470.

67. Farini A, Sitzia C, Navarro C, D'Antona G, Belicchi M, Parolini D, Del Fraro G, Razini P, Bottinelli R, Meregalli M, Torrente Y: Absence of T and B lymphocytes modulates dystrophic features in dysferlin deficient animal model.Exp Cell Res 2012, 318:1160–1174.

68. Mokhtarian A, Lefaucheur JP, Even PC, Sebille A: Hindlimb immobilization applied to 21-day-old mdx mice prevents the occurrence of muscle degeneration.J Appl Physiol 1999, 86:924–931.

69. Torres LF, Duchen LW: The mutant mdx: inherited myopathy in the mouse. Morphological studies of nerves, muscles and end-plates.Brain 1987, 110(Pt 2):269–299.

70. DiMario JX, Uzman A, Strohman RC: Fiber regeneration is not persistent in dystrophic (MDX) mouse skeletal muscle.Dev Biol 1991, 148:314–321.

71. Ikeda M, Kihara A, Igarashi Y: Sphingosine-1-phosphate lyase SPL is an endoplasmic reticulum-resident, integral membrane protein with the pyridoxal 5′-phosphate binding domain exposed to the cytosol.Biochem Biophys Res Commun 2004, 325:338–343.

72. Hait NC, Allegood J, Maceyka M, Strub GM, Harikumar KB, Singh SK, Luo C, Marmorstein R, Kordula T, Milstien S, Spiegel S: Regulation of histone acetylation in the nucleus by sphingosine-1-phosphate.Science 2009, 325:1254–1257.

73. Colussi C, Mozzetta C, Gurtner A, Illi B, Rosati J, Straino S, Ragone G, Pescatori M, Zaccagnini G, Antonini A, Minetti G, Martelli F, Piaggio G, Gallinari P, Steinkuhler C, Clementi E, Dell'Aversana C, Altucci L, Mai A, Capogrossi MC, Puri PL, Gaetano C: HDAC2 blockade

by nitric oxide and histone deacetylase inhibitors reveals a common target in Duchenne muscular dystrophy treatment.Proc Natl Acad Sci USA 2008, 105:19183–19187.

74. Iezzi S, Di Padova M, Serra C, Caretti G, Simone C, Maklan E, Minetti G, Zhao P, Hoffman EP, Puri PL, Sartorelli V: Deacetylase inhibitors increase muscle cell size by promoting myoblast recruitment and fusion through induction of follistatin.Dev Cell 2004, 6:673–684.

75. Morissette MR, Cook SA, Buranasombati C, Rosenberg MA, Rosenzweig A: Myostatin inhibits IGF-I-induced myotube hypertrophy through Akt.Am J Physiol 2009, 297:C1124–C1132.

76. Zammit PS, Partridge TA: Sizing up muscular dystrophy.Nat Med 2002, 8:1355–1356.

77. Smyth SS, Sciorra VA, Sigal YJ, Pamuklar Z, Wang Z, Xu Y, Prestwich GD, Morris AJ: Lipid phosphate phosphatases regulate lysophosphatidic acid production and signaling in platelets: studies using chemical inhibitors of lipid phosphate phosphatase activity.J Biol Chem 2003, 278:43214–43223.

78. Brinkmann V, Billich A, Baumruker T, Heining P, Schmouder R, Francis G, Aradhye S, Burtin P: Fingolimod (FTY720): discovery and development of an oral drug to treat multiple sclerosis.Nat Rev Drug Discov 2010, 9:883–897.

79. Kennedy PC, Zhu R, Huang T, Tomsig JL, Mathews TP, David M, Peyruchaud O, Macdonald TL, Lynch KR: Characterization of a sphingosine 1-phosphate receptor antagonist prodrug.J Pharmacol Exp Ther 2011, 338:879–889.

Chapter 4

Collagen producing cells and PDGFRα signaling in fibrosis

Primer

With muscular dystrophy, the accumulation of connective tissue is acknowledged as an obstacle for regeneration (1). Therapeutic interventions, including gene therapy, have not proved sufficient to overcome the severe fibrosis that is present in advanced stages of muscular dystrophy (2). Yet, little is known about the cellular and molecular mechanisms that promote fibrosis in muscular dystrophy. Mesenchymal progenitors of the skeletal muscle have been described to express components of fibrosis (3), specifically the pro-collagens. However, without cell-specific reporters, the nature of collagen synthesis makes the identification of collagen producing cells inherently difficult. Therefore, we sought to characterize the collagen producing cells in skeletal muscle and describe the molecular interactions that promote fibrosis in muscular dystrophy using a novel genetic reporter, the Collagen1a1-GFP reporter, which is expressed by pro-fibrotic cells (4, 5).

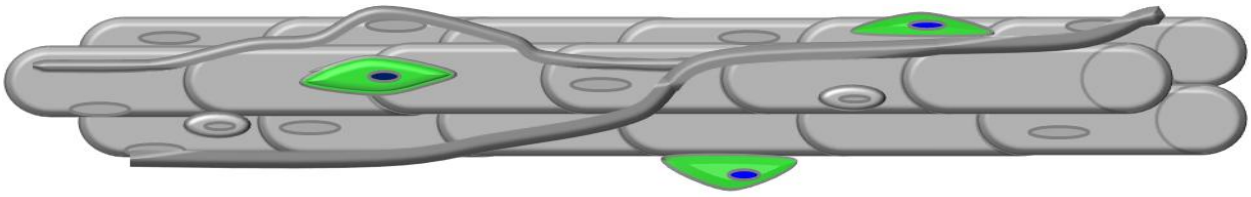

collagen producing cells

1. Zhou L, Lu H. Targeting fibrosis in Duchenne muscular dystrophy. Journal of neuropathology and experimental neurology. 2010;69(8):771-6. PubMed PMID: 20613637.
2. Bostick B, Shin JH, Yue Y, Wasala NB, Lai Y, Duan D. AAV micro-dystrophin gene therapy alleviates stress-induced cardiac death but not myocardial fibrosis in >21-m-old mdx mice, an end-stage model of Duchenne muscular dystrophy cardiomyopathy. Journal of molecular and cellular cardiology. 2012;53(2):217-22. doi: 10.1016/j.yjmcc.2012.05.002. PubMed PMID: 22587991; PubMed Central PMCID: PMC3389274.
3. Uezumi A, Ito T, Morikawa D, Shimizu N, Yoneda T, Segawa M, et al. Fibrosis and adipogenesis originate from a common mesenchymal progenitor in skeletal muscle. Journal of cell science. 2011;124(Pt 21):3654-64. PubMed PMID: 22045730.
4. Lin SL, Kisseleva T, Brenner DA, Duffield JS. Pericytes and perivascular fibroblasts are the primary source of collagen-producing cells in obstructive fibrosis of the kidney. The American journal of pathology. 2008;173(6):1617-27. doi: 10.2353/ajpath.2008.080433. PubMed PMID: 19008372; PubMed Central PMCID: PMC2626374.
5. Ieronimakis N, Hays AL, Janebodin K, Mahoney WM, Jr., Duffield JS, Majesky MW, et al. Coronary adventitial cells are linked to perivascular cardiac fibrosis via TGFbeta1 signaling in the mdx mouse model of Duchenne muscular dystrophy. Journal of molecular and cellular cardiology. 2013;63:122-34. doi: 10.1016/j.yjmcc.2013.07.014. PubMed PMID: 23911435; PubMed Central PMCID: PMC3834000.

PDGFRα signaling promotes the fibrotic response of collagen producing cells in Duchene Muscular Dystrophy.

Nicholas Ieronimakis[1], Aislinn Hays[1], Amalthiya Prasad[1], Kajohnkiart Janebodin[2], Jeremy S. Duffield[1,3,4], Morayma Reyes[1].

Affilliations:

[1]Department of Pathology, School of Medicine, University of Washington, USA.

[1]Department of Pathology, School of Medicine, University of Washington, USA.

[2]Department of Anatomy, School of Dentistry, Mahidol University, Thailand.

[3]Department of Medicine, School of Medicine, University of Washington, USA.

[4]Discovery Research, Biogen Idec Inc. USA.

Abstract

Fibrosis is a prominent facet of pathology in Duchene Muscular Dystrophy (DMD). Yet the cellular and molecular mechanisms responsible for DMD fibrosis are not well understood. Utilizing the Collagen1a1-GFP reporter in the mdx mouse model, we explored the mechanisms of fibrosis and observed that PDGFRα signaling is involved in the pro-fibrotic response of collagen producing cells in DMD. PDGFRα signaling is transiently upregulated during non-diseased muscle regeneration but when constitutively activated results in muscle fibrosis. In response to continuous muscle damage and repair that occurs with muscular dystrophy, PDGFRα+ cells are activated by muscle fiber-derived PDGF-AA. Treatment of mdx mice with

Crenolanib, a selective PDGFRα inhibitor, reduced fibrosis and improved muscle strength. This correlated with reductions of phosphorylated-Src, a downstream effector of PDGFRα signaling. Such results present a novel mechanism for DMD fibrosis mediated by PDGFRα and provides a new therapeutic target for ameliorating fibrosis

Introduction

Duchene Muscular Dystrophy (DMD) is a fatal disease that primarily affects skeletal and cardiac muscles. With disease progression, connective tissue accumulates in degenerating cardiac and skeletal muscles; a process commonly referred to as fibrosis1. Although fibrosis is the most prominent pathological feature and a reliable determinant of disease progression, the cellular and molecular milieu that governs fibrosis in DMD remains largely uncharacterized1-3. Skeletal muscle mesenchymal progenitors capable of differentiating into fibroblasts and adipocytes have been identified 4,5,6. These mesenchymal progenitors are PDGFRα+ cells that have been associated with the pathogenesis in mdx and DMD skeletal muscles7,8. Recently, these mesenchymal progenitors in the skeletal muscle and heart have been shown to express pro-fibrotic genes expression in response to TGFβ1 and PDGF-AA in culture7,9. Imatinib, a broad spectrum tyrosine kinase inhibitor, has also been shown to decrease fibrosis in mdx skeletal muscles by inhibiting c-Abl and PDGFR signaling10,11. Constitutive activation of PDGFRα can induce systemic fibrosis in non-diseased mice while pro-fibrotic cells present following cardiotoxin injury also express PDGFRα4,7,12. Such studies indicate that pro-fibrotic muscle cells can express PDGFRα and that this pathway has the potential to induce fibrosis. In spite of such evidence, it remains unclear if PDGFRα signaling promotes fibrosis in DMD. In addition,

the contribution of PDGFRα expressing cells to the collagen producing population responsible for the development of fibrosis in muscular dystrophy, remains unresolved.

In this study we examined the involvement of PDGFRα signaling in the disease progression and development of fibrosis in both human and mouse dystrophic muscles. Utilizing the Collagen1a1-GFP (Col1a1-GFP) reporter of pro-collagen producing cells13, we have previously shown that the majority of pro-fibrotic cells in mdx hearts, are also PDGFRα+9. Herein this report, we have extended our study of Col1a1-GFP cells to the mdx skeletal muscles. In mdx, Col1a1-GFP cells are abundant in regions of muscle degeneration and regeneration, highlighting their role in the accumulation of connective tissue that occurs with muscular dystrophy. As previously observed in mdx hearts9, Col1a1-GFP cells isolated from mdx skeletal muscles also express Collagen3α1 and are prominent in fibrotic areas with excessive type III collagen deposition that propagates with age and disease progression.

As with the heart9, the majority of Col1a1-GFP+ cells in mdx skeletal muscles are also positive for PDGFRα. Interestingly, the expression of Pdgfrα is elevated in mdx muscles and shortly following acute injury also in wt muscles. The elevation of Pdgfrα expression is accompanied by increases of pro-collagen expression in both injured wt and diseased mdx muscles. Both Col1a1-GFP + and PDGFRα-nGFP+ cells are abundant in regions of regeneration in wt and mdx muscles and near necrotic fibers in mdx. PDGFRα-Cre+ labeled cells are abundant at the onset of degeneration in mdx diaphragms, whereas constitutive activation of the PDGFRα kinase during the course of normal muscle injury results in fibrosis reminiscent of muscular dystrophy. In turn, we observed PDGFRα+ cells and the PDGF-AA ligand are also prominent in DMD skeletal muscle. Altogether such results highlight the role of collagen producing cells and

PDGFRα signaling during the restoration and accumulation of connective tissue that occurs in response to muscle damage.

Exposure to Crenolanib, a potent and selective inhibitor of PDGFRα, reduced the fibrotic response of Col1a1-GFP+ cells in culture. Treatment of mdx mice with Crenolanib resulted in decreased collagen production, increased regeneration and strength of skeletal muscle. The reduced fibrotic response of Pdgfrα expressing cells in vivo and in vitro correlated with a reduction of phosphorylated-PDGFRα. Although the exact signaling cascade of PDGFRα mediated fibrosis remains unknown, in Crenolanib treated diaphragms we observed a decrease of phosphorylated-Src; a known downstream effector of PDGFRα signaling that has been reported to induce collagen synthesis in systemic schlerosis 14,15. In contrast, phosphorylation of c-Abl which has also been reported downstream of PDGFRα and Src, was not significantly altered15. Altogether, our study indicates that PDGFRα signaling is activated and directly promotes fibrosis in DMD. Such evidence implicates PDGFRα signaling in the development of fibrosis in chronic muscle disease and presents a viable target for anti-fibrotic therapies for Duchenne muscular dystrophy.

Results

Collagen1α1-GFP cells are responsible for connective tissue accumulation in dystrophic muscles.

Skeletal muscle fibrosis in DMD is characterized by the accumulation of type I and III collagens 16. In cardiac muscle, fibroblasts are recognized as a heterogeneity population with various expression patterns and developmental origins17,18. Yet the cells responsible for collagen production and consequential accumulation of connective tissue with dystrophy, remain ill characterized in skeletal muscles. The identification of fibrotic cells is inherently hampered by

the nature of collagen synthesis which begins intracellularly, with the expression and production pro-collagens, and ends with the assembly of collagen fibrils in the extracellular space 19. Therefore, collagen producing cells are not easily distinguishable from other cells types, such as inflammatory, that also occupy damaged tissue and influence fibrosis in disease or injury 20. The capability to trace collagen producing cells is fundamental to our understanding of the mechanisms and progression of fibrosis in DMD muscles. Therefore, to study the process of fibrosis in dystrophic skeletal muscles we utilized mdx mice that harbor a reporter of collagen type I production; the Col1a1-GFP allele9,13. In comparison to wt mice, Col1a1-GFP + cells in mdx diaphragms are abundant in regions of pathology. Alterations in connective tissue and muscle architecture, highlighted by type I collagen staining and presence of GFP+ cells, was prominent in diseased diaphragms and quadriceps of mdx mice (Fig. 1). This remodeling is characteristic of degeneration and regeneration cycles that occur with progression of muscular dystrophy and presumably results in fibrosis, as muscles lose their capacity to repair. In turn, Col1a1-GFP + cells are closely associated with muscle fibers positive for sarcoplasmic fibronectin, an indicator of degenerating muscle21, and α-smooth muscle actin (αSMA) which is expressed by regenerating fibers22 (Fig. 2a and 2b). This repeated process of damage and repair is associated with the accumulation of collagen types I and III; the main components of connective tissue in mdx muscle fibrosis23-26. Although expression of Col1a1-GFP is indicative of pro-collagen1a1 production, it remained unclear if GFP+ cells were also the source of type III collagen. Therefore, we FACS-isolated Col1a1-GFP+ and negative cells to compare their expression of Collagen3a1 by quantitative-reverse transcription PCR (q-RT-PCR). Results indicate that GFP+ cells isolated from mdx diaphragms expressed significant levels of Collagen1a1 and Collagen3a1. In contrast, other populations present in fibrosis, endothelial

(CD31+, Sca1+, CD45-) cells and macrophages (CD45+, F4/80+), did not express these pro-collagens relative to Col1a1-GFP+ cells (Fig. 2c).

To understand the progression of fibrosis, we compared different ages of mdx:Col1a1-GFP with staining for type III collagen, which accumulates with age in dystrophic muscles26. Diaphragms from mdx mice showed thickening of endomysial type III collagen by 4MO of age (Fig. 3a). Accordingly GFP+ cells were located in areas of collagen III accumulation. In quadriceps muscles which show less severe pathology vs. the diaphragm, (Fig. 3b) accumulation of type III

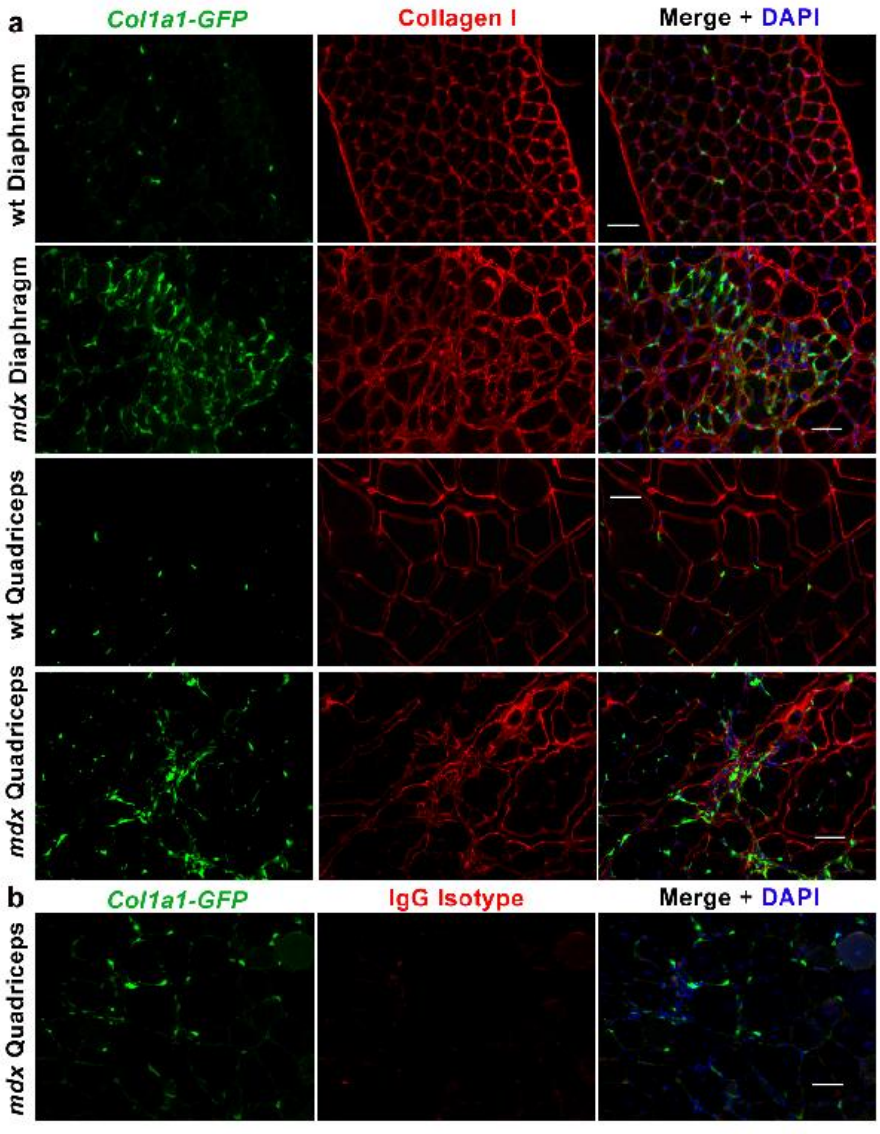

Figure 1: Col1a1-GFP cells are active in dystrophic skeletal muscles from *mdx* mice.(**a**) Immunoflourescence analysis of diaphragms and quadriceps from male 4MO wt and mdx:Col1a1-GFP mice reveals that GFP+ cells are prominent in regions where connective tissue alterations are occurring in dystrophic muscles. Staining for type I collagen highlights areas of muscle pathology where the accumulation GFP+ cells is observed. (**b**) IgG isotype to the anti-collagen I antibody compared in parallel to control for non-specific staining. Scale bars = 50µm.

collagen was evident by 14MO of age (Fig. 3c)27. The type III collagen was also concentrated in the perimysium surrounding large vessels, where Col1a1-GFP cells were also prominent in both mdx diaphragm and quadriceps (Supplemental Fig. 1a). This pattern was also observed in aged hearts from the same mdx mice (Supplementary Fig. 2a). In addition, type VI collagen which is also unregulated in DMD28, was also present in fibrotic regions occupied by Col1a1-GFP+ cells (Supplemental Fig. 1b).

To characterize the molecular signature of Col1a1-GFP+ cells in skeletal muscle, we FACS-analyzed diaphragms at various ages and compared our findings with

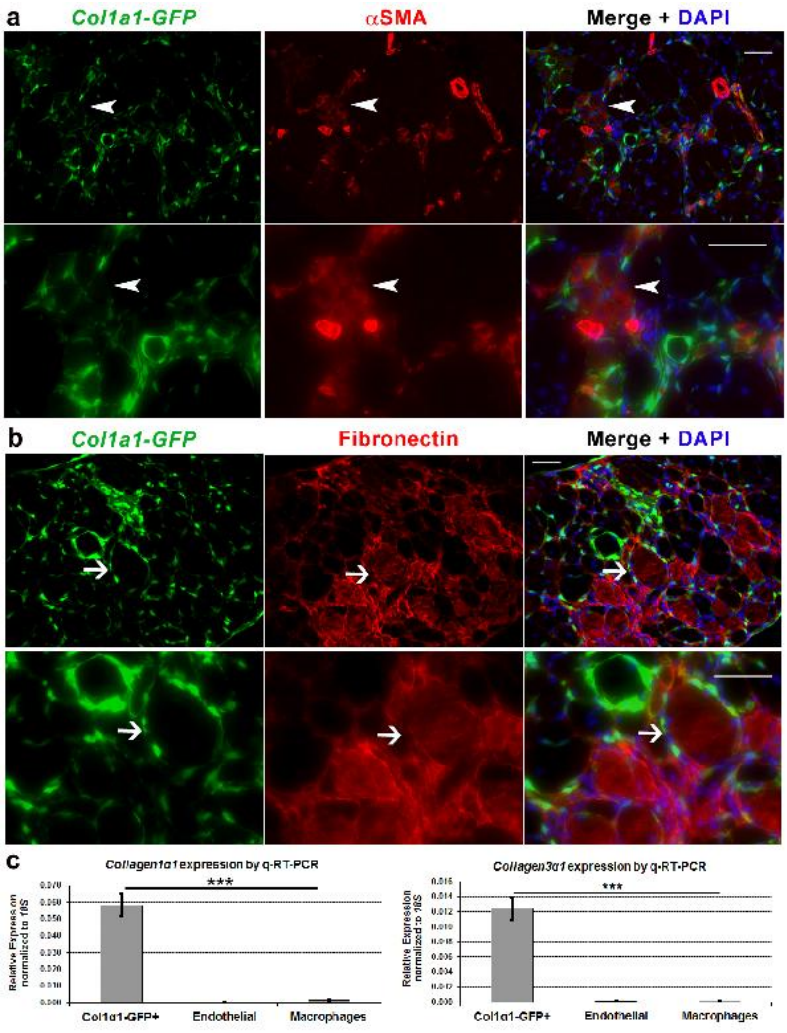

Figure 2: Col1a1-GFP cells produce collagen for regeneration and degeneration that occurs with muscular dystrophy.(**a**) Staining in *mdx* diaphragms from a 4MO mdx:Col1a1-GFP male reveals the concentration of GFP+ cells near regenerating α-Smooth Muscle Actin (αSMA) αSMA+ muscle fibers (arrowhead). A higher magnification of the same regions is shown in the lower row. (**b**) GFP+ cells are also adjacent to degenerating fibers that stain positive for sarcomeric Fibronectin in the same tissue (arrow). Higher magnification of the same regions is once more in the lower row. Scale bars = 50μm. (**c**) quantitative Reverse-Transcription PCR (q-RT-PCR) for Collagens1α1 and 3α1 was done on FACS-sorted cells from diaphragm muscles of 12MO mdx:Col1a1-GFP+ males (n=3). Relative to other populations implicated in collagen synthesis, endothelial cells (Sca1+,CD31+, CD45-) and macrophages (CD45+, F4/80+), *Col1a1-GFP*+ cells expressed significantly higher levels of pro-collagens. *** P<0.0005 by single factor ANOVA. Error bars indicate

immunohistological stainings. By FACS-analysis, GFP+ cells did not express hematopoietic or endothelial markers, CD45 or CD31respectively (Fig. 4a)29,30. In contrast, ~50% of GFP+ cells were PDGFRα+ at 4 months (MO) of age in wt vs. mdx diaphragms. With age, the number of GFP+ cell also positive for PDGFRα+ climbed to
90% at 12MO and was near 87% at 20MO in mdx diaphragms. The proportion of GFP+ cells also positive for PDGFRα in mdx hearts remained ~80% between 4, 12, and 20MO hearts (Supplemental Fig. 2b). The majority of GFP+,PDGFRα+ cells were also Sca1+ in aged diaphragms and hearts of mdx mice (Fig.4a and Supplemental Fig. 2b). By histological analysis, GFP+ cells in mdx diaphragms were confirmed positive for PDGFRα+, but negative for vascular markers BS1 and NG2, which label endothelial cells and pericytes respectively (Fig. 4b) 31,32. Therefore, the majority of (Col1a1-GFP+) in aged mdx skeletal muscles match the profile of collagen producing cells that we have previously characterized in the heart (9).
Recently, skeletal muscle PDGFRα+ cells have been reported to give rise to type I collagen producing cells in vitro and promote regeneration following toxin induced injury by their expression of pro-myogenic factors 4,5,7. Toxin injury in non-diseased muscle leads to a robust myogenic response that results in near complete regeneration within 14 days33. Despite the severity of damage and alteration to the muscle architecture that occur with toxin injury, there is no fibrosis suggesting that collagen production is restricted to the needs of muscle regeneration and restoration of damaged connective tissue33. With recurring damage in diseased mdx muscles, excessive deposition and thickening of the connective tissue occurs, suggesting that fibrosis results from the unbalanced accumulation of collagen during chronic cycles of muscle

regeneration and unresolved degeneration. Therefore, to gain insight on the process of connective tissue restoration, we examined the relationship between Col1a1-GFP collagen producing cells and Myf5nlacZ expressing myogenic cells following cardiotoxin (CTX) injury in wt mice34.

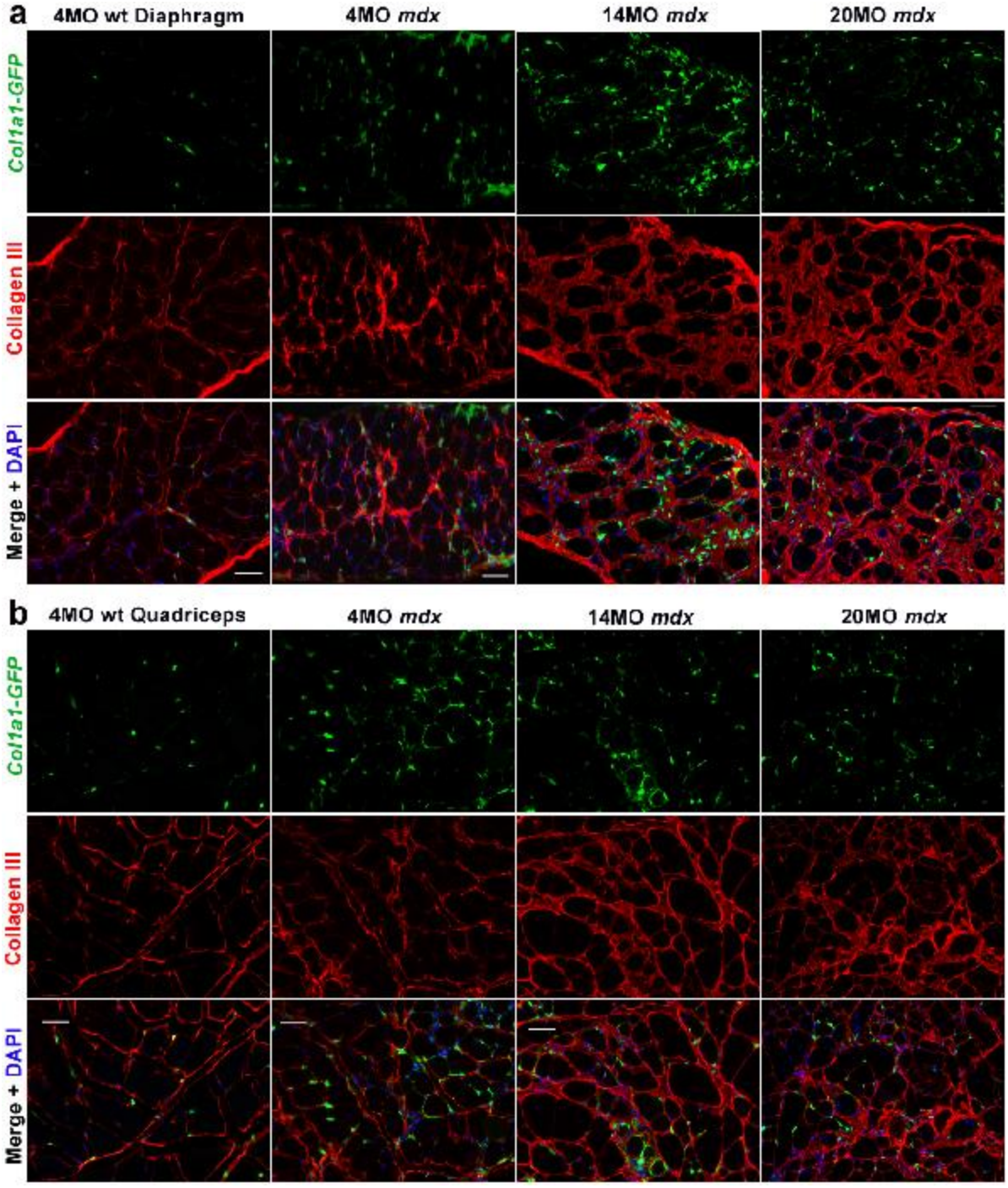

Figure 3: Col1a1-GFP cells are responsible for the accumulation of fibrosis that occurs with disease progression.(a) Staining's for type III collagen highlights the role of Col1a1-GFP+ cells in the development of fibrosis that occurs with age and disease progression in mdx diaphragms. This accumulation is observed as early as 4MO in mdx vs. wt diaphragms. (**b**) In contrast, limb muscles are less affected in mdx mice. The buildup of type III collagen occupied by GFP+ cells was not obvious until 14MO in the quadriceps from the same mdx mice shown. Scale bars = 50μm.

Following CTX injection, the myogenic response peaks at day 3 post injury in wt muscles33,35. This was evident by the prominence of Myf5nlacZ+ cells in CTX injured Tibialis Anterior (TA) muscles vs. the uninjured contra laterals (Fig. 5a). In turn, Col1a1-GFP+ cells were also abundant and within regenerating areas of muscle and in close proximity to myogenic cells and newly regenerated muscle fibers expressing αSMA (Fig. 5b). This association indicates that GFP+ collagen producing cells are active in parallel with myogenisis. This correlated with elevated expression of pro-collagens at day 3 and decline at day 14 post CTX injury (Fig. 5c). In addition, the expression of Pdgfrα and its ligand Pdgf-a, showed the same pattern of increase during the peak of myogenesis at day 3 and declined at day 14 when regeneration is concluding. Analogous to these results, Pdgfrα expression was significantly elevated in mdx vs. wt skeletal and cardiac muscles, although Pdgf-a was only elevated in mdx diaphragms at the age group examined;12 month old wt and mdx (Supplemental Fig. 3). These results suggest that the role of collagen producing cells and PDGFRα+ signaling in normal muscle repair is the restoration of the connective tissue surrounding regenerating myofibers; a process altered in muscular dystrophy.

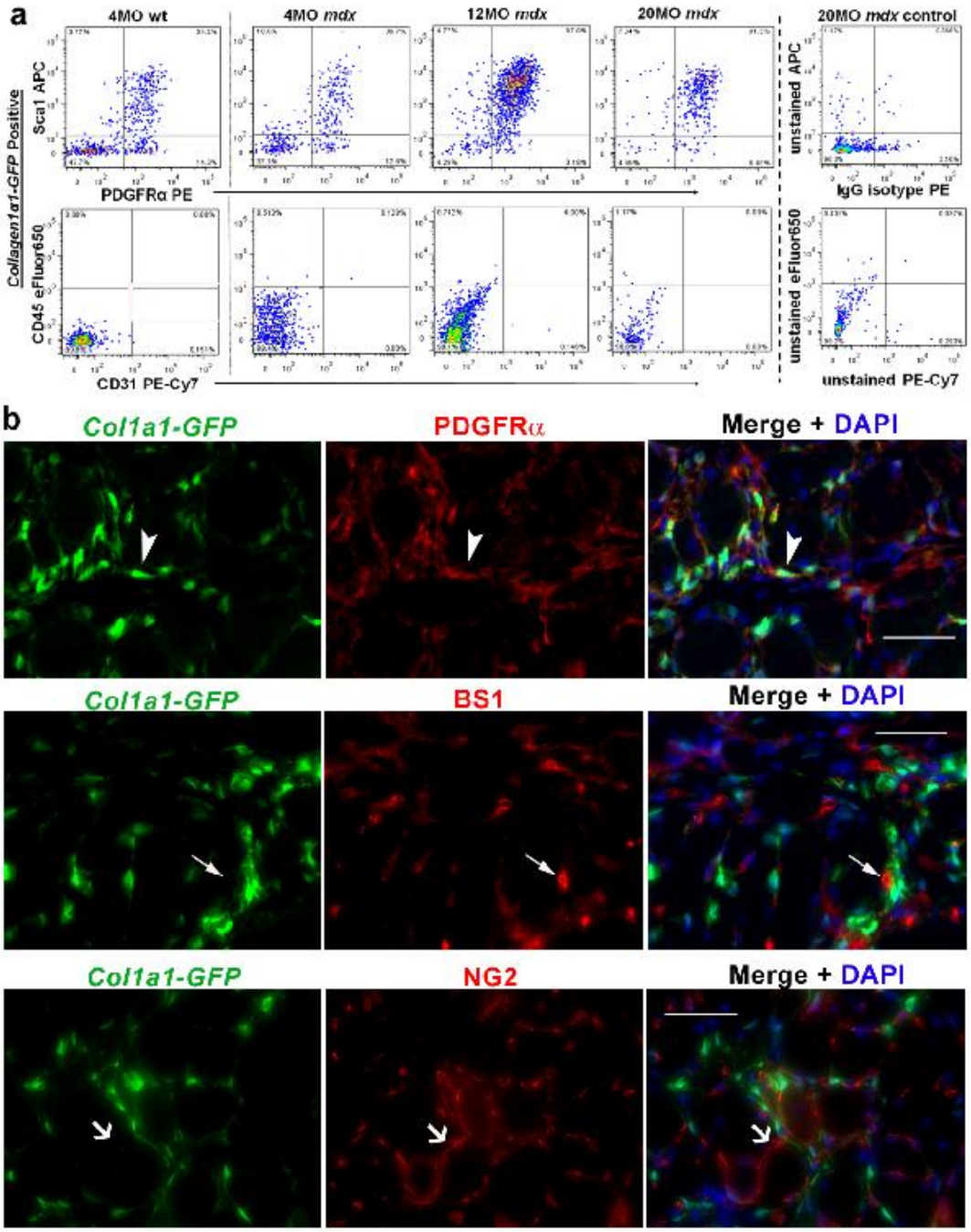

Figure 4: FACS-analysis reveals that the majority of Col1a1-GFP+ cells are also positive for PDGFRα. (a) FACS-analysis of the Col1a1-GFP population in wt and *mdx* diaphragms (n=3 males per age group) reveals that GFP+ cells lack CD45 and CD31, but the majority are positive for PDGFRα and Sca1 by 12MO of age in *mdx* mice. Staining done in parallel with an IgG isoptype for PDGFRα and unstained controls (dot plots on far right column) were referenced for gating. (**b**) Immunofluorescence analysis confirm that GFP+ cells are also PDGFRα+ (arrowhead), but lack vascular markers BS1 (filled arrow) and NG2 (line arrow). Depicted are staining's from 14MO male mdx:Col1a1-GFP diaphragms. Scale bars = 50μm.

Figure 5: Increases in *Col1a1-GFP* cells and Pdgf gene expression occur in parallel to the peak of myogenic cell response in damaged wt muscle. (a) Comparisons of uninjured and cardiotoxin (CTX) injured Tibialis Anterior (TA) muscles from a wt:Col1a1-GFP:Myf5^{nlacZ} dual reporter mouse (1 ½ MO male) reveals the response of GFP+ collagen producing cells in parallel with X-gal+ myogenic precursors to muscle injury. In uninjured muscle Myf5^{nlacZ} expressing cells (arrowhead) are distal to Col1a1-GFP+ cells. In contrast, X-gal+ and GFP+ cells are abundant and in close proximity in damaged regions of muscle at the peak of myogenic cell response, 3 days following cardiotoxin injection. (**b**) In addition to Myf5^{nlacZ} expressing cells (arrowhead), GFP+ cells were also adjacent to regenerating fibers labeled by sarcomeric αSMA (arrow). Scale bars = 50μm. (**c**) q-RT-PCR analysis of whole injured and uninjured TA muscles (n=3 TAs from 12MO males per time point), reveals elevated expression of collagens1α1 and 3α1 coincides with the response of Col1a1-GFP+ observed 3 days post cardiotoxin (CTX) injury. In addition, we observed Pdgfrα and the Pdgf-a ligand were also elevated at 3 days post CTX and reduced to near uninjured levels as regeneration concluded, 14 post injury. # P=0.08, * P=<0.05, **P<0.005 by single factor Anova. Error bars indicate ±SEM.

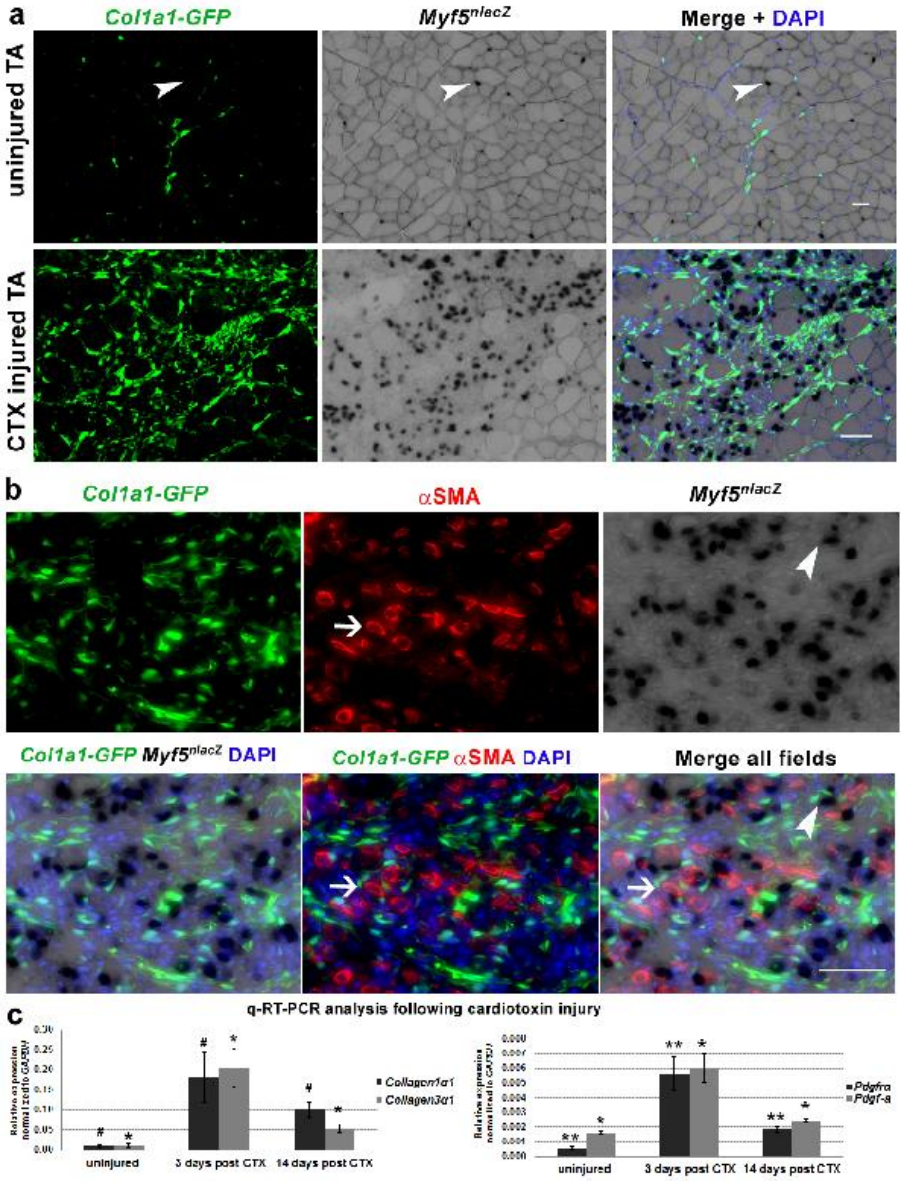

necrotic and regenerating fibers in dystrophic muscles (Fig. 6c). To study the response of the PDGFRα cells to the onset of dystrophy, we generated mdx mice carrying the PDGFRα-Cre allele and mT/mG flox reporter 36,37. In mdx muscle, the presence of PDGFRα-Cre labeled cells (membrane-EGFP+) at 6 weeks of age was similar to wt and became prominent by 8 weeks (Fig. 7a-b), a

timeframe consistent with the commencement of muscular dystrophy in mdx diaphragms 11,26,38. This patterning of Col1a1-GFP and PDGFRα-GFP or Cre labeled populations highlights the association between collagen production and Pdgfrα expression during the processes of skeletal muscle regeneration and degeneration.

Utilizing the cre-lox system, Olson E. and Soriano P. (2009)12 demonstrated the potential of constitutive PDGFRα-phosphorylation to induce systemic fibrosis over the course of 6-8 months. Coincidently, PDGFR-phosphorylation is elevated in mdx skeletal muscle11, while expression is increased during muscle repair (Fig. 5c). Therefore, in the context of skeletal muscle injury and repair we tested if the constitutive activation of the PDGFR- signaling would result in excessive connective tissue deposition. Utilizing a similar strategy, we generated PDGFRα ΔD842V 12 and PDGFRβ ΔD536A 39 flox mice containing the tamoxifen inducible PDGFRαCreER allele40. In these models, we induced constitutive PDGFR activation just prior to CTX injury in order to compare the potential of each receptor signaling to elevate collagen deposition during the process of muscle repair. Histological analysis shows that injury in PDGFRα ΔD842V muscles lead to excessive connective tissue reminiscent of mdx muscle pathology (Fig. 7c). In contrast, injured PDGFRβ ΔD536A mutant muscles did not show obvious fibrosis, yet did not repair as robustly as Cre-negative control muscles. Uninjured muscles appeared relatively similar between each model. Such data indicated that excessive PDGFRα activation during the process of muscle regeneration can result in fibrosis. In turn activation of PDGFRβ may also influence the response of collagen producing cells, but with less avidity in comparison to PDGFRα.

Figure 6: PDGFRα-nGFP share a similar profile to Col1a1-GFP cells and accordingly respond to muscle degeneration and regeneration. (a) FACS-comparison of diaphragms from *Col1a1-GFP* and PDGFRα-nGFP mice (7-8MO males) reveals a similar profile between GFP+ populations; negative for CD45 and CD31, but the majority being positive for Sca1 and CD34. (**b**) As with Col1a1-GFP+ cells PDGFRα-nGFP+ cells in the endomysium and perimysium near vessels (arrowhead) and respond en-mass 3 days following cardiotoxin (CTX) injury (depicted are TAs from a 1½ MO wt:PDGFRα-nGFP male). (**c**) Similarly, in *mdx* muscles PDGFRα-nGFP+ cells are concentrated near areas with degenerating fibers labeled by mouse IgG (arrowhead) and regions of regeneration containing αSMA+ fibers and Myf5^{nlacZ} expressing myogenic cells (arrow). Shown are quadriceps from a 3MO male mdx:PDGFRα-nGFP:Myf5^{nlacZ} double reporter mouse. Scale bars = 50um.

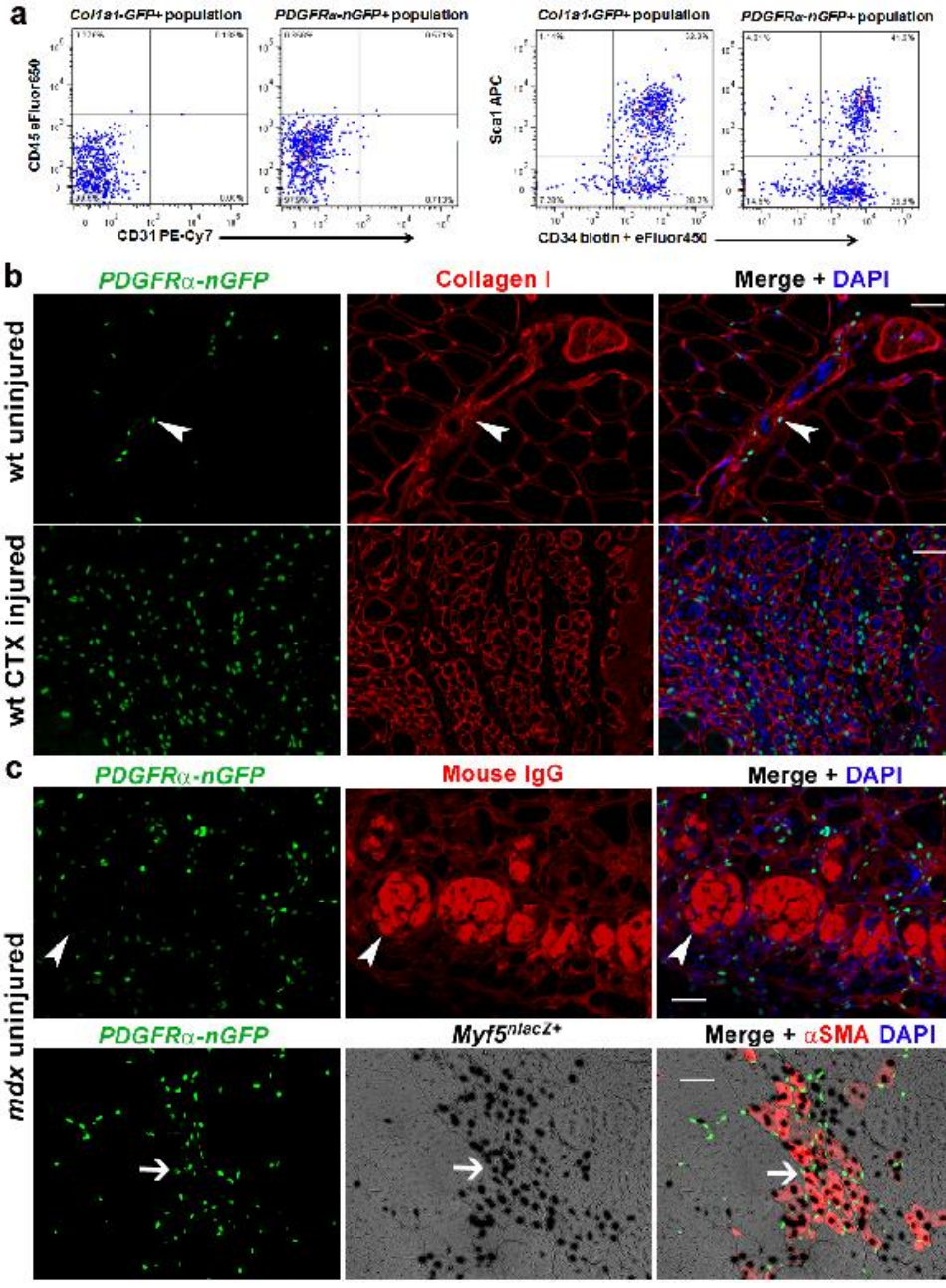

In so far we have demonstrated the presence and potential of PDGFRα signaling in collagen producing cells in promoting excessive connective tissue deposition. Just recently elevated numbers of PDGFRα+ cells have been shown to co-localize with

fibrosis in DMD muscles8. Our own examination of DMD muscles supports the presence of PDGFRα+ cells in the regions of connective tissue thickening (Fig. 8a). Collagen accumulation was pronounced in perimysium and surrounding vessels in DMD muscle (Fig. 8b); sites where Col1a1-GFP cells were also concentrated in mdx muscles (Supplementary Fig. 1). In turn, staining for PDGF-AA ligand showed increased intensity in DMD and mdx muscle fibers (Fig. 8c-d). Altogether, these results suggest that the activation of PDGFRα signaling in muscular dystrophy promotes connective tissue accumulation. Ominously, dystrophic muscle fibers may promote fibrosis in a paracrine fashion via production and secretion of the PDGF-AA ligand.

Inhibition of PDGFRα signaling ameliorates muscular dystrophy fibrosis. With the knowledge that PDGFRα is expressed by collagen producing cells and altered in DMD, we tested if pharmacological inhibition of this pathway can perturb the fibrotic response. Crenolanib is a potent tyrosine kinase inhibitor selective for PDGFRα, currently being tested in phase

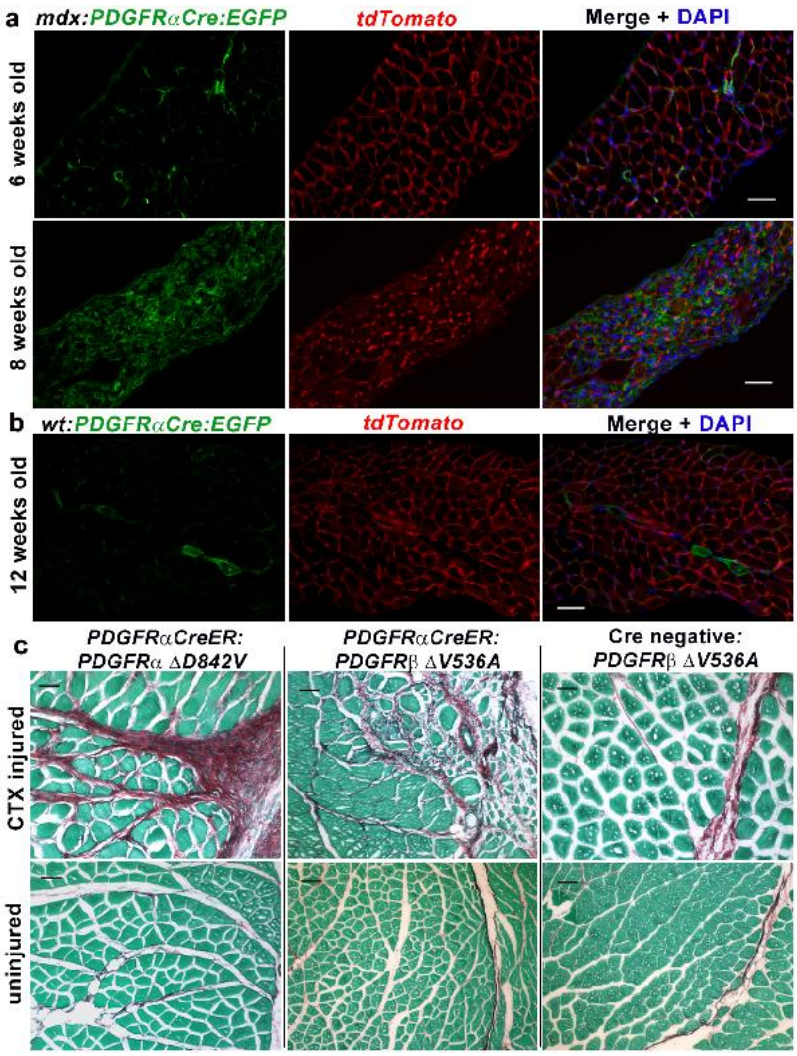

Figure 7: PDGFRα expressing cells are prominent early in dystrophy while constitutive activation can lead to fibrosis in non-diseases muscles following injury.(**a**) Diaphragms from male mdx:PDGFRαCre**:**mT/mG flox mice reveal the response of Pdgfrα expressing cells and their progeny occurs at the onset of muscular dystrophy between 6-8 weeks of age. (**b**) In contrast, diaphragms from wt:PDGFRαCre**:**mT/mG male mice even at 12 weeks appear similar to 6 week old *mdx*; a timepoint just prior to the onset of dystrophy. (**c**) Depicted is fast green and sirius red staining's of injured (top row) and uninjured (bottom row) contralateral quadriceps from each respective cross (all 3MO females), injected with cardiotoxin (CTX) 3 weeks following tamoxifen induction. Constitutive activation of PDGFRα signaling in PDGFRα expressing cells via tamoxifen induction of PDGFRαCreER:ΔD842V flox mice (left column), resulted in fibrosis by day 14 following cardiotoxin (CTX) injury. In contrast, constitutive activation of PDGFRβ (middle column) induced in parallel with PDGFRαCreER:ΔD536A mice, did not result in neither complete regeneration or fibrosis (red staining) by day 14 post injury. Cre negative controls (right column) showed normal collagen deposition reminiscent of uninjured muscles. Scale bars = 50μm.

II clinical trials for PDGFR associated cancers41-43. In comparison to Imatinib, Crenolanib has significantly greater avidity towards PDGFRα kinase activity including mutant variants such as ΔD842V41. Therefore, we chose to administer Crenolanib to Col1a1-GFP cells first in vitro, to evaluate the potential of PDGFRα inhibition towards reducing the pro-fibrotic response of collagen producing cells. In turn, Col1a1-GFP+ cells treated 10ng/ml PDGF-AA significantly elevated their expression of both collagens1α1 and 3α1 (Supplementary Fig. 4a). This response was inhibited with the addition of 1μM Crenolanib. In contrast, stimulation with the same concentration of PDGF-BB did not result in a pro-fibrotic response, validating the PDGF-AA ligand-induced differential signaling, which in turns results in pro-collagen expression. Western blot analysis confirmed the inhibitory effect of Crenloanib in reducing PDGFRα phosphorylation when cells are stimulated with PDGF-AA (Supplementary Fig. 4a). Accordingly, we expanded our studies of PDGFRα inhibition to mdx mice in order to evaluate the potential of Crenolanib in reducing the pro-fibrotic response of collagen producing cells in vivo.

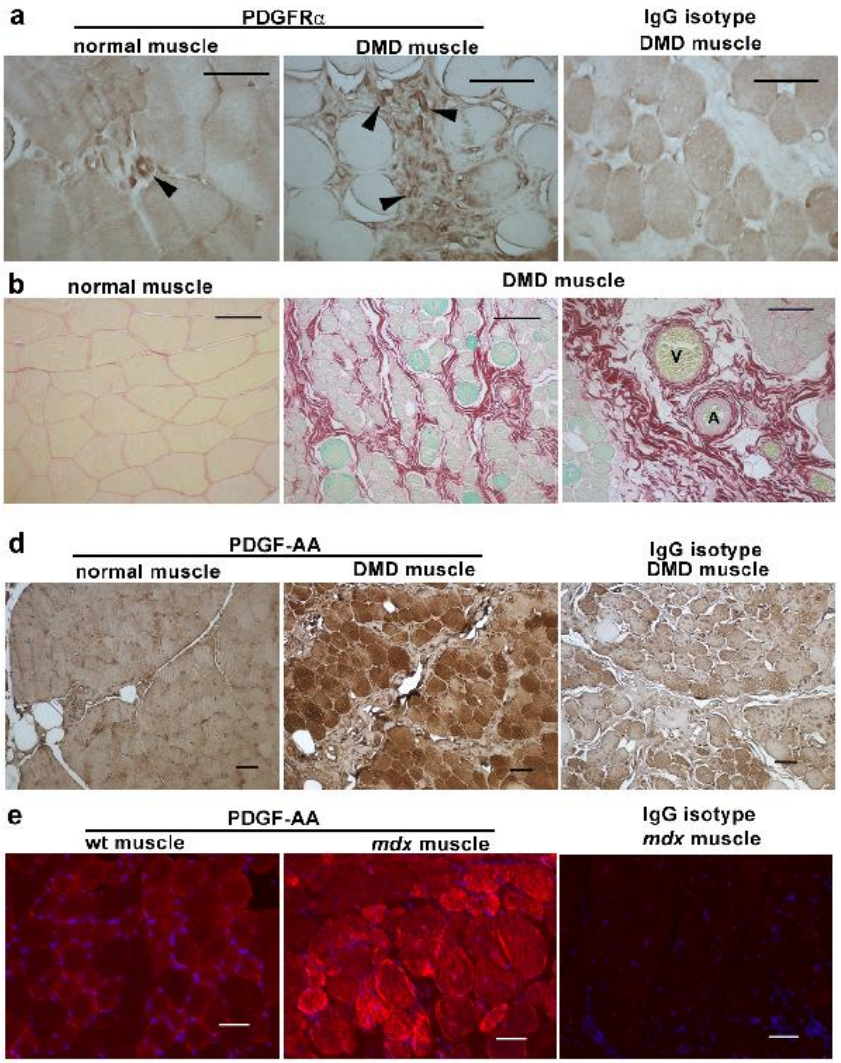

Figure 8: PDGFRα+ cells and the PDGF-AA ligand are concentrated in DMD muscles**.**(**a**) DAB staining reveals an elevated presence of PDGFRα+ cells (arrowheads) in biopsies from DMD vs. non-diseases quadriceps from 8-10 years-old males. (**b**) Fast green and sirius red staining of same muscles, highlights the fibrosis in the endomysium and perimysium, particularly near vessels, veins (V) and arteries (A), where PDGFRα+ cells are observed in human and mouse muscles. (**c**) DAB staining for PDGF-AA on the same DMD and normal muscles, reveals a strong presence of this ligand in dystrophic muscles. (**D**) In turn, PDGF-AA staining was also more intense in mdx vs wt quadriceps. Depicted are sections from 24MO wt and 18MO mdx males. Scale bars = 50µm.

Treatment was administered for 4 weeks in the drinking water ad lib, beginning at 8 weeks of age; a timeframe when elevated numbers of PDGFRα expressing cells are evident (Fig 7a), just prior to the development of fibrosis in mdx diaphragms11,26. Based on published pharmokinetic44, a dose of 0.03mg/ml Crenolanib in the drinking water was chosen for animals to receive approximately 5mg/kg Crenolanib per day in order to achieve sufficient inhibition of PDGFRα. Control mice were treated with an equal amount of the vehicle (DMSO). Following 4 weeks of treatment, muscle strength was initially tested by ex-vivo myography (Fig. 9a); an assay commonly used to measure functional improvement in mdx muscles45. Results show that

Crenolanib treated mdx mice had significantly greater isometric force in both EDL muscles and diaphragm strips. To understand the factors and mechanisms that contributed to this functional gain, we examined changes in the muscles connective tissue. Indeed, fibrosis and its components were reduced with Crenolanib treatment. Histopathology of diaphragm muscles shows reduced collagen deposition by picrosirius red staining (Fig. 9b). Molecular analysis indicated a significant reduction in the expression of collagens3α1 (Fig.9c). In contrast, the expression of Pdgf receptors and ligands did not change (Fig. 9d), suggesting that treatment does not result in downregulation of the inhibited pathway. Western blot analysis of diaphragm muscles shows a significant decline in type III collagen and fibronectin which also accumulates with fibrosis and is present in necrotic fibers (Fig. 9e). These reductions in connective tissue and fibrotic components correlated with reduced phosphorylation of PDGFRα and its downstream effector Src (Fig. 9f). In contrast phosphorylation of c-Abl, which is the main target of Imatinib11, did not change with Crenolanib. Of note, reductions in fibrotic components and PDGFRα-phosphorylation were also detected in Crenolanib treated hearts (Supplementary Fig. 5). Interestingly, the phosphorylation of Src was not different in these same hearts suggesting that the downstream effectors of PDGFRα may be tissue or disease progression dependent. To assess if reductions in fibrosis resulted in increased regeneration, we compared myogenic factors in Crenolanib vs. vehicle treated mdx:Col1a1-GFP muscles. As previously shown, collagen producing cells are involved in regeneration (Fig. 4a and 5b). Once more we observed Col1a1-GFP+ in close proximity to regenerating fibers positive for sarcoplasmic αSMA, which were more abundant in Crenolanib treated diaphragm and EDL muscles (Fig.10a and Supplementary Fig. 6). Molecular analysis confirms the elevated expression of αSMA in Crenolanib treated diaphragm muscles, suggesting that reductions in fibrosis make the environment more

permissive for regeneration (Fig.10b). Further comparisons treated muscles shows significantly elevated expression of the myogenic regulatory factor Pax7, a specific marker of satellite cells, but not Myf5 or Myod, genes expressed by satellite cells and myoblasts 34,46,47 (Fig. 10b) with Crenolanib. The increase of Pax7 transcript suggests that the amelioration of fibrosis resulted in greater satellite cell renewal during the course of treatment 46.

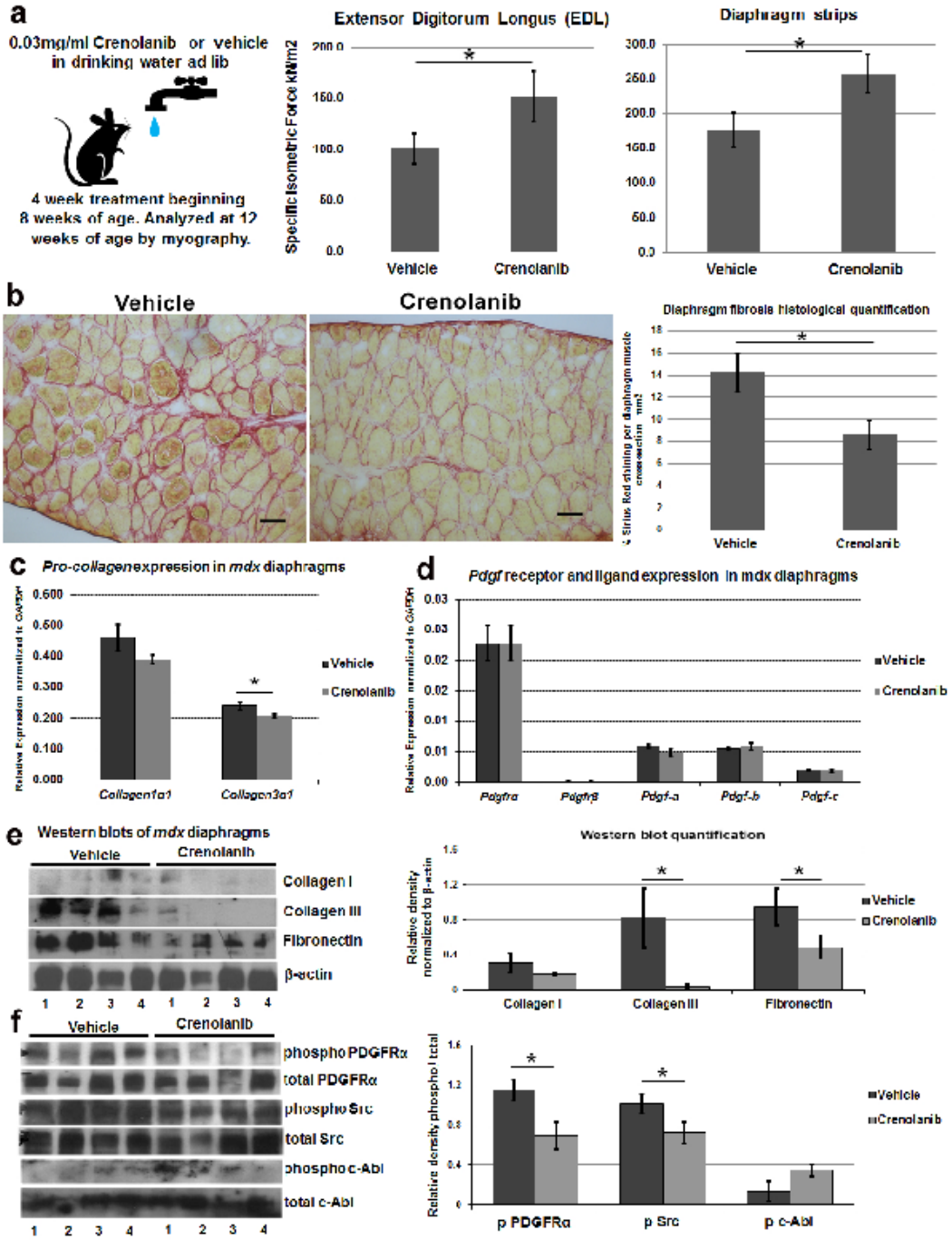

Figure 9: Inhibition of PDGFRα signaling and its downstream effector Src but not c-Abl, results in decreased fibrosis and improved muscle strength of mdx muscles. (**a**) Cartoon depicting treatment of mdx mice with Crenolanib or vehicle (n=6 males per treatment). Myography of these treated mice reveals improved muscle strength in EDL and diaphragm muscles with Crenolanib. (**b**) Histopathology analysis of sirius red staining shows reduced collagen deposition with Crenolanib (n=4) treatment in mdx diaphragms. In turn, the expression of Collagen3α1 was reduced. Scale bars = 50μm. (**d**) Treatment with Crenolanib (n=4 per treatment) did not alter expression of Pdgf genes. (**e**) Western blot analysis confirms a significant reduction in type III collagen and also fibronectin in diaphragms from the same Crenolanib treated mdx mice (n=4 per treatment). (**f**) Further analysis of treated diaphragms indicates the decrease in fibrotic components with Crenolanib are attributed to reduced PDGFRα phosphorylation, possibly signaling through its downstream effector Src but not c-Abl. * P=<0.05 by Student's *t*-test. Error bars indicate ±SEM.

Discussion

Fibrosis in muscular dystrophy is widely recognized as a barrier to regeneration, yet remains ill studied. Utilizing an assortment of genetic models and molecular methods, our present study reveals the involvement of PDGFRα signaling in collagen producing cells during alterations in connective tissue. In the absence of disease, collagen producing cells restore the connective tissue in damaged muscles. This process is associated with elevated pro-collagen production and PDGFRα signaling, indicated by increased receptor and ligand expression, as Col1α1-GFP+ cells respond to injury in coordination with myogenic precursors (Fig. 5). In contrast, dystrophic muscles undergo continuous cycles of degeneration/regeneration, which maintains the response of Col1α1-GFP+ cells and PDGFRα signaling. Increased PDGFRα-phosphorylation11 and expression by mesenchymal progenitors that have potential to express collagens4,5,7,8, suggests a role for this pathway in the pathology of muscular dystrophy. The expression of PDGFRα by collagen producing cells in vivo (Fig. 4) and presence of the PDGF-AA ligand in dystrophic muscles (Fig. 8b) indicates a paracrine role of signaling that remains activated in response to chronic injury. PDGF-AA is expressed by developing muscles but absent in the somite's of Myf5 null mutants48. Consequently, it is entirely possibly that PDGF signaling in muscular

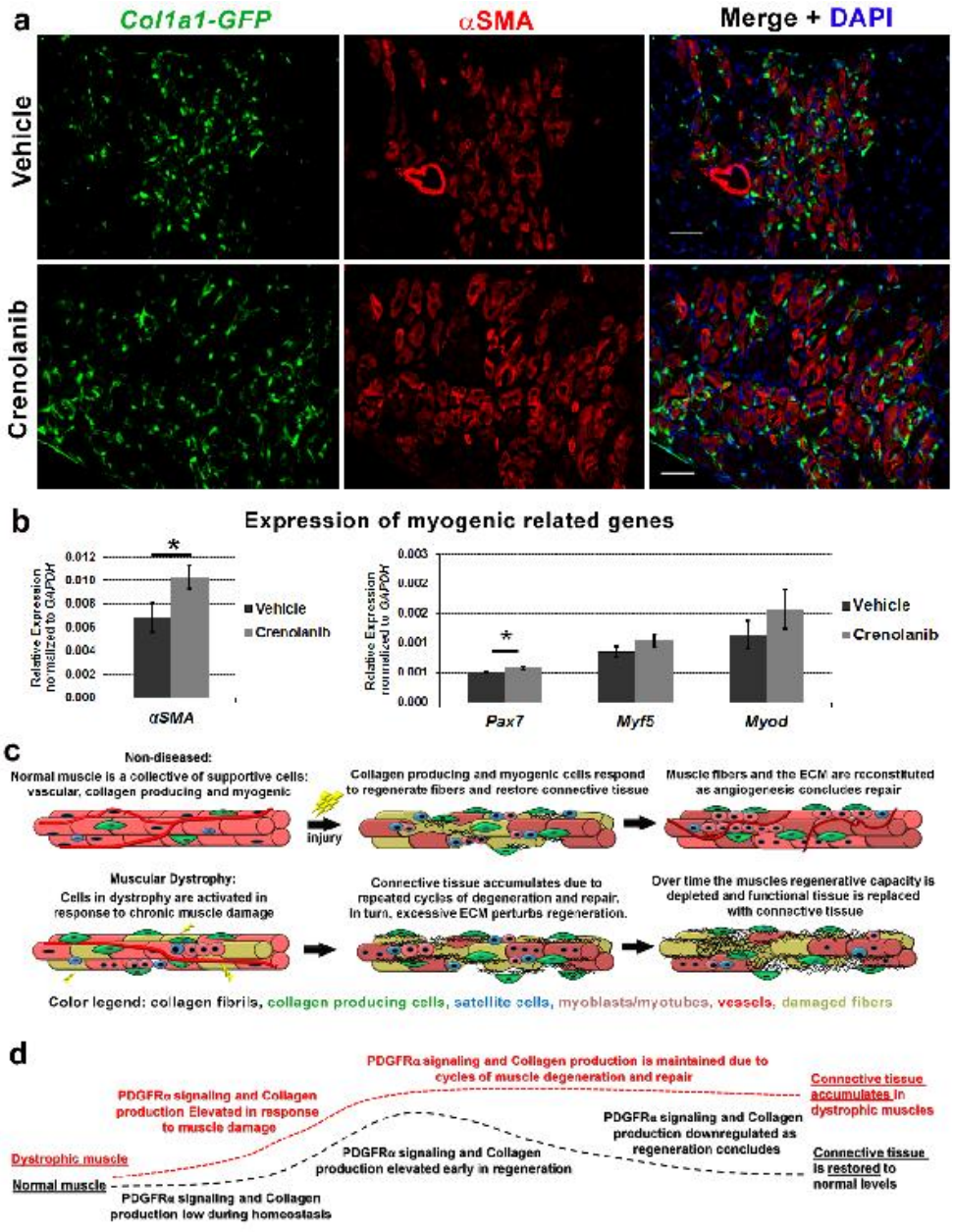

Figure 10: Regeneration in mdx muscles is improved with Crenolanib inhibition of PDGFRα signaling. (a) Diaphragms from age matched mdx:Col1a1-GFP mice, treated in parallel to the mdx mice depicted in Fig. 9, showed GFP+ cells concentrated near a greater number of αSMA+ regenerating fibers with Crenolanib. Scale bars = 50μm. (**b**) q-RT-PCR analysis of the same diaphragm muscles from Fig. 10, not only validates the increase in αSMA expression with Crenolanib, but also reveals greater Pax7 transcript suggesting that more satellite cell self-renewal occurred. (**c**) Illustrative model summarizing our findings and cellular responses to injury in normal and dystrophic muscles. (**d**) Illustration presenting the potential mechanism of continuous PDGFRα signaling and fibrosis with muscular dystrophy.

dystrophy is a reactivation of the development program that occurs in response to muscle repair. Therefore, we hypothesis that continuous activation of PDGFRα signaling in collagen producing cells and the resulting fibrosis are a consequence of the chronic injury and repair that occurs in dystrophic muscles. In contrast, non-diseased muscles downregulate PDGFRα signaling once the muscles connective tissue has been restored, during the process of regeneration (modeled in Fig. 10c-d).

In addition to the aforementioned data, the capability of PDGFRα signaling to promote fibrosis when constitutively activated during the repair process in non-diseased muscles (Fig. 7c), supports our hypothesis. Consequently, inhibition of PDGFRα with Crenolanib resulted in reduced fibrosis and functional improvement of mdx muscles (Fig. 9-10). Such results not only implicate PDGFRα signaling in the fibrotic response of collagen producing cells, but also present a viable target for reducing connective tissue accumulation in DMD.

PDGFRα signaling can mediate cellular responses through several pathways among them Ras-MAPK, PI3K, and Src 49,50. Yet the cascade by which PDGFRα stimulation leads to collagen production remains unknown. Reductions in mdx muscle fibrosis with Imatinib have been attributed to PDGFR and c-Abl tyrosine-kinase inhibition11. Our data indicates that independent of c-Abl, selective inhibition of PDGFRα can reduce fibrosis in mdx muscles (Fig. 9b-f). This was associated with decreased Src phosphorylation, a downstream mediator of PDGF signaling that can mediate pro-collagen expression in vitro 51,52. Further studies are needed to define the signaling cascade by which PDGFRα, perhaps via Src, mediates the pro-fibrotic response of collagen producing cells in skeletal muscles. Although, c-Abl may also potentiate collagen transcription, c-Abl inhibition with Imatinib has been associated cardiomyocyte toxicity and heart failure in cancer patients 53. Such a side effect may compound the cardiomyopathy prevalent in the majority of DMD patients 54. Therefore, anti-fibrotic therapies that selectively target PDGFRα signaling may prove efficacious and safer than broad spectrum tyrosine-kinase inhibitors.

Chapter 4 References

1 Klingler, W., Jurkat-Rott, K., Lehmann-Horn, F. & Schleip, R. The role of fibrosis in Duchenne muscular dystrophy. Acta myologica : myopathies and cardiomyopathies : official journal of the Mediterranean Society of Myology / edited by the Gaetano Conte Academy for the study of striated muscle diseases **31**, 184-195 (2012).

2 Kharraz, Y., Guerra, J., Pessina, P., Serrano, A. L. & Munoz-Canoves, P. Understanding the Process of Fibrosis in Duchenne Muscular Dystrophy. BioMed research international **2014**, 965631, doi:10.1155/2014/965631 (2014).

3 Desguerre, I. et al. Endomysial fibrosis in Duchenne muscular dystrophy: a marker of poor outcome associated with macrophage alternative activation. Journal of neuropathology and experimental neurology **68**, 762-773, doi:10.1097/NEN.0b013e3181aa31c2 (2009).

4 Uezumi, A., Fukada, S., Yamamoto, N., Takeda, S. & Tsuchida, K. Mesenchymal progenitors distinct from satellite cells contribute to ectopic fat cell formation in skeletal muscle. Nature cell biology **12**, 143-152, doi:10.1038/ncb2014 (2010).

5 Joe, A. W. et al. Muscle injury activates resident fibro/adipogenic progenitors that facilitate myogenesis. Nature cell biology **12**, 153-163, doi:10.1038/ncb2015 (2010).

6 Dulauroy, S., Di Carlo, S. E., Langa, F., Eberl, G. & Peduto, L. Lineage tracing and genetic ablation of ADAM12(+) perivascular cells identify a major source of profibrotic cells during acute tissue injury. Nature medicine **18**, 1262-1270, doi:10.1038/nm.2848 (2012).

7 Uezumi, A. et al. Fibrosis and adipogenesis originate from a common mesenchymal progenitor in skeletal muscle. Journal of cell science **124**, 3654-3664 (2011).

8 Uezumi, A. et al. Identification and characterization of PDGFRalpha+ mesenchymal progenitors in human skeletal muscle. Cell death & disease **5**, e1186, doi:10.1038/cddis.2014.161 (2014).

9 Ieronimakis, N. et al. Coronary adventitial cells are linked to perivascular cardiac fibrosis via TGFbeta1 signaling in the mdx mouse model of Duchenne muscular dystrophy. Journal of molecular and cellular cardiology **63**, 122-134, doi:10.1016/j.yjmcc.2013.07.014 (2013).

10 Ito, T. et al. Imatinib attenuates severe mouse dystrophy and inhibits proliferation and fibrosis-marker expression in muscle mesenchymal progenitors. Neuromuscul Disord **23**, 349-356, doi:10.1016/j.nmd.2012.10.025 (2013).

11 Huang, P., Zhao, X. S., Fields, M., Ransohoff, R. M. & Zhou, L. Imatinib attenuates skeletal muscle dystrophy in mdx mice. FASEB journal : official publication of the Federation of American Societies for Experimental Biology **23**, 2539-2548, doi:10.1096/fj.09-129833 (2009).

12 Olson, L. E. & Soriano, P. Increased PDGFRalpha activation disrupts connective tissue development and drives systemic fibrosis. Developmental cell **16**, 303-313 (2009).

13 Lin, S. L., Kisseleva, T., Brenner, D. A. & Duffield, J. S. Pericytes and perivascular fibroblasts are the primary source of collagen-producing cells in obstructive fibrosis of the kidney. The American journal of pathology **173**, 1617-1627, doi:10.2353/ajpath.2008.080433 (2008).

14 Skhirtladze, C. et al. Src kinases in systemic sclerosis: central roles in fibroblast activation and in skin fibrosis. Arthritis and rheumatism **58**, 1475-1484, doi:10.1002/art.23436 (2008).

15 Plattner, R., Kadlec, L., DeMali, K. A., Kazlauskas, A. & Pendergast, A. M. c-Abl is activated by growth factors and Src family kinases and has a role in the cellular response to PDGF. Genes & development **13**, 2400-2411 (1999).

16 Foidart, M., Foidart, J. M. & Engel, W. K. Collagen localization in normal and fibrotic human skeletal muscle. Archives of neurology **38**, 152-157 (1981).

17 Zeisberg, E. M. & Kalluri, R. Origins of cardiac fibroblasts. Circulation research **107**, 1304-1312, doi:10.1161/CIRCRESAHA.110.231910 (2010).

18 Zeisberg, E. M. et al. Endothelial-to-mesenchymal transition contributes to cardiac fibrosis. Nature medicine **13**, 952-961, doi:10.1038/nm1613 (2007).

19 Muiznieks, L. D. & Keeley, F. W. Molecular assembly and mechanical properties of the extracellular matrix: A fibrous protein perspective. Biochimica et biophysica acta **1832**, 866-875, doi:10.1016/j.bbadis.2012.11.022 (2013).

20 Mann, C. J. et al. Aberrant repair and fibrosis development in skeletal muscle. Skeletal muscle **1**, 21, doi:10.1186/2044-5040-1-21 (2011).

21 Gulati, A. K., Reddi, A. H. & Zalewski, A. A. Distribution of fibronectin in normal and regenerating skeletal muscle. The Anatomical record **204**, 175-183, doi:10.1002/ar.1092040302 (1982).

22 Springer, M. L., Ozawa, C. R. & Blau, H. M. Transient production of alpha-smooth muscle actin by skeletal myoblasts during differentiation in culture and following intramuscular implantation. Cell motility and the cytoskeleton **51**, 177-186, doi:10.1002/cm.10022 (2002).

23 Hantai, D., Labat-Robert, J., Grimaud, J. A. & Fardeau, M. Fibronectin, laminin, type I, III and IV collagens in Duchenne's muscular dystrophy, congenital muscular dystrophies and congenital myopathies: an immunocytochemical study. Connective tissue research **13**, 273-281 (1985).

24 Marshall, P. A., Williams, P. E. & Goldspink, G. Accumulation of collagen and altered fiber-type ratios as indicators of abnormal muscle gene expression in the mdx dystrophic mouse. Muscle & nerve **12**, 528-537, doi:10.1002/mus.880120703 (1989).

25 Goldspink, G., Fernandes, K., Williams, P. E. & Wells, D. J. Age-related changes in collagen gene expression in the muscles of mdx dystrophic and normal mice. Neuromuscul Disord **4**, 183-191 (1994).

26 Zhou, L. et al. Temporal and spatial mRNA expression patterns of TGF-beta1, 2, 3 and TbetaRI, II, III in skeletal muscles of mdx mice. Neuromuscul Disord **16**, 32-38, doi:10.1016/j.nmd.2005.09.009 (2006).

27 Chamberlain, J. S., Metzger, J., Reyes, M., Townsend, D. & Faulkner, J. A. Dystrophin-deficient mdx mice display a reduced life span and are susceptible to spontaneous rhabdomyosarcoma. FASEB journal : official publication of the Federation of American Societies for Experimental Biology **21**, 2195-2204, doi:10.1096/fj.06-7353com (2007).

28 Sabatelli, P. et al. Expression of collagen VI alpha5 and alpha6 chains in human muscle and in Duchenne muscular dystrophy-related muscle fibrosis. Matrix biology : journal of the International Society for Matrix Biology **31**, 187-196, doi:10.1016/j.matbio.2011.12.003 (2012).

29 Watt, S. M., Gschmeissner, S. E. & Bates, P. A. PECAM-1: its expression and function as a cell adhesion molecule on hemopoietic and endothelial cells. Leukemia & lymphoma **17**, 229-244, doi:10.3109/10428199509056827 (1995).

30 Charbonneau, H., Tonks, N. K., Walsh, K. A. & Fischer, E. H. The leukocyte common antigen (CD45): a putative receptor-linked protein tyrosine phosphatase. Proceedings of the National Academy of Sciences of the United States of America **85**, 7182-7186 (1988).

31 Yeh, H. I., Dupont, E., Coppen, S., Rothery, S. & Severs, N. J. Gap junction localization and connexin expression in cytochemically identified endothelial cells of arterial tissue. J Histochem Cytochem **45**, 539-550 (1997).

32 Ozerdem, U., Grako, K. A., Dahlin-Huppe, K., Monosov, E. & Stallcup, W. B. NG2 proteoglycan is expressed exclusively by mural cells during vascular morphogenesis. Developmental dynamics : an official publication of the American Association of Anatomists **222**, 218-227, doi:10.1002/dvdy.1200 (2001).

33 Yan, Z. et al. Highly coordinated gene regulation in mouse skeletal muscle regeneration. The Journal of biological chemistry **278**, 8826-8836, doi:10.1074/jbc.M209879200 (2003).

34 Beauchamp, J. R. et al. Expression of CD34 and Myf5 defines the majority of quiescent adult skeletal muscle satellite cells. The Journal of cell biology **151**, 1221-1234 (2000).

35 Ieronimakis, N. et al. Absence of CD34 on murine skeletal muscle satellite cells marks a reversible state of activation during acute injury. PloS one **5**, e10920, doi:10.1371/journal.pone.0010920 (2010).

36 Roesch, K. et al. The transcriptome of retinal Muller glial cells. The Journal of comparative neurology **509**, 225-238, doi:10.1002/cne.21730 (2008).

37 Muzumdar, M. D., Tasic, B., Miyamichi, K., Li, L. & Luo, L. A global double-fluorescent Cre reporter mouse. Genesis **45**, 593-605, doi:10.1002/dvg.20335 (2007).

38 DiMario, J. X., Uzman, A. & Strohman, R. C. Fiber regeneration is not persistent in dystrophic (MDX) mouse skeletal muscle. Developmental biology **148**, 314-321 (1991).

39 Olson, L. E. & Soriano, P. PDGFRbeta signaling regulates mural cell plasticity and inhibits fat development. Developmental cell **20**, 815-826, doi:10.1016/j.devcel.2011.04.019 (2011).

40 Kang, S. H., Fukaya, M., Yang, J. K., Rothstein, J. D. & Bergles, D. E. NG2+ CNS glial progenitors remain committed to the oligodendrocyte lineage in postnatal life and following neurodegeneration. Neuron **68**, 668-681, doi:10.1016/j.neuron.2010.09.009 (2010).

41 Heinrich, M. C. et al. Crenolanib inhibits the drug-resistant PDGFRA D842V mutation associated with imatinib-resistant gastrointestinal stromal tumors. Clinical cancer research : an official journal of the American Association for Cancer Research **18**, 4375-4384, doi:10.1158/1078-0432.CCR-12-0625 (2012).

42 Lewis, N. L. et al. Phase I study of the safety, tolerability, and pharmacokinetics of oral CP-868,596, a highly specific platelet-derived growth factor receptor tyrosine kinase inhibitor in patients with advanced cancers. Journal of clinical oncology : official journal of the American Society of Clinical Oncology **27**, 5262-5269, doi:10.1200/JCO.2009.21.8487 (2009).

43 Dai, J. et al. Large-scale analysis of PDGFRA mutations in melanomas and evaluation of their sensitivity to tyrosine kinase inhibitors imatinib and crenolanib. Clinical cancer research : an official journal of the American Association for Cancer Research **19**, 6935-6942, doi:10.1158/1078-0432.CCR-13-1266 (2013).

44 Zimmerman, E. I. et al. Crenolanib is active against models of drug-resistant FLT3-ITD-positive acute myeloid leukemia. Blood **122**, 3607-3615, doi:10.1182/blood-2013-07-513044 (2013).

45 Faulkner, J. A., Ng, R., Davis, C. S., Li, S. & Chamberlain, J. S. Diaphragm muscle strip preparation for evaluation of gene therapies in mdx mice. Clinical and experimental pharmacology & physiology **35**, 725-729, doi:10.1111/j.1440-1681.2007.04865.x (2008).

46 Zammit, P. S. et al. Pax7 and myogenic progression in skeletal muscle satellite cells. Journal of cell science **119**, 1824-1832, doi:10.1242/jcs.02908 (2006).

47 Relaix, F., Rocancourt, D., Mansouri, A. & Buckingham, M. A Pax3/Pax7-dependent population of skeletal muscle progenitor cells. Nature **435**, 948-953, doi:10.1038/nature03594 (2005).

48 Tallquist, M. D., Weismann, K. E., Hellstrom, M. & Soriano, P. Early myotome specification regulates PDGFA expression and axial skeleton development. Development **127**, 5059-5070 (2000).

49 Tallquist, M. & Kazlauskas, A. PDGF signaling in cells and mice. Cytokine & growth factor reviews **15**, 205-213, doi:10.1016/j.cytogfr.2004.03.003 (2004).

50 Andrae, J., Gallini, R. & Betsholtz, C. Role of platelet-derived growth factors in physiology and medicine. Genes & development **22**, 1276-1312, doi:10.1101/gad.1653708 (2008).

51 Mishra, R., Zhu, L., Eckert, R. L. & Simonson, M. S. TGF-beta-regulated collagen type I accumulation: role of Src-based signals. American journal of physiology. Cell physiology **292**, C1361-1369, doi:10.1152/ajpcell.00370.2006 (2007).

52 Abraham, J. et al. An adaptive Src-PDGFRA-Raf axis in rhabdomyosarcoma. Biochemical and biophysical research communications **426**, 363-368, doi:10.1016/j.bbrc.2012.08.092 (2012).

53 Kerkela, R. et al. Cardiotoxicity of the cancer therapeutic agent imatinib mesylate. Nature medicine **12**, 908-916, doi:10.1038/nm1446 (2006).

54 Sultan, A. & Fayaz, M. Prevalence of cardiomyopathy in Duchenne and Becker's muscular dystrophy. J Ayub Med Coll Abbottabad **20**, 7-13 (2008).

Methods

Animals

All mouse models described were maintained on a C57BL/6J background and all mdx carried the 4Cv allele1. Specific allele and mouse details are listed in the supplemental table S1. Muscle injuries when listed were done by single injections of 10nM cardiotoxin (Sigma) directly into TA (20µl) or Quadriceps (40µl). For inducible Cre activation (Fig. 7c), 100µl of 20mg/ml tamoxifen suspended in corn oil, was injected intraperitonealy daily for 5 consecutive days, then allowed to clear for 3 weeks prior to cardiotoxin injury. Myography was conducted and specific isometric force was calculated as previously specified2. All mouse procedures were authorized by the UW Institutional Animal Care and Use Committee (IACUC).

S1. Mouse Strains / Alleles

Type	Strain Name	Jackson Labs Catalog #	References
wt	C57BL/6J	000664	
mdx	B6Ros.Cg-*DMDmdx-4Cv/J*	002378	[1]
Col1α1-GFP	C57BL6-pCol9GFP-HS4,5 transgene allele.	Not available	[3-6]
Myf5^{nlacZ}	Stock *Myf5tmPas*/j	018626	[7, 8]
PDGFRα-nGFP	B6.129S4-Pdgfra tm11(EGFP)*Sor*/J	007669	[9]
PDGFRα-Cre	C57BL/6-Tg(Pdgfra-cre)1Clc/J	013148	[10]
mT/mG flox	B6.129(Cg)-*Gt(ROSA)26Sor*$^{tm4(ACTB-tdTomato,-EGFP)Luo}$/J	007676	[11]
PDGFRαCreER	B6N.Cg-Tg(Pdgfra-cre/ERT)467Dbe/J	018280	[12]
ΔD842V flox	B6.129S4-*Pdgfra*^{tm12Sor}/J	018433	[13]
ΔD536A flox	STOCK *Pdgfrb*$^{tm13(Pdgfrb)Sor}$/J	018434	[14]

Tissue processing and staining's

Paraffin embedded human muscle sections were acquired from the UW Neuropathology division, anonymous to any patient identification information. Mouse tissues containing GFP reporters were excised and immediately submerged in 4% formaldehyde (made from paraformaldehyde powder suspended in PBS) for 2 hours at 4oC. Tissue was then passed

through a gradient of sucrose in PBS beginning with 10% and 20% (incubated 30min each time), then left in 30% overnight at 4oC. Muscles were then frozen in OCT and cross-sections were subsequently cut in a cryostat at 8μM thick. In the absence of a fluorescent reporter, muscles were frozen fresh without fixation in OCT. In this case cross-sections were post fixed with 4% formaldehyde for 10 minutes prior to antibody staining's. For all sirius red and fast green staining's, tissues were first fixed with ice cold methanol and then stained by the standard method15. Staining's with X-gal were followed as before2 and conducted prior to antibody stainings. For the majority of antibody staining's tissue was first blocked with 10% goat serum or horse serum (when the primary was goat) for 30 min, washed with PBS with 1%BSA three times then the primary antibody was administered. Following three washes with PBS, secondary antibodies conjugated to AlexaFlour's (Invitrogen) were administered for 1hr at dilutions of 1:1000 in PBS with 1%BSA. For PDGFRα and PDGF-AA stainings in human muscle, tissue was deparrafinized by passing through 4x 5min changes of xylenes followed by rehydration through an alcohol gradient of 100%, 90%, 70% and 50% ethanol for 5 min each. Human sections were then treated for antigen retrieval by incubating with sodium citrate buffer pH6 containing Tween20 for 20 min at 95oC, prior to blocking with 10% goat serum for 30min and then incubating with the primary antibodies overnight at 4oC. biotinylated secondary antibodies added the next day for 1 hour and streptavidin-DAB staining was completed following the manufacturer protocol (Vector Labs). Staining for PDGF-AA in mouse tissue also required antigen retrieval, done as mentioned above, and worked only in fresh frozen tissue that was post fixed with 4% formaldehyde for 10 min. Dilutions and incubation times for all primary antibodies are listed in the supplementary S2. Fluorescent photos were captured with a Zeiss Aviovert200 with mRM monochromatic camera then colored and merged in Adobe Photoshop

CS2. Brightness and contrast levels were adjusted equally between experimental and control staining's. Sirius red staining's were captured with a Nikon Eclipse E400 microscope with DS-Fi1 color camera.

S2. Histology Antibodies

Antigen	Conjugate	Host	Clone	Manufacturer	Dilution	Incubation
Collagen I	purified	Rabbit	polyclonal	Abcam ab292 or ab21286)	1:400	overnight
Collagen III	purified	Goat	polyclonal	Southern Biotec A4611	1:100	overnight
Collagen VI	purified	Rabbit	polyclonal	Abcam ab6588	1:200	overnight
Fibronectin	Purified	Rabbit	Polyclonal	Sigma SAB4500863	1:100	4 hours
αSMA	Cy3	Mouse	1A4	Sigma	1:500	1 hour
PDGFRα (mouse)	purified	Goat	polyclonal	R&D AF1062	1:200	overnight
Sca1 (Ly6A/E)	PE or APC	Rat	30-F11	eBioscience	1:200	2 hours
NG2	purified	Rabbit	polyclonal	Millipore (AB5320)	1:400	2 hours
mouse IgG	AlexaFluor®594	Chicken	polyclonal	Invitrogen	1:1000	1 hour
PDGF-AA (mouse and human)	purified	Rabbit	polyclonal	Millipore	1:100	overnight
PDGFRα (human)	Purified	Rabbit	Polyclonal	Bioss bs-0231R	1:100	overnight
Isotype IgG	purified	Rabbit	polyclonal	Vector Labs	Same FC 1°	overnight
Isotype IgG	purified	Goat	polyclonal	Vector Labs	Same FC 1°	overnight

Histology Secondary Antibodies

anti-Rat IgG	AlexaFluor®594or 647	Chicken	polyclonal	Invitrogen	1:1000	1 hour
anti-Rabbit IgG	AlexaFluor®594 or 647	Goat	polyclonal	Invitrogen	1:1000	1 hour
anti-Goat IgG	AlexaFluor®594 or 647	Rabbit	polyclonal	Invitrogen	1:1000	1 hour
anti-Rabbit IgG	Biotin	Horse	polyclonal	Vector	1:200	1 hour

Cell isolations and culture

Cells for molecular analysis and culture were all isolated by FACS from mononuclear cell preparations enriched by digesting a collection of limb muscles (TAs, Gastrocnemius's and Quadriceps') with collagenase and displace (both from Worthington). Procedures for muscle digestion and FACS were followed as previously described8, 16. Antibodiy details used for FACS are listed in supplementary table S3. FACS-isolation and data acquisition was done with an Aria III and Diva software (BD). Post-acquisition analysis and graph generation was done with FlowJo v7.6.5 for PC. Following acquisition, cells were FACS-sorted directly into RLT buffer (Omega Bio-Tek) for molecular analysis or DMEM-HG with 10% FCS for culture. Cultured Col1α1-GFP+ cells used for in vitro studies were the same as previously reported3; FACS-sorted from male 4MO wt:Col1α1-GFP+ hearts were expanded in DMEM-HG with 10% FCS + PenStrep at 37oC, 5%CO2 and 5%O2. These cells were seeded in 12 well plates and treatments were replicated with a minimum of 3 wells per condition. DMSO (vehicle), 10ng/ml PDGF-AA, 10ng/ml PDGF-BB, or 10ng/ml PDGF-AA (all recombinant mouse from Shenandoah Biotech) + 1μM Crenolanib (from Selleck and Chemietek) in a basal media of DMEM-HG with 5%FCS + PenStrep was added for 4 days at 37oC, 5%CO2 and 5%O2. PDGF ligands were from and Crenolanib was from Following treatment, cells were washed with ice cold PBS and scraped off with RLT buffer for molecular analysis. For western blot analysis, cells were expanded in 100mm tissue culture plates and stimulated with 10ng/ml PDGF-AA with and without 1μM Crenolanib. Cells were then collected by scraping in RIPA buffer containing protease and phosphatase inhibitors (all from Thermo/Pierce) 30 minutes following treatments.

S3. FACS Antibodies and Streptavidin Conjugates					
Antigen	**Conjugate**	**Host**	**Clone**	**Manufacturer**	**Dilution**
CD31 (PECAM-1)	PE-Cy7	Rat	390	eBioscience	3µl/10^6 cells
CD45 (Ly-5)	eFluor®650	Rat	30-F11	eBioscience	3µl/10^6 cells
Sca1 (Ly-6 A/E)	APC	Rat	D7	eBioscience	1.5µl/10^6 cells
PDGFRα	PE	Rat	APA5	eBioscience	1.5µl/10^6 cells
CD34	Biotin	Rat	RAM34	eBioscience	3µl/10^6 cells
Fc block (CD16/32)	Purified	Rat	93	eBioscience	1µl/10^6 cells
Streptavidin	eFluor®450	n/a		eBioscience	1.5µl/10^6 cells
Rat IgG Isotype	PE	Rat	eBR2a	eBioscience	3µl/10^6 cells

Molecular analysis of cells and tissue

RNA from cells was isolated using E.Z.N.A isolation kit (Omega Bio-Tek) and from tissue by Trizol (Invitrogen), following manufacturers protocols. Muscle tissue for RNA isolation was first ground with a mortar and pestle under liquid nitrogen, to a fine powder prior to suspension in Trizol. Generation of cDNA and quantitative-PCR analysis was done as previously reported 3 and normalized by single delta Ct method. q-RT-PCR data was analyzed and graphs generated using Microsoft Excel. Primer sequences for q-RT-PCR are listed in the supplementary table S4. For protein isolation whole muscle tissue was ground once more to a fine powder, suspended in RIPA buffer containing protease and phosphatase inhibitors (Thermo/Pierce), and then homogenized with a Tissue-Tearor (BioSpec). Protein content was quantified by BSA assay (Thermo/Pierce) and 35µg protein from each respective sample was loaded per well in 4-20% Tris-Glycine gel (NuSep). Following SDS-PAGE, proteins were transferred onto a PVDF membrane via semi-dry transfer then blocked with in TBS-T with 5%BSA for 1 hour prior to probing with any primary antibodies. Membranes were probed with primary antibodies typically overnight and secondary antibodies for 1 hour in TBS-T with 5%BSA at 4oC. Antibodies against

phosphorylated proteins were probed first and then membranes were stripped with 2x 5min incubations with 6M GnHCl solution and then re-probed with antibodies against the total the protein content for each respective target. Proteins were imaged by chemiluminescence (Thermo/Pierce) and quantifications were done using ImageJ. Western blot antibodies with dilutions are listed in the supplementary table S4.

S4. Western blot primary antibodies

Antigen	Conjugate	Host	Clone	Manufacturer	Dilution	Incubation
Collagen I	purified	Rabbit	polyclonal	Abcam ab292	1:1000	overnight
Collagen III	purified	Rabbit	polyclonal	Sigma SAB45000367	1:1000	overnight
Fibronectin	Purified	Rabbit	polyclonal	Thermo/Pierce PA1-23693	1:1000	overnight
PDGFRα phosphor-Tyr849	purified	Rabbit	polyclonal	Sigma SAB4504655	1:1000	overnight
PDGFRα	purified	Rat	APA5	eBioscience	1:750	overnight
Src phosphor-Tyr418	purified	Mouse	monoclonal	ECM SM3761	1:500	overnight
Src	purified	Mouse	monoclonal	ECM SM2591	1:500	overnight
c-Abl phosphor-Tyr412	Purified	Rabbit	polyclonal	ECM AP1271	1:750	overnight
c-Abl	Purified	Mouse	monoclonal	ECM AP2091	1:500	overnight
B-actin	Purified	Rabbit	polyclonal	BioVision 3662	1:2000	overnight
Western blot secondary antibodies						
anti-Rabbit IgG	HRP	goat	polyclonal	BioRad 170-6515	1:5000	1 hour
anti-Rat IgG	HRP	rabbit	polyclonal	Thermo/Pierce PA1-28573	1:5000	1 hour
anti-Mouse IgG	HRP	goat	polyclonal	BioRad 170-6516	1:5000	1 hour

S4. q-RT-PCR primer sequences

Gene	Forward primer (5' → 3')	Reverse primer (5' → 3')	Reference
Collagen 1α1	ACGGCTGCACGAGTCACAC	GGCAGGCGGGAGGTCTT	[17]
Collagen 3α1	GTTCTAGAGGATGGCTGTACTAAACACA	TTGCCTTGCGTGTTTGATATTC	[17]
Pdgfrα	CAAACCCTGAGACCACAATG	TCCCCCAACAGTAACCCAAG	[18]
Pdgfrβ	GTCTGGTCTTTTGGGATCCT	AAGGCTGGTTACAGTTTGGC	n/a
Pdgf-a	GTCCAGGTGAGGTTAGAGG	CACGGAGGAGAACAAAGAC	[18]
Pdgf-b	TGTCCCTGCCTCTTTCCACT	GCAGACTGAAGGGCACATGA	[19]
Pdgf-c	AGGTTGTCTCCTGGTCAAGC	CCTGCGTTTCCTCTACACAC	[18]
GAPDH	GGGAAGCCCATCACCATCT	GCCTCACCCCATTTGATGTT	[16]
18S rRNA	TTGACGGAAGGGCACCACCAG	GCACCACCACCCACGGAATCG	[20]

Statistical Analysis

Student's t-test or Anova when appropriate, were used for statistical analyses and computation of P-values.. All error bars represent the standard error of the mean (SEM).

Chapter 4 Methods References

1. Chapman VM, Miller DR, Armstrong D, Caskey CT. Recovery of induced mutations for x chromosome-linked muscular dystrophy in mice. Proceedings of the National Academy of Sciences of the United States of America. 1989;86:1292-1296

2. Ieronimakis N, Pantoja M, Hays AL, Dosey TL, Qi J, Fischer KA, Hoofnagle AN, Sadilek M, Chamberlain JS, Ruohola-Baker H, Reyes M. Increased sphingosine-1-phosphate improves muscle regeneration in acutely injured mdx mice. Skeletal muscle. 2013;3:20

3. Ieronimakis N, Hays AL, Janebodin K, Mahoney WM, Jr., Duffield JS, Majesky MW, Reyes M. Coronary adventitial cells are linked to perivascular cardiac fibrosis via tgfbeta1 signaling in the mdx mouse model of duchenne muscular dystrophy. Journal of molecular and cellular cardiology. 2013;63:122-134

4. Lin SL, Kisseleva T, Brenner DA, Duffield JS. Pericytes and perivascular fibroblasts are the primary source of collagen-producing cells in obstructive fibrosis of the kidney. The American journal of pathology. 2008;173:1617-1627

5. Krempen K, Grotkopp D, Hall K, Bache A, Gillan A, Rippe RA, Brenner DA, Breindl M. Far upstream regulatory elements enhance position-independent and uterus-specific expression of the murine alpha1(i) collagen promoter in transgenic mice. Gene expression. 1999;8:151-163

6. Yata Y, Scanga A, Gillan A, Yang L, Reif S, Breindl M, Brenner DA, Rippe RA. Dnase i-hypersensitive sites enhance alpha1(i) collagen gene expression in hepatic stellate cells. Hepatology (Baltimore, Md. 2003;37:267-276

7. Tajbakhsh S, Bober E, Babinet C, Pournin S, Arnold H, Buckingham M. Gene targeting the myf-5 locus with nlacz reveals expression of this myogenic factor in mature skeletal muscle fibres as well as early embryonic muscle. Developmental dynamics : an official publication of the American Association of Anatomists. 1996;206:291-300

8. Ieronimakis N, Balasundaram G, Rainey S, Srirangam K, Yablonka-Reuveni Z, Reyes M. Absence of cd34 on murine skeletal muscle satellite cells marks a reversible state of activation during acute injury. PloS one. 2010;5:e10920

9. Hamilton TG, Klinghoffer RA, Corrin PD, Soriano P. Evolutionary divergence of platelet-derived growth factor alpha receptor signaling mechanisms. Molecular and cellular biology. 2003;23:4013-4025

10. Roesch K, Jadhav AP, Trimarchi JM, Stadler MB, Roska B, Sun BB, Cepko CL. The transcriptome of retinal muller glial cells. The Journal of comparative neurology. 2008;509:225-238

11. Muzumdar MD, Tasic B, Miyamichi K, Li L, Luo L. A global double-fluorescent cre reporter mouse. Genesis. 2007;45:593-605

12. Kang SH, Fukaya M, Yang JK, Rothstein JD, Bergles DE. Ng2+ cns glial progenitors remain committed to the oligodendrocyte lineage in postnatal life and following neurodegeneration. Neuron. 2010;68:668-681

13. Olson LE, Soriano P. Increased pdgfralpha activation disrupts connective tissue development and drives systemic fibrosis. Developmental cell. 2009;16:303-313

14. Olson LE, Soriano P. Pdgfrbeta signaling regulates mural cell plasticity and inhibits fat development. Developmental cell. 2011;20:815-826

15. J K. Histological and histochemical methods: Theory and practice. Cold Spring Harbor Laboratory Press. 2008

16. Ieronimakis N, Balasundaram G, Reyes M. Direct isolation, culture and transplant of mouse skeletal muscle derived endothelial cells with angiogenic potential. PloS one. 2008;3:e0001753

17. Kenyon NJ, Ward RW, McGrew G, Last JA. Tgf-beta1 causes airway fibrosis and increased collagen i and iii mrna in mice. Thorax. 2003;58:772-777

18. Chen X, Aravindakshan J, Yang Y, Tiwari-Pandey R, Sairam MR. Aberrant expression of pdgf ligands and receptors in the tumor prone ovary of follitropin receptor knockout (forko) mouse. Carcinogenesis. 2006;27:903-915

19. Fukai N, Kenagy RD, Chen L, Gao L, Daum G, Clowes AW. Syndecan-1: An inhibitor of arterial smooth muscle cell growth and intimal hyperplasia. Arteriosclerosis, thrombosis, and vascular biology. 2009;29:1356-1362

20. Au CG, Butler TL, Sherwood MC, Egan JR, North KN, Winlaw DS. Increased connective tissue growth factor associated with cardiac fibrosis in the mdx mouse model of dystrophic cardiomyopathy. International journal of experimental pathology. 2010;92:57-65

Chapter 4 Supplementary Figures

Figure S1: Type III and VI collagens are concentrated with *Col1a1-GFP* cells in perimysial fibrosis of mdx skeletal muscles.(**a**) Staining for type III collagen in diaphragms and quadriceps from male 20MO mdx:Col1a1-GFP mice highlights the concentration GFP+ cells in perimysial fibrosis, particularly surrounding vessels labeled with αSMA. (**b**) A similar pattern of accumulation was observed with type VI collagen in serial sections from the same mice. (**b**) IgG isotype to the anti-collagen III antibody was stained in parallel to control for non-specific staining. Scale bars = 50µm.

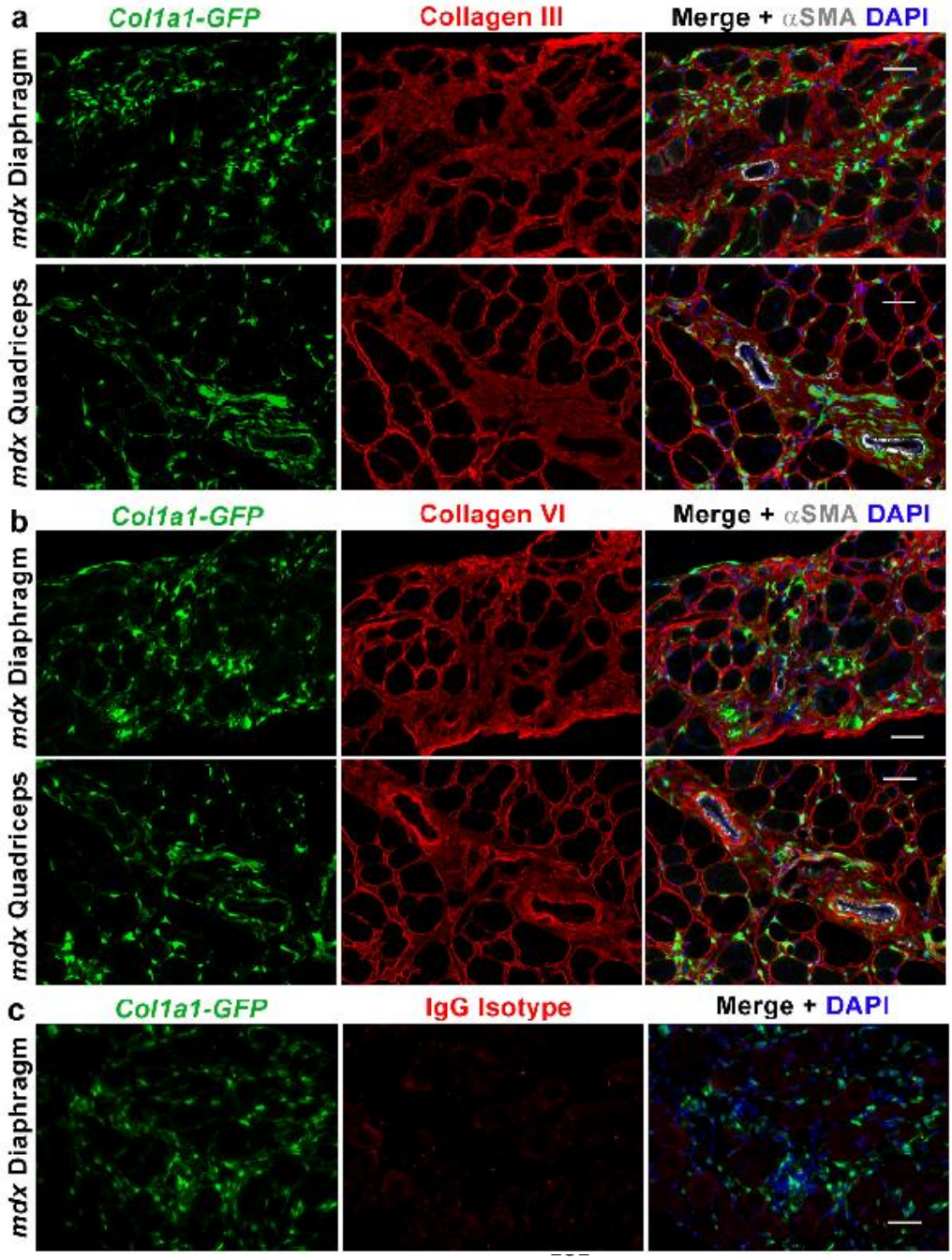

Figure S2: Col1a1-GFP cells in *mdx* hearts share a similar localization with type III collagen and molecular signature by FACS .(a) Heart sections from the same mdx:Col1a1-GFP mice shown in Fig. 3, highlight the accumulation of type III collagen with age and concentration of GFP+ in these fibrotic areas. Scale bars = 50μm. (b) FAC-analysis of hearts from the same wt and mdx:Col1a1-GFP male mice (n=3 per age) depicted in Fig. 4, indicates that the molecular signature of the GFP+ majority remains positive for PDGFRα and Sca1, but negative for CD45 and CD31 with age in mdx hearts.

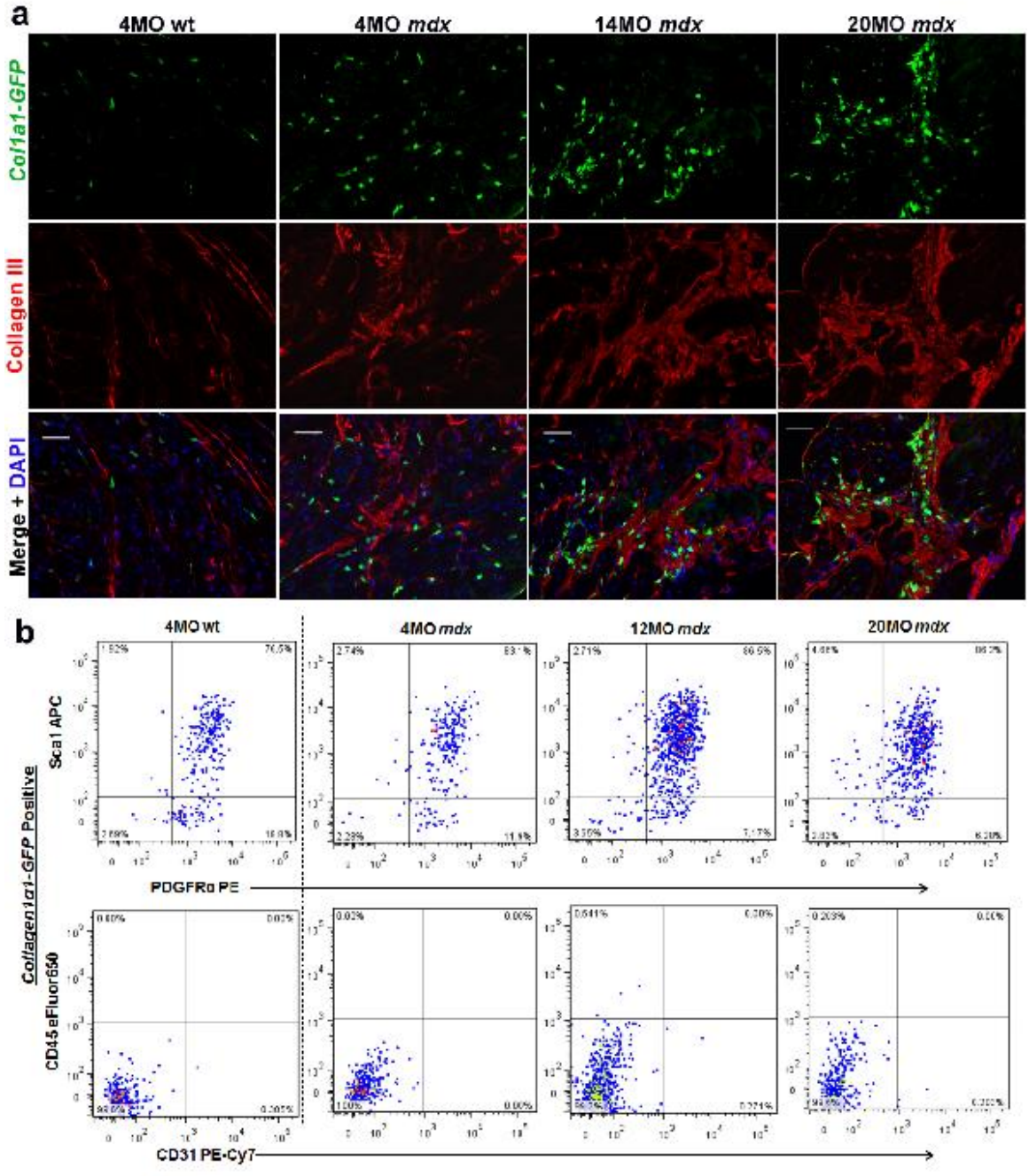

Figure S3: The expression of Pdgfrα is elevated in mdx vs. wt muscles.(a) q-RT-PCR analysis for Pdgfrα reveals increased expression in Tibialis Anterior's (TA), diaphragms and hearts collected from 12MO (n=3 per condition) mdx vs. wt mice; from. (b) Further analysis of the same samples, indicates that the expression of the Pdgf-a ligand was significantly higher only in mdx diaphragms at this. * P=<0.05 by Student's t-test. Error bars indicate ±SEM

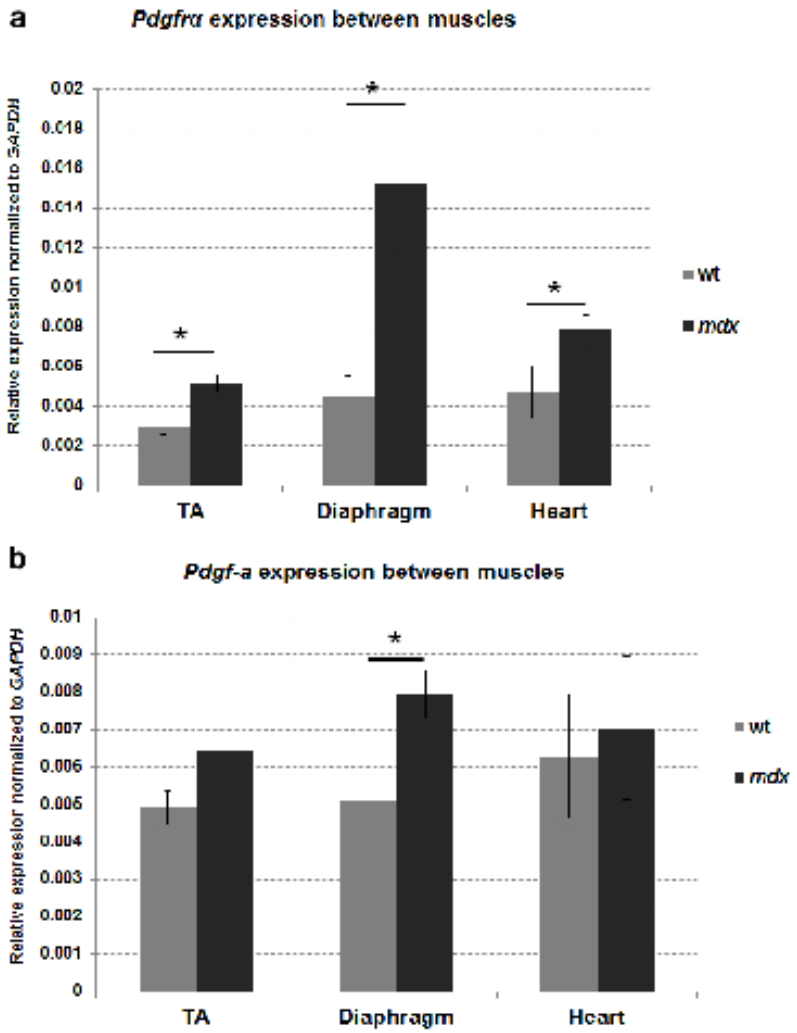

Figure S4: Inhibition of PDGFRα reduces pro-collagen expression in cultured *Col1a1-GFP*+ cells.(a) Cultured *Col1a1-GFP*+ cells were treated with DMEM with 5%FCS+PenStrep containing either vehicle (DMS), 10ng/ml of PDGF-AA, PDGF-BB, or PDGF-AA + 1μM Crenolanib; a selective inhibitor of PDGFRα. Cells were kept in each respective media for 4 days then collected for q-RT-PCR analysis for pro-collagens, a minimum of 3 replicate wells from twelve well plates, was analyzed for each condition. Results indicate treatment with PDGF-AA but not PDGF-BB can potentiate *Collagen1α1* and *3α1* expression. In contrast, the addition of Crenolanib inhibited the response of collagen producing cells to PDGF-AA. *P<0.05, ***P<0.00005 by single factor Anova.. Error bars indicate ±SEM. (b) To confirm these effects were in response to PDGFRα activation and inhibition, *Col1a1-GFP*+ cells were stimulated for 30 minutes with 10ng/ml PDGF-AA or PDGF-AA + 1μM Crenolanib (same basal media). Western blot analysis confirms the phosphorylation of PDGFRα with PDGF-AA stimulation and inhibition this response with Crenolanib.

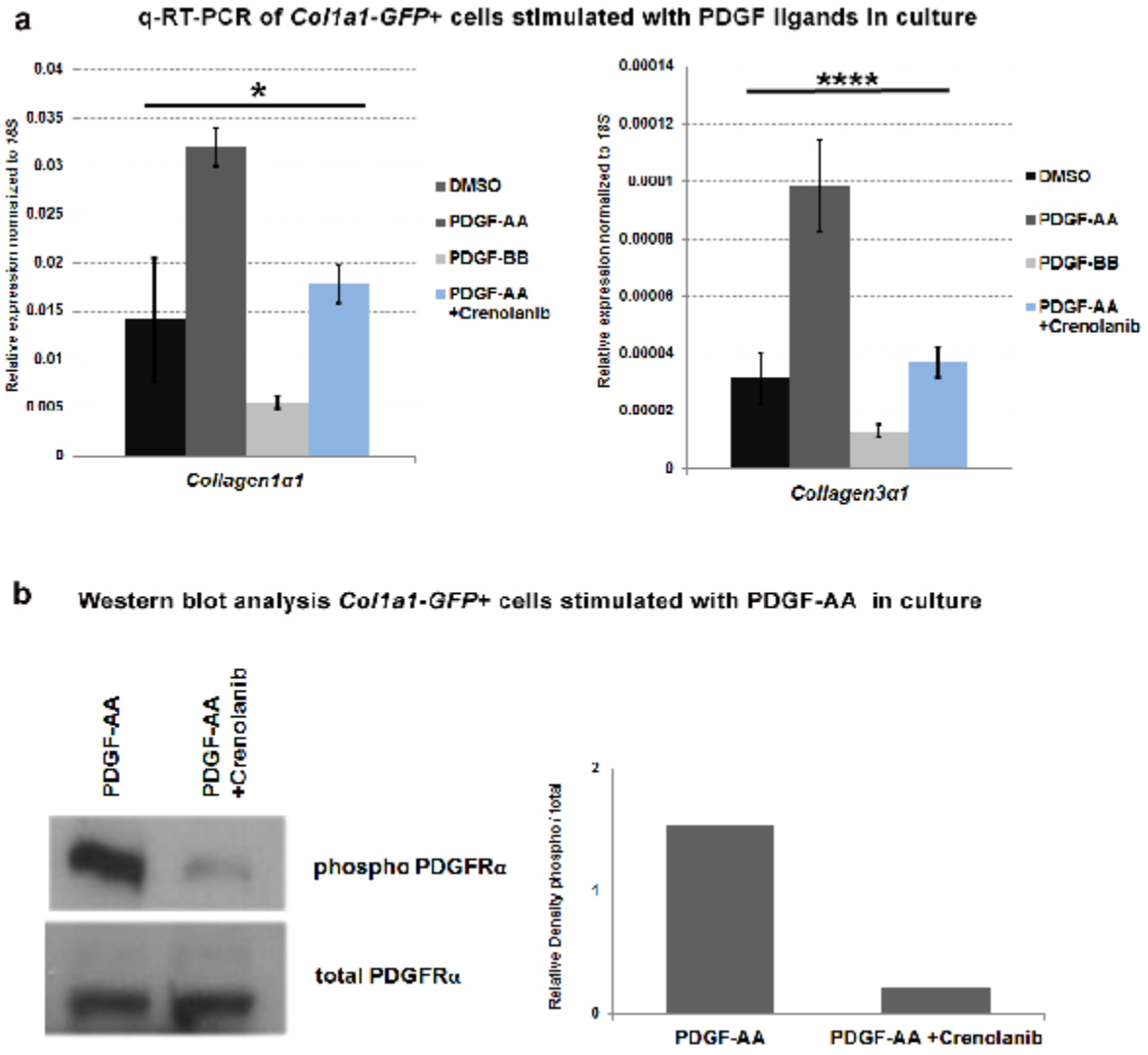

Figure S5: Treatment with Crenolanib reduced PDGFRα signaling and fibrosis in *mdx* heart.(a) Analogous to the results observed in diaphragm muscles, hearts from the same *mdx* mice analyzed in Fig. 9b-f showed reduced cardiac pathology by sirius red staining, with Crenolanib. (b) q-RT-PCR analysis of these same hearts (n=4 per treatment) reveals significantly reduced expression of *Collagen3α1*. (c) Western blot analysis supports the reduction *Collagen3α1* as type III collagen and fibronectin were significantly reduced with Crenolanib treatment in the same heart samples. (d) Once more, the reductions in these components of fibrosis, coincide with the inhibition of PDGFRα signaling in hearts from Crenolanib treated *mdx* mice. Howeevr, in contrast to diaphragms, Scr phosphorylation was not different with Crenolanib. * P=<0.05 by Student's *t*-test. Error bars indicate ±SEM.

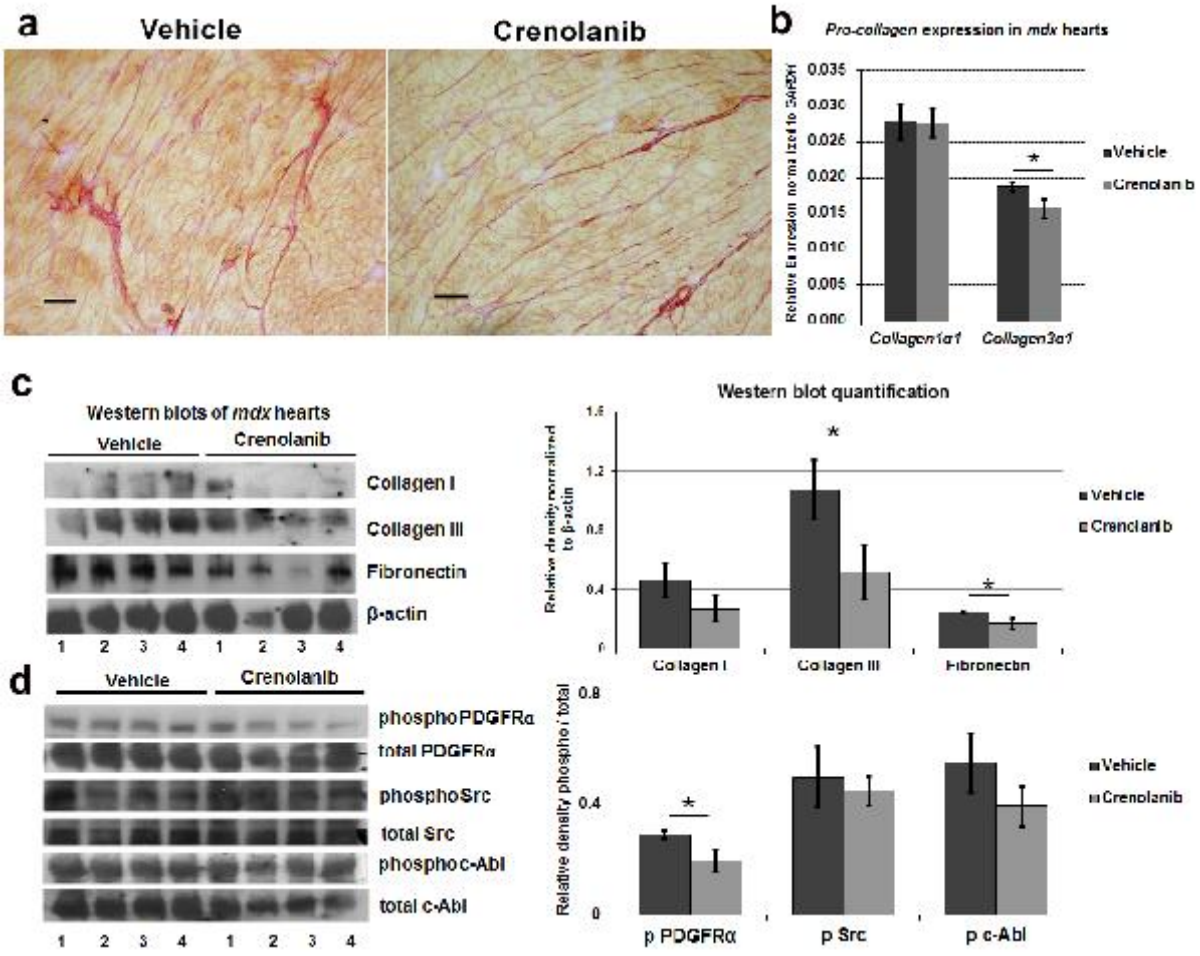

Figure S6: Treatment with Crenolanib reduced PDGFRα signaling and fibrosis in *mdx* heart. EDL muscles from the same mdx:Col1a1-GFP mice depicted in Fig. 10a, show more αSMA+ regenerating muscles fibers with Crenolanib treatment. Scale bars = 50μm.

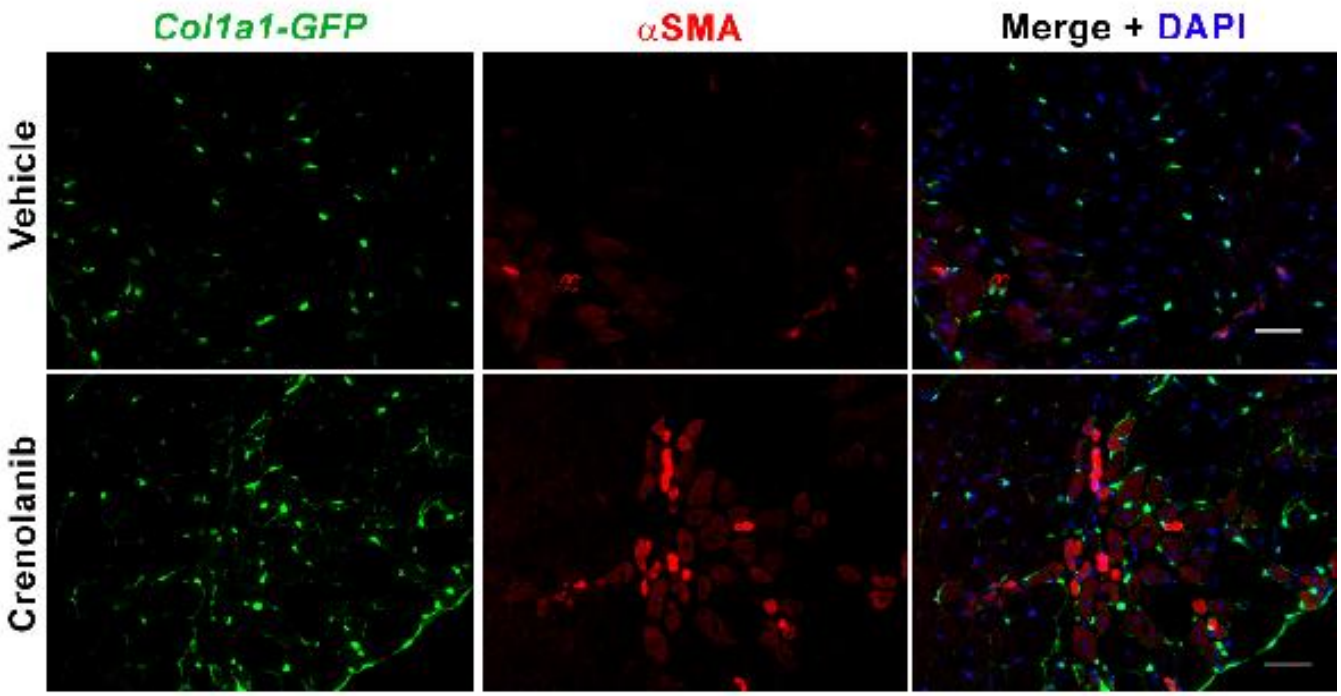

Conclusion

Summary of Results

Classically, DMD has been perceived to be a singular disease affecting muscle fiber function. However, many studies to date, including our own, demonstrate that this is a multi-faceted disease that involves and affects several cell populations (1-4). Interdependence between cellular compartments is governed by paracrine signaling, which is altered in this disease (e.g., S1P (Chapter 3) and PDGFRα (Chapter 4)). The reliance of each cellular population on one another, presents interesting and novel questions that can expand our understanding of muscle cell biology. Herein, we have described two signaling pathways (S1P and PDGFRα) that are altered and directly influence the cellular responses to muscle regeneration (illustrated in Figure 6). The consequences of these alterations are reduced regeneration capacity by satellite cells and increased fibrosis mediated by collagen producing cells. Although endothelial cells are affected with muscular dystrophy, it remains unclear if their capacity to synthesize S1P is altered and results in the reductions we observed in mdx muscles. Therefore, further investigation of sphingosine biology is warranted to specifically identify the components of S1P synthesis that are altered with disease. In contrast, over-activation of PDGFRα results in greater connective tissue accumulation that perturbs regeneration. Elevated levels of the PDGF-AA ligand by dystrophic fibers, is the likely antagonist of this pro-fibrotic signaling. What remains unanswered is the mechanism by which PDGF-AA production occurs in skeletal muscles. The molecular interactions within muscle fibers that occur with chronic damage and repair will require further investigation in order to elucidate this mechanism. In spite of the gaps in knowledge that remain, future research focused on cellular interactions can yield benefits not just for DMD but other

diseases in which alterations in signaling influence cellular responses to tissue degeneration and regeneration.

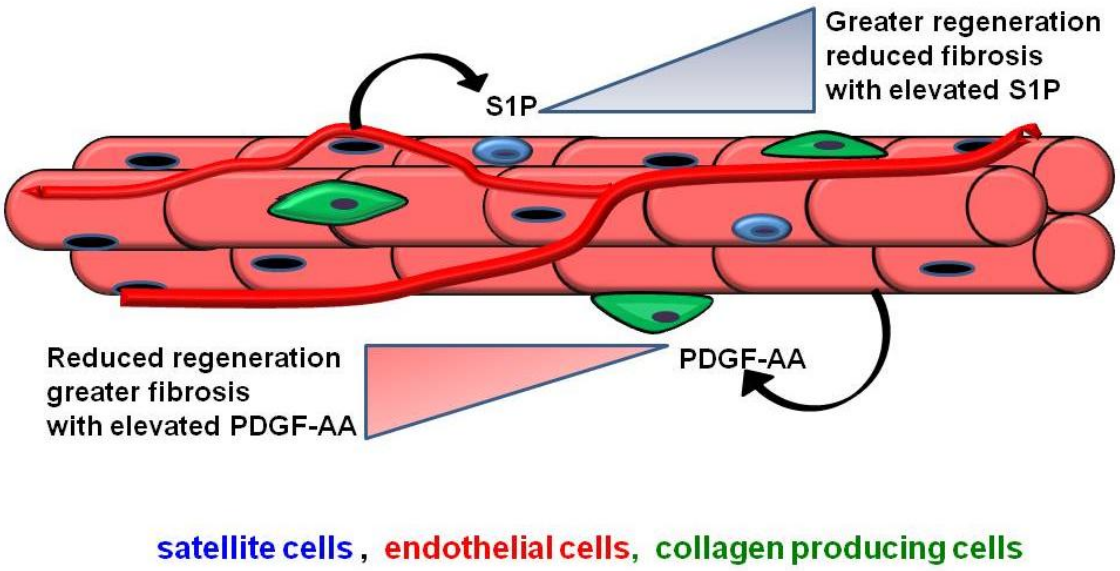

Figure 6. Modeled are the opposing effects of S1P and PDGF-AA on skeletal muscle that occurs with muscular dystrophy. Although S1P content is reduced in dystrophic muscles, pharmacological elevation can promote satellite cell-mediated muscle regeneration and disrupt the accumulation of fibrosis. In contrast, PDGF-AA and the activation of PDGFRα in collagen producing cells promotes fibrosis in muscular dystrophy. Inhibition of PDGFRα signaling can perturb the production and accumulation of excessive connective tissue, which in turn is makes muscle more permission for regeneration.

Muscle wasting that occurs with aging may also be influence by cellular and molecular interactions. Although PDGFRα and S1P signaling have yet to be examined in the field of aging research, it is entirely possible that these mechanisms are conserved between dystrophic and aging-related muscle repair and degeneration. The likelihood stems from the shared pathology present in both DMD and sarcopenia: fat infiltration and fibrosis of the skeletal muscles (5-7). In addition, satellite cell impairment and decline in fast twitch fibers also prevalent between dystrophy and aging (8-11). Therefore, cellular and molecular signaling pathways warrant examination in the context of age related muscle wasting.

Future Directions in Basic Biology

The insight shed by our studies only scratches the surface of the cellular and molecular interactions responsible for muscle regeneration and pathogenesis. In particular, the direct mechanisms by which S1P and PDGFRα influence cellular responses in normal regeneration vs. muscular dystrophy requires significantly more research effort. Genetic ablation and activation of these pathways in satellite cells and collagen producing cells in vivo would provide significant insight of the role of S1P and PDGFRα signaling within these respective cell populations. Specific genetic alterations can be accomplished by utilizing Cre-lox recombination in the mouse model (12). This technology has been vital in fate mapping and delineating signaling requirements within specific cellular compartments (13, 14). In turn, the downstream cascade by which satellite cells are impaired and collagen-producing cells are pathogenic, can be resolved by this approach. Within our own lab, we have already begun follow-up research utilizing Cre-lox alleles to address specific questions about satellite cell-S1P biology and PDGFRα signaling in collagen-producing cells.

As previously discussed, S1PR1-3 are the predominant S1P receptors expressed in skeletal muscle (15). While S1PR2- and S1PR3-null mice show no obvious muscle defects, S1PR1-null mice are embryonic lethal; therefore, its requirement during myogenesis remains unresolved (16). Although, S1PR2-null mice show perturbed muscle repair following toxin injury, this may be a consequence of non-myogenic cell impairment (17). In contrast, we observed S1PR3 was mostly localized to endothelial cells, although satellite cells may express this receptor at low levels (Figure 7) (Chapter 3). Interestingly, newly regenerated fibers contain

perinuclear phophorylated-S1PR1 (18). Altogether, our data suggests that S1PR1 is likely the most vital of the three S1PRs for satellite cell myogensis. Therefore, we plan to address this question by ablating S1PR1 specifically in satellite cells using an inducible Cre driven by the endogenous Pax7 promoter, crossed into S1PR1 lox/lox mice (19, 20). Utilizing this system, S1PR1 can be conditionally ablated in satellite cells (19, 21). This inducible system will also allow us to address the temporal requirements for S1PR1 in satellite cells of postnatal muscles. If S1PR1 signaling is essential for myogenesis, we should observe an impairment in satellite cell-mediated regeneration in adult muscle. Alternatively, we can also assess the developmental requirement for S1PR1 in satellite cell precursors, which also express Pax7 (21). It is entirely possible that S1PR1, is essential for satellite cell maturation and homeostasis. In this case we should observe a decline in satellite cells following Cre induction following postnatal development or in adult muscle respectively. This approach will also be informative for identifing downstream effectors of S1PR1 signaling in satellite cells. Presumably, a phenotype in S1PR1-null satellite cells will result in alterations in signaling that can be traced by transcriptional and molecular comparisons to wild-type satellite cells. Future studies should address long standing questions about the requirement for S1PR1 in myogenic cells and identify downstream transcriptional targets that regulate this signaling. Knowledge of the S1PR1signaling cascade would be invaluable for designing small molecules or peptides that can modulate cellular responses. Such specific drugs may hold significant therapeutic potency if they prove effective for enhancing the regenerative potential of satellite cells.

Analogous to the requirement for S1PR1 in satellite cells, it remains unknown if PDGFRα is essential for the pro-fibrotic signaling that occurs in skeletal muscle collagen producing cells in vivo. In fact, the specific cascade by which PDGFRα results in pro-collagen

expression in vivo remains unknown (22, 23). Elucidating the downstream effectors would provide significant insight on the process of fibrosis and may present more specific pharmacological targets. In order to address this question, we are also currently generating PDGFRα lox/lox mice that harbor the tamoxifen inducible Cre driven by the Col1a1 promoter. With this model, we will be able to assess the requirement for PDGFRα signaling in collagen producing cells during homeostasis and following muscle injury. Once more, transcriptional and molecular comparisons between wild-type and PDGFRα knockout cells should identify the factors that mediate collagen expression. Specifically, we can untangle the downstream effecter of PDGFRα mediated pro-collagen expression in the skeletal muscle. These reporter mice would be invaluable in confirming the role of PDGFRα signaling in the pathogenesis of muscular dystrophy. However, crossing Cre-lox into the mdx background requires significant animal generations and funding.

Clinical Potential

The aforementioned mouse studies are aimed at understanding the novel biology of S1P and PDGFRα signaling in specific cellular populations of the skeletal muscle. However, these follow-up studies may not have immediate clinical implications. Therefore, we will capitalize on the results we have observed with THI and Crenolanib for alleviating the pathogenesis of muscular dystrophy (Chapters 3 and 4). Currently, we are examining the utility of THI-oxime (LX2931) for the treatment of muscular dystrophy. THI-oxime is a derivative of THI with greater solubility that has already passed FDA safety and toxicology studies, and it has completed a Phase II clinical trial for Rheumatoid arthritis (24, 25). In contrast, THI is not under clinical development and would require significantly more financial and temporal investment to assess its safety, toxicology and begin testing in humans. Thus, repurposing THI-oxime for the

treatment of DMD would accelerate the development of S1P-targeted therapies for muscle wasting. Future research should focus on the potential of S1P altering compounds, such as THI-oxime, to regenerate muscles in mdx mice, in order to repurpose available drugs for the immediate treatment of DMD. Careful dosing of S1P elevating drugs will have to be evaluated in order to avoid potential side-effects, such as infection or cancer, that may occur with immune suppression (25).

In contrast to THI, Crenolanib has had significant clinical development and is currently in Phase II clinical trials for juvenile glioblastoma (26, 27). If more pre-clinical studies, including pharmodynamics and dosing in dystrophic animals can be accomplished, Crenolanib may also be repurposed for DMD if shown to be efficacious. Ultimately, therapies using a combination of anti-fibrotic and pro-regenerative drugs, such as THI-oxime and Crenolanib, may prove more efficacious for perturbing muscle wasting in DMD and perhaps sarcopenia. Future research into these therapies warrants the significant investment in time and money. If such therapies prove successful, the economic and moral benefits resulting from the reduction of morbidity and mortality in patients suffering from muscle wasting diseases will far outweigh the initial investments.

Research Barriers

Although future studies of muscle regeneration in the context of disease and aging would yield tremendous economic and population health benefits, the National Institute of Health (NIH) often funds singular studies that focus only on one molecule or gene, while ignoring the cellular and molecular interactions that directly influence pathogenesis. The ineffectiveness of such singular approaches is evident economically; despite millions of dollars spent by the NIH

towards muscular dystrophy research, a cure remains far from reach and not a single treatment has passed FDA approval within the past 20 years. Yet the financial burden of families with DMD children has steadily increased to an average of $60,000 per year/per child affected by muscular dystrophy (28). Irrespective of the financial burdens, the grim reality is that children afflicted with DMD will not only face incredible hardship but will die, pure and simple, and as a scientific community we have failed them. It is my personal belief that science has moved so far from the bedside, we as a community have become too enamored with our own agendas to the point that NIH funding policies gravely overlook the needs of patients, such as those afflicted with DMD.

References

1. Palladino M, Gatto I, Neri V, Straino S, Smith RC, Silver M, et al. Angiogenic impairment of the vascular endothelium: a novel mechanism and potential therapeutic target in muscular dystrophy. Arteriosclerosis, thrombosis, and vascular biology. 2013;33(12):2867-76. doi: 10.1161/ATVBAHA.112.301172. PubMed PMID: 24072696.
2. Ieronimakis N, Hays AL, Janebodin K, Mahoney WM, Jr., Duffield JS, Majesky MW, et al. Coronary adventitial cells are linked to perivascular cardiac fibrosis via TGFbeta1 signaling in the mdx mouse model of Duchenne muscular dystrophy. Journal of molecular and cellular cardiology. 2013;63:122-34. doi: 10.1016/j.yjmcc.2013.07.014. PubMed PMID: 23911435.
3. Uezumi A, Ito T, Morikawa D, Shimizu N, Yoneda T, Segawa M, et al. Fibrosis and adipogenesis originate from a common mesenchymal progenitor in skeletal muscle. Journal of cell science. 2011;124(Pt 21):3654-64. PubMed PMID: 22045730.
4. Luz MA, Marques MJ, Santo Neto H. Impaired regeneration of dystrophin-deficient muscle fibers is caused by exhaustion of myogenic cells. Brazilian journal of medical and biological research = Revista brasileira de pesquisas medicas e biologicas / Sociedade Brasileira de Biofisica [et al]. 2002;35(6):691-5. PubMed PMID: 12045834.
5. Cros D, Harnden P, Pellissier JF, Serratrice G. Muscle hypertrophy in Duchenne muscular dystrophy. A pathological and morphometric study. Journal of neurology. 1989;236(1):43-7. PubMed PMID: 2915226.
6. Corcoran MP, Lamon-Fava S, Fielding RA. Skeletal muscle lipid deposition and insulin resistance: effect of dietary fatty acids and exercise. The American journal of clinical nutrition. 2007;85(3):662-77. PubMed PMID: 17344486.
7. Mann CJ, Perdiguero E, Kharraz Y, Aguilar S, Pessina P, Serrano AL, et al. Aberrant repair and fibrosis development in skeletal muscle. Skeletal muscle. 2011;1(1):21. doi: 10.1186/2044-5040-1-21. PubMed PMID: 21798099; PubMed Central PMCID: PMC3156644.
8. Webster C, Silberstein L, Hays AP, Blau HM. Fast muscle fibers are preferentially affected in Duchenne muscular dystrophy. Cell. 1988;52(4):503-13. PubMed PMID: 3342447.
9. Day K, Shefer G, Shearer A, Yablonka-Reuveni Z. The depletion of skeletal muscle satellite cells with age is concomitant with reduced capacity of single progenitors to produce reserve progeny. Developmental biology. 2010;340(2):330-43. doi: 10.1016/j.ydbio.2010.01.006. PubMed PMID: 20079729; PubMed Central PMCID: PMC2854302.
10. Blau HM, Webster C, Pavlath GK. Defective myoblasts identified in Duchenne muscular dystrophy. Proceedings of the National Academy of Sciences of the United States of America. 1983;80(15):4856-60. PubMed PMID: 6576361; PubMed Central PMCID: PMC384144.
11. Gibson MC, Schultz E. Age-related differences in absolute numbers of skeletal muscle satellite cells. Muscle & nerve. 1983;6(8):574-80. doi: 10.1002/mus.880060807. PubMed PMID: 6646160.
12. Nagy A. Cre recombinase: the universal reagent for genome tailoring. Genesis. 2000;26(2):99-109. PubMed PMID: 10686599.

13. Jaisser F. Inducible gene expression and gene modification in transgenic mice. Journal of the American Society of Nephrology : JASN. 2000;11 Suppl 16:S95-S100. PubMed PMID: 11065338.
14. Kos CH. Cre/loxP system for generating tissue-specific knockout mouse models. Nutrition reviews. 2004;62(6 Pt 1):243-6. PubMed PMID: 15291397.
15. Danieli-Betto D, Peron S, Germinario E, Zanin M, Sorci G, Franzoso S, et al. Sphingosine 1-phosphate signaling is involved in skeletal muscle regeneration. American journal of physiology Cell physiology. 2010;298(3):C550-8. doi: 10.1152/ajpcell.00072.2009. PubMed PMID: 20042733.
16. Liu Y, Wada R, Yamashita T, Mi Y, Deng CX, Hobson JP, et al. Edg-1, the G protein-coupled receptor for sphingosine-1-phosphate, is essential for vascular maturation. The Journal of clinical investigation. 2000;106(8):951-61. doi: 10.1172/JCI10905. PubMed PMID: 11032855; PubMed Central PMCID: PMC314347.
17. Germinario E, Peron S, Toniolo L, Betto R, Cencetti F, Donati C, et al. S1P2 receptor promotes mouse skeletal muscle regeneration. Journal of applied physiology. 2012;113(5):707-13. doi: 10.1152/japplphysiol.00300.2012. PubMed PMID: 22744969.
18. Ieronimakis N, Pantoja M, Hays AL, Dosey TL, Qi J, Fischer KA, et al. Increased sphingosine-1-phosphate improves muscle regeneration in acutely injured mdx mice. Skeletal muscle. 2013;3(1):20. doi: 10.1186/2044-5040-3-20. PubMed PMID: 23915702; PubMed Central PMCID: PMC3750760.
19. Lepper C, Conway SJ, Fan CM. Adult satellite cells and embryonic muscle progenitors have distinct genetic requirements. Nature. 2009;460(7255):627-31. doi: 10.1038/nature08209. PubMed PMID: 19554048; PubMed Central PMCID: PMC2767162.
20. Allende ML, Yamashita T, Proia RL. G-protein-coupled receptor S1P1 acts within endothelial cells to regulate vascular maturation. Blood. 2003;102(10):3665-7. doi: 10.1182/blood-2003-02-0460. PubMed PMID: 12869509.
21. Seale P, Sabourin LA, Girgis-Gabardo A, Mansouri A, Gruss P, Rudnicki MA. Pax7 is required for the specification of myogenic satellite cells. Cell. 2000;102(6):777-86. PubMed PMID: 11030621.
22. Andrae J, Gallini R, Betsholtz C. Role of platelet-derived growth factors in physiology and medicine. Genes & development. 2008;22(10):1276-312. doi: 10.1101/gad.1653708. PubMed PMID: 18483217; PubMed Central PMCID: PMC2732412.
23. Bonner JC. Regulation of PDGF and its receptors in fibrotic diseases. Cytokine & growth factor reviews. 2004;15(4):255-73. doi: 10.1016/j.cytogfr.2004.03.006. PubMed PMID: 15207816.
24. Bagdanoff JT, Donoviel MS, Nouraldeen A, Carlsen M, Jessop TC, Tarver J, et al. Inhibition of sphingosine 1-phosphate lyase for the treatment of rheumatoid arthritis: discovery of (E)-1-(4-((1R,2S,3R)-1,2,3,4-tetrahydroxybutyl)-1H-imidazol-2-yl)ethanone oxime (LX2931) and (1R,2S,3R)-1-(2-(isoxazol-3-yl)-1H-imidazol-4-yl)butane-1,2,3,4-tetraol (LX2932). Journal of medicinal chemistry. 2010;53(24):8650-62. doi: 10.1021/jm101183p. PubMed PMID: 21090716.
25. Bagdanoff JT, Donoviel MS, Nouraldeen A, Tarver J, Fu Q, Carlsen M, et al. Inhibition of sphingosine-1-phosphate lyase for the treatment of autoimmune disorders. Journal of medicinal chemistry. 2009;52(13):3941-53. doi: 10.1021/jm900278w. PubMed PMID: 19489538.

26. Lewis NL, Lewis LD, Eder JP, Reddy NJ, Guo F, Pierce KJ, et al. Phase I study of the safety, tolerability, and pharmacokinetics of oral CP-868,596, a highly specific platelet-derived growth factor receptor tyrosine kinase inhibitor in patients with advanced cancers. Journal of clinical oncology : official journal of the American Society of Clinical Oncology. 2009;27(31):5262-9. doi: 10.1200/JCO.2009.21.8487. PubMed PMID: 19738123; PubMed Central PMCID: PMC2773478.
27. Heinrich MC, Griffith D, McKinley A, Patterson J, Presnell A, Ramachandran A, et al. Crenolanib inhibits the drug-resistant PDGFRA D842V mutation associated with imatinib-resistant gastrointestinal stromal tumors. Clinical cancer research : an official journal of the American Association for Cancer Research. 2012;18(16):4375-84. doi: 10.1158/1078-0432.CCR-12-0625. PubMed PMID: 22745105.
28. Landfeldt E, Lindgren P, Bell CF, Schmitt C, Guglieri M, Straub V, et al. The burden of Duchenne muscular dystrophy: An international, cross-sectional study. Neurology. 2014. doi: 10.1212/WNL.0000000000000669. PubMed PMID: 24991029.

Personal Perspective

In 2002, I separated from the United States Air Force to peruse a career in biological science. Having served on the battlefields of Afghanistan, my motivation stemmed from the lack of treatments in regenerative medicine available to wounded soldiers. At the time, it was a golden age for science; the human genome had just been completed and breakthroughs in stem cell biology were taking shape. Therefore, I was motivated and hopeful that with the right training, perseverance and hard work, I may contribute to the development of treatments for my former colleagues in arms. When I began working on skeletal muscle biology in 2006, my dream was coming to fruition and I did not regret having left a promising and stable career in the military.

Fast forward 12 years later, and now as a junior scientist, the future of biological research is bleak as my dreams are in peril. This dark horizon does not only affect scientist but also patients and taxpayers alike. The problems stems not just from federal budget cuts, but from the corruption at the level of NIH and inefficiency of academic research. Billions have already been spent with few results. All the while, indirect costs at academic institutions continue to rise and consume a significant portion of the already strained NIH budget. This diverts valuable research dollars to the propagation of obstructive administration and bureaucracy. With greater funding disparity, the environment becomes more toxic as scientist become increasingly motivated by survival and personal gain; ideas are stolen, grant reviewers sabotage competitors, and political alliances dictate funding and publications. Therefore, the appearance that the scientific community is infallible and seeks to advance our knowledge and benefit public health is far from reality. In contrast, science has become a feudal system in which mighty lords (the most recognized PIs) dictate every aspect and compete for the gold coffers of public money. In turn,

the peasantry (graduate students and post-docs) toil and fight for scraps while being exploited for ideas and labor. Great kingdoms (academic institutions) compete to attract these lords, so that their realms claim a share of the riches. Unfortunately, this cynical description is a small dose of the tattered landscape of biological research.

This scenario is highlighted by the fact that there exists an enormous disparity between the number of PhD trainees and post-docs vs. the number of faculty positions. Although this issue is has been recognized for over two decades (1-3), little has been or is currently being done to address it. Ultimately, the only benefactors of this crisis are senior investigators who have available to them a throng of expendable PhDs to exploit. In turn, investigators are focused on publishing papers and acquiring grants to pay for runaway institutional costs, which themselves provide little return. This cycle continues to repeat, irrespective of the few benefits the public has received for many billions of dollars in funding spent. Therefore, the ultimate losers are not just PhD graduates, whom most will ultimately have to seek careers outside of research, but more importantly the taxpayers and patients.

Such waste of research resources with little public return has been no more evident than in the field of cancer research. A quote from Dr. Linus Pauling, a two time Nobel laureate sums up the dilemma: “Everyone should know that most cancer research is largely a fraud and that the major cancer research organizations are derelict in their duties to the people who support them.” A testament to this quote is a Pubmed search for “HeLa cells” yields >80,000 publications. HeLa cells were originally derived in 1953 from human epithelial cervical cancer and have been wrought with controversy ranging from numerous contaminations to ethical issues surrounding their isolation (4). Irrespective of these issues, HeLa cells have become the most common tissue culture model not just for studying a range of cancers but also cellular process ranging from

autophagy to apoptosis. Yet the relevancy of this immortalized cell line which is aneuploidy and has multiple other genetic mutations, often comes into question (5). Particularly, the relevance stems from the fact that cancers are heterogeneous populations, often containing a mix of transformed and normal cells with varying genetic alterations (6). The cancer field having recognized the heterogeneous nature of malignancies continues to rely on HeLa cells, which cannot accurately define tumors. This often results in research that is focused on one pathway, studied with cell lines that do not represent in vivo characteristics, and results that cannot be clinically translated (7). Once more, this failure of research to attain tangible insights that benefit the public will continue, so long as the self-interests of academic institutions and corruption at NIH permit.

Unfortunately, the field of muscle research is not immune from this mismanagement. All too often researchers in the skeletal muscle biology receive notoriety and funding despite the lack of novelty or relevancy towards the treatment of dystrophy or other muscle diseases. Analogous to HeLa cells, the C2C12 cell line has been widely used to study myogenesis and model satellite cell biology in culture, with often misleading results. Currently Pubmed holds over 4000 publication referencing C2C12s, including reports that myoblasts can differentiate into chondrogenic and mesenchymal lineages (8, 9). Recent lineage tracing studies have unilaterally proven that satellite cells and their myoblast progeny do not undergo chondrogenic or osteogenic conversion in vivo (10, 11). This puts in question the relevance of many studies that make interpretations solely on experiments conducted with C2C12. Despite the shortcomings of C2C12s, NIH continues to fund such studies that yield little insight on the actual myogenic process which occurs in vivo. Unfortunately, such misappropriation also extends to studies that examine satellite cells in vivo. A prime example lies with a high profile paper published in 2008

by a group from Harvard in the journal of Cell (12). In this study the authors claim to have discovered a "distinct population of skeletal muscle precursors (SMPs)" that can improve dystrophic muscle function upon transplantation. This study was carried out with significant funding from several public and private institutions including the NIH. Yet the conclusions of this study are extremely flawed as the authors main claim that SMPs are a population of muscle stem cells distinct from the already recognized satellite cell population is simply untrue. Furthermore, the functional benefits resulting from cell transplants were skewed as normalizations covered the fact that there were several mock transplanted muscles with greater strength than muscles transplanted with SMPs. Despite these discrepancies and official protest by an expert in the field (13), this manuscript has been cited by at least 149 scientific articles and the investigators continues to receive substantial public funding and notoriety. However, the clinical relevancy and contribution to the treatment of muscular dystrophy by this research remains to be seen.

In retrospect our own contributions to understanding the cellular and molecular mechanism of dystrophy and potential therapeutics, may never reach the bedside. Until the system of research changes and patients welfare instead of funding and notoriety become a greater concern, science will continue to plummet into the abyss. This is further compounded by continued reductions in public funds and increases in indirect costs that academic institutions continue to siphon from bona-fide research dollars. However, this disastrous course can be averted, if we as scientists take on greater personal accountability and interest for patient's welfare. The old system, by which PIs exploit graduate students and post-docs in the race for notoriety and funding, must change. A more collaborative environment where scientist work as teams with the common goal of treating diseases, can yield more discoveries with direct public

benefit. This type of organization has worked well for the fields of engineering, computer and physical sciences, which have blossomed and changed our world in recent years. Only when taxpayers and patients receive greater return, will public funding for research warrant expansion. In closing, if the culture of science is to survive we must adapt a passion for discovery and treating the ill. Otherwise, we will continue to fratricide our community and leave a trail of failures, littered with the ghosts of those we could have saved.

References

1. Kennedy TJ, Jr. Graduate education in the biomedical sciences: critical observations on training for research careers. Academic medicine : journal of the Association of American Medical Colleges. 1994;69(10):779-99. PubMed PMID: 7916789.
2. Domer JE, Garry RF, Guth PS, Walters MR, Fisher JW. On the crisis in biomedical education: is there an overproduction of biomedical PhDs? Academic medicine : journal of the Association of American Medical Colleges. 1996;71(8):876-85. PubMed PMID: 9125964.
3. Juliano RL, Oxford GS. Critical issues in PhD training for biomedical scientists. Academic medicine : journal of the Association of American Medical Colleges. 2001;76(10):1005-12. PubMed PMID: 11597839.
4. Lucey BP, Nelson-Rees WA, Hutchins GM. Henrietta Lacks, HeLa cells, and cell culture contamination. Archives of pathology & laboratory medicine. 2009;133(9):1463-7. doi: 10.1043/1543-2165-133.9.1463. PubMed PMID: 19722756.
5. Adey A, Burton JN, Kitzman JO, Hiatt JB, Lewis AP, Martin BK, et al. The haplotype-resolved genome and epigenome of the aneuploid HeLa cancer cell line. Nature. 2013;500(7461):207-11. doi: 10.1038/nature12064. PubMed PMID: 23925245; PubMed Central PMCID: PMC3740412.
6. Meacham CE, Morrison SJ. Tumour heterogeneity and cancer cell plasticity. Nature. 2013;501(7467):328-37. doi: 10.1038/nature12624. PubMed PMID: 24048065.
7. Begley CG, Ellis LM. Drug development: Raise standards for preclinical cancer research. Nature. 2012;483(7391):531-3. doi: 10.1038/483531a. PubMed PMID: 22460880.
8. Katagiri T, Yamaguchi A, Komaki M, Abe E, Takahashi N, Ikeda T, et al. Bone morphogenetic protein-2 converts the differentiation pathway of C2C12 myoblasts into the osteoblast lineage. The Journal of cell biology. 1994;127(6 Pt 1):1755-66. PubMed PMID: 7798324; PubMed Central PMCID: PMC2120318.
9. Yeow K, Phillips B, Dani C, Cabane C, Amri EZ, Derijard B. Inhibition of myogenesis enables adipogenic trans-differentiation in the C2C12 myogenic cell line. FEBS letters. 2001;506(2):157-62. PubMed PMID: 11591391.
10. Kanisicak O, Mendez JJ, Yamamoto S, Yamamoto M, Goldhamer DJ. Progenitors of skeletal muscle satellite cells express the muscle determination gene, MyoD. Developmental biology. 2009;332(1):131-41. doi: 10.1016/j.ydbio.2009.05.554. PubMed PMID: 19464281; PubMed Central PMCID: PMC2728477.
11. Lepper C, Fan CM. Inducible lineage tracing of Pax7-descendant cells reveals embryonic origin of adult satellite cells. Genesis. 2010;48(7):424-36. doi: 10.1002/dvg.20630. PubMed PMID: 20641127; PubMed Central PMCID: PMC3113517.
12. Cerletti M, Jurga S, Witczak CA, Hirshman MF, Shadrach JL, Goodyear LJ, et al. Highly efficient, functional engraftment of skeletal muscle stem cells in dystrophic muscles. Cell. 2008;134(1):37-47. doi: 10.1016/j.cell.2008.05.049. PubMed PMID: 18614009; PubMed Central PMCID: PMC3665268.
13. Partridge T. Denominator problems in a muscle stem cell study? Cell. 2008;135(6):997-8; author reply 8-9. doi: 10.1016/j.cell.2008.11.033. PubMed PMID: 19070565.

Appendix

List of additional publications authored during period of graduate research.

1. Rosuvastatin reduces neointima formation in a rat model of balloon injury. Preusch M, Vanakaris A, Bea F, Ieronimakis N, Shimizu T, Konstandin M, Morris-Rosenfeld S, Albrecht C, Kranzöfer A, Katus A, Kranzöfer R. European Journal of Medical Research. 2010.

2. Genetic elevation of sphingosine 1-phosphate suppresses dystrophic muscle phenotype in Drosophila. Pantoja M, Fisher F, Ieronimakis N, Reyes M, Ruohola-Baker H. Development. 2012.

3. Defective ephrinB2 reverse signaling promotes capillary rarefaction and fibrosis after kidney injury. Kida Y, Ieronimakis N, Shrimpf C, Reyes M, Acher-Palmer A, Duffield J. Journal of the American Society of Nephrology. 2012.

4 VEGFR2-dependent angiogenic capacity of pericyte-like dental pulp stem cells. Janebodin K, Buranaphatthana W, Ieronimakis N, Reyes M. Journal of Dental Research. 2013.

5. An in vitro culture system for long-term expansion of epithelial and mesenchymal salivary gland cells: role of TGFβ1 in salivary gland epithelial and mesenchymal differentiation. Janebodin K, Buranaphatthana W, Ieronimakis N, Hays A, Reyes M. Biomed Research International. 2013.

6. Coronary adventitial cells are linked to perivascular cardiac fibrosis via TGFβ1 signaling in the mdx mouse model of Duchenne Muscular Dystrophy. Ieronimakis N, Hays A, Janebodin K, Mahoney W, Duffield J, Majesky M, Reyes M. Journal of Molecular and Cellular Cardiology. 2013.

7. Molecular mechanism of sphingosine 1-phosphate action in Duchenne Muscular Dystrophy. Nguyen-Tran DH, Hait N, Sperber H, Qi J, Fischer K, Ieronimakis N, Pantoja M, Hays A, Allegood J, Reyes M, Spiegel S, Ruohola-Baker H. Disease Models & Mechanism. 2013.

8. Isolation, characterization, and transplant of cardiac endothelial cells. Pratumvinit B, Reesukumal K, Janebodin K, Ieronimakis N, Reyes M. Biomed Res Int. 2013.

9. Nanopatterned muscle cell patches enhanced myogenesis and dystrophin expression in a mouse model of muscular dystrophy. Yang H, Ieronimakis N, Tsui J, Kim H, Suh , Reyes M, Kim D. Biomaterials. 2014.

10. Chlamydia Pneumoniae infection of lungs and macrophages indirectly stimulates the phenotypic conversion of smooth muscle cells and mesenchymal stem cells: potential roles in vascular calcification and fibrosis. Rosenfeld M, Cabbage S, Ieronimakis N, Preusch M, Lee, A, Ricks J, Janebodin K, Hays A, Wijelath E, Reyes M, Campbell, Lee A. Pathogens and Disease. 2014.